# Development of a High Throughput Method
# For the discovery of selective propene oxidation catalysts

Dissertation

zur Erlangung des Grades
des Doktors der Ingenieurwissenschaften
der Naturwissenschaftlich-Technischen Fakultät III
Chemie, Pharmazie, Bio- und Werkstoffwissenschaften

der Universität des Saarlandes

von

Su, Woongsik

Saarbrücken

2012

| | |
|---|---|
| Tag des Kolloquiums: | 26. 02. 2013 |
| Dekan: | Prof. Dr. V. Helms |
| Berichterstatter: | Prof. Dr. W.F. Maier |
| | Prof. Dr. J. Jauch |
| Vorsitz: | Prof. Dr. E. Heinzle |
| Akad. Mitarbeiter: | Dr. A. Rammo |

*To my beloved mother*

*&*

*To my respectable Professor Dr. W. F. Maier*

# Acknowledgement

First of all, I would like to express my sincere and deepest gratitude to my Prof. Dr. W. F. Maier for giving me the opportunity to work in his department under his excellent supervision. His expert guidance, advice, support, open mind, encouragements, and suggestions throughout the whole thesis have been crucial for the completion of the work described in thesis.

Secondly, I thank Prof. Dr. J. Jauch for his agreement to review this dissertation.

I would like to thank Prof. Dr. K. Stöwe for his advice during the project as well as for his assistance with the XRD measurements.

I also thank Mr. R. Richter for his perceptive comments and his ongoing efforts to help me in the high-throughput reactor development. In addition, I thank Mrs. H. Höltzen for her helpful feedback and for enriching my understanding of analytic method, and Mr. C. Thome for his technical support concerning the development of the required software.

I gratefully acknowledge financial support to this project from the Deutscher Akademischer Austauschdienst (DAAD).

In addition, special thanks go to Dr. Bauke Albada for putting a lot of effort and time into reading and correcting the manuscript—Thanks you so much!

I thank all my colleagues, especially, William, Nicola, and Katrina, for their support and helpful suggestions. I would like to extend my undying gratitude to my mother, Lee younghae, for her love and support. Also, I wish to thank my father, Su seongdo, who I would give anything to have seen me finish this project.

There have been a number of people whose names are not mentioned, but without whom this thesis could not have been completed. I would like to express my deepest gratitude to all of them.

# Abstract

The main focus of this thesis lies in the development of a high-throughput method for the discovery of catalysts for selective oxidation of propene. For this, a new 10-fold parallel reactor was constructed, validated, and tested for selective oxidation of propene to acrolein or propene oxide. Catalysts for these conversions were prepared by combinatorial chemistry approaches and subsequently screened in high-throughput techniques. Following a sol-gel procedure approximately 2200 catalysts have been prepared, and they were tested with the help of a stage robot reactor as primary screening and a 10-fold parallel reactor as secondary screening. Using the stage robot reactor, several catalysts consisting of Cu-containing mixed oxides have been discovered that were active for propene-oxide production, but they could not be confirmed by conventional tests. In the case of acrolein-production, a $Pd_{10}Ga_{45}Cu_{45}$ catalyst has been found with the best activity. Among Mo-based catalysts, $Mo_{94}Ru_4Te_2$ and $Mo_{88}Sn_8Te_4$ showed very high propene conversion to acrolein with yield of 25% at 375 °C and yield of 28% at 400 °C, respectively.

# Zusammenfassung

Der Schwerpunkt dieser Arbeit liegt in der Entwicklung einer Hochdurchsatz-Methode für die Entdeckung selektiver Propen-Oxidationskatalysatoren. Dafür wurde ein neuer 10-fach-Parallelreaktor entwickelt, validiert und getestet für selektive Oxidation von Propen zu Acrolein oder Propenoxid, indem kombinatorische chemische Vorgehensweisen zusammen mit Hochdurchsatz-Screening-Techniken genutzt wurden. Einem Sol-Gel-Verfahren folgend, wurden etwa 2200 Katalysatoren mit Hilfe eines Stage-Robot-Reaktors als primäres Screening und eines 10-fach-Parallelreaktors als sekundäres Screening vorbereitet und getestet. Durch einen Stage-Robot-Reaktor wurde entdeckt, dass einige Katalysatoren, bestehend aus Cu-fassenden vermischten Oxiden, aktiv Propen-Oxide produzieren, jedoch wurde es nicht durch herkömmliche Tests bestätigt. Bezüglich Acrolein-Produktion wurde ein $Pd_{10}Ga_{45}Cu_{45}$-Katalysator aufgrund seiner Aktivität als bester befunden. Unter den Mo-basierten Katalysatoren zeigten $Mo_{94}Ru_4Te_2$ und $Mo_{88}Sn_8Te_4$ sehr hohe Propen-Konversion in Bezug auf Acrolein mit einer Ausbeute von 25% bei 375°C beziehungsweise 28% bei 400°C.

# Contents

# Ⅰ. Introduction

Nowadays, developments in computer-technology related to automation and data mining has opened the door to high-throughput experimentation in both industry and academy. Reducing the scale of experimentation has many advantages in terms of cost and safety. Hence there is no need in catalyst testing on a larger scale than necessary. However, high-throughput testing of catalysts has to provide meaningful and reliable data.

Our group has developed several high-throughput methods using spectroscopic methods and a stage robot reactor for the discovery of catalysts. Although methods are successful in primary screening, their application is limited when applied to selective reaction like complex partial oxidation reactions. Therefore, a new 10-fold parallel reactor that is suitable as a second screening method and which includes a Micro-GC for analysis has been developed. The developed reactor has been validated for feasibility and reliability by analyzing the test-results at each channel.

In order to study the performance of the new 10-fold parallel reactor, selective oxidation of propene has been chosen as test-reaction. The results show that it is possible to optimize catalyst composition and oxidation-protocol via secondary screening after hits obtained in the primary screening.

This thesis is outlined as follows. At the beginning of chapter 1, combinatorial chemistry including synthesis, information technology and testing is briefly reviewed. Chapter 2 will touch on selective oxidation catalysts.

In the ‘Result and Discussion’ part, chapter 3 will show how the new high-throughput reactor based has been developed. Subsequently, the experimental results of catalyst-discovery for the oxidation of propene to propene oxide in chapter 4, propene to acrolein in chapter 5, and propene to acrolein with molybdenum in chapter 6 will be reported.

Lastly, the experimental setup and the catalyst preparation method based on sol-gel will be described in detail in chapter 7.

# 1 Combinatorial chemistry

The application of catalyst technology in the chemical industry is essential for maintaining our current level of development. In fact, more than over 90% of all chemical processes utilize catalysts and 60% of chemical productions of over 7000 compounds worth over $3 trillion per annum are produced using catalysis. At the moment, about 100 catalyst manufacturing companies exist globally[1]. It is clear that catalytic technologies have a vital role in the economic development of the chemical industry in the 21$^{th}$ century. Controlling selectivity and conversion of new catalytic processes can enhance the chemical productivity by reducing production costs and saving resources. This contributes to the world Gross National Product (GNP) by driving environment friendly and energy-efficient technologies, which later on can provide new challenges for catalysis research[2, 3].

In spite of this importance, finding or developing new catalysts is a difficult procedure since it relies on a number of scientific disciplines covering at least chemistry, physics, and mechanics.

Therefore, it is expected that combinatorial methods can be very useful for the discovery of new catalysts in a reliable and efficient way since many different aspects of catalyst-design can be screened simultaneously in a parallel manner. For example, researchers in the pharmaceutical industry have reduced both time and cost for producing effective and competitive new drugs. Combinatorial chemistry is regarded as one of the major technologies developed[4], and it has become an integral part of drug discovery in intelligent and systematic searches of large-parameter spaces based on the screening of diverse chemical libraries[5, 6]. Although the concept of combinatorial chemistry originated from *combinatorics* in drug discovery, these days combinatorial analysis is widely applied to life sciences or engineering such as semiconductors, superconductors, catalyst, polymers, materials, fuel cell, coating and organic dyes[7-12].

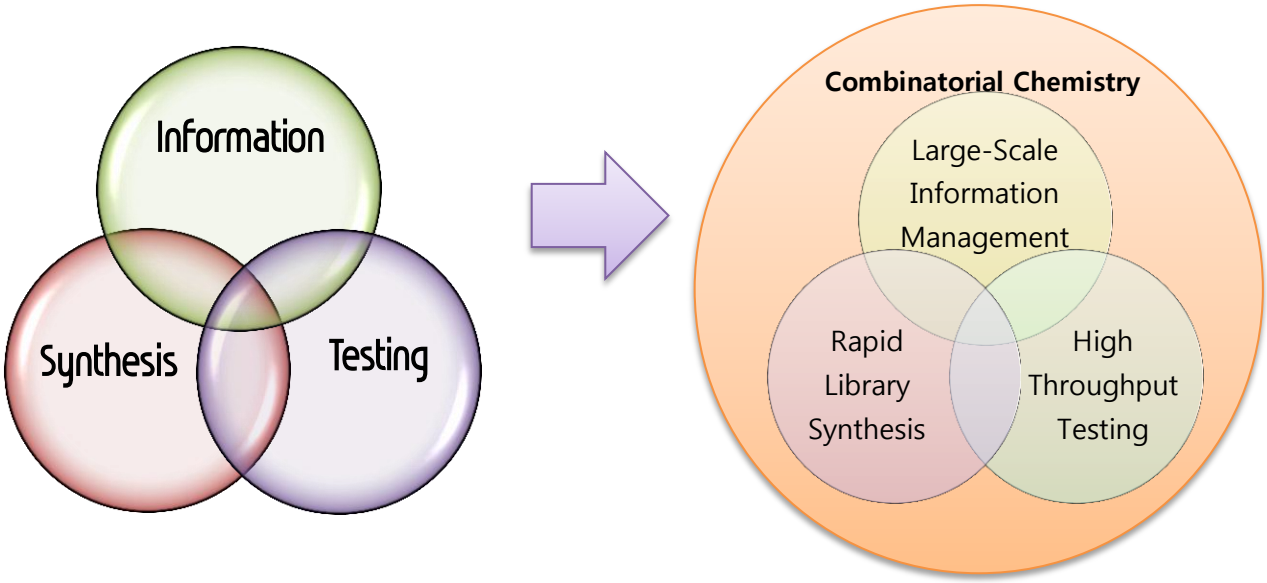


Figure 1.1 Key areas of combinatorial chemistry [1]

Combinatorial chemistry is an innovative methodology to find activity or selectivity among large diversities of libraries, which are synthesized, analyzed, and tested as shown in Figure 1.1 left. Apart from synthesis and testing, the development and use of a sophisticated high-capacity information-management system are essential for this procedure because of the vast amount of data generated. Eventually, successful implementation of combinatorial approaches requires all components, such as rapid library synthesis, large-scale information management and high-throughput testing. These components must function smoothly so that bottlenecks will not control the speed of an entire process[1].

## *1.1 Synthesis*

Since the synthesis of new materials is often the rate-limiting step, speeding up this process can increase the chance of discovering totally new and unexpected catalytic materials compared to the classical methods. Combinatorial approaches in this regard include several manners of the substance preparation and systematic synthesis.

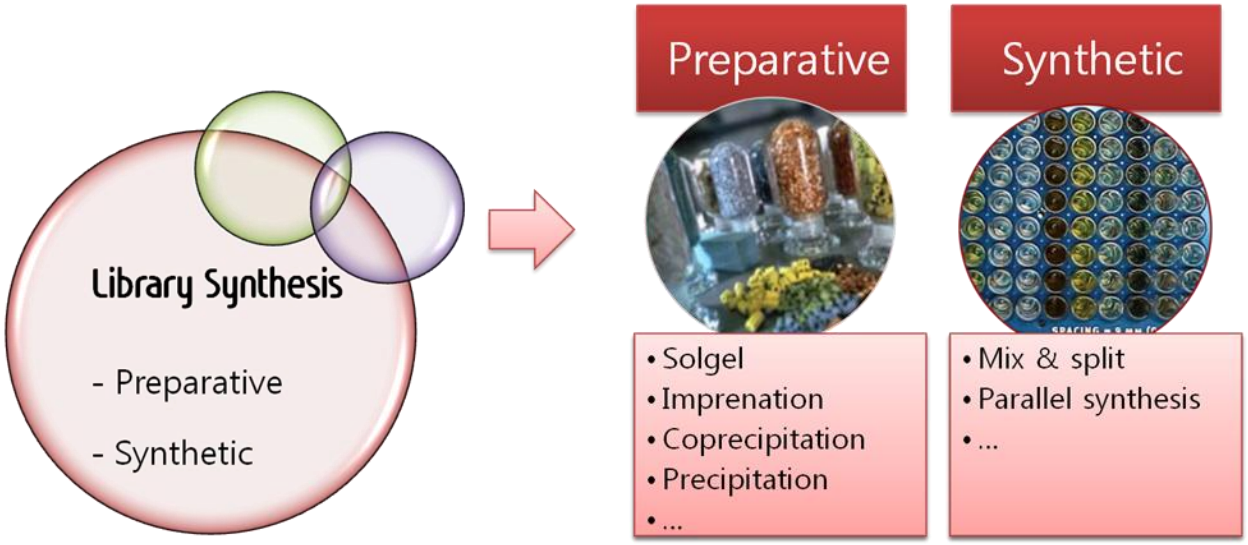


Figure 1.2 Information of library synthesis[13]

For catalyst synthesis, impregnation, multiple co-precipitation, evaporation, extrusion, spray-drying, ionic exchanges, sol–gel synthesis and hydrothermal synthesis have been applied to combinatorial chemistry[14]. However, in this thesis, the focus will be on sol-gel synthesis for catalytic preparation.

### *1.1.1 Preparation of the sol-gel*

Sol-gel synthesis is a well-known bottom-up method to produce nanoparticles[15, 16] in various fields such as optical materials, protection films, porous films, thin films, coating for fiber optics, carbon nanotubes, window insulator, polymers, micro-capsulation, and biomaterial[17-21]. M. Ebelmen in France reported the first silica gels in 1845[22, 23] and Faraday synthesized the oldest sols prepared in a laboratory[24]. The sol-gel process has advantages such as high purity, good homogeneity of raw material, low processing temperature, good shape ability, and easy control of new composition. In contrast, high cost of raw materials, health hazards of organic solution, cracking during the drying phase, long processing time and sensitivity to atmosphere conditions are the main disadvantages[25].

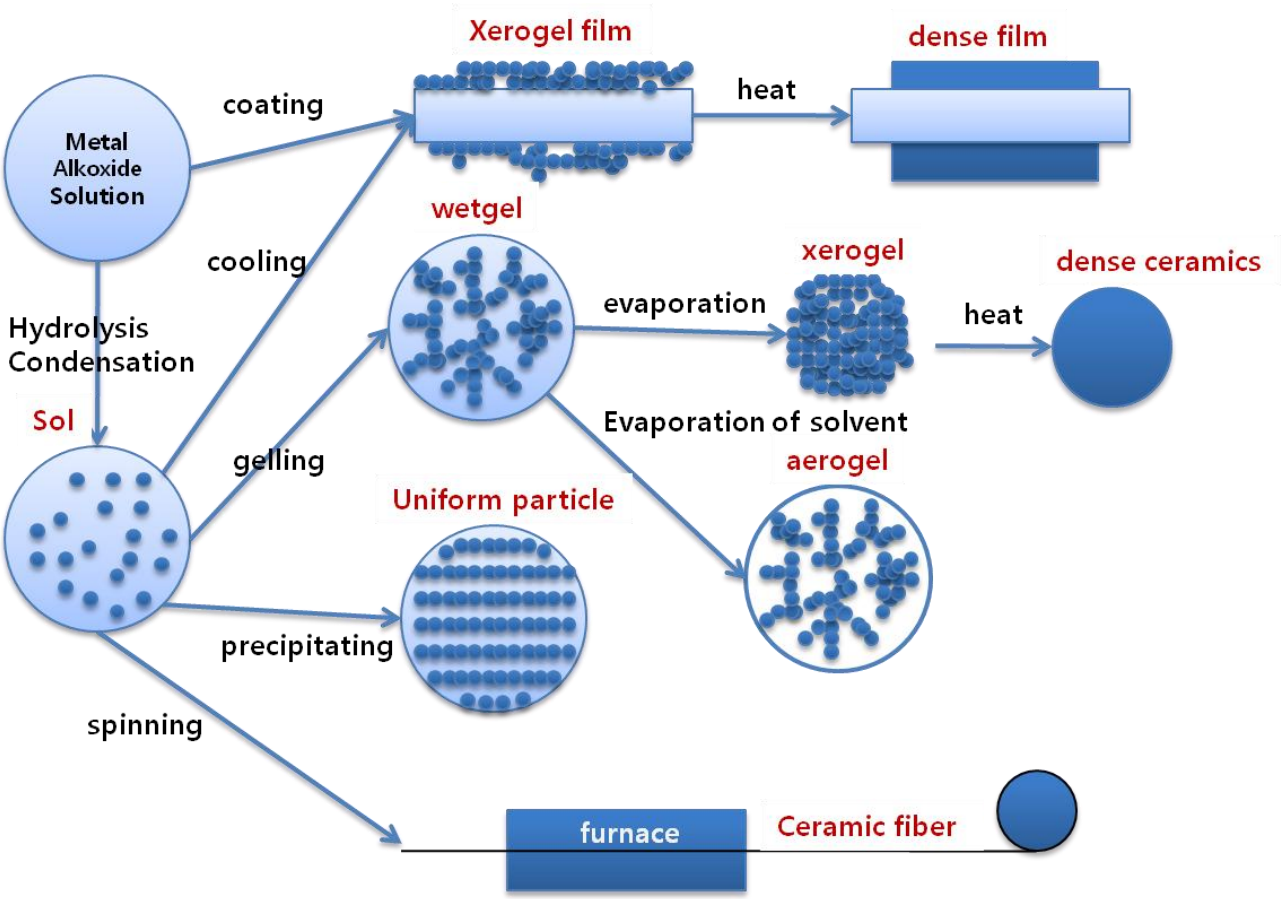


Figure 1.3 Detail information of sol-gel process with steps[26]

As is shown in Figure 1.3, depending on the conditions used in each, the sol phase can be converted into dense films, dense ceramics, aerogels, uniform particles and ceramic fibers. While the sol state represents a stable state in which colloid particles in the liquid phase are distributed with mobility for a long period of time, the gel state results in solidification through hydrolysis and condensation, ultimately resulting in the loss of mobility. Metal alkoxides like $LiOCH_3$ and $NaOCH_3$, and silicium- or germanium-based sol-gel precursors like $Si(OC_2H_5)_4$ and $Ge(OC_2H_5)_4$, are well-known starting materials for sol-gel synthesis because of their high solubility in water.

Sol-gel processes of amorphous or crystalline materials are based on low-temperature hydrolysis and condensation of hydrolysable precursors as in the following figures.

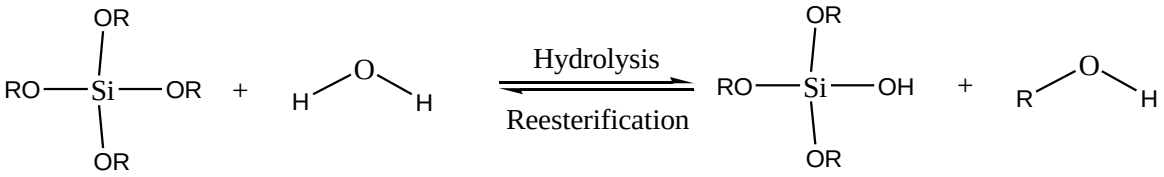


Figure 1.4 Hydrolysis on sol-gel process

The hydrolysis reaction replaces alkoxide groups (OR) with hydroxyl groups (OH) as depicted in the above reaction scheme.

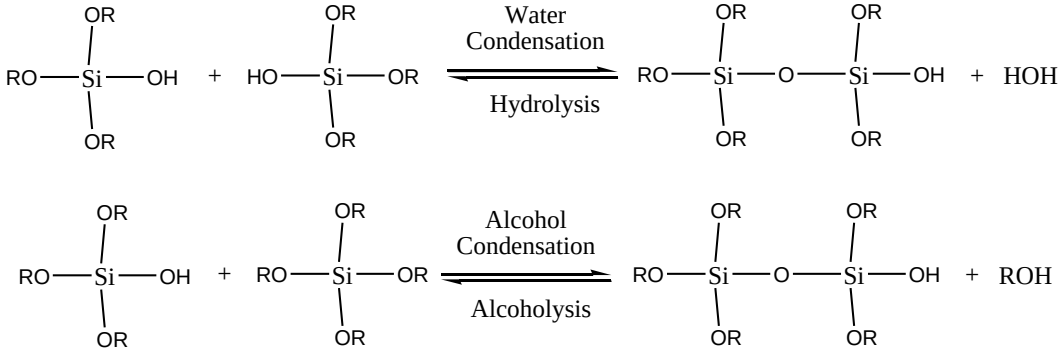


Figure 1.5 Condensations on sol-gel process

In the condensation reactions (water condensation or alcohol condensation), the silanol groups (Si-OR) produce siloxane bonds (Si-O-Si), ultimately resulting in a process of polymerization that leads to larger silicon-containing molecules[27]. Sol-gel synthesis can be classified as 'acidic' (pH 1.5-6), 'basic' (pH 8-11), or 'neutral' (pH 7), depending on the pH value of the solution in which the reaction is performed. Although hydrolysis or condensation can occur without adding catalyst, acid or basic catalyst can accelerate the hydrolysis or condensation reaction. Hydrochloric acid (HCl) and ammonia ($NH_3$) are generally used in acid- and base-catalyzed methods, respectively. Apart from these, acetic acid, KOH, amines, KF, and HF can be used as a catalyst[28].

Figure 1.6 and Figure 1.7 describe the synthesis of amorphous porous silica prepared by either the acid- or base-catalyzed hydrolysis of tetraethoxysilane (TEOS)[29], a starting material that is often used in the preparation of silica aerogels[30].

- Acid-Catalyzed Mechanism

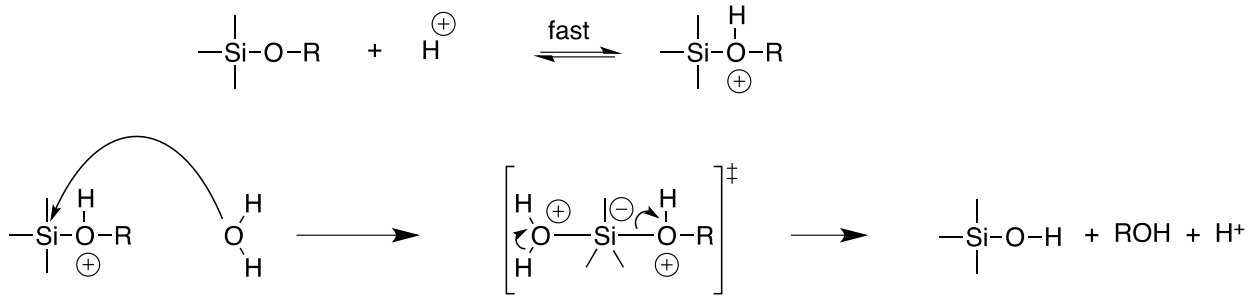


Figure 1.6 Acid-catalyzed hydrolysis

In the acid-catalyzed process, the oxygen atom of the silylether is rapidly protonated. As a result, 1) electron density is withdrawn from the silicon atom making it more susceptible to attack from water, and 2) the R-O fraction of the molecule is already turned into a good leaving-group.

- Base-Catalyzed Mechanism

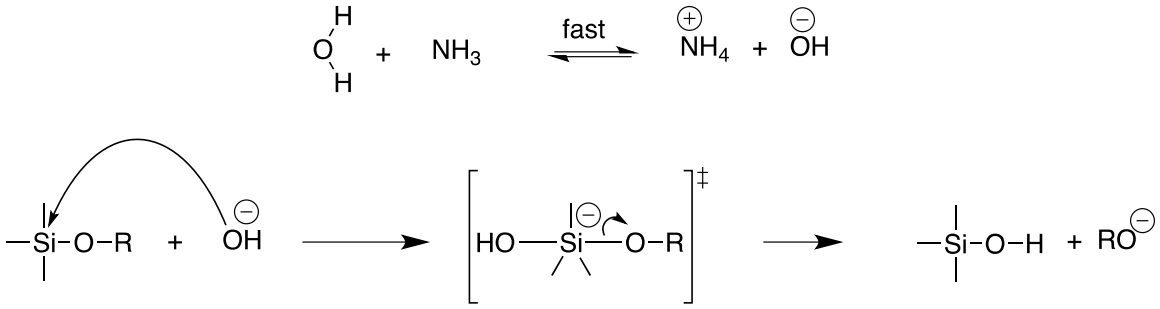


Figure 1.7 Base-catalyzed hydrolysis

In contrast, the base catalyzed sol-gel formation is caused by a hydroxylion. Because the hydroxide-ion is nucleophilic, it can attack the electropositive silicon atom[31] as shown in Figure 1.7.

The relative rate of hydrolysis and condensation in the sol-gel process is dependent on the pH in the solution. Under acidic conditions, the rate of hydrolysis is faster than condensation, resulting in a poorly branched gel. On the other hand, under alkaline conditions the hydrolysis rate is slow and the dissociation of water is rapid, resulting in a highly branched gel[32]. Although many factors affect the structure of the sol-gel network, the difference of gelation between acid- and base-catalyzed conditions is dominant and can be visualized as in Figure 1.8. The former yields linear or randomly branched polymers, which entangle and form additional branches, whereas the latter yields more highly branched discrete clusters.

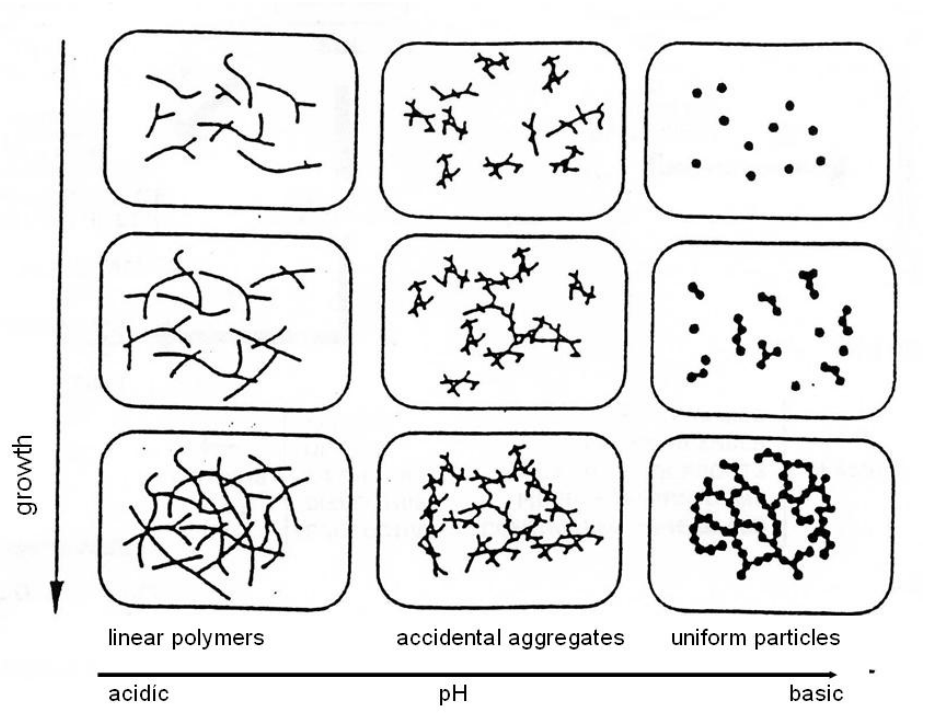


Figure 1.8 Effect of pH on sol-gel network formation[33]

### *1.1.2 Synthetic methods in combinatorial chemistry*

Similar to the synthesis of combinatorial libraries, there are two main methods by which sol-gels can be prepared: a split & pool and parallel synthesis.

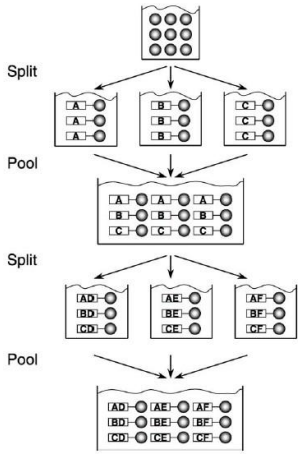


| | A | B | C | D | E |
|---|---|---|---|---|---|
| A | AA | BA | CA | DA | EA |
| B | AB | BB | CB | DB | EB |
| C | AC | BC* | CC | DC | EC |
| D | AD | BD | CD | DD | ED |
| E | AE | BE | CE | DE | EE |

Figure 1.9 Basic scheme of the Split & Pool-principle[34] versus that of parallel synthesis[35]

Houghton published a "tag-bag method" for the rapid synthesis of multiple peptides in 1985, which is nowadays referred to as the split & pool methodology. In this method, each bag contains polymeric resin "beads" for separation and isolation, wherein the mean bead diameter exceeds the mean pore diameter of the polymeric membrane of the bag. After repeating split and pool steps for several times, where during each step a different monomer is coupled, a highly diverse library is produced covering a wide range of samples. Immobilization of the discrete members of this library on solid-supports like resin-beads allows the efficient testing of libraries[34, 36]. Other commonly used synonyms in the field of combinatorial chemistry are "split-mix", "split-combine", "one bead – one compound" and "selectide-process"[37]. Importantly, the identity of the library member has to be identified after the screening by either a direct determination of the structure of the member or by and indirect method in which tags, that were introduced during the synthesis, could be deciphered after screening of the library.

Alternatively, parallel synthesis allows different chemical compositions to be prepared in parallel, using a number of reaction vessels and a robot programmed to add the appropriate reagents to each other. The library construction speed of parallel synthesis is slower than with the split-mix synthesis, but it is easy to trace the chemical reaction and to identify the chemical structure of the active compound. Therefore, it has broadly been used in inorganic and organometallic chemistry[38, 39], polymer synthesis[40], medicinal chemistry[41], drug discovery[42], catalysis synthesis[43], material discovery[12], solid phase extraction[44] and organic synthesis[45]. Multiple parallel procedures in combinatorial technology have been developed based on this parallel synthesis[35].

## *1.2 Information technology*

From the use of systematically acquired data and data-mining technologies, combinatorial methods can help scientists to discover trends and patterns of structure—activity relations from large databases for the development of catalysts. Finding a global maximum instead of a local maximum in the activity-profile of a catalyst by a mathematical solving-system is a major challenge in this regard. To improve initial hits and to find ways for catalyst discovery, rational methods have been applied in the design of experiments as plotted in the following Figure 1.10.

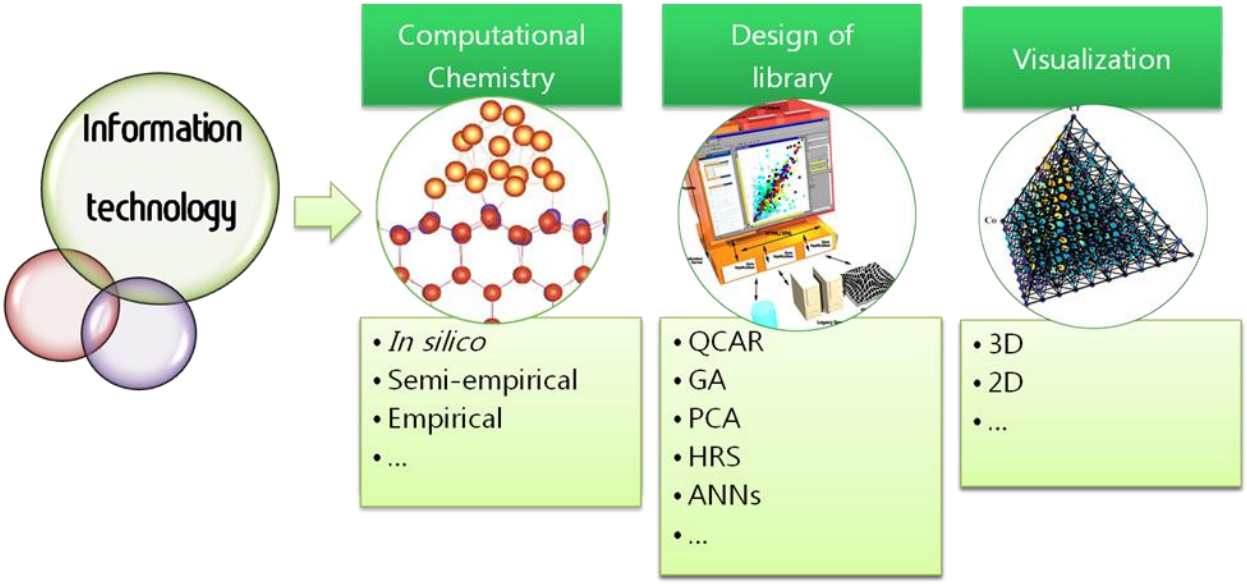


Figure 1.10 Basic scheme of information technology system

### *1.2.1 Computational Chemistry*

Over the last decades, significant progress has been made in computational strategies for information management. For example, quantum-chemical approach, Monte Carlo (MC) and density function theory (DFT) have been developed as so-called *in silico* methods.

Mechanisms of methanol decomposition on platinum[46], reaction rates for an elementary process on the surface of solid catalyst in different zeolite framework structures[47], and Brønsted acidity of active sites on the microscopic surface of silica-alumina and silica magnesia[48] are simulated by quantum-chemical approaches. Density Function Theory (DFT) calculations are applied to gain an understanding in the temperature and/or pressure dependency of the interaction between oxygen and silver in a known oxidation catalyst[49], and it helps to simulate various fields such as catalytic reaction, reactivity, mechanisms, barriers and kinetics[50-54]. A Monte Carlo (MC) with natural parallelism method has been implemented to save the power of computing resources[55].

Recently, Miyamoto *et al.* have introduced the term of "Combinatorial Computational Chemistry" and implemented it with the high-throughput screening of catalysts and materials. The adsorption energies of NO and water on various ion-exchanged ZSM-5 for design of deNox catalyst[56] was investigated, and the most stable adsorption state of NO on Ir model cluster was demonstrated in the design of precious metal catalysts for deNOx[57]. An active catalyst for methanol synthesis is also

implemented, and the result of calculation showed that $Cu^{+}$-cation is the active center in the industrial $Cu/ZnO/Al_2O_3$ catalyst[58]. This simulation of a theoretical approach is based on quantum chemical and molecular dynamics methods[59] and shows the beneficial use of computers in catalyst discovery.

Volcano shaped plots of catalyst activities against catalyst composition is a useful empirical method in catalysis as it relates the activity to the strength of adsorption of intermediates at the surface of the active material[60]. These relationships within catalysts have been applied to different experimental conditions ranging from atmospheric to high pressure, various temperature of reaction[61], and transitions of metal sulfide catalyst[62]. Also, electro catalytic materials for hydrogen evolution on 256 pure metals and surface alloys have been studied and found to fit the volcano plot[63]. Although this empirical approach is usually reliable, it is very time-consuming and costly to obtain reliable data.

Therefore, semi-empirical methods that use parameters derived from experimental data can also decrease computation time. Gordeeva *et al.* have introduced "An Original Semi-empirical Approach to Computer-Assisted synthesis" on the combination of pure combinatorial methods with a small knowledge base that included several empirical rules[64].

### *1.2.2 Design of the catalyst library*

Due to the data explosion in combinatory chemistry, managing the flow of data with design concepts and extracting useful information from this data using a data mining concept has become essential. However, the design of a library for discovering or optimizing new catalysts is not straightforward since a number of factors have to be considered, such as the type of elements, suitable precursors and concentrations, functional group variations, the order of the addition of reagents during the preparation, the solvents, modifiers and additives used during preparation, treatment and reaction times, pretreatment, activation procedures, and molecular descriptors related to structural features and so on. Therefore, the experiments need to be planned in an intelligent way before combinatorial experiments can be initiated. In addition, researchers should recognize problems and select the response variable for experimental design with factors, levels and range. This design of experiment (DoE) relies on complex statistical and optimization algorithm, allowing the effective determination of those parameters as well as parameter interactions, which have a main effect on the desired properties during experiment[65].

A very well-known evolutionary process[66], Genetic Algorism (GA), was introduced by Wöhler[67]. Although GA has been developed as a machine learning technique in drug industry[67], it has also been used for the generation of catalytic quality[68]. In addition, Optimal Design Of Experiments (ODOE), optimization strategy for the development of heterogeneous catalytic material has been studied using a stochastic strategy based on GA[69]. Recently, several approaches to the combination of GA and artificial neural networks (ANN) have been represented.

The main idea of artificial neural networks (ANN) is based on the concept of neurons in biology, which mimics signal-processing in a way like neurons process signals from the environment. It combines GA and ANN, which leads to acceleration of the process of catalyst-discovery. The approach, supplemented by an artificial neural network with the genetic algorithm software for establishing relationships between catalyst compositions, is illustrated for finding the catalyst for the oxidative dehydrogenation of propane[70] and optimizing olefin epoxidation catalysts[71] or methanol synthesis catalyst based on Cu oxide[72].

### *1.2.3 Visualization of the data obtained in HTE*

For showing the results of high-throughput experimentation efficiently and selecting the next generation of catalysts rationally, several visualization methods have been developed as illustrated in the following Figure 1.11.

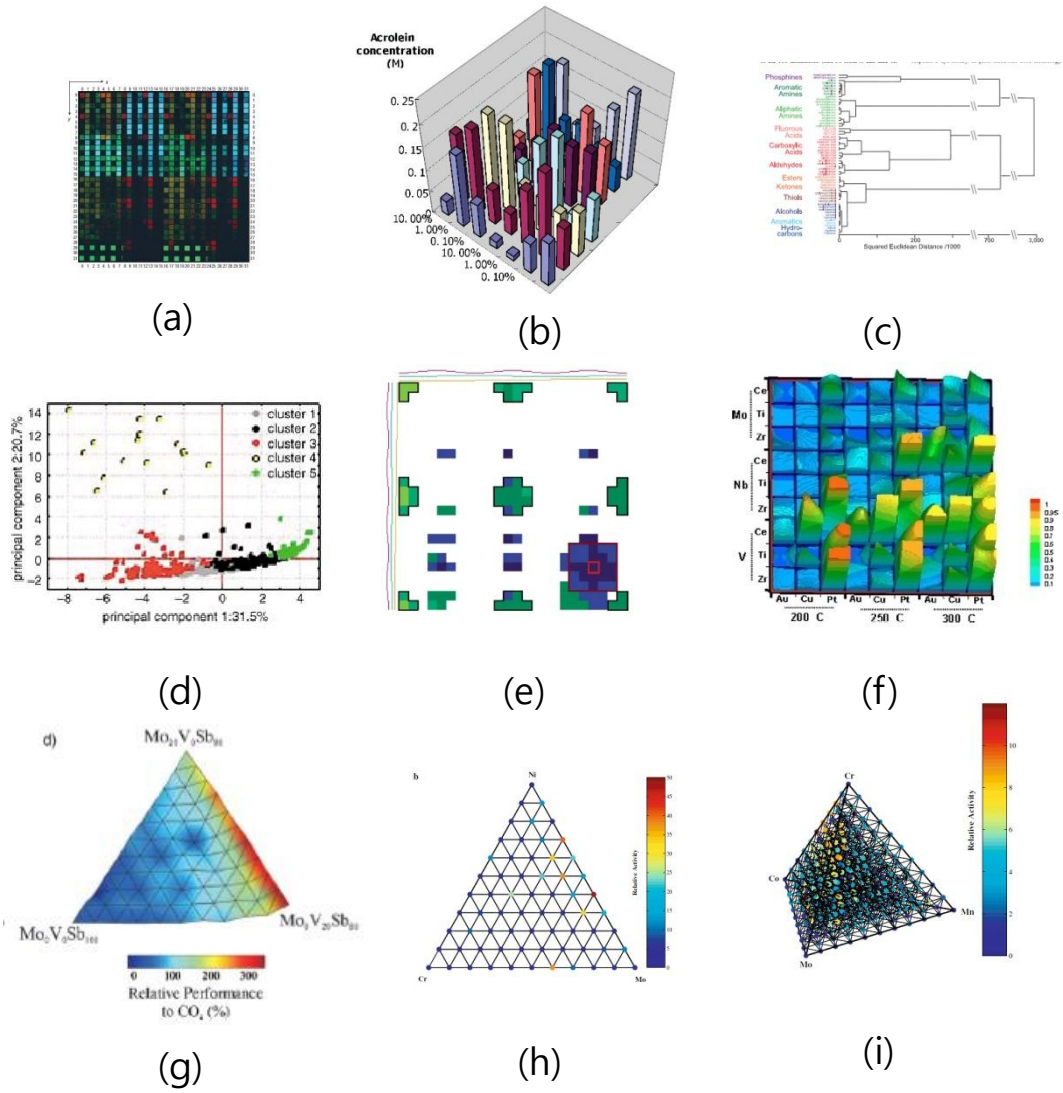


Figure 1.11 different visualization methods [10, 11, 73-77]

Various ways of visualization have been developed for the mapping of data into parameter space. For example, the photograph of a luminescent material's library (a) is shown in the two dimensions diagram[11], and acrolein concentrations (b) of samples collected from catalysts in a library is shown by excel program.[77] Holographic research strategy (HRS) (e) showed how to handle a bulk of data by implementing the visualization scheme[76]. Results of a k-means cluster analysis based on eight principal components (PC) in the projection (d) are presented[73]. Our research group has developed different methods, such as the ternary (g) composition of catalytic activity[78], the mapping of parameter spaces (h) for Quantitative composition activity relationships (QCARs) and quaternary composition spaces (i) with the help of Support vector machines (SVMs), multilevel B-splines, or

Kriging [74, 79]. Apart from these, the statistical commercial program Spotfire can help to visualize broad data sets using different visualization algorithms.

## *1.3 Testing for HTE that is needed in catalyst design*

Classical catalyst tests are miniaturized, automated, and coupled with combinatorial tools. Suitable techniques for the analysis of catalyst results include GC, MS and IR, and characterization tools like XRD and XPS.

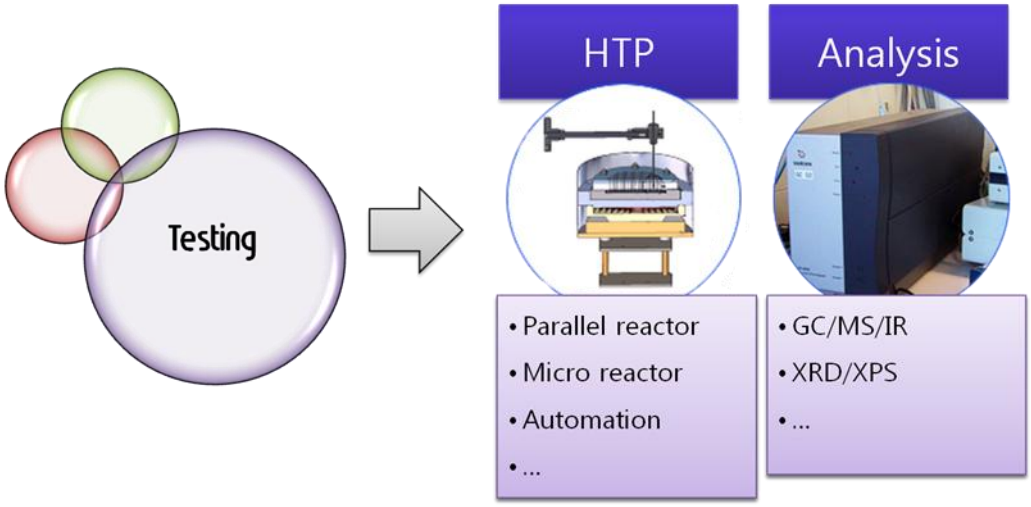


Figure 1.12 Basic scheme of testing

### *1.3.1 High-throughput experimentation (HTE)*

Since classical catalyst testing in laboratory reactors requires careful experimentation and data interpretation based on the concept of trial-and-error, the development tends to be slow. However, a method based on the high-throughput screening of catalysts increases the possibility to find an optimal catalytic system for a certain transformation.

Miniaturization or microfabrication should increase speed of catalyst screening and decrease the consumption of resources. As a result, these applications should help chemical experiments to gain a number of advantages concerning chemical synthesis, chemical kinetics studies, and process development[80]. Based on these concepts, several techniques were developed that decrease the reaction volume and use small amounts of catalysts. For example, 384 parallel reactions reactor[81], 625-parallel single-bead reactor[82], and 207-parallel reactor[83] were developed. These high-

throughput reactors can explore a broad experimental space and may include thousands of experiments as a primary screening, but they are not sufficient to assess the viability of hits as development candidates and to optimize catalyst formulation for activity and selectivity.

In academies, several reactors to improve the accuracy of results were developed based on the concept of packed-bed reactor for gas-solid mixed-phase reaction as follows. In 2006, a 64-channel reactor module has been used for discovering free nonpyrophoric catalytic materials for the water–gas shift reaction (WGSR)[68]. Kiener *et al.* in the Max-Planck-Institut in Mülheim developed a 49-channel parallel flow reactor for high pressure processes, applying it to development of methanol synthesis catalysts in 2002[84] and to the selective catalytic reduction of NO with $C_3H_6$[85] in 2007. A 64-channel parallel fixed-bed reactor was developed to investigate propylene oxidation catalysts[77] in 2007. Catalysts for hydrocyanic acid formation from methane and ammonia were studied by a high-throughput approach in a 48-parallel channel fixed-bed reactor[86] in 2008.

Although these studies described above were successful with newly developed high-throughput reactors, they are still insufficient to be substituted for conventional experimentations because reaction chambers were over-simplified and modified. Six-flow parallel reactor[87] and four parallel reactors[88] developed in academies can obtain almost the same result as conventional tests since these reactors are simply connecting several conventional reactors. Similar to these, such industrial reactors, a 16 parallel fixed bed reactor[89] by Symyx Technologies or parallel reactor by hte AG were developed.

In addition, another design approach of high-throughput reactors in a long-term perspective has been applied to three-phase reactions, which have largely been neglected because they are difficult to design, and their construction must consider that its application requires elevated temperatures and pressures. In this respect, the catalytic screening of three-phase reactions in 2001 is introduced to study the catalytic hydrogenation of crotonaldehyde over bimetallic samples[90]. However, it still remains to solve engineering problems such as stirrer design, the purging and introduction of pressurized gases, and the sealing of the entire system.

### *1.3.2 Analysis of conversion*

To date, a number of instruments are implemented based on combinatorial chemistry for analysis or characterization of experimental results as high-throughput methods. Especially gas chromatography

(GC) and liquid chromatography (LC) are techniques widely used for the separation and analysis of gas samples in the chemical industry and help the acquisition of thermodynamic and kinetic data.

In 2007 Oliver Trapp reviewed gas chromatographic techniques in high-throughput screening in catalysis[91, 92]. It covers both on- and off-line screening techniques of sequential or parallelized high-throughput multiplexing GC. Mass spectrometry (MS) was also implemented for a high-throughput flow injection analysis on the purity estimation of combinatorial chemistry synthesis[93] and especially micro reactor supported MS is applied for testing heterogeneous catalyst library[94].

Furthermore, combinations of multiple analytic techniques have been implemented for combinatorial chemistry, for example, gas chromatography-mass spectrometry (GC-MS) for microbial metabolism analysis[95] and several applications of liquid chromatography-mass spectrometry (LC-MS) related to interfacing, ionization and mass analysis, pharmaceutical sciences and biochemistry [96-98]. Also, a high-performance liquid chromatography tandem mass spectrometric assay (HPLC-MS) has been introduced for the sample-pooling approach in pharmacokinetic studies[99]. For the discovery of new polyolefin catalysts, using high-throughput screening techniques to support polymer characterization method has been described with FT-IR[13].

### *1.3.3 Expected tendency of future development in HTE*

Combinatorial chemistry and high-throughput experimentation save both time and cost for research and development, and are, therefore, rapidly entering industrial laboratories. Academia still remains hesitant and even opposes in part due to huge investments required at the beginning of a project[100].

It is well known that heterogeneous catalysts are complex materials of ill-defined structures and mechanism. Catalyst performance is dependent on elemental composition, formulation, morphology, size, size distribution and processing variables. Since the parameter space that is needed to optimize catalysts is quite large, traditional one-at-a-time approaches of synthesis and testing are slow and inefficient. High-throughput methods in heterogeneous catalysis allow the synthesis and testing of large numbers of materials and are increasingly applied for catalytic and other functional applications in academic and industrial laboratories[89]. Despite the initially severe skepticism as to the possibility of obtaining meaningful catalytic data by HTE approaches, the technology becomes more and more accepted. Nowadays most major chemical companies have closed strategic collaborations with service providers, such as Symyx technologies, Chemspeed, hte Akiengesellschaft, AMTEC, INM, SINTEF, the AG, or Avantium or have their own internal efforts.

In addition, the combinatorial chemistry combined with HTE is now a core technology in many major chemical or material companies such as BASF, Bosch, Degussa, UOP, P&G, GE, Bayer, DuPont, DOW and many others[101].

# 2 Selective oxidation of propene

Selective oxidation of small molecules to valuable products is an important reaction both in fundamental and industrial catalysis. It produces about 25% of the industrial organic chemicals and intermediates used for the production of fine chemicals and pharmaceuticals worldwide. The main products of this conversion are acrolein, acrylic acid, acrylonitrile, methacrylic acid, MTBE, maleic anhydride, phthalic anhydride, ethylene and propylene oxide, etc[102].

These reactions have the common feature that the desired products are often not the most favorable thermodynamically. If the strength of C-H bond of a particular hydrocarbon is stronger than the intermediate of its partial oxidized product, the reaction has a tendency to proceed to total oxidation of carbon-atoms to $CO_2$. Moreover, to activate reactants, reaction conditions need high temperatures that sometimes lead to complete disintegration of the partially oxidized products[103]. In other words, on the route to the thermodynamically favorable total oxidation of hydrocarbons to $CO_2$, catalysts are needed that accelerate certain desired chemical transformations, possibly by providing alternative reaction routes or mechanisms.

Depending on the reaction conditions, a number of partially oxidized products can be formed before carbon oxides are formed. Selective oxidations of hydrocarbon have a long history and are often carried out with oxygen, air, water and sometimes $CO_2$. Understanding factors that account for the activity and selectivity of these reactions is important in discovering new catalysts[104]. In 2002, Grasselli enumerated seven fundamental principles for a selective heterogeneous oxidation catalyst:

1. lattice oxygen;
2. metal oxygen bond strength;
3. host structure;
4. redox chemistry;
5. multifunctionality of active sites;
6. site isolation;
7. phase cooperation.

These principles, referred to as "seven pillars", are very helpful to understand structure, surface and dynamic properties of metal oxide catalysts on an atomic level[102].

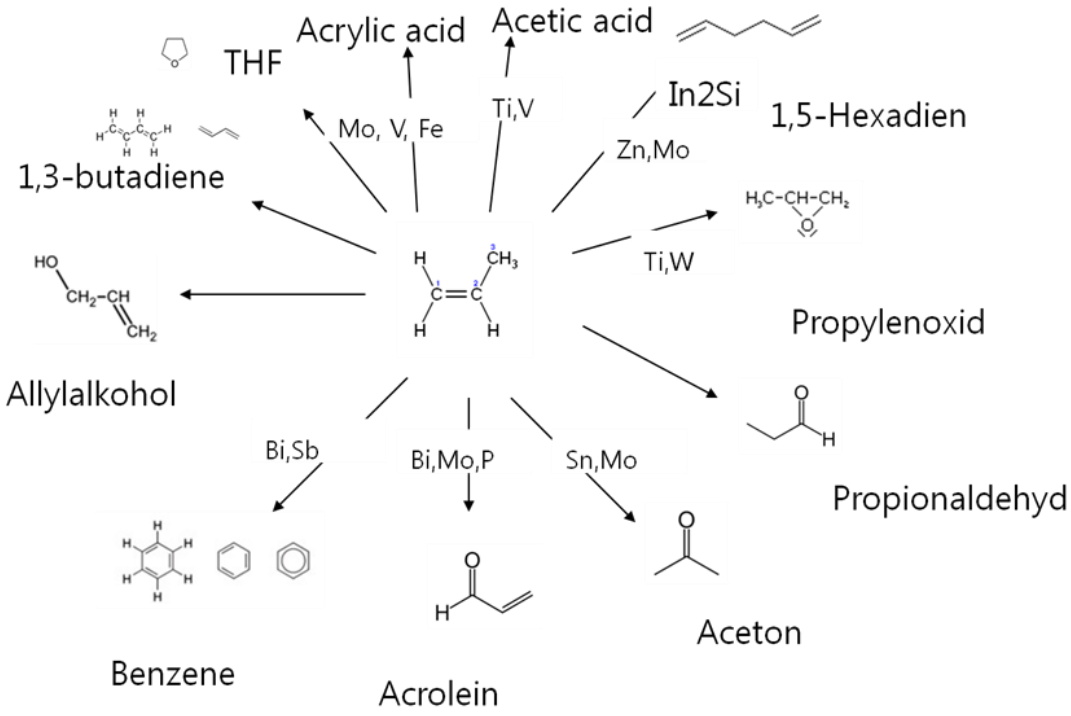


Figure 2.1 Summary of propene selective oxidation routes [105]

For specific cases of the oxidation of propene, Figure 2.1 gives a summary of the routes available (see also appendix). The mechanism and kinetics of propylene oxidation catalysts have been extensively studied, and several comprehensive reviews have appeared in the literature[106-108].

## *2.1 Selective oxidation of propene to propene oxide*

In the chemical industry, propene oxide is an important starting-material. In fact, over 10% of all propene produced is converted into propene oxide. To date, there are two well-known commercialized propene oxidation processes, such as the chlorohydrin process and the Halcon process[109]. The chlorohydrin process causes severe environmental pollution because it produces environmentally benign chlorinated organic byproducts as well as calcium chloride. Alternatively, in 2003, BASF and Dow Chemical started up new HPPO (Hydrogen-peroxide-propylen-oxide) process. However, this causes equimolar amounts of co-products requiring huge capital investment for the clean-up process.

Therefore, a direct production route from propene to propene oxide is highly desirable. Gold and copper have a proved reputation to be the most useful elements for this conversion. In order to reach commercial viability of gold-based catalyst like Au/Ti[109, 110], it needs to improve superior performance with respect to efficient $H_2$ consumption and resilience to catalyst deactivation. Cu based catalysts, such as Cu/silica catalyst Cu/silica[111] and NaCl-Modified VCe1−x Cux[112], are other alternatives for the epoxidation of propylene with direct molecular oxygen as the oxidant. However, these catalysts were still insufficient to apply in industry.

TS-1 (titanium silicalite-1) has been applied in the HPPO process. In the reaction unit, the catalytic epoxidation of propene is carried out using hydrogen peroxide ($H_2O_2$) and methanol at a temperature of 40-50 °C and 4 bar[113]. The disadvantageous use of costly hydrogen peroxide was solved by *in situ* production of this oxidizing reagent. For example, hydrogen peroxide synthesis from hydrogen and oxygen using anthrahydroquinones is implemented in combination with the oxidation of quinines using a bubble column and the palladium-catalyzed hydrogenation of quinines using a slurry, fixed-bed or monolith reactor[114].

## *2.2 Selective oxidation of propene to acrolein*

From the moment acrolein was produced commercially in 1938, the capacity of worldwide-refined acrolein increased to about 113,000 ton/yr in 1995. It has a variety of very valuable uses, for example, resins, glycerin, polyurethane, propylene glycol, acrylic acid, acrylonitrile, glycerol methionine and pharmaceuticals[115].

Acrolein is produced industrially through oxidation of propene or from glycerol and propane. Although efforts are underway to use propane as feedstock for the acrolein synthesis, it is still difficult to commercialize[116]. Similarly, commercializing acrolein production by dehydration of glycerol was abandoned because of the low efficiency of the process and the high cost of glycerol. Lately, this topic has attracted renewed interest in academic research due to an increase in the availability of glycerol as a result of enlarged biodiesel production [117-119]. As it increases the usefulness of biomass, a number of studies about acrolein production from glycerol have recently been reported [119-122]. Most studies are based on the fact that when glycerol is heated to 280 °C over solid acids, it decomposes into acrolein.

For the discovery of selective oxidation catalysts of propylene to acrolein, there have been several approaches with molybdate (MoBi[123, 124], MoSb[125], MoTe[126, 127]), vanadium($V_2O_5$[107],

$V_2O_5/Nb_2O_5$[128]) or iron (FeSb[129], $Fe_2(MoO_4)_3$ doped with Bi or Te[130]). A major milestone was achieved when SOHIO in 1959 introduced a bismuth molybdates catalyst with outstanding activity and selectivity on the selective oxidation reaction of hydrocarbons. The typical process conditions are a reaction temperature at 300–400 °C with pressures of 1.5–2.5 kPa and a feed-gas with 5 - 10 % propene, mixed with air and inert diluents. Subsequently, multicomponent metal-oxides containing bismuth, molybdenum, and tungsten have been used to enhance catalytic performance for the propene oxidation catalyst to acrolein[103]. The other effective catalyst of MoVNb(Te, Sb) [131] was discovered by the Mitsubishi Chemical Company. Academia and industries studied it with regard to the catalytic performance of single-phase[132], of support with Te-free or Te-containing[133], of K doping[134], and of Ph influence[135, 136]. The MoVSb Oxide catalyst was applied to several reactions such as partial oxidation of Isobutane [137], selective oxidation of propane to acrylic acid[138] and selective oxidation propane to acrolein[139].

Nowadays, modern catalysts for selective oxidation are composed of at least four transition metals in at least two complex oxide phases. For example, a complex multicomponent oxide catalyst based on Bi, Fe and Co molybdate is used for the partial oxidation of propylene to acrolein[140]. In fact, all commercial processes in operation utilize multicomponent metal oxide catalysts. In addition, acrolein produced using this catalyst is used to produce acrylic acid (AA) by selective oxidation, or acrylonitrile (AN) through ammoxidation, both of which are important for manufacture of plastics, polymers, fibers and synthetic rubbers.

The mechanism of acrolein production from propene can be expressed as follows. Industrial acrolein is produced by selective oxidation of propene without affecting the double bond by a suitable catalyst (1).

$$CH_3\text{-}CH{=}CH_2 + O_2 \leftrightarrow CH_2{=}CH\text{-}CH{=}O + H_2O \quad (1)$$

Side reactions that lead to the total oxidation of propene (2) and acrolein (3) are:

$$CH_3\text{-}CH{=}CH_2 + \tfrac{9}{2}O_2 \leftrightarrow 3CO_2 + 3H_2O \quad (2)$$

$$CH_2{=}CH\text{-}CH{=}O + \tfrac{7}{2}O_2 \leftrightarrow 3CO_2 + 2H_2O \quad (3)$$

Acrylic acid (4) is produced as a secondary product.

$$CH_2{=}CH\text{-}CH{=}O + \tfrac{1}{2}O_2 \leftrightarrow CH_2{=}CH\text{-}C(O)\text{-}OH \quad (4)$$

# Ⅱ. Result and discussion

## 3 Development of a high-throughput reactor

Over the last several years, high-throughput methods and combinatorial chemistry have been developed as experimental methods enabling both the synthesis of numerous samples and the examination of their properties in a short time. High-throughput does not necessarily mean that a large number of overly simplistic experiments have been performed. On the contrary, if reliable data needs to be generated it requires a thoughtful design of the experiments and needs to be based on a sophisticated concept and heavily relies on the handling of data produced by a high-speed reactor as cutting edge technology. In this chapter, the development of a new high-throughput reactor that can provide reliable data for discovering new catalysts will be described.

### *3.1 Motivation for the work described in this thesis*

The Maier group at Saarland University successfully applied an IR camera in several studies for the development of heterogeneous catalysts[141, 142]. However, this application is often restricted to total oxidation reactions because it cannot differentiate between catalysts that are responsible for intermediately oxidized products since it operates through the registration of the heat of reaction.

To solve this drawback, an open-well high-throughput reactor system, referred to Stage-Robot Reactor (SRR), has been developed by previous researchers. It assists in the identification of the various products in the reaction of complex partial oxidation by using analytical instruments such as GC and MS. Regardless of the benefit that the simultaneous analysis of diverse products can have, the different design that a reaction chamber of a SRR has in comparison to a fixed-bed reactor limits the generation of reliable data, and thus severely affects the optimization of certain catalysts and its later application in the scaling up of the process[143]. In this, the main problems are the open reactor and phenomenon of catalyst instability like activation/deactivation, which happens during the catalytic process.

Because of this reason, hits from a primary screening in the SRR should be ranked and evaluated further in a secondary screening using a more advanced reactor. This reactor allows a better which assessment of the application of hits as candidates and allows further optimization of the catalyst

formulation. In addition, new screening technology employed must closely mimic the various commercial processes and is at least as precise as conventional laboratory methods. In summary, the goal is to develop a more efficient and reliable high-throughput reactor that allows the entire system to operate under conventional conditions[144].

It is expected that the new reactor provides accurate data for the discovery of new catalyst that reach the global maximum in the activity-profile of the catalyst-composition and conversion of starting material into desired products instead of a local maximum.

For the development of the reactor, three concepts of miniaturization, automation and parallel processing are determined to be crucial:

1) Development of a highly accurate reactor that can be applied in the scale-up and optimization of chemical composition as secondary screening method.
2) Validation of the efficiency of the developed high-throughput reactor using different experimental conditions.
3) Application of the new high-throughput reactor in the actual catalyst discovery for selective propene oxidation system.

This study described in this thesis will treat the following issues:

A. Solving problems of the SRR for further testing to obtain larger quantities of data by:

- Developing, implementing and leading new high-throughput reactor as a key technology.
- Improvement of the reproducibility of catalysts discovered by new high-throughput reactor.
- Combining possibilities of the SRR as a primary screening method, and the newly developed high-throughput reactor as secondary screening method.

B. Formulate and deploy plans for discovering and optimizing the catalysts by:

- Development and application of combinatorial chemistry and high-throughput experimentation tools to investigate catalyst for the selective oxidation of propene.

- Confirmation of properties of the best catalysts by high-throughput experiments of a scale-up process through conventional gas-phase reaction tests.
- Characterization of new catalysts by the study of their properties at fundamental levels using various instruments

For this, a 10-fold parallel reactor consisting of 10 mini tube reactors will be developed and tested for the selective oxidation of propene by a fast-screening procedure of heterogeneously catalyzed gas-solid reactions. The objective of this study is not only to develop a high-throughput system, but also to validate the new reactor as a secondary screening method.

## *3.2 Reactor design issues that need to be considered*

Generally, various preliminary questions for the design of a commercial reactor should be answered before embarking on the detailed construction of general issues[145]:

- What are the concerns when it comes to has to temperature progression, i.e. constant, rising, falling, etc?
- Are additional instruments required?
- What should be the size of particles used for catalytic reaction?
- What type of reactor is best for development, for example, plug flow, mixed flow, CSTR, fluidized bed, 3 phase reactor, recycle reactor and multistate?

In the answering of these definable problems, heterogeneous catalysis, material science and reactor engineering are playing key roles[146].

In this study, the plug-flow reactor or fixed-bed reactor has been considered as the model of high-throughput reactor development. Because it is continuously operating with a stream of gas or concurrent stream of gas, it is a common reactor in industrial plants and is also the most widely used reactor in hydrocarbon processing. On the other hand, it is used in the academic laboratories for experiments that evaluate new catalysts to monitor the commercial production of catalysts and to assess the effect of change of feedstock or operating variables on processes.

Generally, both individual porous-catalyst particles and phenomenon in reactions are important for the concept of developing reactors. For example, the effects of unsteady-state heat and mass transfer, and the influence of inhomogeneities and stagnant regions or back-mixing in the reactor should be considered for reactor operation in process control as well as in development[147]. However, these questions were not considered initially since minimization of reaction chambers had been planned in advance in order to minimize the effect of their design on the outcome of the catalytic reaction, thus make it more relevant as model-reactor for a pilot plant or commercial reactor.

## *3.3 New developing concept*

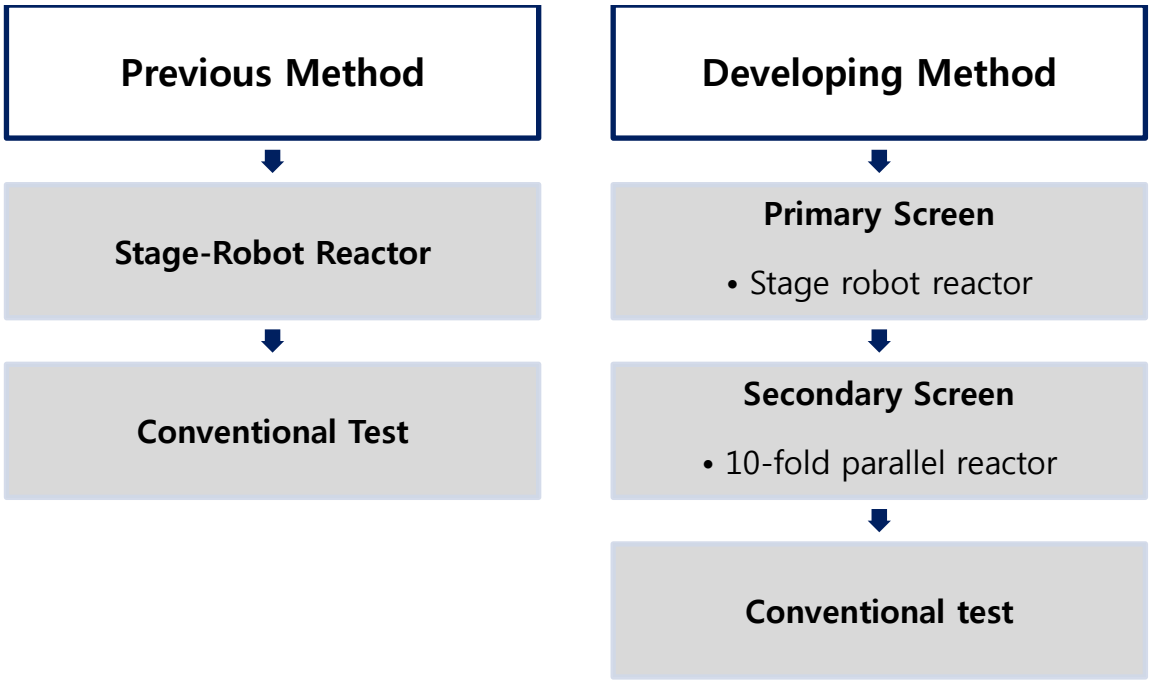


Figure 3.1 Previous method (left) vs. developing method (right)

Figure 3.1 outlines the concept of pervious methods and that of the new method developed for catalyst discovery. As discussed in the previous chapter, the stage robot reactor (SRR) developed by our group was confronted with the restriction of identifying various oxidized products in catalyst optimization and discovery of complex reactions. As is well known, research directed toward the discovery and optimization of new catalysts by means of conventional testing is an expensive, time-consuming process that includes high degrees of uncertainty in their reproducibility. Thus, to overcome such limitations of catalyst discovery and to extend the capabilities of our high-

throughput program with the stage robot reactor, we designed and implemented a fully integrated, high-throughput discovery and optimization infrastructure by developing a 10-fold parallel reactor as secondary screening method, as shown in the diagram of Figure 3.1[13].

Three screening systems were considered as follows:

1) A stage robot as a primary screening device: it can rapidly identify catalyst activity, and identify and refuse an inactive catalyst by observing the hit. At the same time, it allows a number of broad ranges of the catalyst's candidates and conditions to be evaluated.
2) A new secondary screening method is used to study catalyst performance, the relationship between catalyst structure and activity, and catalyzed process.
3) Final results can be validated in a conventional test.

As a consequence, it is expected that time and resources will be saved toward maximizing catalyst performance by checking only those catalyst candidates, which show the most promising performance. While conventional catalytic tests take more than one day using a manual operation system, the 10-fold parallel reactor can measure up to 10 catalysts under an automated work flow within one day.

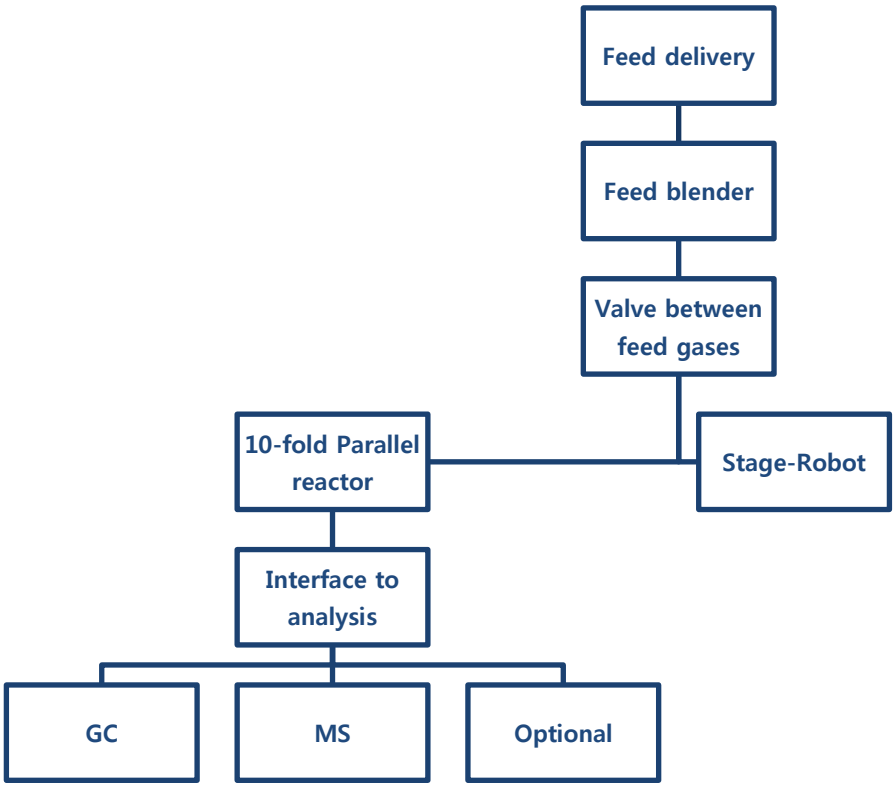


Figure 3.2 Schematic representation of an idealized generic structure for a catalyst test and analysis system

New generic structure for the stage robot reactor and the 10-fold parallel system involved the same feed system consisting of feed delivery, feed blender and valve between feed-gases. The mixed gas is split into two flows when performing either the 10-fold parallel reactor or the stage robot. On-line gas chromatography (GC), mass spectrometry (MS) and optional various gas sensors for analyzing catalyst performance could be implemented.

## *3.4 Schematic design of the reactor system*

### *3.4.1 Overall system design*

The 10-fold parallel reactor module for screening of heterogeneous catalysts enables catalyst testing under conditions that are equal to those of fixed-bed reactors. Especially, the rate by which experiments could be performed was significantly increased by testing 10 catalysts at the same using an automated system. In other words, processes can be carried out under identical reaction conditions as in a miniature glass tube reactor but were coupled with an online micro-gas chromatograph and a data-acquisition system.

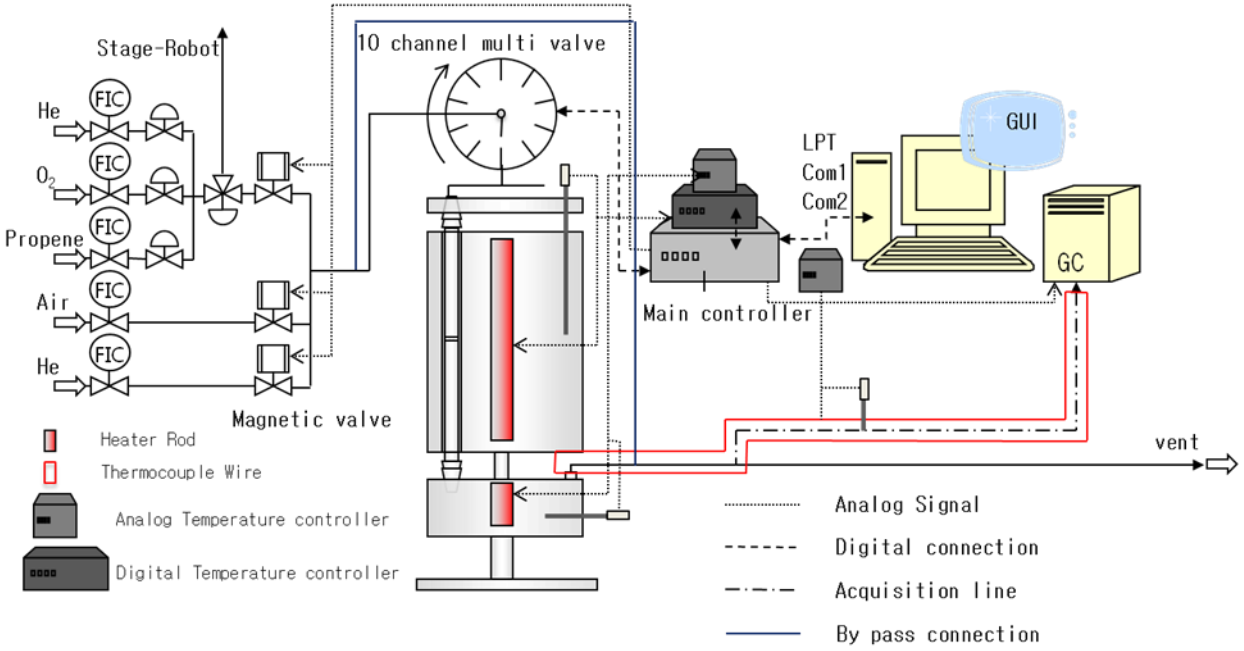


Figure 3.3 Outline of reactor system

Figure 3.3 shows a schematic outline of the new 10-fold parallel reactor system. A 10-channel multi valve (1 x 10, Valco Instrument) in the feed-gas inlet allows fast switching between the different channels. The main setup consists of two cylindrical modules called the central and splitting module. The main part of a central module is assigned to 11 channels using 10 fixed-bed reactors, which are concentrically arranged with regard to the axis of the module. To avoid condensation, polymerization or thermal decomposition of products, a temperature above 100 ºC is required throughout the entire system during the process. Therefore, the splitting module and the output piping including the product-gas-tube to the GC were installed with heater rod and thermocouple wire, respectively. For automation of the system, an electric circuit as a main interface was developed to communicate with each instrument through LPT, Com1 and Com2. In addition, a GUI interface mode was developed with the C++ programming language for controlling and monitoring the catalytic experiment. Subsequently, sequential analysis of the reaction products contained in the effluent gas was performed by Micro-GC.

### *3.4.2 10-fold parallel reactor design*

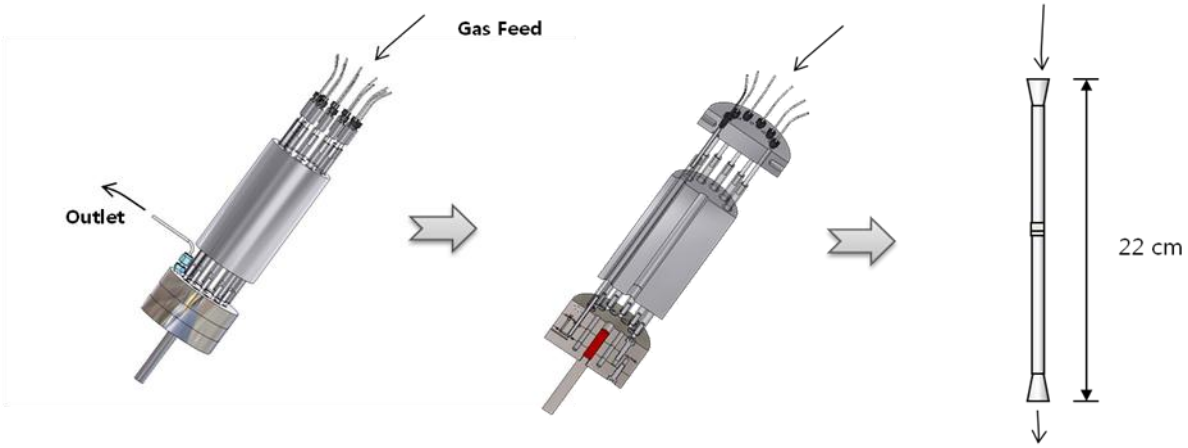


Figure 3.4 High-throughput testing equipment: (a) view on the 10-fold parallel reactor module consisting of two modules (b) a cross-sectional view of reactor (c) fixed-bed tube reactor used in this system

The 10-fold parallel reactor designed in this work contains a central module (height = 15 cm, diameter = 8 cm) with 11 channels (height = 15 cm, internal diameter = 11 mm) based on a miniature concept. It was made of an aluminum alloy that possesses good heat conduction. To ensure isothermal conditions in the reaction zone, in this system, these channels were equally

distributed under rotational symmetry. Heating was provided by an inner electrical heater rod (height = 13 cm, diameter = 1 cm). Axial temperature profiles are controlled by thermocouples placed in an empty tube reactor at the 11$^{th}$ channel, and it has been shown that the radial temperature deviation does not exceed 4 K. The reactor was tested to keep the entire system stable at a temperature up to a maximum of 400 °C with a flow rate up to 50 mL/min. The miniature glass tube reactor (height = 22 cm, inner diameter = 5 mm and outer diameter = 8 mm) containing grid filter (diameter = 5 mm, thickness = 3 mm, porosity 0.27) were implemented for catalytic test as shown (c) in Figure 3.5. Each tube reactor was filled with 100–300 mg of catalytic material of 100–300 μm. The rest of catalysts in the filter of the used tube reactor were cleaned by using the ultra-sonic equipment and by heating in a diluted $HNO_3$ acid solution.

## *3.5 Consecutive parallel reactor*

During the last decade, several parallel reactors have been developed (16 parallels Amtec Germany, 16 parallel Flowrence, hte). The possible system of flow stream can be divided into three concepts based on the position of the Multi-Position Valves (MVs) as shown in the following Figure 3.5.

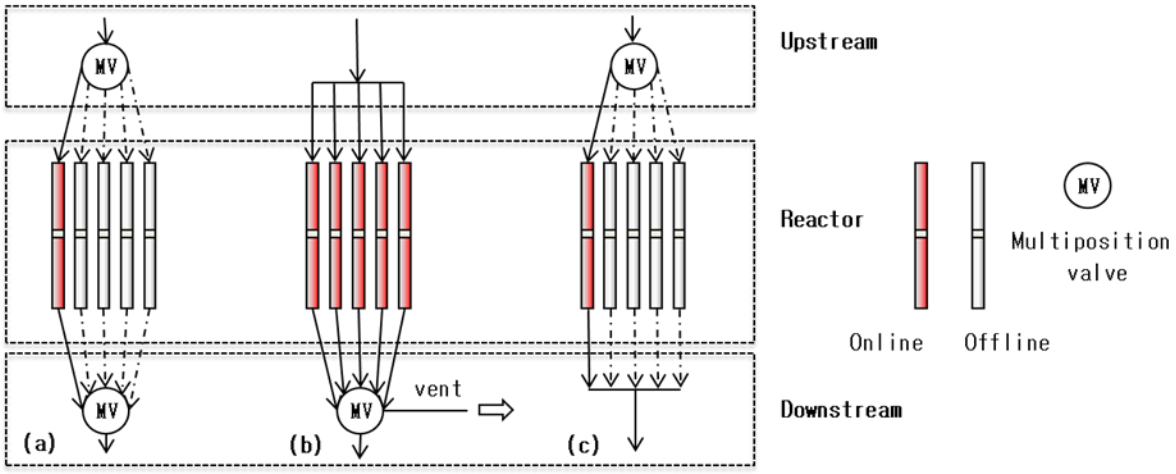


Figure 3.5 Schematic flow-sheet of (a) MV's at both sides (b) one downstream MV, and (c) one upstream MV

The high-throughput instrument requires a good user interface, be fast and relatively inexpensive. Obviously, using two multi-position valves (figure 3.5, example a) fails to meet the last criterion. Although implementing MVs both upstream and downstream probably produces the most accurate

results, the application of one MV installed downstream (b) is general sufficient for the development of parallel reactors.

However, the concept of installing one MV downstream leads to another problem:

while a specific channel is measured, all other channels remain under continuous flow. This creates two drawbacks. First, to observe the activation or deactivation of catalytic material accurately, the designed structure of the reactor should be tested, so that the total flow rate is equally distributed through all channels and have the same pressure drop. Furthermore, supplying a continuous flow to all channels simultaneously significantly increases expenses due to feed-gas consumption.

Installing MV either upstream or downstream of the catalyst bed is of importance to establish 'flow concept' in the parallel reactor. An upstream MV (c) causes a high risk that effluent gas analyzed can be contaminated by gases from the rest of the operating channel. Because of this, so far, the parallel reactor development has generally used to set up MV's positioned downstream (b). Disadvantages connected with the upstream positioned MV could be avoided using a splitting module. Here, it will be elucidated how this system works to neglect the contamination of effluent gas in each channel.

### *3.5.1 Design of splitting module*

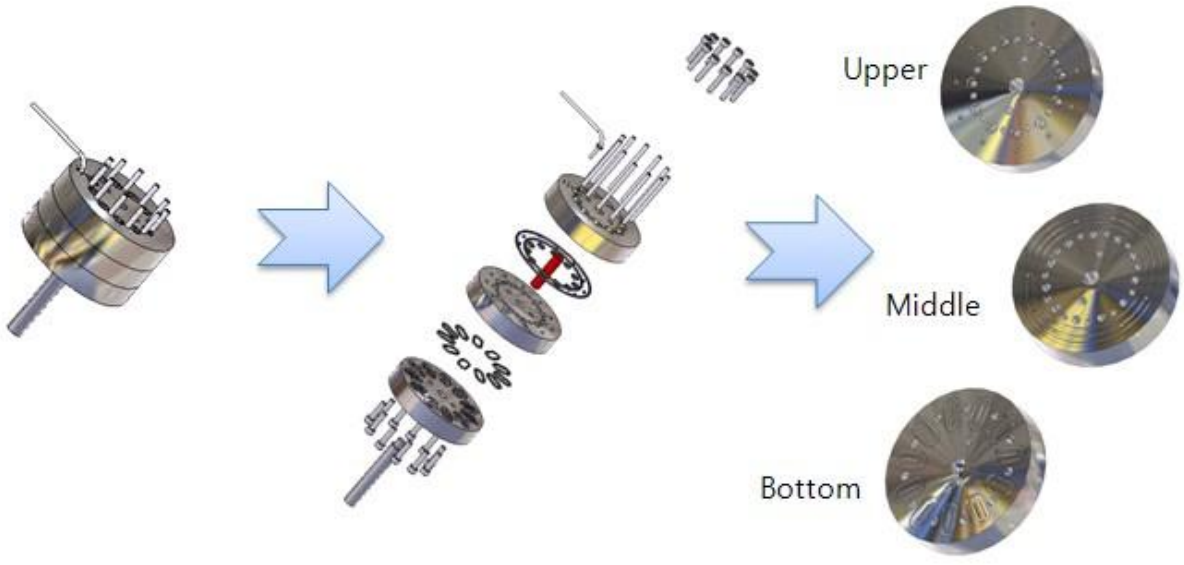


Figure 3.6 Effluent gas splitting module downstream

To solve the gas contamination problem in the case of installing the MV upstream, a gas splitting module was invented and designed by the mechanical engineer R. Richter as shown in Figure 3.6,

which has the function of minimizing or eliminating the influence of gas contamination between online and offline columns. It is comprised of three parts such as upper plate (height = 20 mm, diameter = 20 mm), middle plate (height = 18 mm, diameter = 20 mm) and bottom plate (height = 20 mm, diameter = 20 mm). In order to avoid corrosion, plates were made of stainless steel ($X_6CrNiMTi_{17-12-2}$). To avoid gas leakage they are enclosed in polished planes by tightening screws and sealing with 23 gaskets (2 sealing rings, 11 sealing O-rings, 11 sealing ellipses). The heating rod (height = 38.1 mm, diameter = 9.6 mm, 100W) in the center of the module allows to keep the temperature above 100 °C. The effluent gas from the online column is passed through a capillary line connected to the Micro-GC.

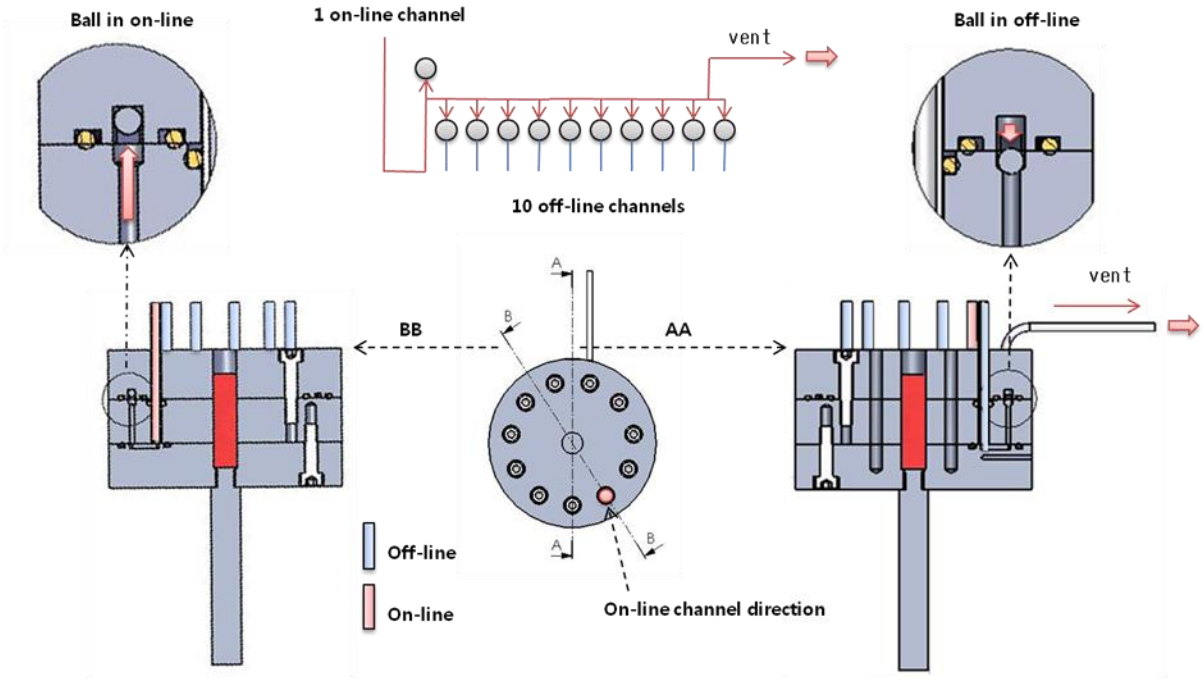


Figure 3.7 Function of module for splitting effluent gas

Our specific technique compared to other high-throughput reactors is the gas splitting module as shown in Figure 3.7. State-of-the-art technology for avoiding gas contamination between on-line and off-line results in the application of fine flow lines (width 2.5 mm) associated with the function of the stainless balls (diameter 3 mm).

Each ball accomplishes opening or shutting each channel by moving its position up and down by overcoming the force of gravity associated with the weight of the ball. The ball in the online channel

is raised by the convection force derived by the flow as shown in the top left of Figure 3.7. In contrast, when one channel is open for flow of flue-gas, the other 10 offline channels remain close by pushing the ball based on the gravity force itself and the convection force of feed-gas as shown in the top right of Figure 3.7.

Although contamination can occur through the narrow gap between the ball and channel based on diffusion effects, this influence may be small enough to be ignored. The extent of error in this regard will be shown in the following chapter on the validation of the reactor performance. The entire design of the splitting module can be seen in the appendix.

### *3.5.2 Comparison of two methods*

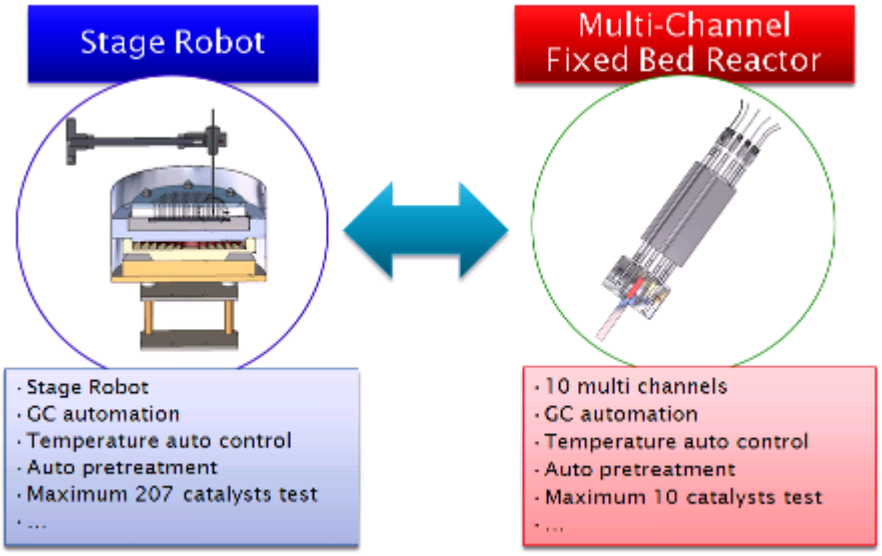


Figure 3.8 Stage robot reactor vs. 10-fold parallel reactor

The so-called ‘multichannel fixed bed reactor’ or ‘10-fold parallel reactor’ was developed for the secondary screening and hit validation. In this chapter the performance of this reactor will be compared with the stage robot reactor (SRR). Both high-throughput methods are used with the Micro-GC as analysis instruments and were automated with temperature control and the pretreatment of catalyst. Despite the fact that the new reactor can carry out tests with a maximum of 10 catalysts compared to 207 in the stage robot reactor, the accuracy is high, which makes it suitable for the optimization of catalysts or scale-enlargements. However, it is unclear which reactor is more suitable for high-throughput experimentation since each reactor has specific advantages and

drawbacks. Ideally, the combination of two high-throughput methods is the best choice for discovering new catalysts in a set of large variables.

To summarize, the stage robot reactor as a primary screening method has to meet the following challenges: tests should be simple, fast and scalable; large variety of catalysts can be tested under steady-state conditions and continuous flow; analysis has to provide a reliable estimate of conversion and selectivity of catalyst; the test results have to be reproducible; all tasks have to be automated under systematic workflow[81].

It is also necessary to confirm promising results in secondary screening methods, which is used to scale up a certain conversion to production scale or screen conditions under conventional test[100]. Therefore, the 10-fold parallel reactor developed by in-house workshop is suitable to take this role as the instrument in secondary screening process.

Evidently, there is a difference between two high-throughput reactors and each reactor has specific criteria to extrapolate catalyst properties in primary screening and secondary screening stages. After all, using both reactors can both enhance the rate of the catalyst testing and harvest on the synergy effect of getting reliable data.

## *3.6 Automation of the reactor*

Prior to developing the software required for performing catalytic tests in the 10-parallel rector, understanding the nature of this task is necessary. Namely, at the beginning those following points are to be taken into consideration:

- What are the component's elements of the task?
- What are the main functions?
- How should different instruments be combined?
- Which is the better way for the communication of instruments?

In order to accomplish this work, the idea of processing is applied to events generated over time, a method that simulates the often-occurring queuing in a heterogeneous catalyst environment. This is referred to as the 'discrete event model' and is a system where components interact via timed events. These discrete steps in the procedure may be classified as 'regulating reactor temperature', 'analyzing product by Micro-GC', 'switching magnetic valve to guide the flow of feed-gas' and

'changing the online channel in Multi-ports valve'. For automation of the reactor, an event model is designed in such a manner that the instruments that analyze the outcome of the reactor are alternatively activated during experimentation. This generates a 'queue events' that is sorted by time. For this, a reference program is developed using C++ (see appendix).

### *3.6.1 Main control box*

Developing the electric circuit as the interface of the whole system has the purpose of controlling the five instruments such as Varian CP-4900 GC, 10 multi position valve, heater, 3 magnetic valves. In addition, this control circuitry should be able to command controlling a current stream channel, reactor temperature and on/off condition of valve through Graphical User Interface (GUI) mode.

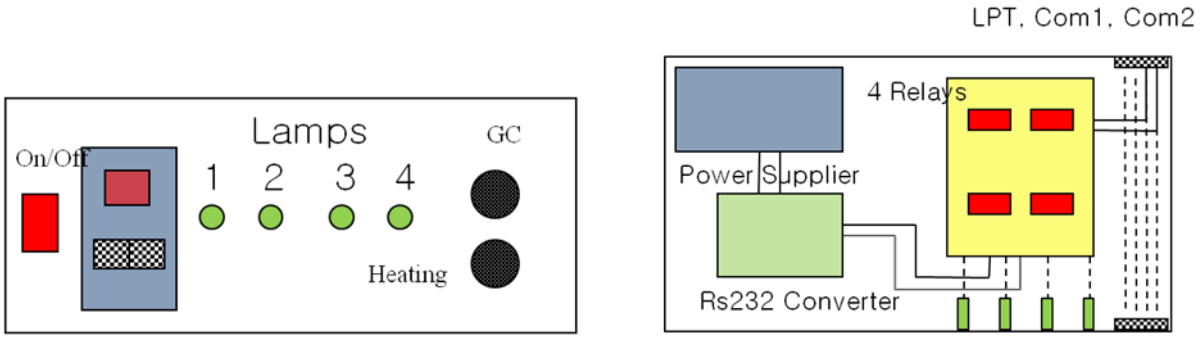


Figure 3.9 Main control box

As shown in above Figure 3.9, the front side of a control box shows the main power switch, the manual control panel of MVs including the monitor screen, 4 on/off LED lamps for magnetic valves, Micro-GC and heating instrument connectors.

The right diagram in Figure 3.9 describes the inside of the box containing the power supplier, RS232 converter and electric circuit. Four relays are applied to downgrade the voltage sending the signal to 4 magnetic valves for controlling the on/off different feed-gases and 4 LED lamps installed with resistors are implemented to show the state of the magnetic valve. For controlling the temperature at the reaction chamber, ADAM-450 (RS-232 to RS-422/RS-485 Isolated converter) was used. Since the temperature controller (dTron) is carried out under RS485, the change of protocol from RS232 to RS485 through COM1 was necessary. All data communication for automation is performed through three ports such as LPT for 'Micro-GC' and 'three magnetic valves', Com1 for 'temperature controller' and Com2 for 'multi-ports valve'.

### *3.6.2 Software development*

In order to control the entire system of the high-throughput process automatically, AutoCat software was developed by means of C++. In addition, some program components in this task were copied from previous IR-testRing software programmed by J.Scheidtmann. The software was programmed and developed based on the concept of user-friendly GUI and total automation.

During the experiment, the process of experiment can be identified in real-time and is carried out independently for an entire day on manual control. The main screen of GUI mode under this software is shown (Figure 3.10), and the main source-code of C++ can be found out in the appendix.

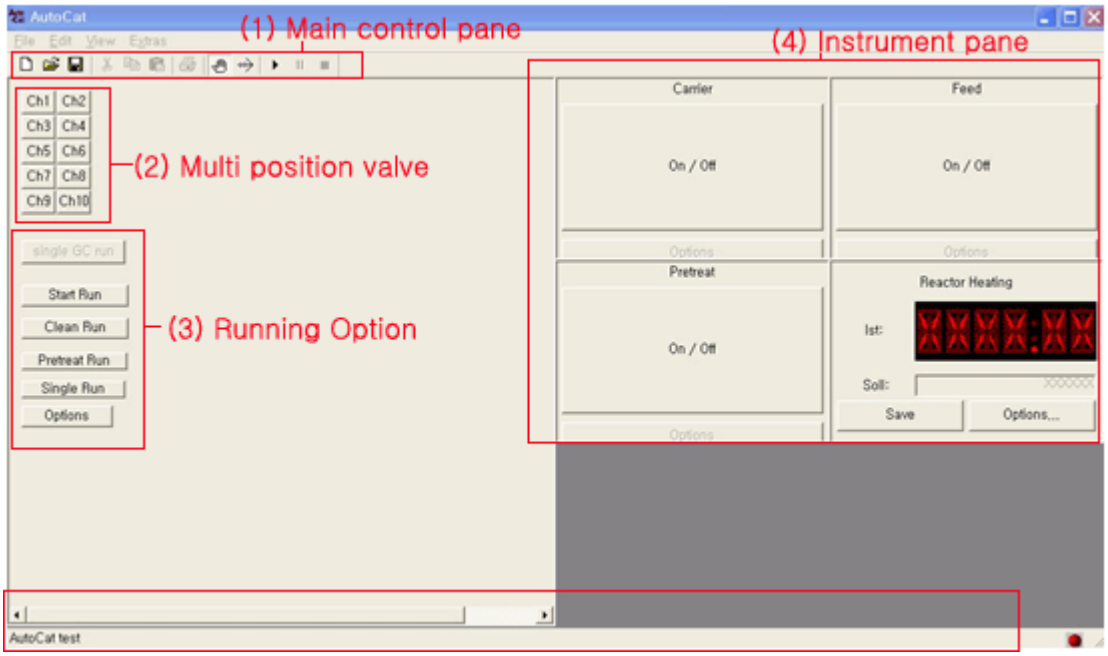


Figure 3.10 Main GUI window for controlling whole process

The main center GUI in the AutoCat software consists of four sectors (Figure 3.10). First, (1) the main control panel has several functions such as changing the screen from main to process-mode, starting a queue of future events, and saving or loading the files for event process. Clicking the button in the (2) panel of the multi position valve can change the current channel by sending the command. The (3) running option part is comprised of several command buttons that can define the specific way of the testing process. Lastly, the instrument windowpane (4) has the role to switch three magnetic valves and control the temperature of the reactor heater. In addition, the bottom of the window shown by the red box presents the current process by showing the time counter in text mode.

Consequently, the AutoCat software can control instruments such as a multi-position valve, three magnetic valves, an electronic heating chamber and a micro-GC. This automatic AutoCat system is provided with an action queue based on time.

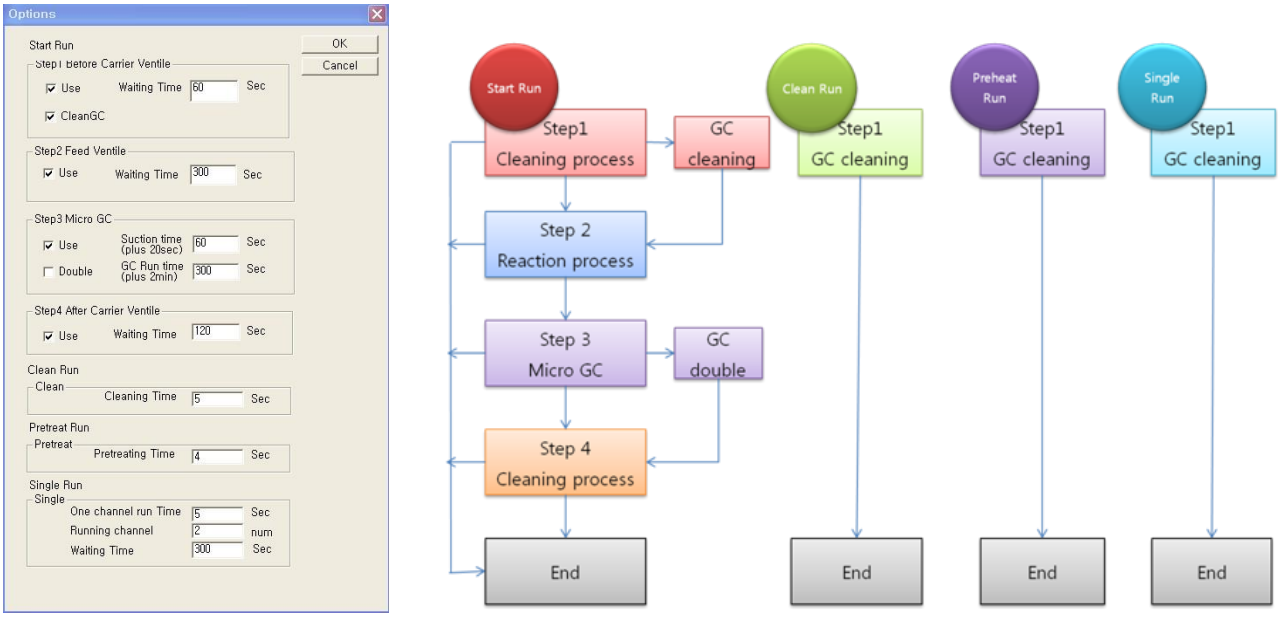


Figure 3.11 GUI option window including the flow chart of the process steps

The basic process called “Star Run” consists of four steps that can be selected by changing the ‘check-box’ and typing the time duration in text box as shown (left part of Figure 3.11). In the first step, each reactor channel and product flow channel of the micro-GC is cleaned by the carrier gas, in this case He or Ar. This avoids impurities originating from chemicals and products of the previous experiments or off-line channels. In the second step, the time to flow feed-gas into the reactor is defined, which in turn defines the time to reach steady condition of reaction. The third step defines sampling time and run time of the micro-GC. In the case of double measurements, it is possible to recheck the results in order to reduce errors. In step 4, the channel that has been used is cleaned by a flow of He, and it also keeps the coherency of the results in each channel. In addition, containing He in previous channels helps to avoid deactivation of catalysts by undesired reactions and the impurity of reaction gas by contamination.

In addition to the basic run, there are three running methods for specific situations based on experimental conditions. “Clean Run” performs the cleaning process of all channels. If it needs to run a preheat treatment for a certain catalyst, “Preheat Run” allows to use different gases, such as,

He, $O_2$ and $H_2$ under different temperature conditions. “Single Run” has a function to carry out tests with only one channel automatically. Flow charts of four different processes are shown on the right side of Figure 3.11.

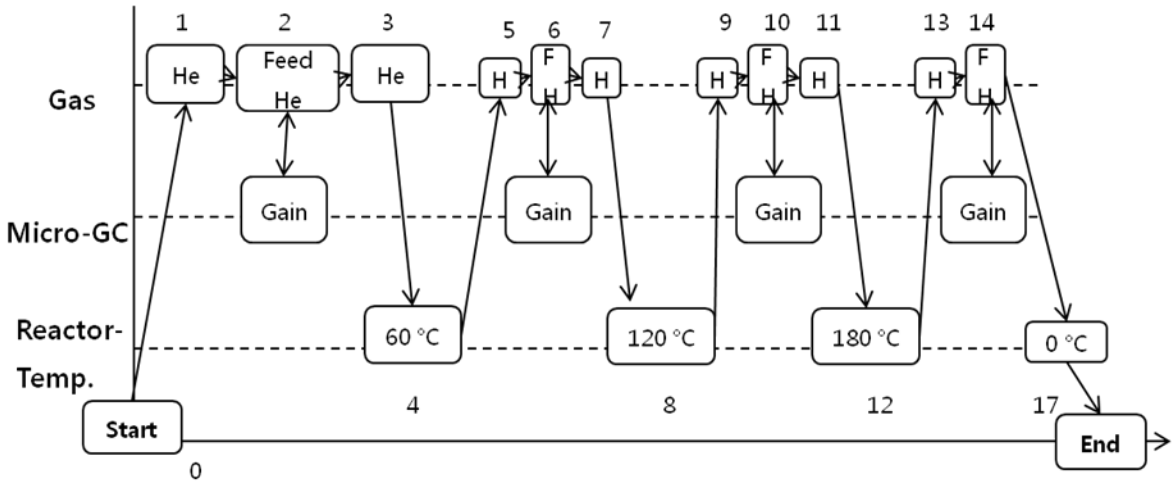


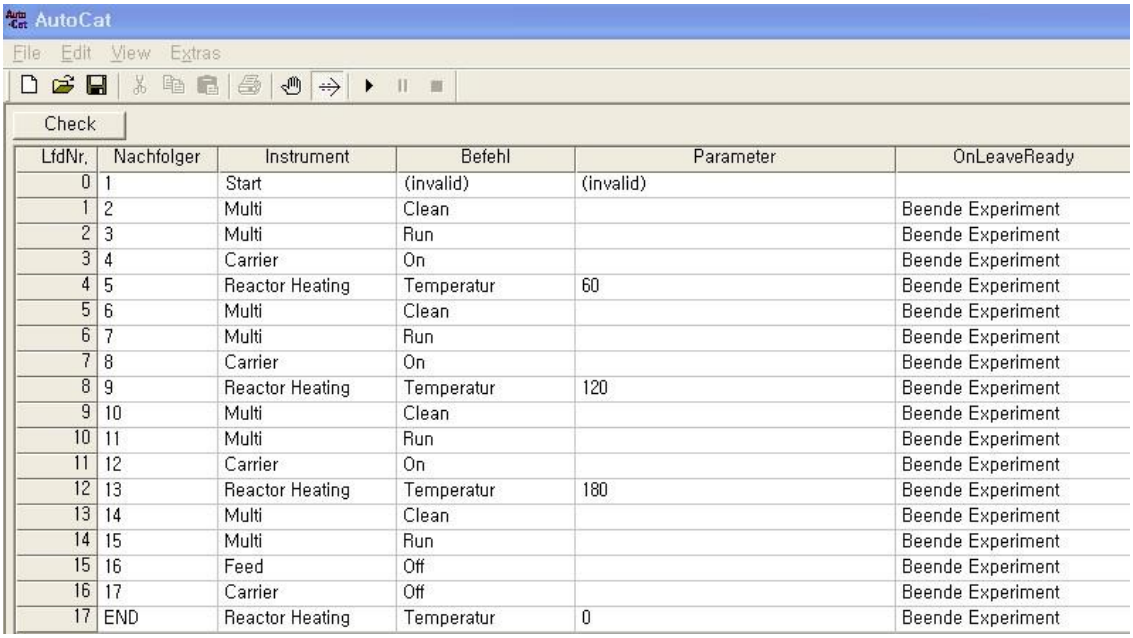


| LfdNr. | Nachfolger | Instrument | Befehl | Parameter | OnLeaveReady |
|---|---|---|---|---|---|
| 0 | 1 | Start | (invalid) | (invalid) | |
| 1 | 2 | Multi | Clean | | Beende Experiment |
| 2 | 3 | Multi | Run | | Beende Experiment |
| 3 | 4 | Carrier | On | | Beende Experiment |
| 4 | 5 | Reactor Heating | Temperatur | 60 | Beende Experiment |
| 5 | 6 | Multi | Clean | | Beende Experiment |
| 6 | 7 | Multi | Run | | Beende Experiment |
| 7 | 8 | Carrier | On | | Beende Experiment |
| 8 | 9 | Reactor Heating | Temperatur | 120 | Beende Experiment |
| 9 | 10 | Multi | Clean | | Beende Experiment |
| 10 | 11 | Multi | Run | | Beende Experiment |
| 11 | 12 | Carrier | On | | Beende Experiment |
| 12 | 13 | Reactor Heating | Temperatur | 180 | Beende Experiment |
| 13 | 14 | Multi | Clean | | Beende Experiment |
| 14 | 15 | Multi | Run | | Beende Experiment |
| 15 | 16 | Feed | Off | | Beende Experiment |
| 16 | 17 | Carrier | Off | | Beende Experiment |
| 17 | END | Reactor Heating | Temperatur | 0 | Beende Experiment |

Figure 3.12 (a) Operation diagram procedure (up) (b) process option screen (down)

The process needed to control the temperature is performed in the point of each temperature, controlling sub steps such as ‘Multi’, ‘Carrier’ and ‘Feed’ and it can be registered depending on different experimental conditions. For example, the option ‘Multi’ under ‘Instrument’ has options such as ‘Start’, ‘Clean’, ‘Preheat’ and ‘Run’. Likewise, ‘Reactor Heating’ under ‘Instrument’ can

control the temperature of the reactor by typing the desired temperature in the text box of the parameter row.

Figure 3.12 shows the process with regard to the queue including 17 sequences. When it starts the program (0), the reactor with command 'Clean' (1) is cleaned by helium gas in the process. This purging process is of importance, so that the results of measurements in each channel are based on identical experimental conditions. When command 'Run' (2) is given, the program begins the measurements of 10 channels by the selected process in the option of 'Start Run' given in Figure 3.12. After that, the magnetic valve is opened (3) in order to flow carrier gas (helium) into the reactor channel during temperature increase to 60 ºC by the command of 'Reactor Heating' (4).

There is a reason why it is necessary to supply gas during the increasing temperature. As is well known, reactor leaking towards air can induce oxidation of the catalysts resulting in their deactivation. Helium gas in this system is purged into the reactor with 1 bar pressure. If no continuous gas supply exists during increasing temperature, the inside pressure of the reactor will be increased by heating gas, which induces the increase of potential to happen the leakage of reactor.

Subsequently, these steps described above were repeated after increasing temperatures as shown in Figure 3.12. When all reaction measurements have been completed, magnetic valves are closed, which lowers the reactor temperature to an ambient levels. These process sequences can be rearranged by using a different combination of 'Start-Run', 'Clean-Run', 'Preheat-Run' and 'Single-Run' based on the desired reaction procedure.

Experimental errors always occur during testing. In order to avoid or minimize these, a double measurement method was implemented in the software of AutoCat as shown on the left side of Figure 3.11. By clicking the check box "double", each step was measured twice. The accuracy of the tests is then increased by the compensation of two measurements. At the same time, the existence of the reactor leakage and the lack of measurements of micro-GC can be identified by monitoring the difference of the measurements obtained at values during the process.

## *3.7 Validation of the reactor*

The main reason for this validation is to have reliable results of each channel with same catalyst under identical reaction conditions. In order to prove consistency at each reactor-tube, 50 mg Hopkalite catalysts is mixed with 100 mg sand for better heat transfer. The temperature has been increased from 23.8 ºC (room temperature) to 150 ºC in 25 ºC increments. Prior to the catalytic

reaction, each channel was purged with helium gas (50 mL/min) and product-gas was analyzed by the Mirco-GC. The experiment was performed in duplicate as described above (Figure 3.11). The flow rate of the feed-gas was maintained with 25 mL/min using gas with a composition of (CO: $O_2$: He = 2: 2: 96).

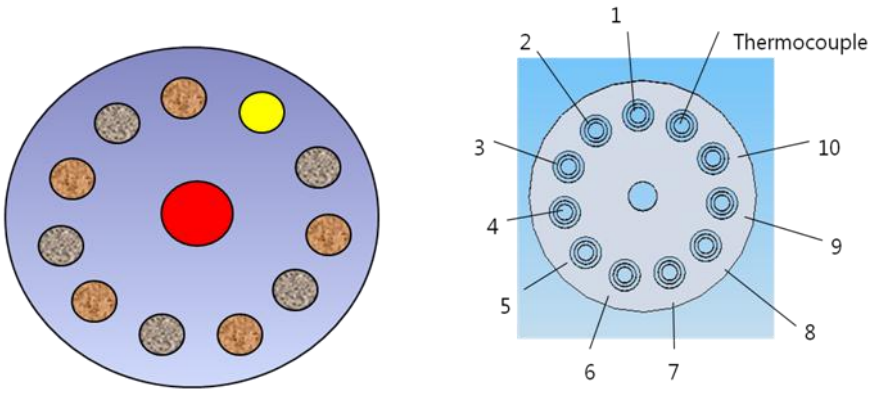


Figure 3.13 Reactor sketch in different channels

As depicted in Figure 3.13, sand and sand-catalyst mixtures were inserted into odd (1, 3, 5, 7, 9) and even number (2, 4, 6, 8, 10) channels, respectively. For this experimental setup, 180 sequences were planned to test the heterogeneous catalytic reaction with Hopcalite.

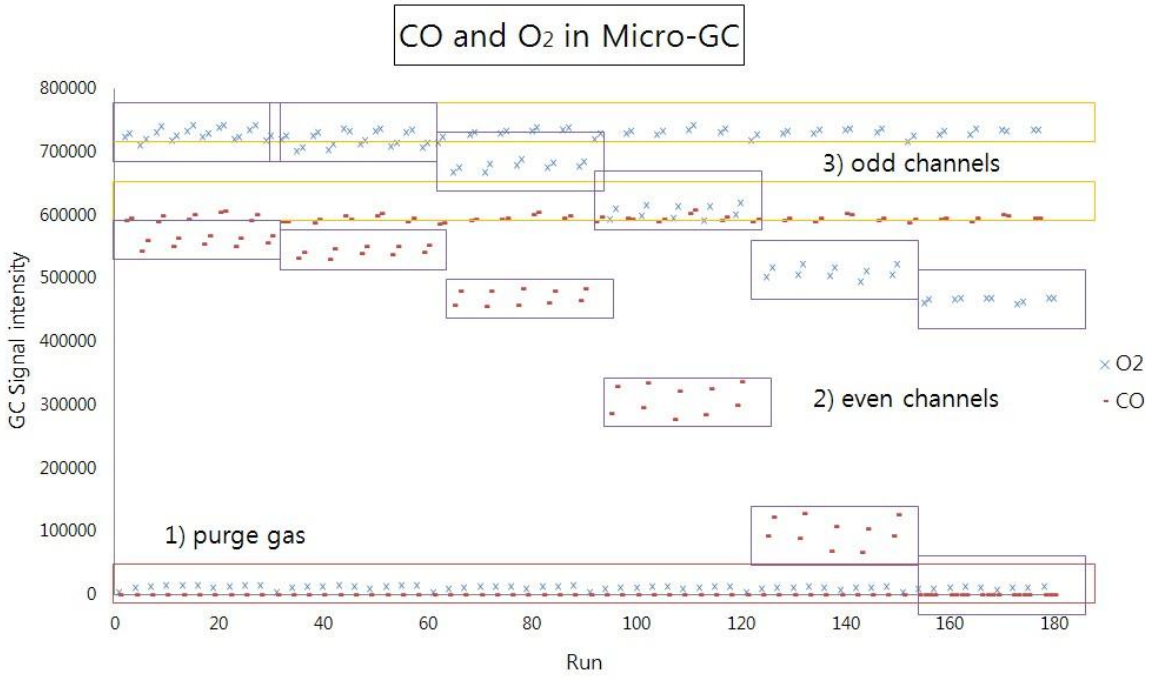


Figure 3.14 Results of sequence test.
Reaction condition: 50 mg of Hopkalite catalyst diluted with 100 mg of sand; particle size of 100-200 μm; total flow rate of 25mL/min ($CO:O_2$:He=2:2:96 vol%)

The difference of experimental results of both even and odd channels, which represent the conversion of CO and $O_2$ measured by the thermal conductivity detector of the Micro-GC, is shown in Figure 3.14. The Y-axis represents the activities of reactants and products based on GC signal intensity. These results can be divided into three parts:

As expected, the analysis of the purge gas (He) showed about zero value of GC signal intensity of $O_2$ and CO (1). On the other hand, while the odd channels (insert send) showed almost no conversion (3), the conversion in the even channels (catalysts) increased with time based on increasing reaction rate through increasing temperature (2). Interestingly, the conversion in the second measurement by the double measurement concept was always higher than the first value, which is indicative a lower conversion of reactants. The origin of this outcome is still unclear, but it is likely that the contamination from the previous sample gas in the suction line of the Micro-GC enhances the signal of the current gas analysis.

Consequently, sequence results show that the process is in accordance with expectations. However, it is still debatable whether the variations of the experimental results are due to the catalytic reaction process or not. The differences in the results should not depend on the channels. In order to evaluate the extent of deviation, the reactor reliability is judged by the differences at each channel.

Experimental results in a box plot are presented as Whisker Diagrams, applied using the Excel program. Whisker plot provides a simple graphical summary of a set of data based on medians. Parameters (Mean, SD, Min, Q1, Median, Q3, Max, Bottom, 2Q Box, 3Q Box, Whisker-, and Whisker+) were tabulated in table 3.1 for even channels and in table 3.2 for odd channels. The data in table 3.1 as well as table 3.2 were calculated according to reference[148].

The positive and negative error span of the plot can be measured by calculation the correlation of Q3 subtracted from Max and Min subtracted from Q1, respectively. 2Q Box and 3Q Box describe the range of median between Q1 and Q3.

Table 3.1 CO conversion data (left) and Whisker data (right) in even channels without Hopkalite

| Even | Temperature step | | | | | |
|---|---|---|---|---|---|---|
| | 33.8 | 50 | 75 | 100 | 125 | 150 |
| 2 | 9.4 | 11.8 | 22.9 | 49.4 | 82.3 | 100.0 |
| | 9.8 | 9.8 | 20.7 | 47.6 | 80.3 | 97.4 |
| 4 | 8.4 | 11.4 | 23.0 | 48.2 | 82.0 | 100.0 |
| | 7.2 | 10.0 | 21.4 | 46.9 | 80.5 | 97.4 |
| 6 | 7.7 | 10.4 | 22.6 | 50.8 | 85.5 | 100.0 |
| | 7.1 | 9.9 | 22.4 | 49.9 | 84.8 | 99.7 |
| 8 | 8.3 | 10.5 | 22.6 | 49.9 | 85.9 | 100.0 |
| | 6.8 | 9.1 | 21.7 | 48.8 | 84.6 | 99.8 |
| 10 | 7.7 | 10.1 | 22.1 | 47.7 | 81.9 | 100.0 |
| | 6.7 | 8.7 | 21.0 | 46.9 | 80.7 | 96.7 |

| Even | Temperature step | | | | | |
|---|---|---|---|---|---|---|
| | 33.8 | 50 | 75 | 100 | 125 | 150 |
| Count | 10 | 10 | 10 | 10 | 10 | 10 |
| Mean | 7.92 | 10.17 | 22.04 | 48.61 | 82.84 | 99.11 |
| SD | 1.06 | 0.94 | 0.80 | 1.36 | 2.16 | 1.34 |
| Min | 6.74 | 8.68 | 20.74 | 46.87 | 80.27 | 96.72 |
| Q1 | 7.12 | 9.82 | 21.46 | 47.63 | 81.00 | 97.99 |
| Median | 7.71 | 10.06 | 22.24 | 48.50 | 82.14 | 99.91 |
| Q3 | 8.37 | 10.48 | 22.62 | 49.79 | 84.77 | 100.00 |
| Max | 9.81 | 11.79 | 23.04 | 50.76 | 85.86 | 100.00 |
| Bottom | 7.12 | 9.82 | 21.46 | 47.63 | 81.00 | 97.99 |
| 2Q Box | 0.58 | 0.24 | 0.78 | 0.88 | 1.15 | 1.92 |
| 3Q Box | 0.66 | 0.42 | 0.38 | 1.28 | 2.63 | 0.09 |
| Whisker- | 0.38 | 1.15 | 0.71 | 0.76 | 0.73 | 1.28 |
| Whisker+ | 1.44 | 1.31 | 0.42 | 0.98 | 1.09 | 0.00 |
| Deviation | 3.07 | 3.12 | 2.30 | 3.89 | 5.59 | 3.28 |

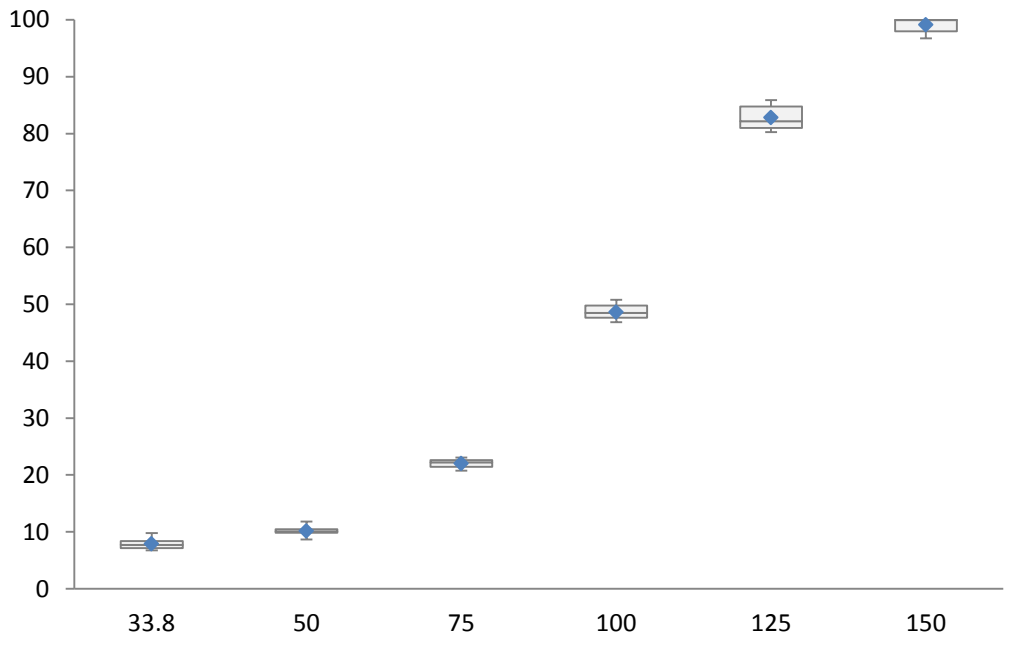


Figure 3.15 Conversion profile with Box plot in even channels

These box plots of Figure 3.15 show that the conversion values of the Hopcalite sample at 5 even-channels increase with increasing temperature. Precisely, the deviation of conversion regarding

temperature ranges from the minimum (2.30; 75°C) to the maximum (5.59; 125°C). Ten data of each temperature, which are five channels with double measurements, were used to calculate the parameters, including the deviation.

Table 3.2 CO conversion data (left) and Whisker data (right) in odd channels with Hopkalite

| Odd | Temperature step | | | | | |
|---|---|---|---|---|---|---|
| | 33.8 | 50 | 75 | 100 | 125 | 150 |
| 1 | 2.7 | 2.9 | 3.7 | 3.0 | 2.9 | 3.3 |
| | 2.2 | 2.9 | 3.3 | 1.9 | 2.4 | 2.5 |
| 3 | 3.1 | 3.3 | 2.7 | 2.2 | 2.7 | 2.5 |
| | 1.6 | 2.5 | 2.3 | 2.3 | 2.2 | 2.2 |
| 5 | 2.3 | 1.6 | 2.3 | 3.1 | 3.0 | 3.1 |
| | 1.1 | 2.5 | 2.0 | 2.3 | 2.2 | 2.0 |
| 7 | 0.7 | 1.4 | 1.3 | 0.9 | 1.0 | 1.3 |
| | 0.1 | 0.8 | 0.7 | 0.0 | 1.1 | 1.4 |
| 9 | 2.7 | 3.0 | 2.2 | 2.7 | 2.7 | 2.0 |
| | 1.3 | 2.1 | 1.6 | 1.8 | 2.2 | 2.1 |

| Odd | Temperature step | | | | | |
|---|---|---|---|---|---|---|
| | 33.8 | 50 | 75 | 100 | 125 | 150 |
| Count | 10 | 10 | 10 | 10 | 10 | 10 |
| Mean | 1.78 | 2.31 | 2.19 | 2.03 | 2.23 | 2.23 |
| SD | 0.97 | 0.81 | 0.90 | 0.96 | 0.69 | 0.64 |
| Min | 0.14 | 0.84 | 0.65 | 0.00 | 1.02 | 1.26 |
| Q1 | 1.17 | 1.74 | 1.67 | 1.85 | 2.17 | 1.99 |
| Median | 1.90 | 2.48 | 2.23 | 2.27 | 2.31 | 2.12 |
| Q3 | 2.59 | 2.92 | 2.62 | 2.58 | 2.71 | 2.51 |
| Max | 3.08 | 3.30 | 3.66 | 3.12 | 2.98 | 3.28 |
| Bottom | 1.17 | 1.74 | 1.67 | 1.85 | 2.17 | 1.99 |
| 2Q Box | 0.72 | 0.74 | 0.56 | 0.41 | 0.14 | 0.13 |
| 3Q Box | 0.69 | 0.44 | 0.39 | 0.31 | 0.40 | 0.39 |
| Whisker- | 1.04 | 0.89 | 1.02 | 1.85 | 1.15 | 0.73 |
| Whisker+ | 0.49 | 0.38 | 1.04 | 0.54 | 0.27 | 0.76 |
| Deviation | 2.94 | 2.46 | 3.01 | 3.12 | 1.96 | 2.02 |

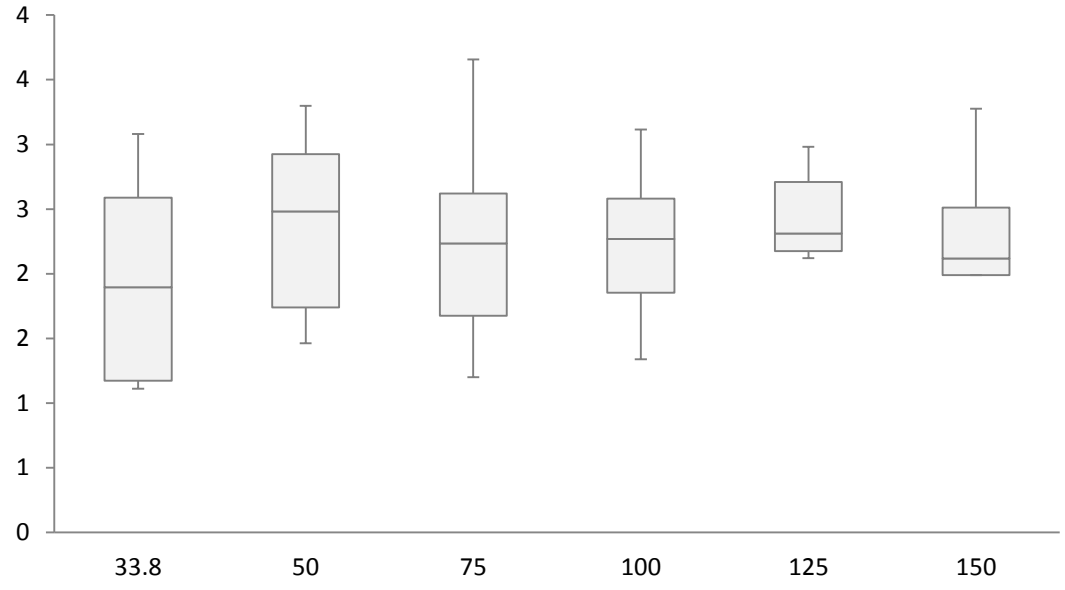


Figure 3.16 Conversion profile with Box plot in odd channels

In the tube reactors that had no catalyst, no reaction should take place, which means the concentration of CO and $O_2$ should be constant. In the other words, the conversion of CO has to remain 0. The measured mean values of conversion with increasing temperature varied from 1.78 to 2.23, which were taken as experimental error. For this, several reasons are possible. First, even though the intersection of online and offline channels are blocked by balls, some diffusion of gas through the seals can take place. Artificial errors, such as calibration mistakes on conversion and small leakages of connections between the tube reactor and each joint, cannot be avoided completely. Furthermore, after purging empty channels with 50 mL He, the trace of the previous gas contaminated in the Miro-GC suction line can add to this error. Apart from these, the reaction can take place without catalysts at high temperatures and trace contamination of catalysts on the reactor will can contribute to the error. The test in each odd channel provided almost identical results, having only small deviation (1.96–3.12).

Although it is shown that the accuracy in each channel still needs improvement, this result clearly showed that the new reactor is promising and reliable and deserves to be applied in high-throughput experimentation. As a first step, the stability or compatibility of this system is tested at a temperature maximum of 400 °C and with atmospheric pressure. Generally, selective oxidation reaction takes place at conditions with temperature below 400 °C. Therefore, this reactor seemed ideal for catalyst screening in selective oxidation.

## *3.8 Simulation of temperature distribution*

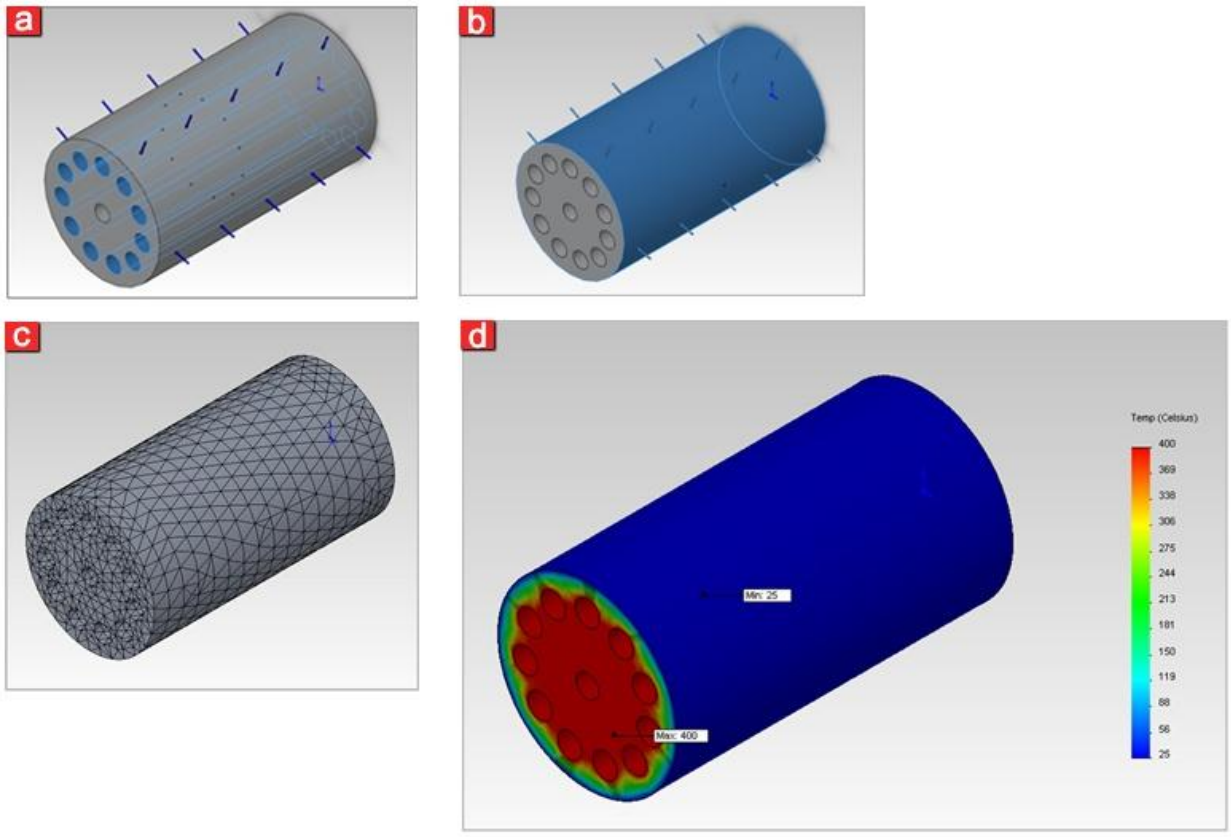


Figure 3.17 3D FEA simulation in the distribution of temperature

BC: Internal holes (a), BC: outside surface (b), FEA mesh (c), and temperature distribution profile (d)

The FEA simulation in the central module was carried out to visualize its temperature distribution at a reaction temperature of 400 °C, shown in Figure 3.17. Aluminum 7079 alloy was chosen as the raw material, containing properties such as the thermal conductivity of 120 W/m.K, the density of 2700 kg/m$^3$ and the specific heat of 960 J/kg.K. A surface with 11 internal holes in Figure 3.17 (a) and an outside surface of the cylinder in Figure 3.17 (b) were considered as boundary conditions with a reaction temperature of 400 °C and a room temperature of 25 °C, respectively. All domains and boundaries were assigned, and then the generation of mesh was performed as presented in Figure 3.17 (c). The generated mesh contains 44996 triangular elements and 68280 nodes. The FEA/SolidWorks coupled computation required about half an hour to obtain the solution of temperature profile in this required condition. Figure 3.17 (d) shows the temperature variation in the solid domain of the central module of the 10-fold parallel reactor.

## 3.9 Operation concepts

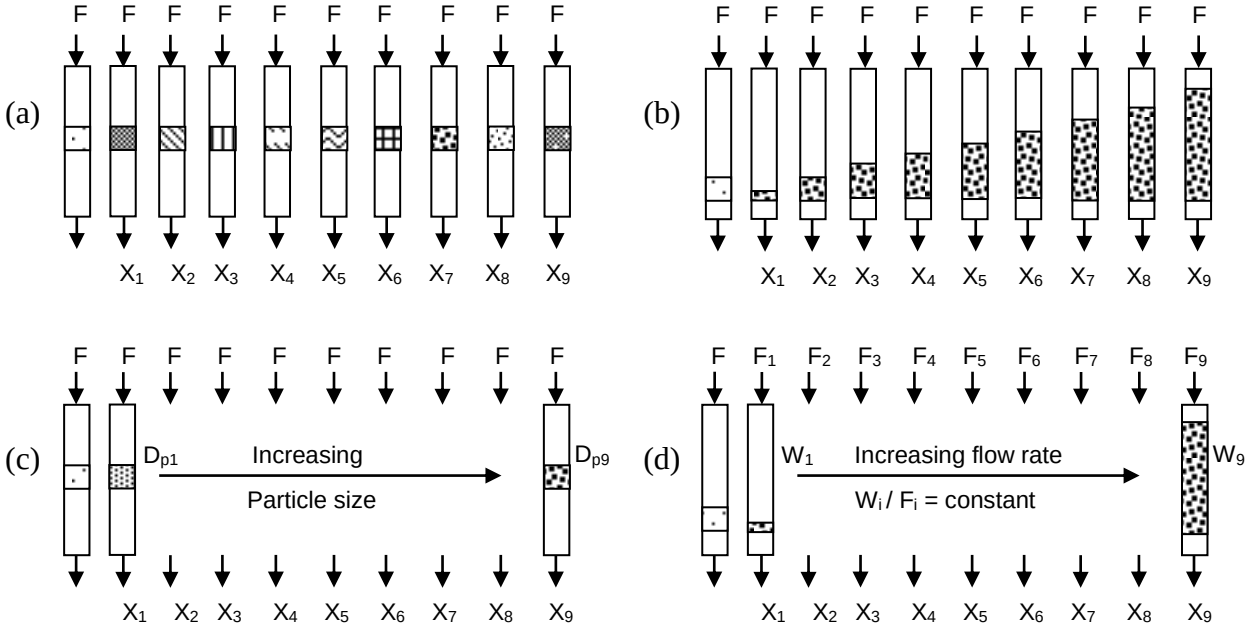


Figure 3.18 Operation concepts in the 10-fold parallel reactor scheme: (a) activity tests and life time experiments; (b) kinetic studies; (c) mass transfer limitation based on porous diffusion (d) mass transfer limitation based on film diffusion

The Figure 3.18 shows different possibilities for experiments[87] possible with the 10-fold parallel reactor setup. Here, possible main applications of the new reactor will briefly be described. Generally, for the purpose of catalyst screening, the reactor can be filled with the same amount of nine different catalysts (it is recommended to use the first tube reactor as reference, since it is also designed to be purged by the carrier gas, helium, during temperature changes) (Figure 3.18a). In contrast, different amounts of the same catalyst can be added to facilitate kinetic studies (Figure 3.18b). By increasing the particle size of the catalyst with the same flow rate, the diagnostic experimental tests for the presence of intra particle limitation (mass transfer limitation based on porous diffusion) is used (Figure 3.18c). Variation of W/F by changing the amount of catalyst W or F allows a broad range of conversions to check for mass transfer limitation based on film diffusion (Figure 3.18d).

Activity and stability tests with the same set catalyst can be performed in a single run using one experimental channel. The 10-fold parallel reactor concept also offers the possibility to investigate the stability of 9 samples of the same catalyst at different conditions simultaneously. Many kinetic

experiments can also be carried out at different temperatures and feed compositions during the screening process.

## *3.10 Design of new rack*

### *3.10.1 Concept*

Based on a bottleneck of library preparation, a new rack has been designed and validated with the idea of increasing the speed of a process for catalyst tests. The previous procedure entails different vessels during each step such as synthesis, aging, drying, calcination and testing, which can be a time consuming and troublesome procedure. For example, each stock solution in synthesis is positioned into 2 mL vials in a rack of 50 vials and exchanged in a steel rack for calcination and is finally transferred into a slate or steel plate for testing. Instead of utilizing vials, rack and plate, it will be a more economical use of time or resource to apply one standard vessel.

In 2001, our group introduced new rack including the part of a synthesis reactor[100]. Although the pipetting unit dispenses liquid or dissolves reagents into the cavities of a microreactor array in the rack, this method remained a problem in reproducibility as an important factor for discovering catalysts by high-throughput screening. Therefore, the manual preparation of the reagent solution again became a common procedure.

The aim of the presenting work is to demonstrate the application of new rack applied in the entire catalyst process, which leads to the new or improved catalyst test with increasing the speed and reproducibility.

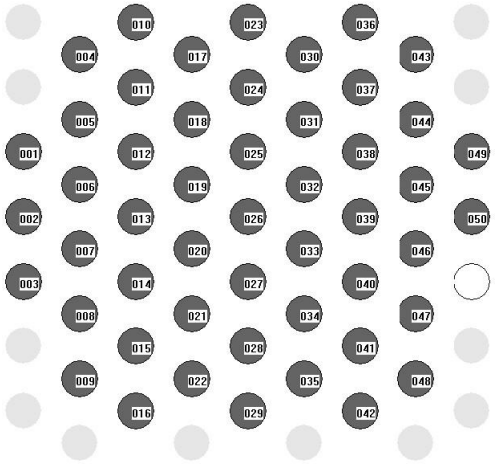


Figure 3.19 Hexagonal library with 51 wells in a new rack

For this purpose, hexagonal aluminum-rack with 51 holes was developed as shown in Figure 3.19; this cylindrical rack was designed to contain maximum 51 GC flasks, placed in the stage robot reactor for catalyst tests.

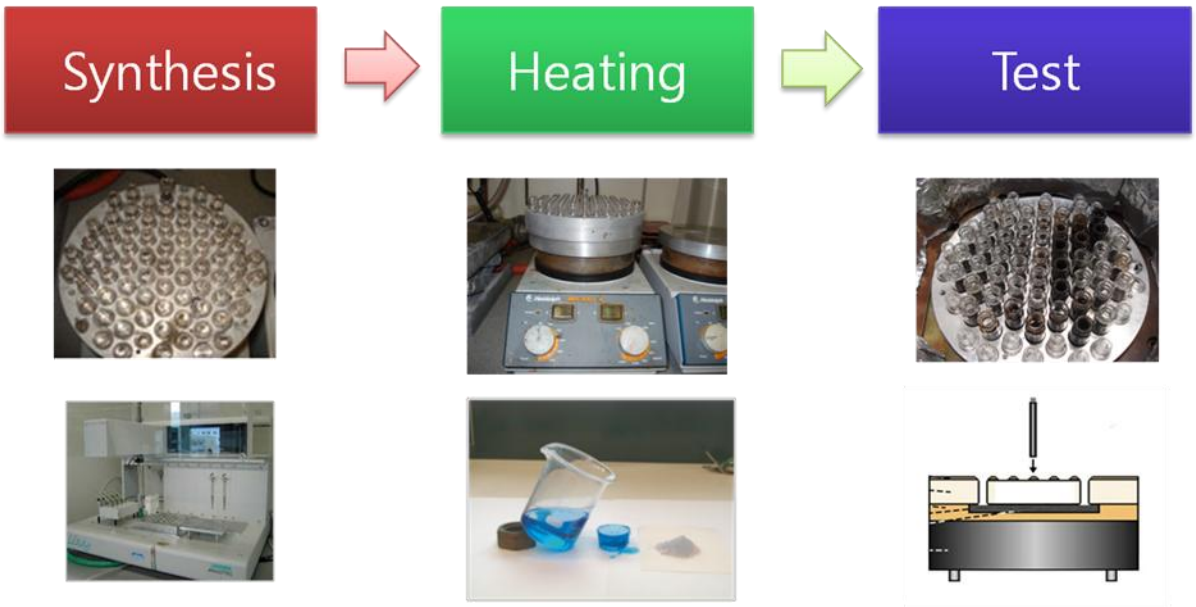


Figure 3.20 Scheme of using a new rack

As described in Figure 3.20, this new type of rack for the stage robot reactor can be used for the catalyst preparation in synthesis, aging or drying and calcinations, or catalyst test, by turns. IR-testRing software, which can control the SRR, was modified to use this new rack. While it decreases the time consumed during catalyst preparation and testing, the accuracy decreased due to the following two reasons. First, in comparison to our previous plate as a rack, the open structure with new rack is more exposed to atmospheric air and moisture, which can disturb the final result of experiments. Next, the reaction may be affected by the kind of HPLC flask material, such as silicate, which has the potential to promote unexpected reactions.

In spite of the problem concerning the less accurate data obtained using this new rack, the time consuming in the entire system decreased. In addition, it was suitable to identify the hits of catalysts in a primary screening process. However, if high accuracy is required, it would be preferable to use the stage robot reactor with the old rack. This work aimed using only one standard vessel is implemented successfully and still valuable to develop for the further instrument because of its

flexibility, convenience and simplicity. Furthermore, there is the potential to apply it to analysis of liquid-liquid or liquid-gas phase reaction.

### *3.10.2 Ternary composition*

To validate the performance of the new rack, a composition spread of potential catalysts composed of Ag, Cu and Mn has been chosen for the selective oxidation of propene. It is important that the entire process of catalyst preparation and testing has been performed with the same rack. In summary, the library of 51 potential catalysts in the new rack has been implemented for the entire process, including catalyst testing in the stage robot reactor for the selective oxidation of propene. This testing used propylene and oxygen atmospheres ($C_3H_6$:$O_2$=4:1) and temperatures of 250 ºC, 300 ºC and 350 ºC. The results were reproducible.

Figure 3.21 shows the result of the direct test of ternary composition containing Ag, Cu and Mn by using the new rack. Visualization of the conversion for propylene to proplyenoxide, acrolein and $CO_2$ were used in a Matlab modeling. Catalytic activities were defined based on the GC signal intensity of unscaled results.

Correlations between catalytic activity and chemical composition reveal that conversion to propylene oxide exists in the wide area of composition spread at 250 ºC. However, the most of active areas of propylene formation at 250 ºC disappeared at 350 ºC, except for the area where the catalyst was composed of $Cu_{0.3}Mn_{0.6}Ag_{0.1}$.

In the case of the conversion to acrolein, similar behavior was seen at 250 ºC and 350 ºC: the most active region was found at the composition of $Cu_{0.8}Mn_{0.2}$. The rest showed relatively low activities of acrolein. This active area of acrolein production was extended at 350 ºC.

The results of the conversion to $CO_2$ show high value in the broad areas of including Mn rich composition at 250 ºC. With increasing the reaction temperature, the catalysts of binary composition of Mn-Ag or Mn-Cu have higher activity at 300 ºC.

Although this result of the new rack maybe less accurate when compared to previous racks such as steel plate, the visualization of ternary composition provided interesting results to recognize a pattern that is useful for decision-making in future primary screening phases.

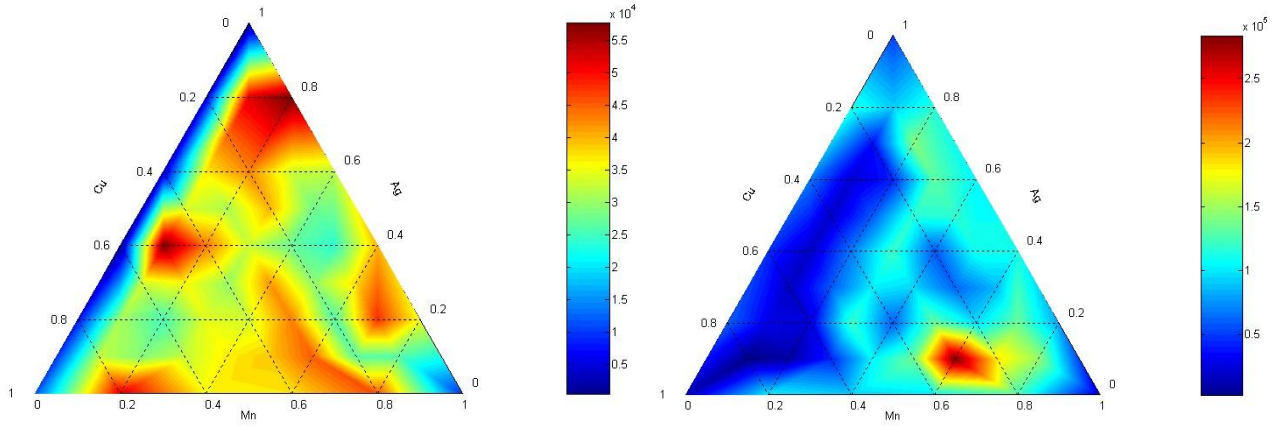


Production of Propylenoxide at 250 ºC (left) and at 350 ºC (right)

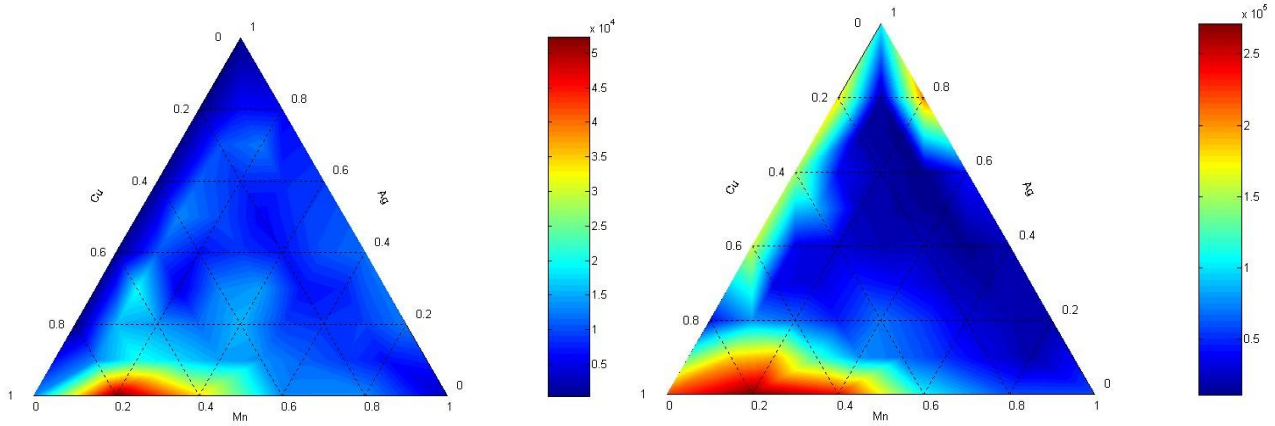


Production of Acrolein at 250 ºC (left) and at 350 ºC (right)

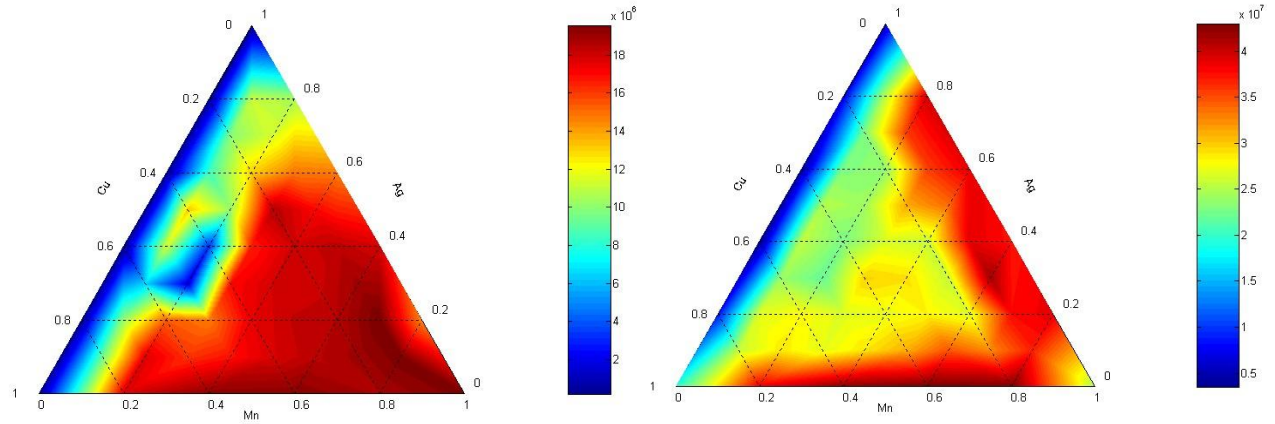


Production of $CO_2$ at 250 ºC (left) and at 350 ºC (right)

Figure 3.21 Ternary composition spread by using hexagonal library.
Reaction conditions: around 400 μmol of catalyst. Total flow rate: 5 mL/min ($C_3H_6$:$O_2$=4:1 vol%)

## *3.11 Conclusion*

The chemical industry promotes the use of miniature reactors since the reduced scale of experimentation has many advantages with respect to cost and safety. There is certainly a global interest in the application of high-throughput miniature reactors.

In this project, a 10-fold parallel reactor has been developed and built by the in-house workshop. This reactor allows us to perform 10 comparable catalytic tests at the same time. So far, most of the parallel reactors rely on one multi-position valve downstream for decreasing the construction price and avoiding the mixture of product-gas. Here, another method has been used where the multi-position valve is implemented upstream: the disadvantageous mixing of product-gas has been solved by developing a new splitting module that seals the channels using a ball valve at each channel.

Moreover, the results of reactor validation show its compatibility for catalyst tests at temperatures up to 400 °C at atmospheric pressure. Because selective oxidation reactions can take place at low reaction temperature, it is expected that the newly developed reactor is suitable for the application to discover heterogeneous catalysts. This high-throughput system can be used as secondary screening systems that are useful for catalyst optimization, analysis, and validation. At least, it will supposedly be safer than a large reactor and less costly in respect of material for catalyst preparation. However, there are still challenges to tackle in the development of such a catalytic reactor before it can be applied in the application at high pressure or high temperature.

Apart from the new reactor, the application of the new rack was successful in saving time for the catalyst-discovery and was used to sample the ternary composition spread of Ag, Cu and Mn. Nevertheless, the application of this rack still requires improvement and modifications to verify its performance for future applications.

# 4 Discovering catalysts for propene to propene oxide conversion

## *4.1 Primary generation by using binary composition*

In our attempt to find new catalysts for propylene oxide production, the first generation of catalysts has been synthesized. Most materials used for the sol-gel synthesis were obtained from commercial sources and used without further purification. A list of the metal complexes used as a matrix was described in table 4.1 and 4.2.

Table 4.1 Elements used for binary composition matrix

| | | | | | | | | | | | | | | | | | |
|---|---|---|---|---|---|---|---|---|---|---|---|---|---|---|---|---|---|
| **H** | | | | | | | | | | | | | | | | | **He** |
| **Li** | **Be** | | | | | | | | | | | **B** | **C** | **N** | **O** | **F** | **Ne** |
| **Na** | **Mg** | | | | | | | | | | | **Al** | **Si** | **P** | **S** | **Cl** | **Ar** |
| **K** | **Ca** | **Sc** | **Ti** | **V** | **Cr** | **Mn** | **Fe** | **Co** | **Ni** | **Cu** | **Zn** | **Ga** | **Ge** | **As** | **Se** | **Br** | **Kr** |
| **Rb** | **Sr** | **Y** | **Zr** | **Nb** | **Mo** | | **Ru** | **Rh** | **Pd** | **Ag** | **Cd** | **In** | **Sn** | **Sb** | **Te** | **I** | **Xe** |
| **Cs** | **Ba** | **Lu** | **Hf** | **Ta** | **W** | **Re** | **Os** | **Ir** | **Pt** | **Au** | **Hg** | **Tl** | **Pb** | **Bi** | **Po** | **At** | **Rn** |
| **Fr** | **Ra** | | | | | | | | | | | | | | | | |
| | | **La** | **Ce** | **Pr** | **Nd** | | **Sm** | **Eu** | **Gd** | **Tb** | **Dy** | **Ho** | **Er** | **Tm** | **Yb** | | |
| | | **Ac** | **Th** | **Pa** | **U** | | | | | | | | | | | | |

Table 4.2 List of used chemicals for binary matrix

| Element | Chemical | Compay | Element | Chemical | Compay |
|---|---|---|---|---|---|
| Ag | Ag $NO_3$ M | ABCR | Re | Re Cl M | Aldrich |
| Al | Al $NO_3$ M | Alfa | Ru | Ru Cl M | Aldrich |
| B | B acid M | Fluka | Sb | Sb Cl M | J. T. Baker |
| Cr | Cr $NO_3$ M | Aldrich | Si | Si $C_8H_2OO_4$ Si M | |
| Cu | Cu $NO_3$ M | Fluka | Sn | Sn Cl M | Aldrich |
| Fe | Fe $NO_3$ M | k.A. | Te | Te Saeure M | Fluka |
| Ga | Ga $NO_3$ M | Aldrich | W | W Cl M | Fluka |
| Ge | Ge O*i*Pr M | Aldrich | Y | Y $NO_3$ M | ABCR |
| Hf | Hf Cl M | Aldrich | Zn | Zn OAc M | Fluka |
| In | In $NO_3$ M | Aldrich | Zr | Zr $ONO_3$ M | Johnson |
| La | La $NO_3$ M | Fluka | Mo | Mo O*i*Pr I | Alfa Aesar |
| Mn | Mn $NO_3$ M | Merck | Bi | Bi 2-Ethylhexanoat M | Strem |
| Nb | Nb OEt M | | Ta | Ta $Cl_5$ M | ABCR |
| Pb | Pb $ClO_4$ M | | | | |

M: methanol, I : isopropanol

For the synthesis of catalysts, stock solutions of 27 precursors in methanol were prepared with 0.25 M according to the following formulation:

The molar ratio of A (0.25 M solution in methanol): B (0.25 M solution in methanol): complexing agent (4-hydroxy-4-methyl-pentanone): acid (propionic acid) was 50:50:695:2. The preparation of $A_{50}B_{50}$ was performed by pipetting the following volumes of single solutions in sequence: 0.25 M A in methanol (600.0 µL, 0.15 µmol), 0.25 M B in methanol (600.0 µL, 0.15 µmol), and complexing agent mixed with propionic acid (8.06 M, 259 µL, 2087 µmol). New catalysts of the systematic binary composition $A_{50}B_{50}$ with 27 materials (Ag, Al, B, Cr, Cu, Fe, Ga, Ge, Hf, In, La, Mn, Nb, Pb, Re, Ru, Sb, Si, Sn, Te, W, Y, Zn, Zr, Ta, Mo, Bi) were set by this recipe. This sol-gel method is similar to those described in reference[83].

In total, 351 catalysts were prepared for binary compositions as summarized in Figure. 4.1. After the pipetting process, the rack was covered and placed on an orbital shaker (Titramax 100; Heidolph) for 3 h. After the lid had been removed, the rack was dried for 6 days at 45 °C for gel formation and catalyst drying. All samples were calcined in an oven at 400 °C for 5 h with a heating rate of 0.2 °C $min^{-1}$. Finally, the 351 catalyst powders obtained were ground in the HPLC flasks with a glass rod and manually transferred into wells in two library plates such as 1G1L and 1G2L, being stainless steel libraries.

| | | | | | | | | | | | | | | | | | | | | | | | |
|---|---|---|---|---|---|---|---|---|---|---|---|---|---|---|---|---|---|---|---|---|---|---|---|
| 1 | AgAl | 31 | AlGa | 61 | BNb | 91 | CrTe | 121 | FeGa | 151 | GaSb | 181 | HfIn | 211 | InZn | 241 | MnY | 271 | PbTa | 301 | SbY | 331 | WY |
| 2 | AgB | 32 | AlGe | 62 | BPb | 92 | CrW | 122 | FeGe | 152 | GaSi | 182 | HfLa | 212 | InZr | 242 | MnZn | 272 | PbMo | 302 | SbZn | 332 | WZn |
| 3 | AgCr | 33 | AlHf | 63 | BRe | 93 | CrY | 123 | FeHf | 153 | GaSn | 183 | HfMn | 213 | InTa | 243 | MnZr | 273 | PbBi | 303 | SbZr | 333 | WZr |
| 4 | AgCu | 34 | AlIn | 64 | BRu | 94 | CrZn | 124 | FeIn | 154 | GaTe | 184 | HfNb | 214 | InMo | 244 | MnTa | 274 | ReRu | 304 | SbTa | 334 | WTa |
| 5 | AgFe | 35 | AlLa | 65 | BSb | 95 | CrZr | 125 | FeLa | 155 | GaW | 185 | HfPb | 215 | InBi | 245 | MnMo | 275 | ReSb | 305 | SbMo | 335 | WMo |
| 6 | AgGa | 36 | AlMn | 66 | BSi | 96 | CrTa | 126 | FeMn | 156 | GaY | 186 | HfRe | 216 | LaMn | 246 | MnBi | 276 | ReSi | 306 | SbBi | 336 | WBi |
| 7 | AgGe | 37 | AlNb | 67 | BSn | 97 | CrMo | 127 | FeNb | 157 | GaZn | 187 | HfRu | 217 | LaNb | 247 | NbPb | 277 | ReSn | 307 | SiSn | 337 | YZn |
| 8 | AgHf | 38 | AlPb | 68 | BTe | 98 | CrBi | 128 | FePb | 158 | GaZr | 188 | HfSb | 218 | LaPb | 248 | NbRe | 278 | ReTe | 308 | SiTe | 338 | YZr |
| 9 | AgIn | 39 | AlRe | 69 | BW | 99 | CuFe | 129 | FeRe | 159 | GaTa | 189 | HfSi | 219 | LaRe | 249 | NbRu | 279 | ReW | 309 | SiW | 339 | YTa |
| 10 | AgLa | 40 | AlRu | 70 | BY | 100 | CuGa | 130 | FeRu | 160 | GaMo | 190 | HfSn | 220 | LaRu | 250 | NbSb | 280 | ReY | 310 | SiY | 340 | YMo |
| 11 | AgMn | 41 | AlSb | 71 | BZn | 101 | CuGe | 131 | FeSb | 161 | GaBi | 191 | HfTe | 221 | LaSb | 251 | NbSi | 281 | ReZn | 311 | SiZn | 341 | YBi |
| 12 | AgNb | 42 | AlSi | 72 | BZr | 102 | CuHf | 132 | FeSi | 162 | GeHf | 192 | HfW | 222 | LaSi | 252 | NbSn | 282 | ReZr | 312 | SiZr | 342 | ZnZr |
| 13 | AgPb | 43 | AlSn | 73 | BTa | 103 | CuIn | 133 | FeSn | 163 | GeIn | 193 | HfY | 223 | LaSn | 253 | NbTe | 283 | ReTa | 313 | SiTa | 343 | ZnTa |
| 14 | AgRe | 44 | AlTe | 74 | BMo | 104 | CuLa | 134 | FeTe | 164 | GeLa | 194 | HfZn | 224 | LaTe | 254 | NbW | 284 | ReMo | 314 | SiMo | 344 | ZnMo |
| 15 | AgRu | 45 | AlW | 75 | BBi | 105 | CuMn | 135 | FeW | 165 | GeMn | 195 | HfZr | 225 | LaW | 255 | NbY | 285 | ReBi | 315 | SiBi | 345 | ZnBi |
| 16 | AgSb | 46 | AlY | 76 | CrCu | 106 | CuNb | 136 | FeY | 166 | GeNb | 196 | HfTa | 226 | LaY | 256 | NbZn | 286 | RuSb | 316 | SnTe | 346 | ZrTa |
| 17 | AgSi | 47 | AlZn | 77 | CrFe | 107 | CuPb | 137 | FeZn | 167 | GePb | 197 | HfMo | 227 | LaZn | 257 | NbZr | 287 | RuSi | 317 | SnW | 347 | ZrMo |
| 18 | AgSn | 48 | AlZr | 78 | CrGa | 108 | CuRe | 138 | FeZr | 168 | GeRe | 198 | HfBi | 228 | LaZr | 258 | NbTa | 288 | RuSn | 318 | SnY | 348 | ZrBi |
| 19 | AgTe | 49 | AlTa | 79 | CrGe | 109 | CuRu | 139 | FeTa | 169 | GeRu | 199 | InLa | 229 | LaTa | 259 | NbMo | 289 | RuTe | 319 | SnZn | 349 | TaMo |
| 20 | AgW | 50 | AlMo | 80 | CrHf | 110 | CuSb | 140 | FeMo | 170 | GeSb | 200 | InMn | 230 | LaMo | 260 | NbBi | 290 | RuW | 320 | SnZr | 350 | TaBi |
| 21 | AgY | 51 | AlBi | 81 | CrIn | 111 | CuSi | 141 | FeBi | 171 | GeSi | 201 | InNb | 231 | LaBi | 261 | PbRe | 291 | RuY | 321 | SnTa | 351 | MoBi |
| 22 | AgZn | 52 | BCr | 82 | CrLa | 112 | CuSn | 142 | GaGe | 172 | GeSn | 202 | InPb | 232 | MnNb | 262 | PbRu | 292 | RuZn | 322 | SnMo | | |
| 23 | AgZr | 53 | BCu | 83 | CrMn | 113 | CuTe | 143 | GaHf | 173 | GeTe | 203 | InRe | 233 | MnPb | 263 | PbSb | 293 | RuZr | 323 | SnBi | | |
| 24 | AgTa | 54 | BFe | 84 | CrNb | 114 | CuW | 144 | GaIn | 174 | GeW | 204 | InRu | 234 | MnRe | 264 | PbSi | 294 | RuTa | 324 | TeW | | |
| 25 | AgMo | 55 | BGa | 85 | CrPb | 115 | CuY | 145 | GaLa | 175 | GeY | 205 | InSb | 235 | MnRu | 265 | PbSn | 295 | RuMo | 325 | TeY | | |
| 26 | AgBi | 56 | BGe | 86 | CrRe | 116 | CuZn | 146 | GaMn | 176 | GeZn | 206 | InSi | 236 | MnSb | 266 | PbTe | 296 | RuBi | 326 | TeZn | | |
| 27 | AlB | 57 | BHf | 87 | CrRu | 117 | CuZr | 147 | GaNb | 177 | GeZr | 207 | InSn | 237 | MnSi | 267 | PbW | 297 | SbSi | 327 | TeZr | | |
| 28 | AlCr | 58 | BIn | 88 | CrSb | 118 | CuTa | 148 | GaPb | 178 | GeTa | 208 | InTe | 238 | MnSn | 268 | PbY | 298 | SbSn | 328 | TeTa | | |
| 29 | AlCu | 59 | BLa | 89 | CrSi | 119 | CuMo | 149 | GaRe | 179 | GeMo | 209 | InW | 239 | MnTe | 269 | PbZn | 299 | SbTe | 329 | TeMo | | |
| 30 | AlFe | 60 | BMn | 90 | CrSn | 120 | CuBi | 150 | GaRu | 180 | GeBi | 210 | InY | 240 | MnW | 270 | PbZr | 300 | SbW | 330 | TeBi | | |

Figure 4.1 Binary composition list

## *4.2 Instrument setup*

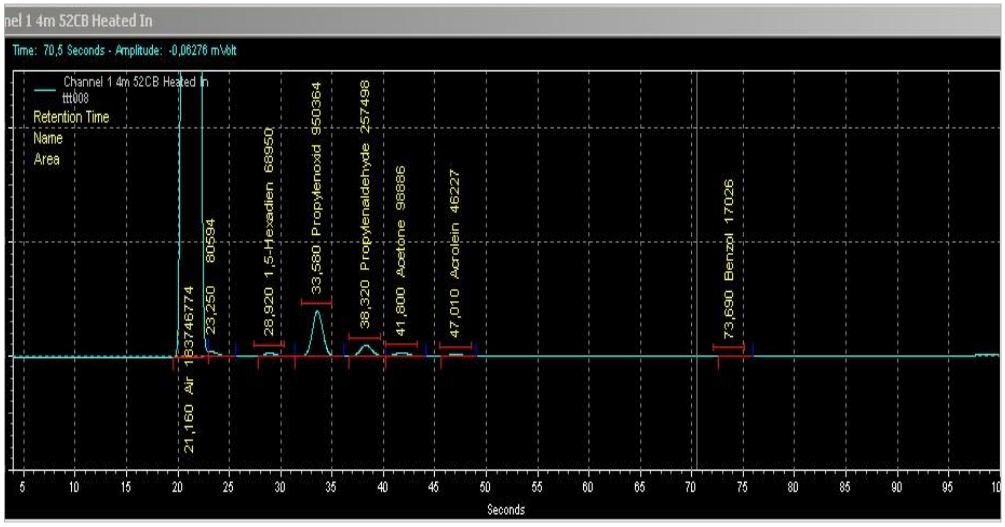


Figure 4.2 Peaks of possible products determined by GC 52CB column

The following conditions of the stage robot reactor were used: a flow rate of 5 mL/min was used at temperatures in a range from 200 °C to 400 °C with increments of 50 °C. Two feed-gas conditions

were used: rich gas 9:1 ($C_3H_6$ 64.8%, $O_2$ 7.2%, $N_2$ 27%) and lean gas 4:1 ($C_3H_6$ 45.6%, $O_2$ 11.4%, $N_2$ 43%) at atmospheric pressure.

For feed and product-gas analyses, a micro-gas chromatograph (model CP 4900; Varian) was used with two packed columns, Porapak Q and polar 52CB. The 52CB column was used in parallel to separate 1,5-hexadien, propylene oxide, propylene aldehyde, acetone, acrolein and benzol as shown in Figure 4.2. In this study, only these 6 oxidized products from propene were considered as main products and other products were considered as side products. The first column, the polar 52CB, was used at a column temperature of 60 °C, injector temperature 110 °C, inject time 80 m sec, initial pressure 50 kP, run time 100 sec and acquisition delay 4 sec. The PPQ column was used at a column temperature of 80 °C, inject temperature 30 °C and inject time 50 m sec and all other conditions were identical to the 52CB. In addition, sample time, sample line temperature and stabilizing time of the Micro-GC were set to 20 sec, 80 °C and 5 sec, respectively. The product peak data received by the Micro-GC were analyzed with the help of the Matlab Program.

## *4.3 Experimental setup and results*

The experiments of both libraries, 1G1L and 1G2L, with the stage robot were carried out with increasing temperatures from 200 °C to 400 °C. Each increment was 50 °C to provide five measurement points. Product-gas (1,5-Hexadiene, Propyleneoxide, Propylenealdehyde, Acetone, Acrolein and Benzol) was analyzed by the gas chromatographic method.

The fuel-lean conditions or stoichiometric reactions save the fuel as feed-stock. However, such conditions have the tendency to increase burning of the fuel. Because of this, the work was carried out in a propene-rich condition with 9:1 and 4:1 flow rates, which caused the experiment to perform with a high $C_3/O_2$ ratio to limit total oxidation. The feed ratios were compatible with the selective oxidation for the formation of propene oxide. Because of less stability of propene oxide, it is expected to carry it out under a fuel-rich condition which used to apply in a membrane reactor or recycling process for such selective oxidation of butane to maleic anhydride[149] [150]. Even though this condition ($C_3/O_2$=9; $C_3/O_2$=4) has the advantage in increasing selective oxidation, the problem of the deactivation of catalysts is increased by especially coking. During catalytic reactions involving hydrocarbons or carbon oxides, side reaction can occur on the catalyst surface leading to the formation of coke or carbon, which tends to cause deactivation of catalysts. Therefore, the

decision for a reliable feed-ratio still remains controversial, depending on using the type of reactor. Moreover, because the stage robot reactor cannot evaluate, elucidate and test the deactivation or pretreatment of catalysts, it is still difficult to explain results under different feed ratio conditions.
Using data visualization to find insight in experimental results is critical to data analysis. For this, the selectivity and conversion were used, which were defined using the following formulas:

$$\text{Propene Conversion} = \frac{(\text{GC siganl inensity of propene})_{\text{in}} - (\text{GC siganl inensity of propene})_{\text{out}}}{(\text{GC siganl inensity of propene})_{\text{in}}} \quad (1)$$

To calculate the conversion and selectivity, the GC signal intensities of reactant and product were used instead of the moles. That means these parameters only show the trend or pattern of the results, and do not provide molar amounts of product produced. However, the global trends should be sufficient for the primary screening.

$$\text{Selectivity of product a} = \frac{\text{GC singal intensity of Propene oxide}}{\sum_{i=1}^{5} P_i(\text{GC singal intensity of Product i})} \quad (2)$$

The symbol of Pa means one among five products. The term $\sum P_i$describes the sum of five products based on
$P_i = \{1{,}5\text{Hexadiene},\ \text{Propyleneoxide},\ \text{Propylenealdehyde},\ \text{Acetone},\ \text{Acrolein},\ \text{Benzol}\}$.
In order to visualize and analyze results, Matlab program (see also appendix) was used as follows.
Since 351 samples with five temperatures were measured, 1755 experimentations were carried out. Such area of high conversion and selectivity is generally interesting for engineers because of commercial reasons. However, it was difficult to analyze the data of the first generation because less selectivity and conversion were shown with a lot of overlapped data. In order to solve this problem, the following normalized expression was used for the conversion and selectivity of representing the hits of the tremendous data. The normalizations of two parameters were calculated by dividing the data by the maximum values of the generation, which means conversion = 1 and selectivity = 1, the maximum values, respectively. The color bar on the right side of Figure 4.3 shows the measured temperature from 200 °C to 400 °C.

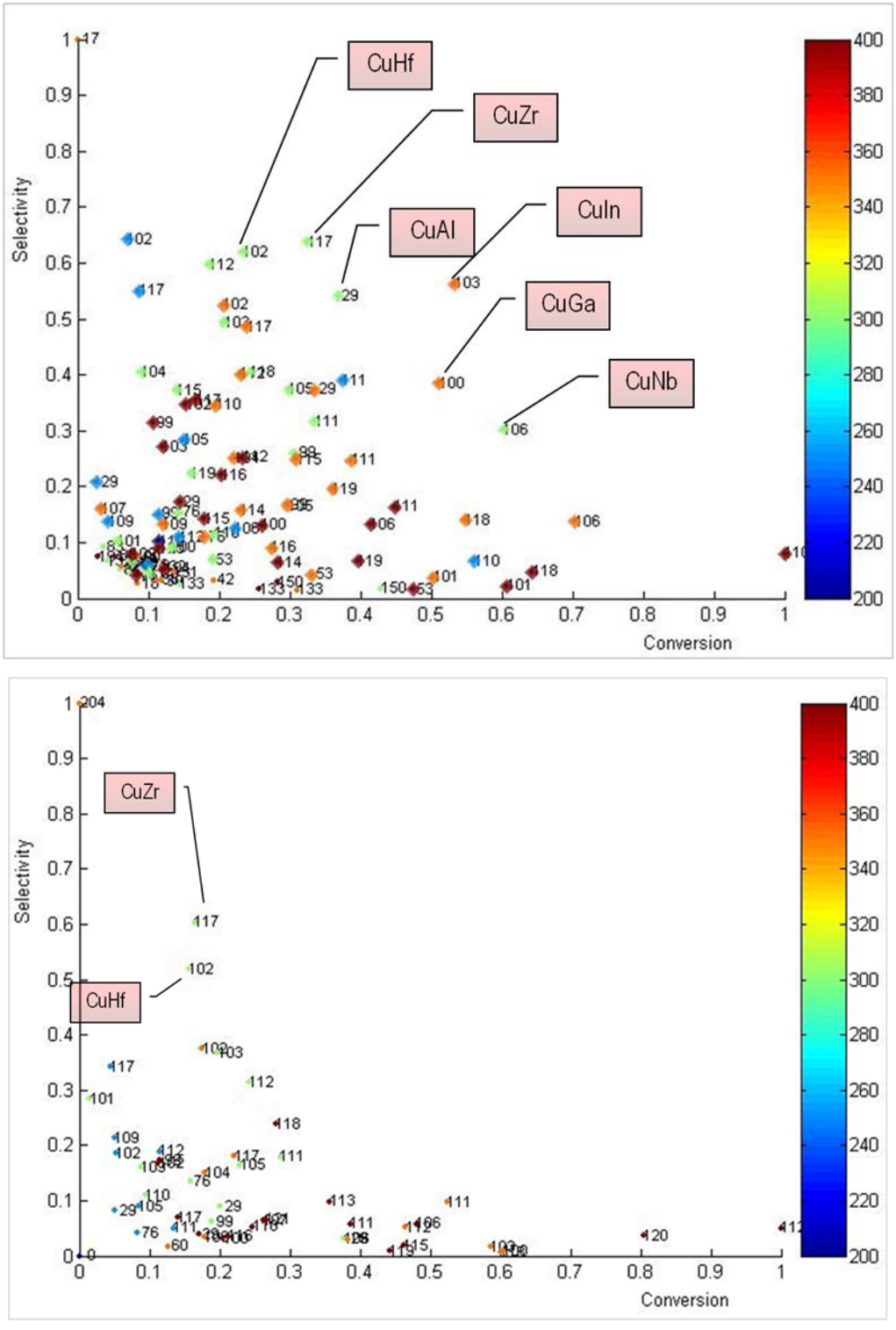


Figure 4.3 Normalization of selectivity vs. conversion with feed-gas ratio 9:1(up) and 4:1(down) for propene oxide Reaction condition: around 400 μmol of catalyst. Total flow rate: 5 mL/min ($C_3H_6$:$O_2$=9:1 and $C_3H_6$:$O_2$=4:1 vol%)

Figure 4.3 describes that, among hit samples, the most active catalysts of the first generation (1G1L, 1G2L), CuHf, CuZr, CuAl, CuIn, CuGa and CuNb show potential as catalysts for propene oxidation with a feed-gas ratio 9:1. An increasing temperature has proportional influence to the conversion. Even more, only CuZr and CuHf show high selectivity with feed-gas ratio 4:1 as well as 9:1, making them very interesting candidates. Moreover, these catalysts have remarkable activity at the low reaction temperature of 300 °C.

Even though the others are potentially good materials for the catalyst propene oxide, they can induce the problem of deactivation of catalysts. Therefore, after runs (351 materials) of the first generation, CuHf and CuZr were selected for the design of second generation.

## *4.4 Secondary generation*

Table 4.3 Summary of library for second generation

| | Library | Key elements | Composition | Doping elements |
|---|---|---|---|---|
| 1 | 2G1L | CuHf, CuZr | CuHfX, CuZrX CuZr, CuHf, CuTi | X=[Hf, Ti, Al, Fe, Mn, La, Nb, Sb, Si, Sn, Zn, Ta, Ru, In] |
| 2 | 2G2L | " | " | " |
| 3 | 2G3L | Cu | CuXY | X,Y=[Mn, Sn, Sb, Cr, In, La, Zr] |

In order to prepare the library for the secondary generation, CuHf and CuZr were chosen as a starting point because they have the best catalytic activity for propene oxidation in the previous experiments. Next, Cu with compositions [0.3, 0.5, 0.7] was combined with the composition of two other elements such as Zr [0.2, 0.4, 0.6] and Hf [0.2, 0.4, 0.6]. The rest of the composition was one of the 14 elements, X=[Hf, Ti, Al, Fe, Mn, La, Nb, Sb, Si, Sn, Zn, Ta, Ru, In]. Based on these compositions of $Cu_aHf_bX_c$ and $Cu_aZr_bX_c$, 84 samples were synthesized. In addition, the binary compositions of $Cu_AZr_B$, $Cu_AHf_B$ and $Cu_ATi_B$ with 0.1 composition increments were prepared. The catalysts for two libraries were prepared using two different sol-gel methods such as the propionic route (2G1L) and ethyl glycol route (2G2L) (please see chapter 7.4 catalyst preparation). Finally, two libraries containing 199 samples were tested by the stage robot reactor.

According to first generation (1G1L, 1G2L), it is shown that Cu has quite good activity in the formation of the propylene oxide. Therefore, another library (2G3L) was prepared with copper containing composition of 7 elements (Mn, Sn, Sb, Cr, In, La, Zr) by using propionic route. Cu [0.3, 0.5, 0.7] was combined $X_AY_B$ to receive 200 samples.

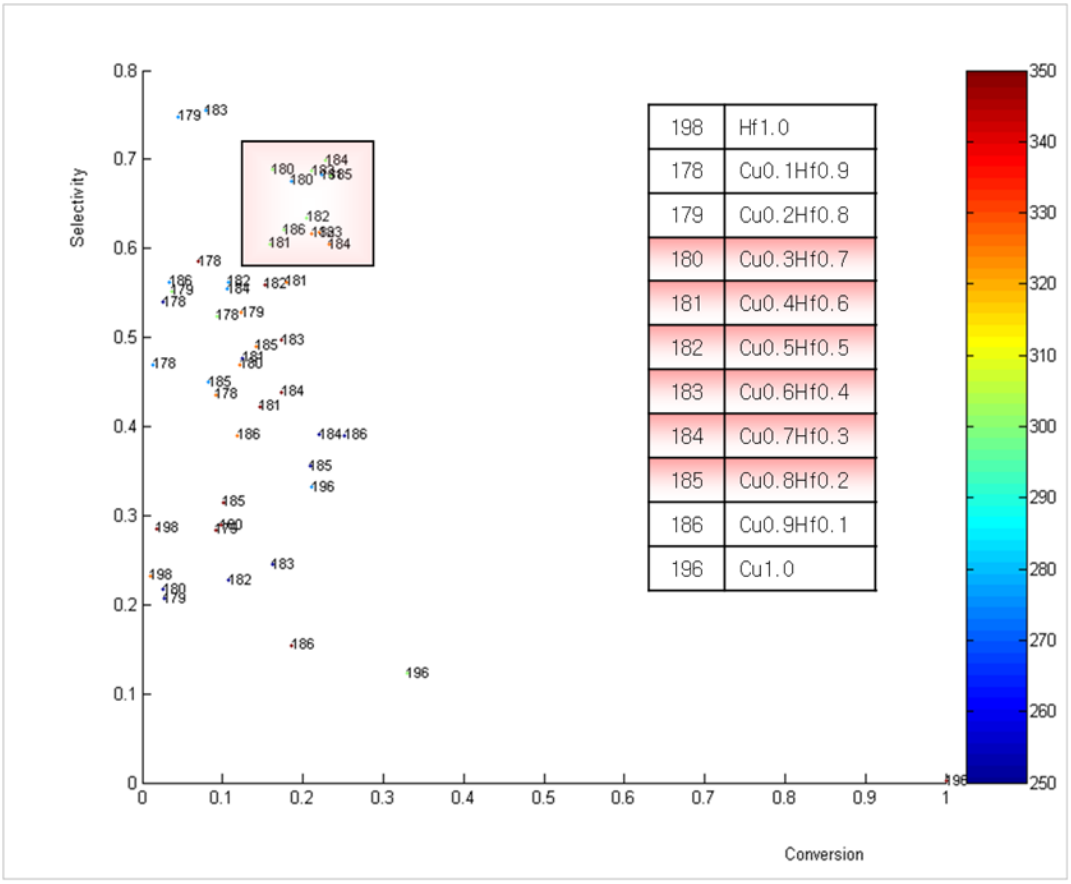


Figure 4.4 Normalization of selectivity vs. conversion for propene oxide in 2G1L (up) and 2G2L (down)
Reaction condition: around 400 μmol of catalyst. Total flow rate: 5 mL/min ($C_3H_6$:$O_2$=1:1 vol%)

These tests were carried out at atmospheric pressure with the stage robot reactor in the temperature range of 250 °C to 350 °C. In order to study the result in oxygen rich conditions, the feed-gas composition of $C_3H_8$:$O_2$ = 1:1 with a total flow rate of 5 mL/min was applied to the propene reaction. Figure 4.4 describes that Cu-Hf and Cu-Ti showed most active for propene oxide production in the two libraries. Especially, $Cu_{0.3\text{-}0.8}Hf_{0.2\text{-}0.7}$ in the library 2G1L showed good selectivity in a broad temperature range between 300 °C and 350 °C. Library 2G2L showed that $Cu_{0.1\text{-}0.7}Ti_{0.3\text{-}0.9}$ were potential catalysts for the selective oxidation propene to propene oxide.

## *4.5 Hit validation by conventional test*

In the library of the second generation, several catalysts ($Cu_{0.3}Zr_{0.4}Sn_{0.3}$, $Cu_{0.5}Hf_{0.2}Sn_{0.3}$, $Cu_{0.7}Hf_{0.2}Sn_{0.1}$, $Cu_{0.3}Hf_{0.2}Zr_{0.5}$, $Cu_{0.8}Zr_{0.2,}$ and the binary composition of Cu-Hf and Cu-Ti) were found active for propene oxide formation. Conventional tests to confirm the activity of the catalysts for propylene oxide formation were studied in a fixed-bed tubular flow reactor (25 mL/min) at atmospheric pressure without a pre reduction of the catalyst. The results were disappointing since there was no activity of propylene oxide. Eventually, the catalysts of conventional testing failed to show reproducibility of catalysts obtained in high-throughput method. The reasons can be explained as follows:

First of all, catalyst scale-up was unsuccessful. It is well known that scaling up catalyst synthesis has always been a problem since catalysts are very sensitive to their method of a preparation. In this study for the high-throughput method, 300–400 μmol of catalysts were prepared, but 500 mg of catalysts were synthesized for conventional testing. It is guessed that the functional catalyst bodies were modified during catalyst scale-up.

Secondly, fast deactivation of catalysts took place during the conventional test. In the high-throughput method with the stage robot, the deactivation of catalysts was not considered and not checked. Nevertheless, sintering, carbon deposition and decreasing of surface area can induce deactivation during conventional tests.

## *4.6 Discussion*

Despite the fact that it was not possible to reproduce the hit obtained in the primary screening by the secondary screening, the results of the high-throughput test are here summarized. Several catalysts of the first generation were found to containing cooper, for examples, CuHf, CuZr, CuAl, CuIn, CuGa and CuNb. It is well known that copper can function as epoxidation catalyst. Cu/silica[111], NaCl-Modified $VCe_{1-X}Cu_X$ Oxide[112], and $Cu/SiO_2$ and Mn-on-$Cu/SiO_2$[151] were reported as the catalysts of propene epoxidation by molecular oxygen as the oxidant.

Li *et al.* showed that keeping the Cu species in its low valence is very important for propylene epoxidation and the role of $H_2$ in the feed-gas helps to keep the Cu species at its low valence[112]. Based on XPS data of Cu $2p_{3/2,}$ it is induced that $Cu^0$ may be the active phase in NaCl-modified $VCe_{1-X}Cu_X$ catalysts for propylene epoxidation. Moreover, increasing the amount of $H_2$ in the feedstock can enhance the PO selectivity and keep the catalyst stable. Consequently, it seems that a reduction process with $H_2$ gas is necessary to get the low-valent Cu species before using Cu based catalysts.

To the best of our knowledge, even though the *in situ* auto reduction process is preferable, no commercial catalyst has been developed. Therefore, it is required either to add $H_2$ in the feed or to reduce the catalyst with hydrogen before using the catalysts. A typical reduction process is performed at 200-300 °C in 5% $H_2$/He for 1-2 h[111, 112]. It seems that, without reduction process, the deactivation of catalysts takes place even faster.

The question remains if the reduction process described above is also necessary in conventional tests for catalysts as discovered in the stage robot reactor. It is still unclear to answer this question. However, the open reactor system of the SRR may be the cause of the different results when compared to the conventional reactor. Since the SRR has a short reaction time in catalyst reactions with the open structure of the reactor, it seems to show the activity of Cu based catalysts in first and second generation.

Moreover, the instability of propylene oxide with different topographical surface on catalysts can produce other products by a post reaction of propylene oxide as well as direct oxidation. For example, the study of selective propene epoxidation with immobilized Au has shown that the catalyst is extremely sensitive to the nanoparticle size and shape, and if particles are larger than 4 nm, the reaction mainly proceeds to catalyzed propene combustion[152].

In view of these problems, of which fast deactivation of catalysts and poor stability of propylene oxide are the most notable, the stage robot reactor still has the problem to develop reliably catalysts, especially when used in optimization or scale-up experiments. For this reason, we have planned to develop a new high-throughput reactor suitable for secondary screening.

# 5 Catalyst for propene to acrolein

After facing difficulties during the selective oxidation of propene to propene oxide, we turned out attention to acrolein as the main product. At the same time, new high-throughput reactor was developed.

## *5.1 Primary screening in ternary composition*

### *5.1.1 1G3L*

It is well known that metals have individual properties concerning absorbing gases on their surfaces. Table 5.1 shows the extent of absorption with gases such as $O_2$, $C_2H_2$, $C_2H_4$, CO, $H_2$, $CO_2$ and $N_2$. It is assumed that, for the selective oxidation of propene to acrolein, the absorption of hydrocarbons, $H_2$ and $O_2$ will affect the reaction. This hypothesis has been considered in the design of new libraries for discovery of new catalysts.

Table 5.1 Ability of metals to chemisorb simple molecules[153]

| Group | Metals | Periodic | $O_2$ | $C_2H_2$ | $C_2H_4$ | CO | $H_2$ | $CO_2$ | $N_2$ |
|---|---|---|---|---|---|---|---|---|---|
| A | Ti, Zr, Hf, | IVA | | | | | | | |
| | V, Nb, Ta, | VA | + | + | + | + | + | + | + |
| | Cr, Mo, W, | VIA | | | | | | | |
| | Fe, Ru, Os | VIIIA | | | | | | | |
| B1 | Ni, Co | VIIIA | + | + | + | + | + | + | - |
| B2 | Rh, Pd, Pt, Ir | VIIIA | + | + | + | + | + | - | - |
| B3 | Mn, Cu | VIIA, I B | + | + | + | + | ± | - | - |
| C | Al, Au | IIIB, B | + | + | + | + | - | - | - |
| D | Li, Na, K | IA | + | + | - | - | - | - | - |
| E | Mg, Ag, Zn, Cd, | IB-VB | | | | | | | |
| | In, Si, Ge, Sn, | | + | - | - | - | - | - | - |
| | Pb, As, Sb, Bi, Pd | | | | | | | | |

+ Strong chemisorptions, ± weak, - unobservable

Stock solutions with 0.25 mol/L concentration were prepared with 27 elements (Ga, Cr, Cu, Cd, Fe, Co, Ni, Zr, V, Zn, Sn, K, Nb, Ca, Ru, Ce, SrBr, Ag, Hf, Cs, W, Re, Ba, Bi, Pb, Pd, Mn). According to the values of chemisorptions in table 5.1, coefficient parameters were used with 0, 0.5 and 1. If there was absorption of gas on the surface of material, the value was 1 and the other case was 0. In the case of lack of data, the value 0.5 was given.

Band-gap (forbidden zone) theory was applied[154, 155]. High band gap decreases the intrinsic conductivity, which has a mutual relation with the catalyst activity. In order to design the ternary composition as $M1_AM2_BM3_C$, preference-factors were calculated with the following formula:

$$\text{Preference-factor} = \sum_{i=1}^{3} E_i(M\,1_i) \times A + \sum_{i=1}^{3} E_i(M\,2_i) \times B + \sum_{i=1}^{3} E_i(M\,3_i) \times C \qquad (1)$$

The parameters used for calculating the preference-factor are shown in the following table 5.2. By the above formula, 200 samples having lower preference factor were filtered to select the candidates of catalyst for ternary composition, based on the assumption that the potential of catalyst to selective oxidation is proportional to the preference factor.

Table 5.2 Parameter of gas absorption and band gap energy

| N | M | $E_1$ ($O_2$) | $E_2$ ($C_nH_n$) | $E_3$ ($H_2$) | $B(M_i)$ | N | M | $E_1$ ($O_2$) | $E_2$ ($C_nH_n$) | $E_3$ ($H_2$) | $B(M_i)$ |
|---|---|---|---|---|---|---|---|---|---|---|---|
| 1 | Ga | 0.5 | 0.5 | 0.5 | 4.5 | 15 | Ru | 1 | 1 | 1 | 0.1 |
| 2 | Cr | 1 | 1 | 1 | 1.7 | 16 | Ce | 0.5 | 0.5 | 0.5 | 1.1 |
| 3 | Cu | 1 | 1 | 1 | 2 | 17 | SrBr | 0.5 | 0.5 | 0.5 | 5.77 |
| 4 | Cd | 1 | 0 | 0 | 2.3 | 18 | Mn | 1 | 1 | 1 | 3.7 |
| 5 | Fe | 1 | 1 | 1 | 2.3 | 19 | Ag | 1 | 0 | 0 | 1.2 |
| 6 | Co | 1 | 1 | 1 | 0.6 | 20 | Hf | 1 | 1 | 1 | 5.6 |
| 7 | Ni | 1 | 1 | 1 | 3.7 | 21 | Cs | 0.5 | 0.5 | 0.5 | 6 |
| 8 | Zr | 1 | 1 | 1 | 5 | 22 | W | 1 | 1 | 1 | 2.8 |
| 9 | V | 1 | 1 | 1 | 2.3 | 23 | Re | 0.5 | 0.5 | 0.5 | 2.3 |
| 10 | Zn | 1 | 0 | 0 | 3.3 | 24 | Ba | 0.5 | 0.5 | 0.5 | 5.1 |
| 11 | Sn | 1 | 0 | 0 | 4.3 | 25 | Bi | 1 | 0 | 0 | 2.9 |
| 12 | K | 1 | 1 | 0 | 6 | 26 | Pb | 1 | 0 | 0 | 2.8 |
| 13 | Nb | 1 | 1 | 1 | 3.5 | 27 | Pd | 0.5 | 0.5 | 0.5 | 1.5 |
| 14 | Ca | 0.5 | 0.5 | 0.5 | 7.5 | | | | | | |

In this regard, two hypothesizes were considered. First, the property of absorbing gases on the surface of materials is a precondition to take place for any reactions like selective oxidation or total oxidation. Therefore, the combination of metals which have a high preference-factor may have a higher chance to perform during the catalytic test. Second, the primary factor for the enhanced activity of catalyst is a lowered band gap with a larger surface area[156]. However, in the case of low band gap, it may tend to proceed to total oxidation, so a high preference factor is considered the expectation value for the design of library in this experiment.

### *5.1.2 1G4L*

A ternary composition of Cr-Ga-X with 24 elements X (Cr, Cd, Fe, Co, Ni, Zr, V, Zn, Sn, K, Nb, Ca, Ru, Ce, SrBr, Ag, $Hf_1$, Cs, W, Re, Ba, Bi, Pb, $Hf_2$) was prepared for the new library (1G4L) by means of the two sol-gel methods, the propionic acid and ethylene glycol route. At the beginning of the composition spread, $Cr_AGa_B$ was defined with A:B = [0.45:0.45, 0.4:0.4, 0.5:0.4, 0.4:0.5], and the rest was added with 24 elements. Through this method, 96×2 samples were synthesized by two recipes. In addition to these, 8 samples based on a binary composition of CrGa were also added to the library. Overall, 200 samples were prepared in this library (1G4L).

## *5.2 The check of hit validation*

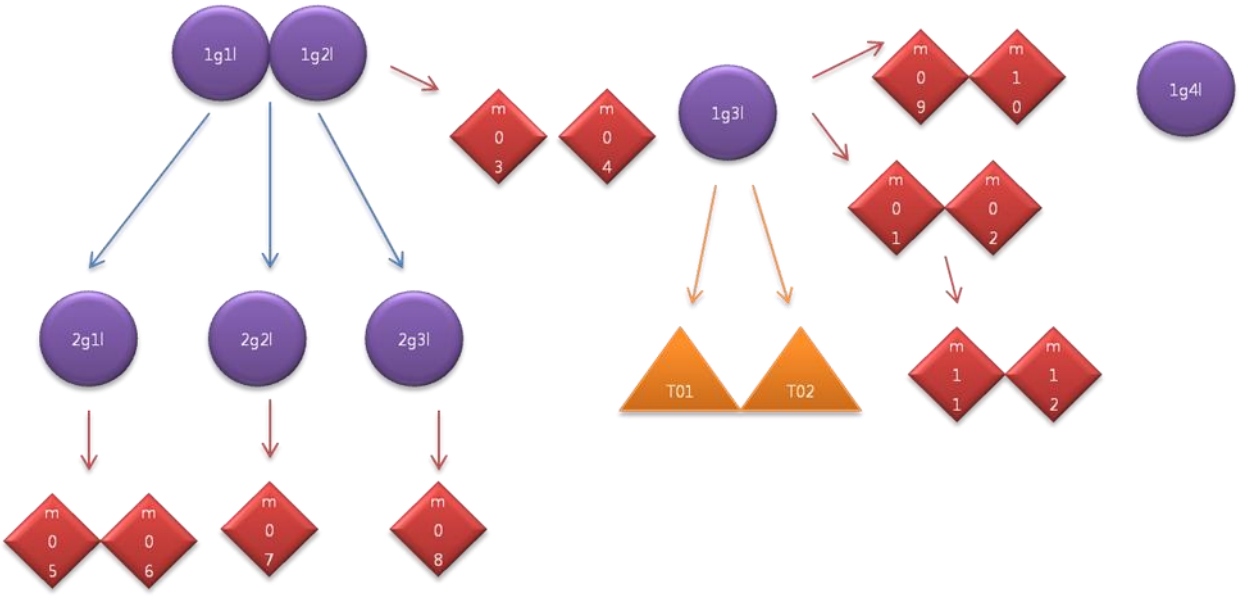


Figure 5.1 Flow chart of library design

After the development of the 10-fold parallel reactor, previous experiments were considered to obtain some information for finding the candidates of catalysts to acrolein production. Therefore, the results of six libraries (1G1L, 1G2L, 2G1L, 2G2L, 2G3L, 1G3L) presented in Figure 5.1 were used to select potential catalysts. A total 12 runs were prepared with the catalyst composition as summarized in table 5.3. Tests of M01–M08 were performed to validate the hits. In addition to these, tests of M09–M10 were done to optimize composition and recipe.

Table 5.3 Chemical composition information for 10-fold parallel reactor

| | M01 | M02 | M03 | M04 | M05 | M06 |
|---|---|---|---|---|---|---|
| 1 | $Cu_{0.3}Ce_{0.3}SrBr_{0.3}$ | Empty | Empty | $Hf_{0.5}Re_{0.5}$ | empty | Empty |
| 2 | $Cu_{0.35}Ce_{0.47}SrBr_{0.18}$ | $Ga_{0.47}Cu_{0.35}Pd_{0.18}$ | $Al_{0.5}Ru_{0.5}$ | $Hf_{0.5}Ru_{0.5}$ | $Cu_{0.3}Hf_{0.2}La_{0.5}$ | $Cu_{0.5}Hf_{0.4}Sn_{0.1}$ |
| 3 | $Cu_{0.4}Zn_{0.3}Ru_{0.3}$ | $Ga_{0.4}Cu_{0.3}Pd_{0.3}$ | $B_{0.5}Cu_{0.5}$ | $Hf_{0.5}Sb_{0.5}$ | $Cu_{0.3}Hf_{0.2}Nb_{0.5}$ | $Cu_{0.3}Zr_{0.2}La_{0.5}$ |
| 4 | $Cu_{0.47}Zn_{0.35}Ru_{0.18}$ | $Ga_{0.35}Cu_{0.47}Pd_{0.18}$ | $Cu_{0.5}Ga_{0.5}$ | $Hf_{0.5}Te_{0.5}$ | $Cu_{0.3}Hf_{0.2}Sb_{0.5}$ | $Cu_{0.3}Zr_{0.4}Nb_{0.3}$ |
| 5 | $Cu_{0.4}Mn_{0.3}Ag_{0.3}$ | $Ga_{0.4}Cu_{0.5}Pd_{0.1}$ | $Cu_{0.5}W_{0.5}$ | $Ag_{0.5}Cu_{0.5}$ | $Cu_{0.3}Zr_{0.5}Hf_{0.2}$ | $Cu_{0.5}Zr_{0.2}La_{0.3}$ |
| 6 | $Cu_{0.4}Mn_{0.3}Ag_{0.3}$ | $Ga_{0.4}Cu_{0.3}Pd_{0.3}$ | $Ge_{0.5}Ru_{0.5}$ | $Al_{0.5}Cu_{0.5}$ | $Cu_{0.3}Hf_{0.4}Sn_{0.3}$ | $Cu_{0.5}Zr_{0.2}Sb_{0.3}$ |
| 7 | $Co_{0.4}Mn_{0.3}Ba_{0.3}$ | $Ga_{0.2}Cu_{0.8}$ | $Ge_{0.5}Sn_{0.5}$ | $Hf_{0.5}Cu_{0.5}$ | $Cu_{0.3}Hf_{0.4}Zn_{0.3}$ | $Cu_{0.7}Zr_{0.2}Ta_{0.1}$ |
| 8 | $Co_{0.47}Mn_{0.35}Ba_{0.18}$ | $Cu_{0.9}Pd_{0.1}$ | $Ge_{0.5}In_{0.5}$ | $Ag_{0.5}Nb_{0.5}$ | $Cu_{0.3}Hf_{0.6}Nb_{0.1}$ | $Cu_{0.6}Hf_{0.4}$ |
| 9 | Re (AuCe) | $Ga_{0.5}Cu_{0.4}Pd_{0.1}$ | $Cr_{0.5}Sb_{0.5}$ | $Cu_{0.5}Nb_{0.5}$ | $Cu_{0.5}Hf_{0.2}La_{0.3}$ | $Cu_{0.9}Ti_{0.1}$ |
| 10 | Re (Hopkalit) | $Cu_{1.0}$ | $Cu_{0.5}In_{0.5}$ | $Fe_{0.5}Mo_{0.5}$ | $Cu_{0.5}Hf_{0.4}Si_{0.1}$ | $Cu_{1.0}$ |
| | M07 | M08 | M09 | M10 | M11 | M12 |
| 1 | Empty | empty | $Ga_{0.4}Cu_{0.3}Pd_{0.3}$ | $Ga_{0.3}Cu_{0.4}Pd_{0.3}$ | $Pd_{0.1}Cu_{0.5}Ga_{0.4}$ | $Mo_{0.91}Pd_{0.03}Cu_{0.03}Ga_{0.03}$ |
| 2 | $Cu_{0.3}Hf_{0.2}Ta_{0.5}$ | $Cu_{0.5}Sb_{0.2}In_{0.3}$ | $Ga_{0.3}Cu_{0.4}Pd_{0.3}$ | $Ga_{0.2}Cu_{0.5}Pd_{0.3}$ | $Pd_{0.1}Cu_{0.5}Ga_{0.4}$ | $Mo_{0.91}Pd_{0.03}Cu_{0.03}Ga_{0.03}$ |
| 3 | $Cu_{0.5}Hf_{0.2}Zn_{0.3}$ | $Cu_{0.5}Mn_{0.3}Cr_{0.2}$ | $Ga_{0.3}Cu_{0.3}Pd_{0.4}$ | $Ga_{0.1}Cu_{0.6}Pd_{0.3}$ | $Pd_{0.1}Cu_{0.5}Ga_{0.4}$ | $Mo_{0.91}Pd_{0.03}Cu_{0.03}Ga_{0.03}$ |
| 4 | $Cu_{0.3}Zr_{0.2}In_{0.5}$ | $Cu_{0.5}Sb_{0.3}In_{0.2}$ | $Ga_{0.4}Cu_{0.3}Pd_{0.3}$ | $Cu_{0.7}Pd_{0.3}$ | $Pd_{0.1}Cu_{0.4}Ga_{0.5}$ | $Mo_{0.91}Pd_{0.03}Cu_{0.03}Ga_{0.03}$ |
| 5 | $Cu_{0.3}Zr_{0.4}Sb_{0.3}$ | $Cu_{0.7}Sn_{0.2}Sb_{0.1}$ | $Ga_{0.3}Cu_{0.4}Pd_{0.3}$ | $Ga_{0.2}Cu_{0.6}Pd_{0.2}$ | $Pd_{0.1}Cu_{0.4}Ga_{0.5}$ | $Mo_{0.82}Pd_{0.06}Cu_{0.06}Ga_{0.06}$ |
| 6 | $Cu_{0.3}Zr_{0.4}Zn_{0.3}$ | $Cu_{0.4}Sn_{0.3}La_{0.3}$ | $Ga_{0.3}Cu_{0.3}Pd_{0.4}$ | $Ga_{0.2}Cu_{0.7}Pd_{0.1}$ | $Pd_{0.1}Cu_{0.4}Ga_{0.5}$ | $Mo_{0.82}Pd_{0.06}Cu_{0.06}Ga_{0.06}$ |
| 7 | $Cu_{0.5}Zr_{0.2}Ti_{0.3}$ | $Cu_{0.4}Sb_{0.3}In_{0.3}$ | $Ga_{0.4}Cu_{0.3}Pd_{0.3}$ | $Ga_{0.1}Cu_{0.8}Pd_{0.1}$ | $Pd_{0.1}Cu_{0.3}Ga_{0.6}$ | $Mo_{0.82}Pd_{0.06}Cu_{0.06}Ga_{0.06}$ |
| 8 | $Cu_{0.7}Zr_{0.2}Hf_{0.1}$ | $Cu_{0.3}Mn_{0.4}Sb_{0.3}$ | $Ga_{0.3}Cu_{0.4}Pd_{0.3}$ | $Ga_{0.3}Cu_{0.3}Pd_{0.4}$ | $Pd_{0.1}Cu_{0.3}Ga_{0.6}$ | $Mo_{0.82}Pd_{0.06}Cu_{0.06}Ga_{0.06}$ |
| 9 | $Cu_{0.9}Ti_{0.1}$ | $Cu_{0.3}Mn_{0.3}La_{0.4}$ | $Ga_{0.3}Cu_{0.3}Pd_{0.4}$ | | $Pd_{0.1}Cu_{0.3}Ga_{0.6}$ | $Mo_{0.91}Pd_{0.03}Cu_{0.03}Ga_{0.03}$ |
| 10 | $Cu_{1.0}$ | $Cu_{0.3}Mn_{0.3}Zr_{0.4}$ | | | | $Mo_{0.82}Pd_{0.06}Cu_{0.06}Ga_{0.06}$ |

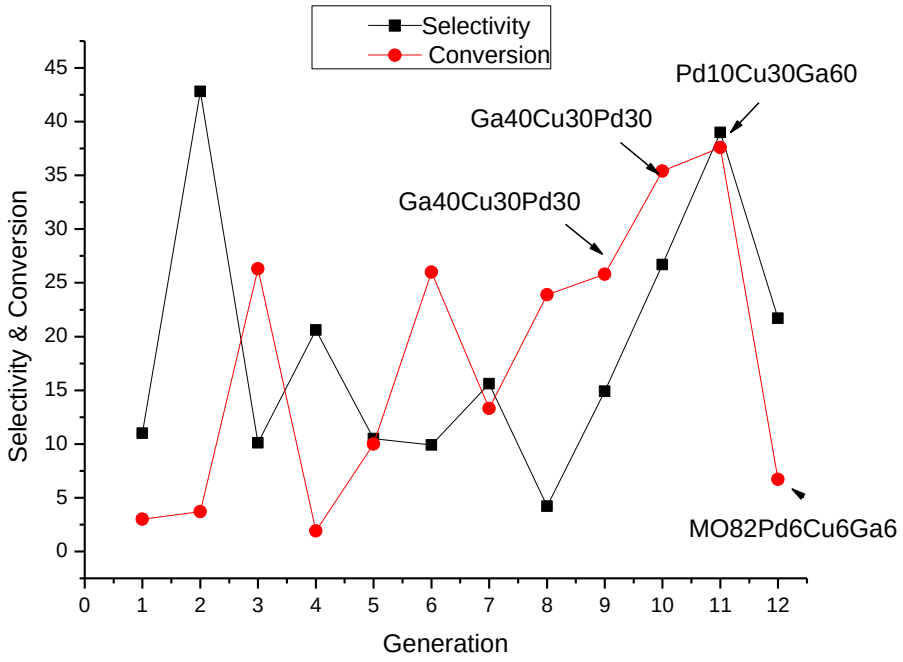


Figure 5.2 Selectivity and conversion through test number

Reaction condition: 50 mg of catalysts diluted with 100 mg of sand with particle size of 100-200 μm. Total flow rate: 25mL/min ($C_3H_6$:$O_2$:He=2:2:96 vol%)

Figure 5.2 shows the selectivity and conversion of the best catalysts in each run of the 10-fold parallel reactor based on the best activity of propene to acrolein. Out of 12 tests, $Pd_{10}Cu_{30}Ga_{60}$ showed the best performance with high selectivity and conversion. The increase of catalytic activity of $Cu_{40}Cu_{30}Pd_{30}$ from test M09 to M10 seems due to the increase of its surface area as shown in table 5.4. The surface area of catalysts was measured by nitrogen adsorption (Sorptomatic 1990, Carlo Erba). In addition to this, the dramatic decrease of activity of $Mo_{82}Pd_6Cu_6Ga_6$ could result from the decrease of surface area from 32.78 $m^2/g$ to 0.65 $m^2/g$. However, the amount of Pd also decreased in the catalysts, which could also be one of the reasons why its activity has decreased.

Table 5.4 Surface area of catalysts, $Ga_{40}Cu_{30}Pd_{30}$ and $MO_{82}Pd_6Cu_6Ga_6$

| Generation | Catalyst | Surface area |
|---|---|---|
| 9 | $Ga_{40}Cu_{30}Pd_{30}$ | 16.74 $m^2/g$ |
| 10 | $Ga_{40}Cu_{30}Pd_{30}$ | 32.78 $m^2/g$ |
| 12 | $MO_{82}Pd_6Cu_6Ga_6$ | 0.65 $m^2/g$ |

## *5.3 Discussion*

According to previous experiments by using the 10-fold parallel reactor, $Pd_{10}Cu_{30}Ga_{60}$ in the generation 11 was found as best potential catalysts for conversion of propene to acrolein. Therefore, the ternary composition spread of Pd-Ga-Cu was planned to examine.

Because of high cost of precious metals, such as Pt, Pd and Ru[157, 158], these are mainly used as doping elements in catalysts. Even though catalysts containing noble metals allow the reaction to run at mild conditions, especially at low temperature, the less noble metal containing catalyst is still suitable from a commercial perspective. For this study, the library (2G4L) was prepared to carry out the test with the stage robot reactor based on catalysts with maximum loading of Pd 10%.

A composition spread library of the mixed oxides of $Cu_{1–100}Pd_{0\text{-}10}Ga_{1\text{-}100}$ was planned with the help of Plattenbau software. Catalysts were transferred to the library plate and reactions at a temperature from 300-400 °C with increments of 50 were performed. The catalyst performance was determined with the GC signal intensity by TCD (thermal conductivity detector).

Figure 5.3 shows the catalytic activity of the ternary composition (Ga-Cu-Pd) spread by Matlab visualization (see also appendix). It describes that $Ga_{45}Pd_{10}Cu_{45}$ shows the best activity for acrolein production at 300 °C. As expected, at low temperature (mild reaction conditions), total oxidation as well as selective oxidation is dependent on the presence of Pd as the key element. Consequently, there is a proportional pattern between the amount of the Pd in catalysts and the acrolein formation.

The other high activity of selective oxidation is found in regions of composition with $Ga_{46}Pd_8Cu_{46}$ and $Ga_{91}Pd_9$. In addition, the binary compositions $Ga_{0–100}Cu_{0–100}$ and low Pd containing areas with $Ga_{0–100}Pd_{0\text{-}5}Cu_{0–100}$ showed relatively low catalytic activity.

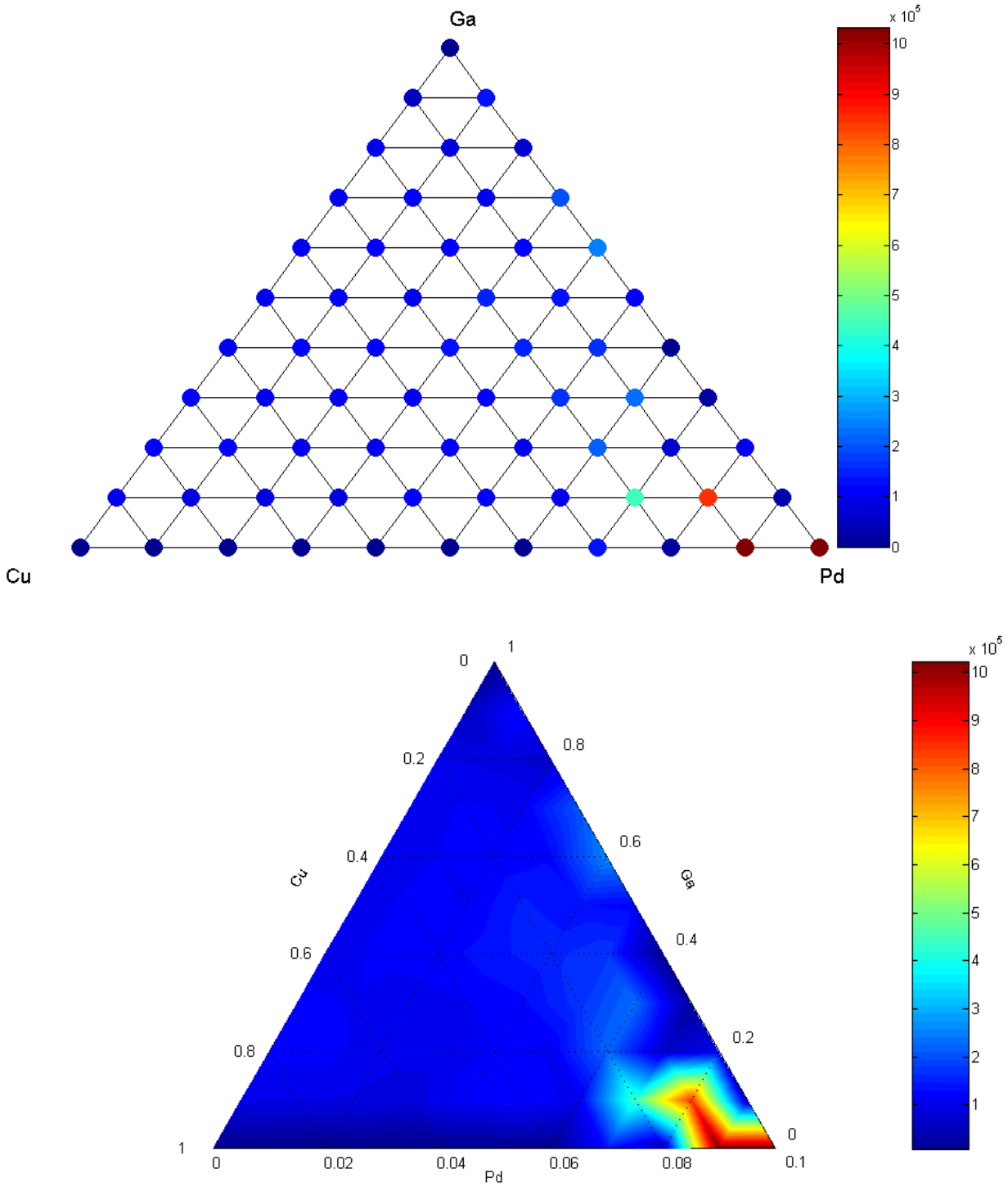


Figure 5.3 Acrolein ternary composition spread of $Cu_{1-100}Pd_{0-10}Ga_{1-100}$ at 300 °C

Reaction condition: around 400 μmol of catalysts. Total flow rate: 5 mL/min ($C_3H_6$:$O_2$=1:1 vol%)

# 6 Mo based catalyst for propene to acrolein

At this moment, a complex multicomponent oxide catalyst based on Bi, Fe and Co molybdate was used for the partial oxidation of propylene to acrolein[140]. In fact, all commercial processes in operation utilize multicomponent metal oxide catalysts including bismuth molybdate and catalysts, have been studied for nearly 40 years[159-162], and have displayed very good activity and selectivity[163]. Recently, there have been several studies using vanadium based catalysts[128, 155].

## *6.1 Primary screening*

The synthesis for this work in primary screening started with the Mo containing catalysts for acrolein formation. Molybdate was chosen as a starting material since it exhibits extraordinarily high thermal stability and is well known for having a function of partial oxidation of olefins. Most materials used for sol-gel synthesis were obtained from commercial sources and used without further purification. A list of the metal complexes used as a matrix is described in Table 6.1 and 6.2.

Table 6.1 Elements used for composition matrix in primary screening

| | | | | | | | | | | | | | | | | | |
|---|---|---|---|---|---|---|---|---|---|---|---|---|---|---|---|---|---|
| **H** | | | | | | | | | | | | | | | | | **He** |
| **Li** | **Be** | | | | | | | | | | | **B** | **C** | **N** | **O** | **F** | **Ne** |
| **Na** | **Mg** | | | | | | | | | | | **Al** | **Si** | **P** | **S** | **Cl** | **Ar** |
| **K** | **Ca** | **Sc** | **Ti** | **V** | **Cr** | **Mn** | **Fe** | **Co** | **Ni** | **Cu** | **Zn** | **Ga** | **Ge** | **As** | **Se** | **Br** | **Kr** |
| **Rb** | **Sr** | **Y** | **Zr** | **Nb** | **Mo** | | **Ru** | **Rh** | **Pd** | **Ag** | **Cd** | **In** | **Sn** | **Sb** | **Te** | **I** | **Xe** |
| **Cs** | **Ba** | **Lu** | **Hf** | **Ta** | **W*** | **Re** | **Os** | **Ir** | **Pt** | **Au** | **Hg** | **Tl** | **Pb** | **Bi** | **Po** | **At** | **Rn** |
| **Fr** | **Ra** | | | | | | | | | | | | | | | | |
| | | **La** | **Ce** | **Pr** | **Nd** | | **Sm** | **Eu** | **Gd** | **Tb** | **Dy** | **Ho** | **Er** | **Tm** | **Yb** | | |
| | | **Ac** | **Th** | **Pa** | **U** | | | | | | | | | | | | |

W*: NaW

For primary screening, two libraries with the 100 samples of 50 different dopants (Ag, Al, Au, B, Ba, Bi, Ca, Ce, Co, Cr, Cs, Cu, Dy, Er, Eu, Fe, Ga, Hf, Ho, In, Ir, K, La, Li, Lu, Mg, Mn, Mo, Na, Nb, Ni, Pb, Pd, Rb, Re, Rh, Ru, Sb, Sc, Si, Sn, Sm, Sr, Te, Ti, V, W, Y, Zn, Zr), as shown in table 6.1, were tested.

Table 6.2 Chemicals used for synthesis in primary screening

| Element | Chemical | Compay | Element | Chemical | Compay |
|---|---|---|---|---|---|
| Ag | $AgNO_3M$ | ABCR | Mg | $MgNO_3M$ | Merck |
| Al | $AlNO_3M$ | Alfa | Mn | $MnNO_3M$ | Merck |
| Au | AuBrM | | Mo | MoO*i*PrI | AlfaAesar |
| B | BAcidM | Fluka | Na | $NaNO_3M$ | Merck |
| Ba* | BaClM | | Nb | NbOEtM | |
| Bi | $Bi_2$EthylhexanoatM | Strem | Ni | $NiNO_3M$ | Aldrich |
| Ca | $CaNO_3M$ | Merck | Pb | $PbClO_4M$ | |
| Ce | $CeNO_3M$ | Fluka | Pd | PdOAcM | |
| Co | $CoNO_3M$ | Fluka | Rb | Rb | |
| Cr | $CrNO_3M$ | Aldrich | Re | ReClM | Aldrich |
| Cs | CsClM | unb. | Rh | RhClM | Aldrich |
| Cu | $CuNO_3M$ | Fluka | Ru | RuClM | Aldrich |
| Dy | $DyNO_3M$ | Aldrich | Sb | SbClM | J.T.Baker |
| Er | $ErNO_3M$ | Aldrich | Sc | $ScNO_3M$ | ABCR |
| Eu | $EuNO_3M$ | STREM | Si | $SiNO_3M$ | |
| Fe | $FeNO_3M$ | k.A. | Sn | SnClM | Aldrich |
| Ga | $GaNO_3M$ | Aldrich | Sm | $SmNO_3M$ | Riedel |
| Hf | HfClM | Aldrich | Sr | SrClM | Merck |
| Ho | $HoNO_3M$ | STREM | Te | TeacidM | Fluka |
| In | $InNO_3M$ | Aldrich | Ti | TiO*i*PrM | Lancaster |
| Ir | IrClM | Aldrich | V | VOO*i*$Pr_3M$ | ABCR |
| K* | $KNO_3M$ | | W* | NaWM | Fluka |
| La | $LaNO_3M$ | Fluka | Y | $YNO_3M$ | ABCR |
| Li | $LiNO_3M$ | Fluka | Zn | ZnOAcM | Fluka |
| Lu | $LuNO_3M$ | Aldrich | Zr | $ZrONO_3M$ | Johnson |

Ba*, K*,W*: addition of $HNO_3$ to avoid precipitation

As is shown in table 6.2, 0.1 M metal precursor solutions in methanol solvent were prepared with 50 metal alkoxides. These doping solutions were placed in 20 mL volume flasks. In the case of some dopants such as K, HaW and Ba, a drop of nitric acid was added to avoid precipitation.

### *6.1.1 First library*

Two binary catalysts including molybdate, $Mo_{96}X_4$ and $Mo_{92}X_8$ mixed oxides, were prepared by modified sol-gel methods based on reference[164]. $(NH_4)_6Mo_7O_{24}{\cdot}4H_2O$ (0.25 atomic mol/L = 0.035 mol/L) were used as starting materials to prepare the initial suspension that contains citric acid with an atomic ratio of C/Mo (Citric acid$\cdot H_2O$ and $(NH_4)_6Mo_7O_{24}{\cdot}4H_2O$) = 3/1 in 130 mL $H_2O$. After that,

a 10 mL $HNO_3$ solution was added into this suspension solution through vigorous stirring to dissolve precipitates.

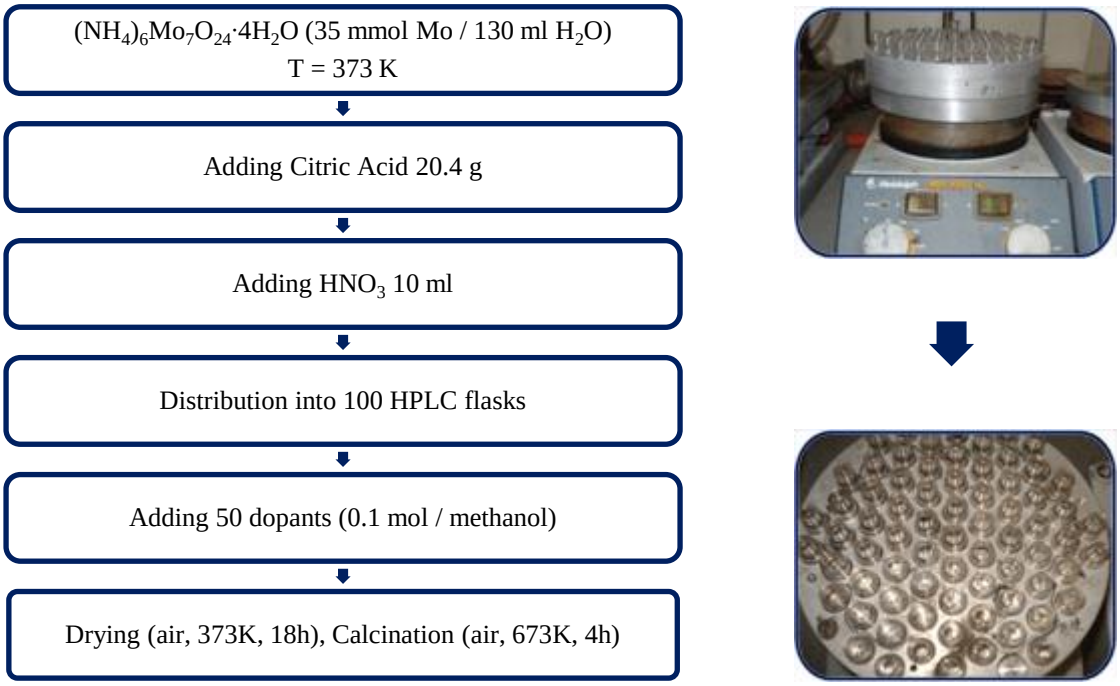


Figure 6.1 Procedure of modified sol-gel synthesis

It is well known that most molybdenum compounds have a very low solubility in water, which results in precipitation. In order to avoid precipitation, it was necessary to use a high synthesis temperature such as 373K. Since commercial pipetting robot (Zinsser Analytic) does not function for maintaining a certain temperature during synthesis, the new racks described in chapter 3.10 were used. By manual pipetting method, the suspension containing $(NH_4)_6Mo_7O_{24}\cdot 4H_2O$, $HNO_3$ and citric acid were distributed into two libraries ($Mo_{96}X_4$ and $Mo_{92}X_8$) as shown in Figure 6.1. 50 different dopants (0.1 mol/ methanol) were manually transferred into each flask. The temperature of 373K was maintained during the synthesis. Consequently, the molar ratio of $Mo_{96}X_4$ and $Mo_{92}X_8$ were dopant (X): matrix ($H_{24}M0_7N_6O_{24}\cdot 4H_2O$): acid ($HNO_3$) = 1:3.4:240 and dopant (X): matrix ($H_{24}M0_7N_6O_{24}\cdot 4H_2O$): acid ($HNO_3$) = 1:1.64:240, respectively. After drying at 100 °C for 3 days and calcinations of up to a temperature of 400 °C, 1G5L library was obtained for using the stage robot.

### *6.1.2 Instrument setup*

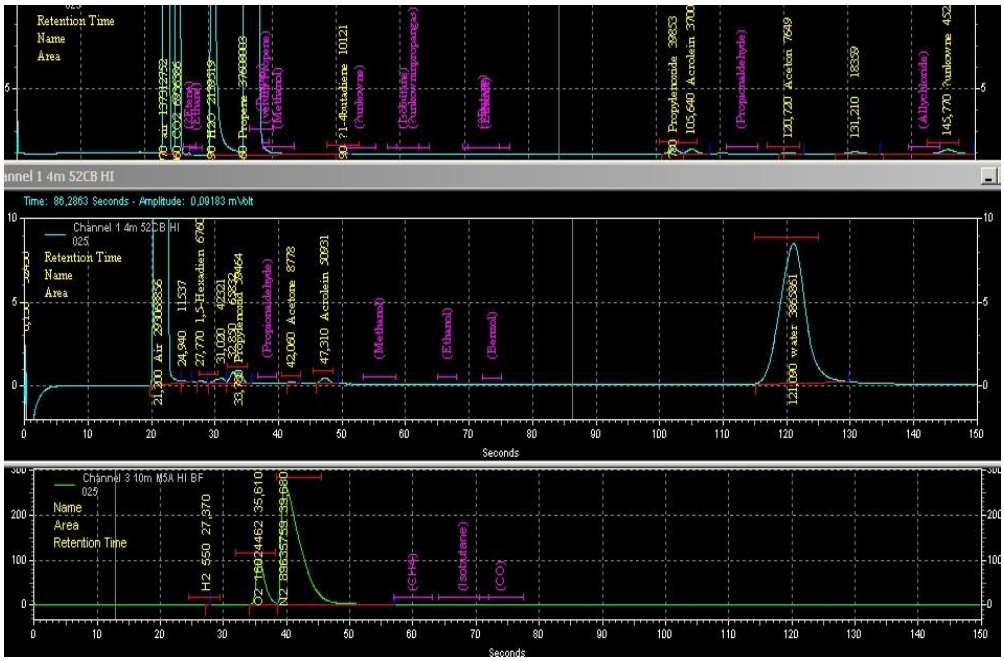


Figure 6.2 Separation peaks in columns of Micro-GC

For this experiment, the Micro-GC equipped three packed columns such as polar, Porapak Q and molecular sieve 5Å, were used in parallel to separate all different products available. These separation peaks in three columns are shown in Figure 6. 2.

The 10-fold parallel reactor was set up with a flow rate of 25mL/min comprising the following gas composition ($C_3H_6$: $O_2$: He=2:2:96). To get a homogenous static condition and to reduce hot spots during the reaction, 50 mg of catalyst was mixed with 100 mg of sand, which had a particle size in a range between 100 μm–200 μm.

### *6.1.3 Test by the Stage Robot Reactor*

100 samples in the first-generation library (1G5L) were tested at 300, 350 and 400 °C. Flow rate and gas composition in the feed-gas were adjusted with 5 mL/min and ($C_3H_6$: $O_2$ = 1:1), respectively.

Figures 6.3–6.5 show the results of the 1G5L library for selective oxidation of propene to acrolein. The test results were analyzed based on visualization in Matlab (see also appendix). For these plots, the activities based on unscaled GC signal intensity have been applied such that very active samples are colored in dark red and can be identified at once. Empty holes in these graphs are represented with gray color.

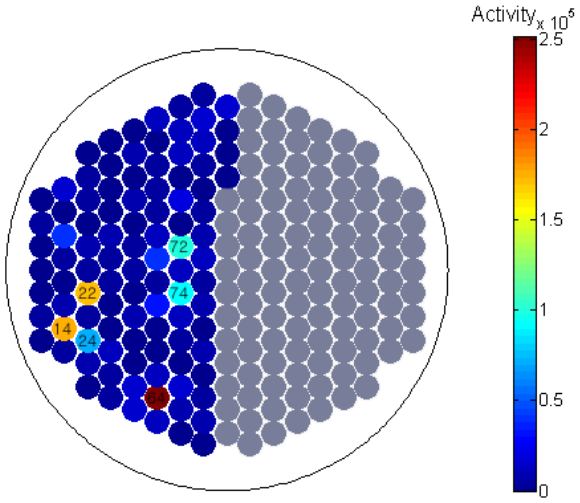


Figure 6.3 Acrolein activity at 300 °C

Reaction condition: around 400 µmol of catalysts. Total flow rate: 5 mL/min ($C_3H_6$:$O_2$=1:1 vol%)

The result of the catalytic test at 300 °C in Figure 6.3 showed that the activities for acrolein formation in 14($Mo_{96}Rh_4$), 22($Mo_{96}Ir_4$), 24($Mo_{96}Ru_4$), 64($Mo_{92}Rh_8$), 72($Mo_{92}Rb_8$) and 74($Mo_{92}Ru_8$) are high compared to the other catalysts. Molybdenum loaded with 8% rhodium showed the best catalytic performance.

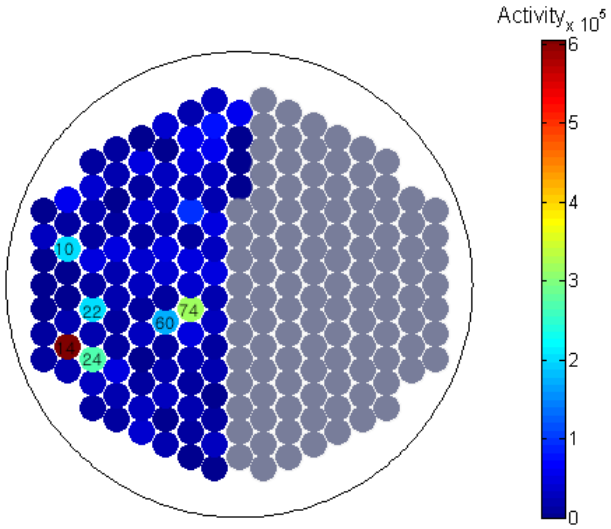


Figure 6.4 Acrolein activity at 350 °C

Reaction condition: around 400 µmol of catalysts. Total flow rate: 5 mL/min ($C_3H_6$:$O_2$=1:1 vol%)

The result of the catalytic test at 350 °C in Figure 6.4 showed the best activities in the holes of 10($Mo_{96}Sn_4$), 14($Mo_{96}Rh_4$), 22($Mo_{96}Ir_4$), 24($Mo_{96}Ru_4$), 60($Mo_{92}Sn_8$) and 74($Mo_{92}Ru_8$). There was no activity of molybdenum doped with Sn at 300 °C, but it improved with the increase of temperature.

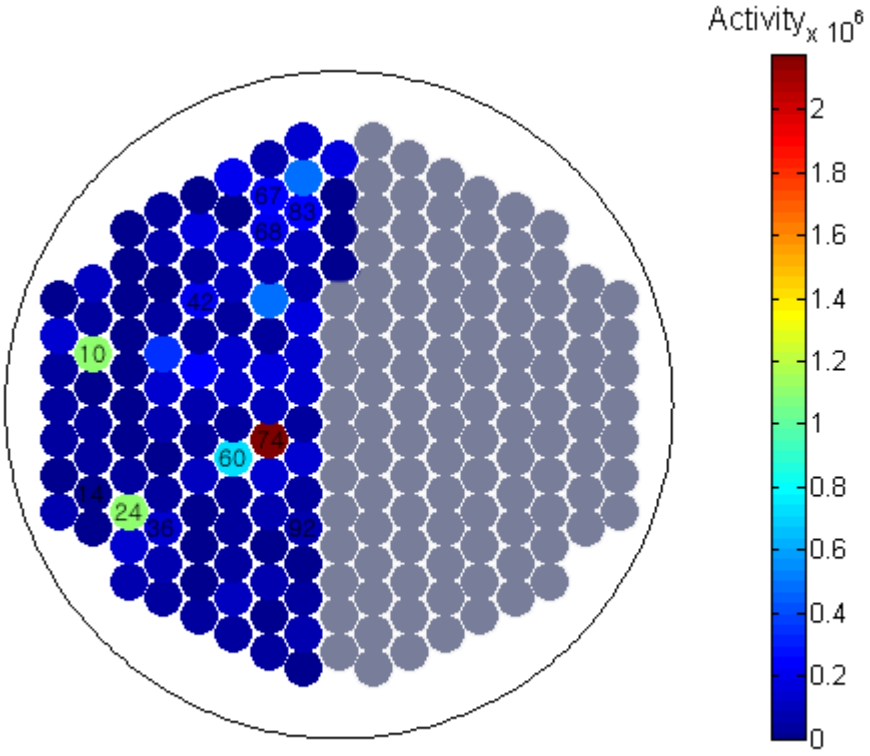


Figure 6.5 Acrolein activity at 400 °C

Reaction condition: around 400 μmol of catalysts. Total flow rate: 5 mL/min ($C_3H_6$:$O_2$=1:1 vol%)

The catalytic tests at 400 °C showed the best activities in the holes of 10($Mo_{96}Sn_4$), 24($Mo_{96}Ru_4$), 60($Mo_{92}Sn_8$) and 74($Mo_{92}Ru_8$). The results clearly illustrate that the Mo based catalysts with Sn and Ru have a good potential for selective oxidation of propene to acrolein. 10($Mo_{96}Sn_4$), 14($Mo_{96}Rh_4$), 24($Mo_{96}Ru_4$), 36($Mo_{96}Te_4$), 42($Mo_{96}Bi_4$), 67($Mo_{92}Er_8$), 68($Mo_{92}Eu_8$), 74($Mo_{92}Ru_8$), 83($Mo_{92}Y_8$) and 92($Mo_{92}Bi_8$) were chosen for hit validation. Although the catalysts of 42($Mo_{96}Bi_4$) and 92($Mo_{92}Bi_8$) did not show high activity in this test, they were chosen because the catalyst of Molybdenum with Bismuth is often used in the catalytic partial oxidation of propene to acrolein[124, 165].

### *6.1.4 Hit validation*

Based on the primary screening, 8 Mo based catalysts containing doping elements (Sn, Ru, Bi, Rh, Te, Er, Eu, Y) were found with high activity of acrolein formation. However, as discussed in the previous chapter, even though hits were identified using the stage robot reactor, it still did not guarantee the same results in conventional experiments because of problems such as catalyst deactivation, scale-up, instability of starting materials and the open structure of the reaction chamber in the stage robot reactor. Therefore, it is required that the hits are validated by conventional tests.

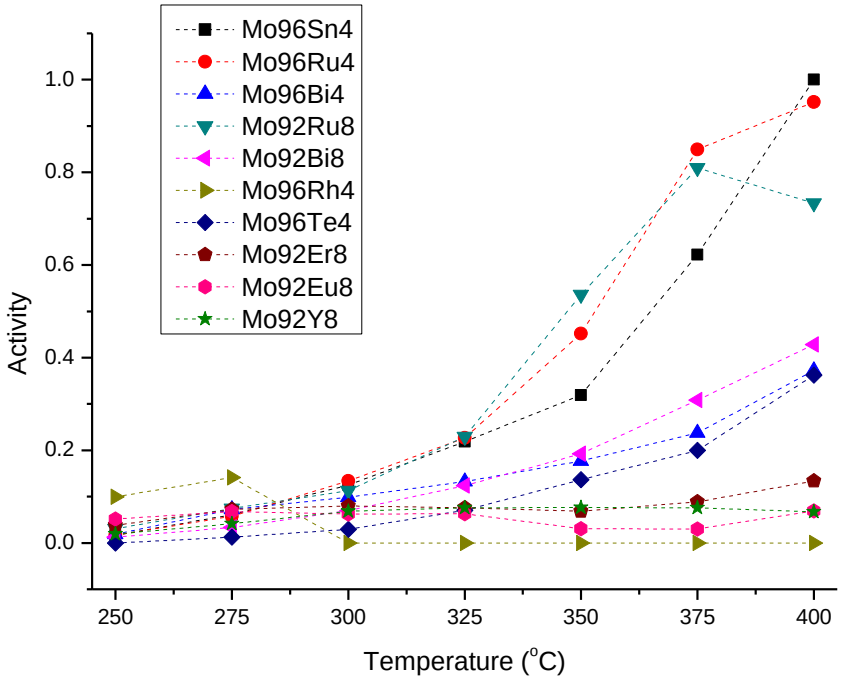


Figure 6.6 Activities of acrolein

Reaction condition: 50 mg of catalysts diluted with 100 mg of sand with particle size of 100-200 μm. Total flow rate: 25mL/min ($C_3H_6$:$O_2$:$N_2$=2:2:96 vol%)

In order to validate the potential candidate of catalysts obtained with the stage robot reactor, the 10-fold parallel reactor was used. The results of the reactant-gas analysis were then used to calculate the values of activity which are defined as:

$$\text{Activity} = \frac{\text{GC singnal intensity of acrolein}}{\text{GC signal intensity of acrolein of } Mo_{96}Sn_4 \text{ at } 400°C} \quad (1)$$

Figure 6.6 shows activity relating to the production of acrolein in the temperature range of 250 to 400 °C. Here, the unscaled GC signal intensity was used for calculating the activity. Normalization of activity was calculated by dividing the value with the GC signal intensity of acrolein of $Mo_{96}Sn_4$ since it was the best value during the process of hit validation. Activity 1 is the value of the GC signal intensity of $Mo_{96}Sn_4$ at 400 °C. Without consideration of selectivity, three catalysts ($Mo_{96}Sn_4$, $Mo_{96}Ru_4$ and $Mo_{96}Ru_4$) showed the highest performance for the selective oxidation of propene to acrolein. The group that had the activity between 0.2 and 0.4 were the catalysts such as $Mo_{96}Bi_4$, $Mo_{92}Bi_8$ and $Mo_{96}Te_4$. Lastly, $Mo_{96}Rh_4$, $Mo_{92}Er_8$, $Mo_{92}Eu_8$ and $Mo_{92}Y_8$ showed less than 0.2 activities over the entire experimental range.

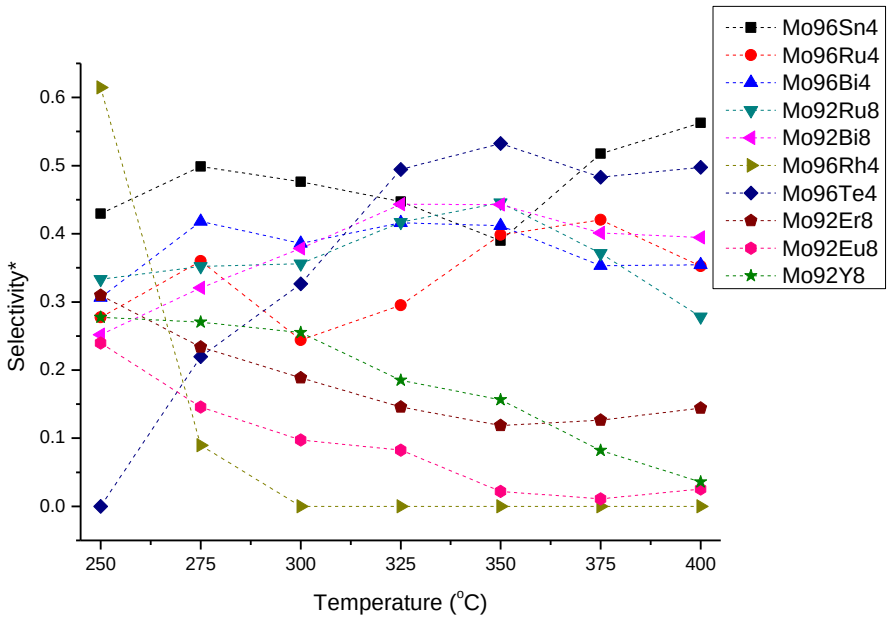


Figure 6.7 Selectivity of acrolein

Reaction condition: 50 mg of catalysts diluted with 100 mg of sand with particle size of 100-200 μm. Total flow rate: 25mL/min ($C_3H_6$:$O_2$:$N_2$=2:2:96 vol%)

To show the extent of selectivity of acrolein, the simplified definition of the selectivity was calculated as follows:

$$\text{Selectivity} = \frac{\text{GC signal intensity of acrolein}}{\text{GC signal intensity of acrolein} + \frac{\text{GC signal intensity of } CO_2}{3}} \quad (1)$$

This value is involved in the combination of the selective oxidation of propene to acrolein and the total oxidation of propene to carbon dioxide. Ru-, Sn- and Bi-doped catalysts in Figure 6.7 showed that the selectivity was higher than 0.3 over the whole experimental range. In contrast, Te containing catalysts showed high selectivity with increasing temperature. Interestingly, $Mo_{96}Rh_4$ showed selectivity around 0.6 at 240 °C and decreased dramatically with increasing temperature.

Based on the result of selectivity, it was predicted that the best candidates would be the catalysts doped with Ru, Sn, Bi and Te. However, despite the high selectivity of $Mo_{96}Bi_4$ and $Mo_{96}Ti_4$, both catalysts were not very active for the production of acrolein (see Fig. 6.3). Therefore, $Mo_{94}Ru_4$ and $Mo_{94}Sn_4$ were chosen as key elements for preparation of the second library after the recheck of 10 potential catalysts. 2G6L was prepared with 100 compositions with 50 dopants including these two elements as a base for composition ($Mo_{94}Ru_4X_2$, $Mo_{94}Sn_4X_2$).

### *6.1.5 Second library*

$Mo_{94}Ru_4X_2$, $Mo_{94}Sn_4X_2$ mixed oxides in the second library (2G6L) were prepared by using the same procedure described for first generation. For example, $Mo_{94}Ru_4X_2$ and $Mo_{94}Sn_4X_2$ matrixes were synthesized pipetting the following volumes of single solutions in sequence: 0.035 M Molybdenum with 0.75 M citric acid monohydrate in water (940 µL) and 0.1 M RuCl(or SnCl) in methanol (100 µL, 10 µmol), 0.1 M X (50 dopants, 100 µL, 5 µmol) in methanol, and nitric acid (50 µL). In short, the molar ratio of first dopant(X): second dopant(RuCl or SnCl): matrix($H_{24}M0_7N_6O_{24}\cdot 4H_2O$): acid ($HNO_3$) was 1:2:6.58:480.

### *6.1.6 Screening of the stage robot*

The result of 2G6L in the library of second generation for the stage robot reactor at 300 °C and 350 °C is shown in the following Figure 6.8. Consequently, four catalysts such as $Mo_{94}Sn_4Te_2$ (36), $Mo_{94}Ru_4Sb_2$ (51), $Mo_{94}Ru_4Te_2$ (86) and $Mo_{94}Ru_4Bi_2$ (92) were chosen as the best catalysts. $Mo_{94}Ru_4Te_2$ (86) especially showed the highest activity from the second generation of library in primary screening method. The results of unscaled GC signal intensity were also used for the activities of acrolein.

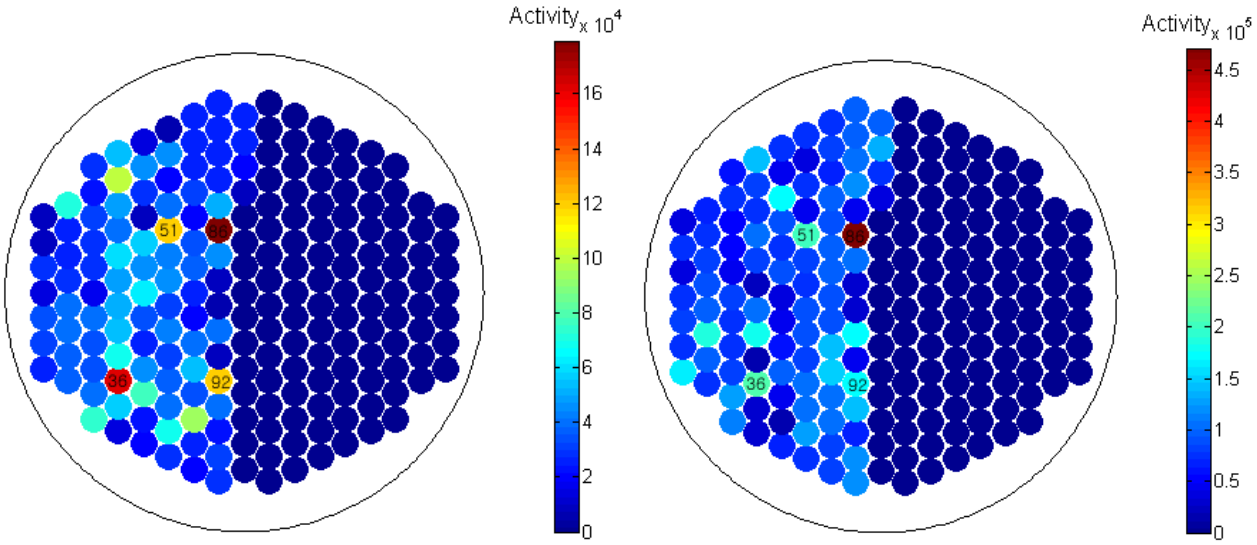


Figure 6.8 Acrolein activity at 300 °C (left) and 350 °C (right)
Reaction condition: around 400 µmol of catalysts. Total flow rate: 5 mL/min ($C_3H_6$:$O_2$=1:1 vol%)

### *6.1.7 Hit validation*

Again for the validation of hits in the second generation, a 10-fold parallel reactor has been used. In order to analyze data precisely, calibration of propene, acrolein, $CO_2$ and CO was completed. The yield(Y) of acrolein, conversion(X) of propene and selectivity(S) of acrolein identify the results of the experiment. Reactant and product signals were calibrated to define their moles in feed and product-gases. Theses parameters were defined as follows:

$$\text{conversion} = \frac{(\text{Mole of } C_3H_6)_{in} - (\text{Mole of } C_3H_6)_{out}}{(\text{Mole of } C_3H_6)_{in}} \quad (1)$$

$$\text{Selectivity} = \frac{\text{Mole of acrolein}}{\text{Mole of acrolein} + \frac{\text{Mole of } CO_2}{3} + \frac{\text{Mole of CO}}{3}} \quad (2)$$

$$\text{Yield} = \text{Conversion} \times \text{Selectivity} \quad (3)$$

For calculating these values, only $CO_2$, CO and acrolein as major products were considered, which means it was assumed that additional propene compounds were negligible and thus were simply ignored. If there are no other products in the reaction without those described above, the values could actually be compatible with real ones such as conversion, selectivity and yield. These parameters with hypothetical assumptions were enough to represent their physical properties of high-throughput results.

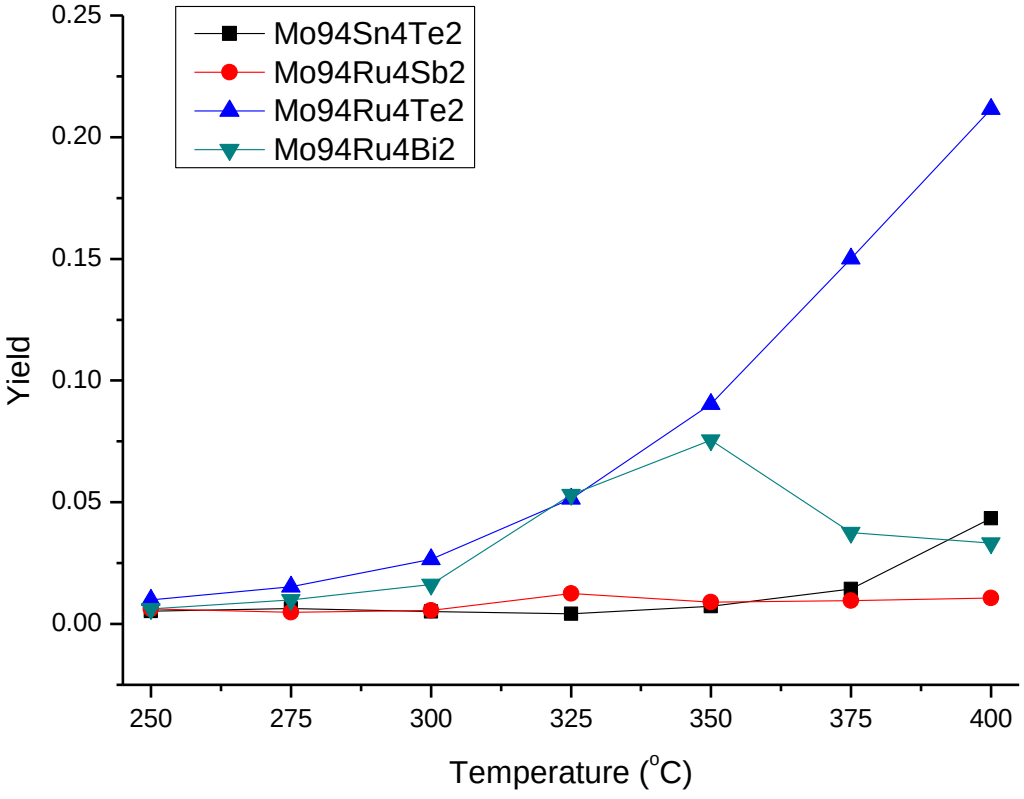


Figure 6.9 Yield of acrolein

Reaction condition: 50 mg of catalysts diluted with 100 mg of sand with particle size of 100-200 μm. Total flow rate: 25mL/min ($C_3H_6$:$O_2$:$N_2$=2:2:96 vol%)

The yields of acrolein obtained by the catalysts in Figure 6.9 show that the yield with the catalyst of $Mo_{94}Ru_4Te_2$ increased up to 25% by increasing reaction temperature from 250 °C to 400 °C. On the other hand, $Mo_{94}Sn_4Te_2$, $Mo_{94}Ru_4Bi_2$ and $Mo_{94}Ru_4Sb_2$ showed relatively low yield of below 5% at 400 °C. In case of $Mo_{94}Ru_4Bi_2$, a slight increase at 350 °C was noted, and after that the value

decreased gradually. Consequently, except for $Mo_{94}Ru_4Te_2$ it seems that the result of hit validation did not correlate with the result of the stage robot reactor.

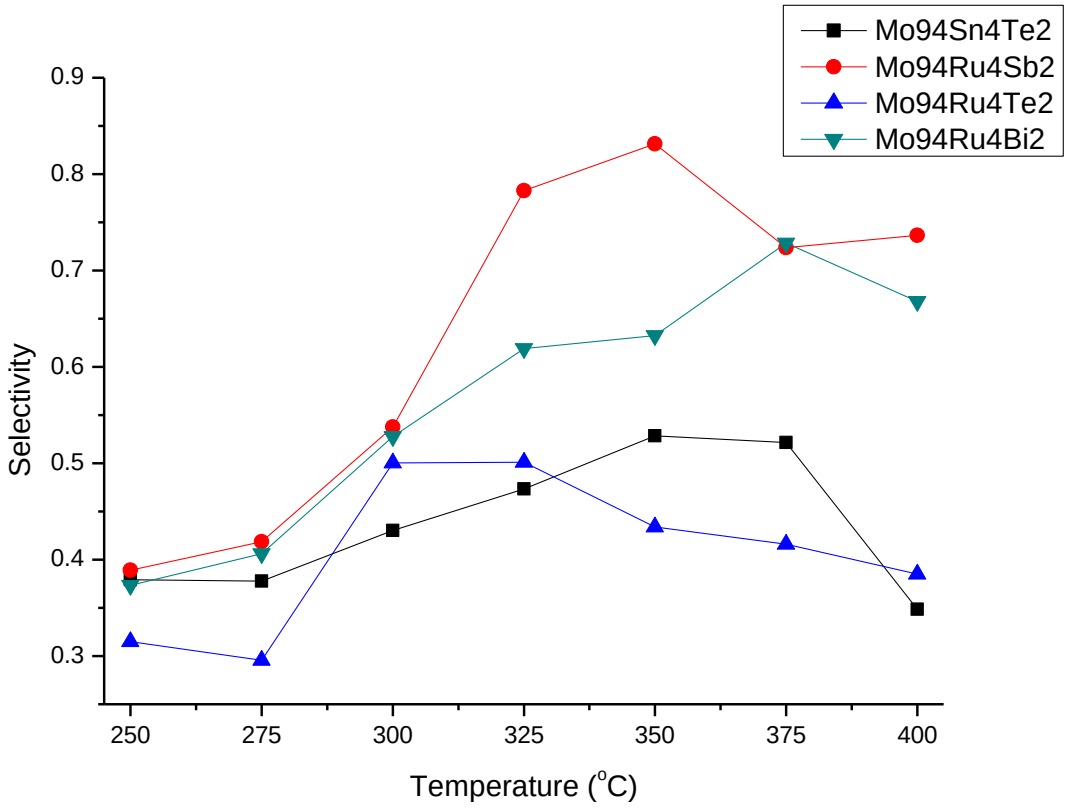


Figure 6.10 Selectivity of acrolein

Reaction condition: 50 mg of catalysts diluted with 100 mg of sand with particle size of 100–200 μm. Total flow rate: 25mL/min ($C_3H_6$:$O_2$:$N_2$=2:2:96 vol%)

Based on the results of selectivity to acrolein in Figure 6.10, $Mo_{94}Ru_4Sb_2$ has the highest selectivity among 4 catalysts whereas it also has the lowest yield in Figure 6.9. In contrast, $Mo_{94}Sn_4Te_2$ and $Mo_{94}Ru_4Te_2$ have less than 50% of selectivity with high yields. Without doubt, these results performed with the parallel-reactor were identical to that of the primary screening by the stage robot reactor, but again, problems such as reproducibility and deactivation of catalysts and reliability of high-throughput reactor may have contributed to validating the hit selection.

Consequently, among four candidates as a potential catalyst, $Mo_{94}Ru_4Te_2$ was found the best hit based on its yield in Figure 6.9. Therefore, this catalyst was chosen as the best candidate for optimization of the catalytic activity in a second approach. At the same time, the remaining catalysts,

$Mo_{94}Sn_4Te_2$, $Mo_{94}Ru_4Bi_2$ and $Mo_{94}Ru_4Sb_2$, which showed less activity, were considered as potential catalysts in a second screening.

### *6.1.8 Ternary composition (Mo-Ru-Te)*

As is shown with the primary screening in Figure 6.9 and Figure 6.10, it was found that the combination of Mo-Ru-Te provided the best catalyst for the selective oxidation of propene to acrolein based on its yield at 400 °C. To study the catalytic efficiency and behavior of Mo-Ru-Te, 55 samples were prepared using the same recipe used for synthesis and the following results were obtained by using the stage robot under the same conditions used in the primary screening. The unscaled GC signal intensity was used for the visualization of the ternary composition for selective oxidation of propene to acrolein in Matlab.

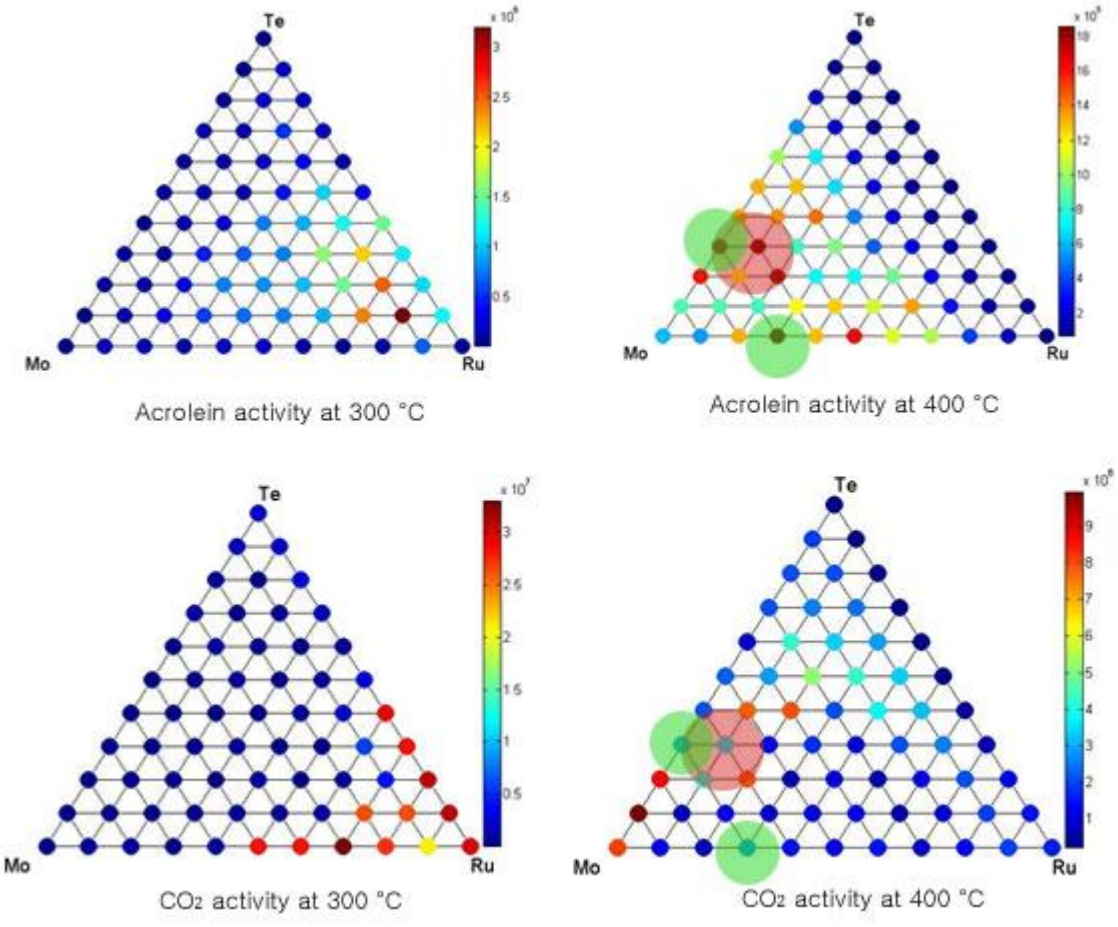


Figure 6.11 Activities of acrolein and $CO_2$ to composition spread at temperature of 300 °C and 400 °C
Reaction condition: around 400 μmol of catalysts. Total flow rate: 5 mL/min ($C_3H_6$:$O_2$=1:1 vol%)

Figure 6.11 describes the activity of catalysts for the selective oxidation to acrolein and for total oxidation to $CO_2$. At the low temperature of 300 °C, the catalyst with high amounts of Ru was more active for total oxidation as well as partial oxidation, most likely because Ru as noble metal enhanced its activity at low temperature. Considering reaction temperatures of 400 °C, Mo contained catalysts had a high potential in the case of binary as well as ternary compositions, which are shown in the green and red transparent area in the right side of Figure 6.11, respectively.

Interestingly, based on the results at 400 °C, some similarities to previous studies were observed. For example, P. Forzatti showed that multicomponent oxide systems (Cd-Te-Mo-O and Mn-Te-Mo-O) based on Mo including small amounts of Te are effective catalysts for the selective oxidation of olefins at 400 °C[166]. This study described that the addition of small amounts of Te in catalysts induced an increase in the conversion of propylene and the yield of acrolein, but only minor changes in the yield of carbon oxides. The data suggests that Te doping to a molybdate matrix should not exceed a maximum of 2 mol%. More than 2 mol% doping was shown to induce decreasing the yield of propylene to acrolein.

## *6.2 Secondary screening*

As is shown in the previous chapter, with the primary screening method based on the stage robot reactor it is possible to screen a large number of samples within a short time and to accumulate a lot of data. However, a catalyst may deactivate rapidly over time due to poisoning or product inhibition or it may require additional time to improve performance such as pretreatment by reduction. In regard to this, our objective in the early stages of the development of high-throughput catalyst research methods was to create a new setup of a secondary workflow that allows broad exploration for catalyst composition, synthesis method, support materials, run conditions and real feeds. Although several manners of using the newly developed reactor are explained in chapter 3.9, in this study the new high-throughput reactor was mainly used for hit validation, optimization of synthesis method and catalyst composition.

### *6.2.1 Instrumental setup*

In the procedure of secondary screening, the parallel-reactor was used for the propene oxidation experiments under reaction temperatures from 250 to 400 °C (523–673K), which resulted in 7

measurement points (25 °C increments). Flow rate and gas composition in the feed-gas were 25mL/min and $C_3H_6$: $O_2$: He=2:2:96, respectively. To achieve homogenous static conditions and to ignore hot spots during the reaction, 50 mg of catalyst were mixed with 100 mg sand, which had a particle size from 100 μm to 200 μm. The setup of the Micro-GC for analysis was identical to the conditions used in the primary screening.

### *6.2.2 Experimental procedure*

Twelve runs of the new 10-fold parallel reactor with changing the synthetic recipe or the composition of catalysts were carried out to optimize the performance of the catalyst. After facing difficulties with the reproducibility of the catalysts, several synthesizes were carried out to find an improved sol-gel recipe. For this experiment, seven diverse parameters were considered to optimize the activity of the catalysts. The information of composition in each generation is shown in the following table 6.3. Catalysts based on 7 elements (Mo, Ru, Te, Sn, Ti, Bi, Sb) were prepared during increasing generation in the secondary screening procedure by using modified sol-gel methods.

Table 6.3 Catalyst composition based on atomic content in each generation

| Num | G1 | G2 | G3 | G4 | G5 | G6 |
|---|---|---|---|---|---|---|
| 1 | $Mo_{94}Ru_4Te_2$ | $Mo_{94}Ru_4Te_2$ | $Mo_{88}Ru_8Te_4$ | $Mo_{94}Ru_4Te_2$ | $Mo_{94}Ru_4Te_2$ | $Mo_{94}Ru_4Te_2$ |
| 2 | $Mo_{92}Ru_4Te_4$ | $Mo_{94}Ru_4Te_2$ | $Mo_{84}Ru_8Te_8$ | $Mo_{94}Ru_4Te_2$ | $Mo_{92}Ru_4Te_4$ | $Mo_{92}Ru_6Te_2$ |
| 3 | $Mo_{90}Ru_4Te_6$ | $Mo_{94}Ru_4Te_2$ | $Mo_{80}Ru_8Te_{12}$ | $Mo_{94}Ru_4Te_2$ | $Mo_{94}Ru_4Te_2$ | $Mo_{90}Ru_6Te_4$ |
| 4 | $Mo_{94}Ru_2Te_4$ | $Mo_{94}Ru_4Te_2$ | $Mo_{88}Ru_8Te_4$ | $Mo_{88}Ru_8Te_{12}$ | $Mo_{94}Ru_4Te_2$ | $Mo_{92}Ru_4Te_4$ |
| 5 | $Mo_{96}Ru_2Te_2$ | $Mo_{94}Ru_4Te_2$ | $Mo_{88}Ru_8Te_4$ | $Mo_{94}Ru_4Te_2$ | $Mo_{92}Ru_4Te_4$ | $Mo_{90}Ru_4Te_6$ |
| 6 | | | | $Mo_{94}Ru_4Te_2$ | $Mo_{94}Ru_4Te_2$ | |
| 7 | | | | $Mo_{94}Ru_4Te_2$ | $Mo_{94}Ru_4Te_2$ | |
| 8 | | | | $Mo_{92}Ru_4Te_4$ | $Mo_{92}Ru_4Te_4$ | |
| 9 | | | | $Mo_{92}Ru_4Te_4$ | $Mo_{94}Ru_4Te_2$ | |
| 10 | | | | | | |

| Num | G7 | G8 | G9 | G10 | G11 | G12 |
|---|---|---|---|---|---|---|
| 1 | $Mo_{94}Ru_4Te_2$ | $Mo_{92}Ru_6Te_2$ | $Mo_{94}Sn_4Te_2$ | $Mo_{94}Sn_4Te_2$ | $Mo_{96}Sn_1Te_2Ti_2$ | $Mo_{94}Sn_4Te_2$ |
| 2 | $Mo_{92}Ru_6Te_2$ | $Mo_{92}Ru_6Te_2$ | $Mo_{94}Ru_4Sb_2$ | $Mo_{94}Sn_4Te_2$ | $Mo_{94}Ru_2Te_2Ti_2$ | $Mo_{90}Sn_8Te_2$ |
| 3 | $Mo_{94}Ru_4Te_2$ | $Mo_{92}Ru_6Te_2$ | $Mo_{94}Ru_4Te_2$ | $Mo_{92}Ru_8$ | $Mo_{94}Ru_2Te_2Ti_2$ | $Mo_{88}Sn_8Te_4$ |
| 4 | $Mo_{92}Ru_6Te_2$ | $Mo_{92}Ru_6Te_2$ | $Mo_{94}Ru_4Bi_2$ | $Mo_{92}Ru_8$ | $Mo_{94}Ru_2Te_2Ti_2$ | $Mo_{92}Sn_4Te_2Ti_2$ |
| 5 | $Mo_{96}Ru_4$ | $Mo_{92}Ru_6Te_2$ | $Mo_{94}Sn_4Te_2$ | $Mo_{94}Sn_4Te_2$ | $Mo_{94}Sn_4Te_2$ | $Mo_{94}Ru_4Te_2$ |
| 6 | $Mo_{94}Ru_6$ | $Mo_{92}Ru_6Te_2$ | $Mo_{92}Sn_6Te_2$ | $Mo_{94}Sn_4Te_2$ | $Mo_{94}Sn_4Te_2$ | $Mo_{90}Ru_8Te_2$ |
| 7 | $Mo_{96}Ru_4$ | $Mo_{92}Ru_6Te_2$ | $Mo_{92}Sn_4Te_4$ | $Mo_{92}Ru_8$ | $Mo_{94}Ru_4Te_2$ | $Mo_{88}Ru_8Te_4$ |
| 8 | $Mo_{94}Ru_6$ | $Mo_{92}Ru_6Te_2$ | $Mo_{94}Sn_4Te_2$ | $Mo_{92}Ru_8$ | $Mo_{94}Ru_4Te_2$ | $Mo_{92}Ru_4Te_2Ti_2$ |
| 9 | | $Mo_{92}Ru_6Te_2$ | | | | |
| 10 | | $Mo_{92}Ru_6Te_2$ | | | | |

### *6.2.3 Catalysts preparation*

Catalyst performance is dependent on catalytic composition as well as preparation parameters (such as type of precursors, mixture of solution, solution Ph, synthetic temperature, calcinations temperature, and carination media) and operation condition (such as temperature, contact time, and reactant concentration). Some of these attributes correlate with catalytic activity, which are called the "descriptor" to design a "diverse" library in order to increase chances for discovering promising regions in the parameter space by HTE[167].

Seven factors, such as material composition, pH in solution, amount of addition of citric acid, mixture with ethylene glycol, aging time of precursors in solution, stirring (rpm) and the type of precursors used were chosen as descriptors in table 6.4.

Table 6.4 Diversity of catalyst synthesis as descriptor

| Num | D1 | D2 | D3 | D4 | D5 | D6 | D7 |
|---|---|---|---|---|---|---|---|
| G1 | O | X | X | X | X | X | X |
| G2 | X | O | X | O | X | X | X |
| G3 | O | O | O | X | X | X | X |
| G4 | O | O | X | X | O | X | X |
| G5 | O | X | O | X | X | X | X |
| G6 | O | X | X | X | X | X | X |
| G7 | O | X | O | X | X | X | X |
| G8 | X | X | X | X | X | X | O |
| G9 | O | X | X | X | O | X | X |
| G10 | O | X | X | X | X | O | X |
| G11 | X | X | X | X | X | X | O |
| G12 | O | X | X | X | X | X | X |

D1: material composition; D2: pH by $HNO_3$; D3: amount of citric acid; D4: mixture with ethylene glycol; D5: aging precursors in solution; D6: stirring rpm; D7: type of precursors

Based on the experimental results with diverse descriptors in each generation, the decision to design the library of the next experiment was made. As mentioned above, seven factors (D1–D7) were considered to have main influence on the activity of catalysts for the success of catalyst discovery. For instance, material composition (D1) was changed in a range of $Mo_{80\text{-}96}Ru_{2\text{-}8}Te_{0\text{-}6}$, $Mo_{80\text{-}96}Sn_{2\text{-}8}Te_{0\text{-}6}$, $Mo_{94}Ru_4Bi_2$, $Mo_{94}Ru_4Sb_2$, $Mo_{92\text{-}96}Sn_{1\text{-}4}Te_2Ti_2$ and $Mo_{92\text{-}96}Ru_{2\text{-}4}Te_2Ti_2$. The value of pH (D2) in solution was changed by adding $HNO_3$ 1-3 mL per flask. The solution of dissolved $(NH_4)_6Mo_7O_{24}{\cdot}4H_2O$ (D3) was added to the amount of citric acid based on weight rate 0–3 (citric

acid/ molybdate matrix). This solution was mixed with ethylene glycol up to 0–2 mL per flask (D4). After dissolving RuCl and SnCl in methanol with 0.1 M, the solution was allowed to age for more than 2 weeks. The procedure of adding Sn and Ru solutions into molybdate solution was carried out with the different rpm 250–300 (D6). Different precursors (D7) of Mo (Ammonium molybdate tetrahydrate, phosphomolybdic acid, Bi(acetonitrile)molybdenum chloride), Bi(Bismuthyl nitrate), Ru(Ruthenium chloride, Ammonium hexachlororuthenate, Ruthenium(Ⅲ) acetylacetonate, Ruthenium(Ⅳ)oxide anhydrous), Sn(Tin chloride, Tintetraisopropoxytin-isoprosal adduct, Tin(Ⅳ)acetate, Tin(Ⅱ)-2,4-pentanedionate), Ti(Titanium(Ⅳ) isopropoxide, Titanium 2-ethylhexoide) and Te(telluric acid) were prepared as starting materials. The detailed recipe of catalyst synthesis in detail can be found in chapter 7.4.

### *6.2.4 The result concerning the temperature range*

Figure 6.12 shows the best results of yield from propene to acrolein at each temperature with increasing temperatures and generations. The yields at different temperatures have been implemented to visualize the results in the range of 250–400 °C. The yield was calculated based the same way as given in chapter 6.1.7. The maximum yields at each temperature were selected to visualize results.

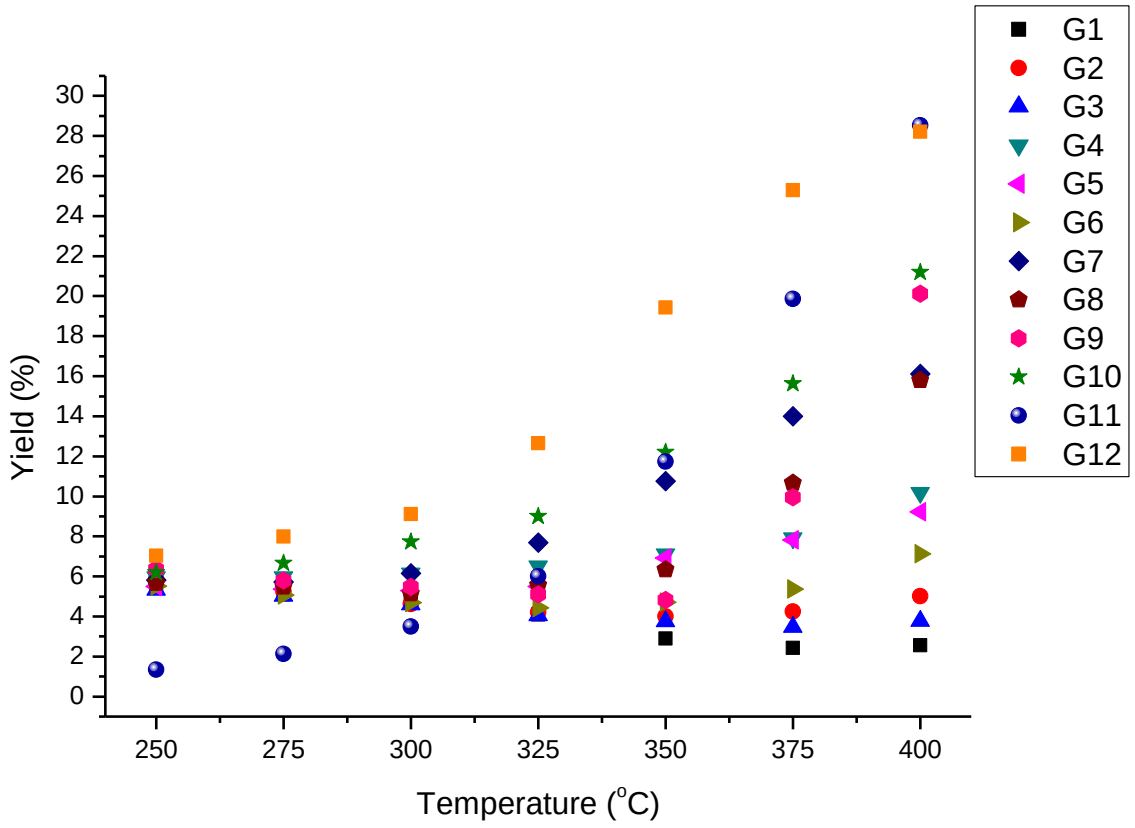


Figure 6.12 Visualization of temperature vs. yield

Reaction condition: 50 mg of catalysts diluted with 100 mg of sand with particle size of 100–200 µm. Total flow rate: 25mL/min ($C_3H_6$:$O_2$:$N_2$=2:2:96 vol%)

The pattern of the graph in Figure 6.12 clearly describes the increasing yield while the generation is performing. At the highest temperature, e.g. 1 as 400 °C, it shows that there is a dramatic increase in yield up to maximum 28%. In contrast, there is a little variation of the yield at 250 °C.

Until the temperature of 350 °C is reached, no exact proportional increase of yield appeared with increasing generations. For example, the results of generation 9 show lower activity compared to the result obtained with the previous generation. However, in the results at 400 °C a clear increase of conversion with a higher generation was observed.

### *6.2.5 The result of selectivity vs. yield with increasing generations*

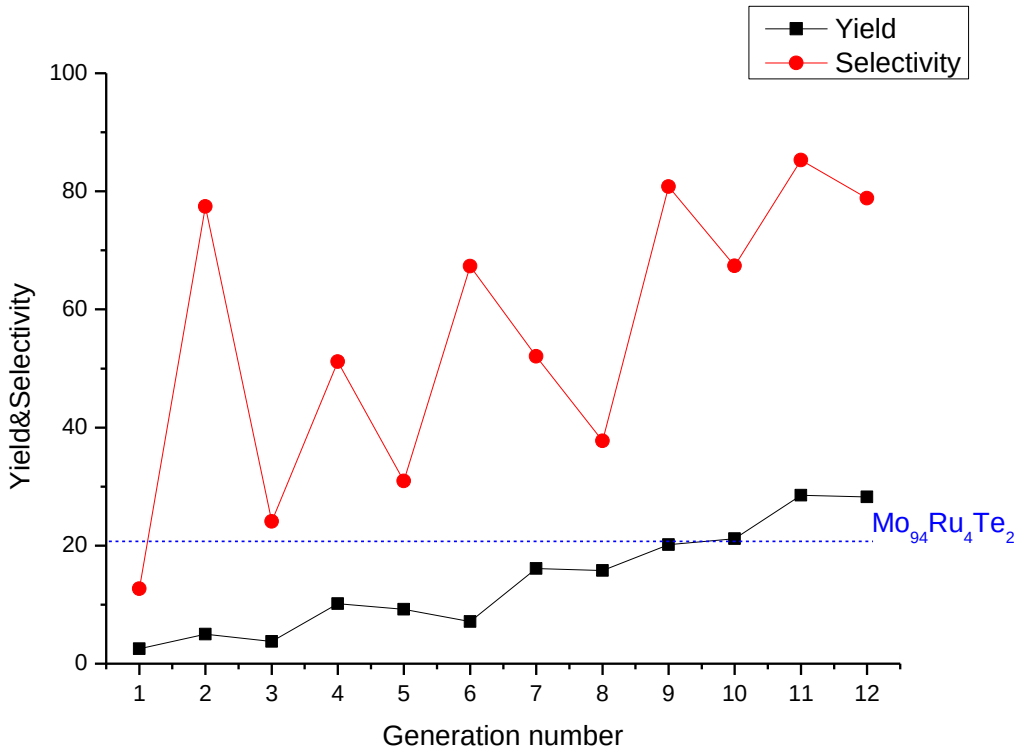


Figure 6.13 Yield & selectivity with increasing generations

Reaction condition: 50 mg of catalysts diluted with 100 mg of sand with particle size of 100–200 μm. Total flow rate: 25mL/min ($C_3H_6$:$O_2$:$N_2$=2:2:96 vol%)

The best results of the maximum yield and selectivity, which are chosen in each generation of 400 °C, are given in Figure 6.13. The value of yield was gradually increased with the rise of the library generation. In contrast, selectivity shows the pattern of fluctuation on the range of generation. During hit validation with the 10-fold parallel reactor, the best catalyst $Mo_{94}Ru_4Te_2$ from the primary screening method showed 21% yield, which was confirmed as the blue dot line of the 9$^{th}$ library generation in Figure 6.13. Eventually, there were difficulties with the reproducibility of the experiment, which showed the best yield in primary screening. It is assumed that the problem resulted from the sensitivity of catalyst preparation. Therefore, the sol-gel method was modified in each generation by changing seven factors as descriptors of diversity in order to identify the best recipe for catalyst preparation.

### *6.2.6 Characterization of surface area*

Table 6.5 Surface areas of catalysts, $Mo_{94}Sn_4Te_2$ and $Mo_{94}Ru_4Te_2$

| Generation | Catalyst | Surface area |
|---|---|---|
| 9 | $Mo_{94}Sn_4Te_2$ | 32.78 $m^2/g$ |
| 10 | $Mo_{94}Ru_4Te_2$ | 57.017 $m^2/g$ |
| 11 | $Mo_{94}Ru_4Te_2$ | 35.22 $m^2/g$ |

Total BET surface areas of the catalysts, measured by nitrogen adsorption (Sorptomatic 1990, Carlo Erba) at the temperature of liquid nitrogen, are shown in table 6.5. The samples were outgassed overnight under vacuum at 200 °C before adsorption.

The catalysts of $Mo_{94}Ru_4Te_2$ and $Mo_{94}Ru_4Te_2$ from the $10^{th}$ and $11^{th}$ library generation show surface areas of 57 and 35 $m^2/g$. The results of $Mo_{94}Ru_4Te_2$ in generation 10 and 11 describe that even though surface area decreased from 57.017 $m^2/g$ to 35.22 $m^2/g$, the yield as well as the selectivity increased.

### *6.2.7 Effects of parameter variation for catalytic activity*

It is often useful to perform pattern recognition to solve certain problems or to find out trend from enormous data in various fields[168-170]. In particular, the pattern search between the catalytic activity and the parameter variation modified for synthesis improvement is necessary for analysis of the problem of catalyst preparation. During the currently discussed study, seven descriptors such as material composition, pH, the amount of citric acid, mixture with ethylene glycol, aging time of stock solution, stirring (rpm) and type of precursors were used.

In order to study the effects of parameter variation, deviation values were calculated in each generation by subtracting the minimum of acrolein yield from the maximum of acrolein yield at each generation as following:

Deviation value (DV) = |maximum yield of acrolein - minimum yield of acrolein|

For convenience in statistical calculations or visualizations, the statistical variable often is normalized or simplified. After calculating the deviation values, they were changed to obtain better magnitudes, according to the scale values tabulated in table 6.6. For example, the deviation values between 1 and 5 were converted into 1.

Table 6.6 Calculation parameters to change magnitude

| Num | Deviation values (yield to acrolein) | Scale values |
|---|---|---|
| 1 | 1≤DV<5 | SV=1 |
| 2 | 5≤DV<10 | SV=2 |
| 3 | 10≤DV<15 | SV=3 |
| 4 | 15≤DV<20 | SV=4 |
| 5 | 20≤DV<25 | SV=5 |
| 6 | 25≤DV<30 | SV=6 |

In the graph below, some trends were observed that correlate to increase yield according to the diversity. However, because the number of data is too low, a clear trend for the aspects D1 to D7 cannot be observed. Furthermore, data of two catalysts, Mo-Ru-Te and Mo-Sn-Te, are combined in visualizing pattern due to the lack of data Mo-Sn-Te. Therefore, these findings may only be true to this special case of Mo-Ru-Te.

Table 6.7 Analysis of parameter variations

| | The deviation value of conversion (DV) | | | | | | | New scaled value (NV) | | | | | | |
|---|---|---|---|---|---|---|---|---|---|---|---|---|---|---|
| G | D1 | D2 | D3 | D4 | D5 | D6 | D7 | D1 | D2 | D3 | D4 | D5 | D6 | D7 |
| 1 | 1.0 | | | | | | | 1 | | | | | | |
| 2 | | 4.1 | | 0.7 | | | | | 1 | | 1 | | | |
| 3 | 1.3 | 1.2 | 1.7 | | | | | 1 | 1 | 1 | | | | |
| 4 | 0.9 | 1.5 | | | 4.5 | | | 1 | 1 | | | 1 | | |
| 5 | 0.3 | | 3.1 | | | | | 1 | | 1 | | | | |
| 6 | 5.4 | | | | | | | 2 | | | | | | |
| 7 | 10.0 | | 11.9 | | | | | 3 | | 3 | | | | |
| 8 | | | | | | | 14.5 | | | | | | | 3 |
| 9 | 3.4 | | | | 21.2 | | | 1 | | | | 5 | | |
| 10 | 20.2 | | | | | 3.2 | | 4 | | | | | 1 | |
| 11 | | | | | | | 26.7 | | | | | | | 6 |
| 12 | 19.4 | | | | | | | 3 | | | | | | |
| | | | | | | | Avg | 1.9 | 1.0 | 1.7 | 1.0 | 3.0 | 1.0 | 4.5 |

$\{1 \leq DV < 5|NV = 1\}, \{5 \leq DV < 10|NV = 2\}, \{10 \leq DV < 15|NV = 3\}, \{15 \leq DV < 20|NV = 4\}, \{20 \leq DV < 25|NV = 5\}, \{25 \leq DV < 30|NV = 6\}$ Avg = average of parameter variations

Considering the ternary composition Mo-Ru(Sn)-Te, 12 library generations were designed by changing descriptor (D1–D7). Each color shows the sensitivity of descriptor with regard to conversion performance. For example, the value of the red color has the highest influences in the increase of conversion based on changing the value of descriptor. In addition, the value of the green color clearly represents less impact. As is shown in table 6.7, the average values of parameter variations (Avg) were calculated to determine the data of Figure 6.14 below.

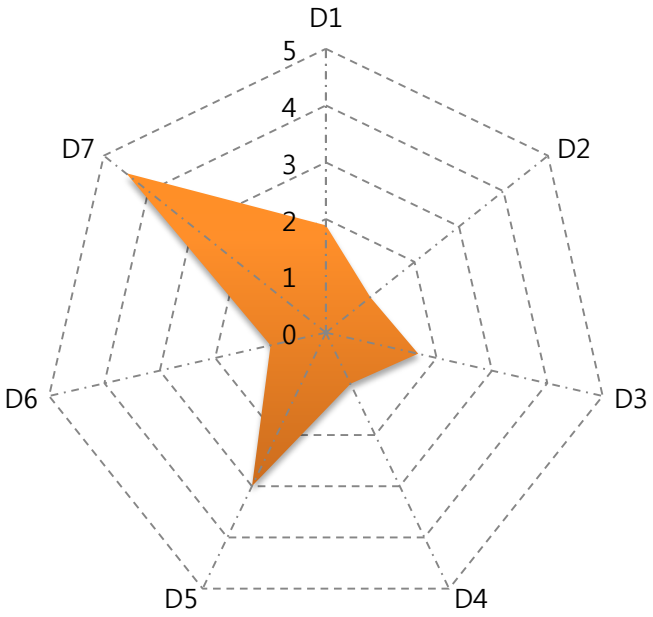


Figure 6.14 The summary of influence of 7 parameter variations along 12 generation
(D1: material composition; D2: pH by $HNO_3$; D3: amount of citric acid; D4: mixture with ethylene glycol; D5: aging precursors in solution; D6: stirring; D7: type of precursors)

Figure 6.14 shows that the aspects of D5 and D7 are the most important key factors to improve catalyst activity. It also shows a medium importance of the aspects is D1 and D3. Lastly, as expected, D2, D4 and D6 are not of much importance. However, the three values cannot be totally neglected.

Aging time of solution (D5) together with type of precursor (D7) was shown as one of the important factors. In order to study this influence, stock solutions of RuCl (0.1 mol/L) and SnCl (0.1 mol/L) as starting material in methanol solvent were used in G5 and G9. The aging time of these stock solutions, especially RuCl, showed a strong effects on the catalytic activity. It was thought that this may result from the change of the oxygen state of precious metal because of absorbing sunlight

during aging time. The role of aging time during catalyst synthesis was unclear. However, it was concluded that the failure of catalyst reproducibility in the secondary screening process was caused by deviations in the aging time of the stock solution.

The type of precursor (D7) was also shown to be an important key factor. Instead of finding the suitable aging time of the metal chloride in methanol, it was decided to seek appropriate precursors. As a result, Tin(IV)2,4-pentanedionate and Ruthenium(III) acetylacetonat were shown to be the best precursors for preparing stock solutions for catalyst synthesis.

Interestingly, materials composition (D1) seemed to be quite unimportant compared to other factors such as D5 and D7. Generally, the chemical composition of catalysts plays a very important role in the catalyst activity. However, by primary screening procedure the span of material composition here was already optimized, which led to less impact on the experimental results.

Although D2, D4 and D6 had little influence in improving their catalytic performance, it was still difficult to draw clear conclusions, because the number of experiments was insufficient to obtain reliable results, and variations of the factors were too small to notice any influence.

In addition to these, this study was not prepared for quantitative analysis, which means that this pattern visualization cannot be perfect because of the lack of data and the previously taken assumptions. Therefore, it cannot compare the absolute difference of 7 descriptors on selective oxidation catalyst from propene to acrolein, but it was enough to show the relative difference based on the pattern concerning catalyst activity.

### *6.2.8 The result of generation 12*

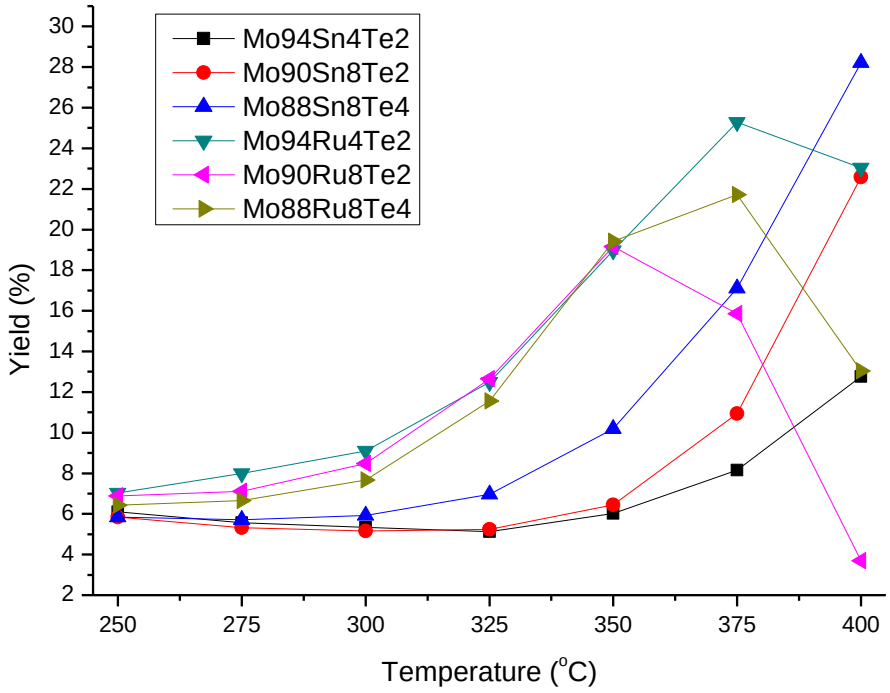


Figure 6.15 Yield of acrolein in generation 12 without catalyst pre-treatment

Reaction condition: 50 mg of catalysts diluted with 100 mg of sand with particle size of 100-200 μm. Total flow rate: 25mL/min ($C_3H_6$:$O_2$:$N_2$=2:2:96 vol%)

So far, two catalyst compositions, Mo-Ru-Te and Mo-Sn-Te, were optimized to generation 12. Although the two catalysts, $Mo_{94}Ru_4Te_2$ and $Mo_{88}Sn_8Te_4$ showed the best yield at 400 °C, they exhibit a totally different behavior with increasing temperature.

In the case of the Sn containing catalyst, the amount of Sn-Te in the Mo-oxide seemed directly proportional to the yield. In addition, the yield increased with increasing temperature. In contrast, the amount of Ru-Te in the Mo-oxide was inversely preoperational to the yield, and after 350 °C the yield of acrolein abruptly decreased.

Based on the result of the composition in $Mo_{94}Ru_4Te_2$ it seems that Ru and Te are best up to a maximum of $Re_4$ and $Te_2$, but $Mo_{88}Sn_8Te_4$ still has potential to increase the amount of Sn and Te in the catalyst so as to increase its yield.

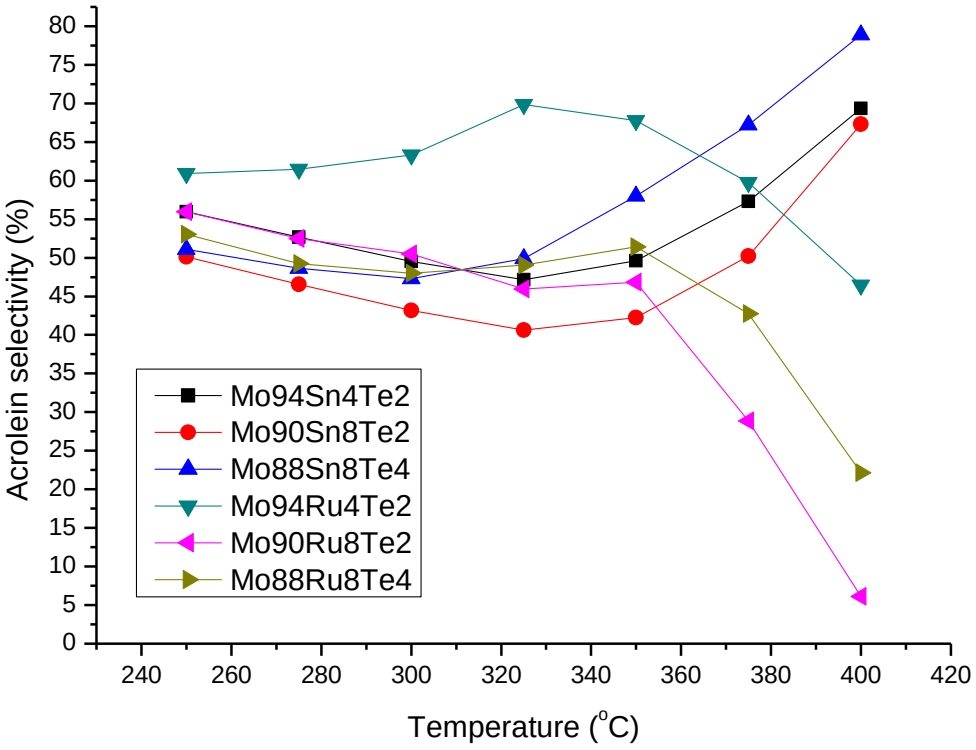


Figure 6.16 Selectivity of acrolein in generation 12 without catalyst pre-treatment

Reaction condition: 50 mg of catalysts diluted with 100 mg of sand with particle size of 100-200 μm. Total flow rate: 25mL/min ($C_3H_6$:$O_2$:$N_2$=2:2:96 vol%)

Figure 6.16 describes that the decrease in the yield of Ru or Sn contained catalyst in Figure 6.15 is associated with the decrease in selectivity to acrolein. In this regard, the higher amount of Ru seems to induce an increase in the total oxidation producing $CO_2$ and $H_2O$ at a temperature more than 350 °C. Eventually, it is of interest to note that the Ru contained catalysts are still better than the Sn contained ones at low temperatures as can be seen from Figure 6.16. In contrast, at high temperatures, the Sn contained catalysts had an outstanding activity for propene conversion to acrolein.

In addition to these results, our study showed that both catalysts were very sensitive according to the conditions of catalyst preparation on sol-gel method. During the optimization processes, the developed catalysts could be further optimized by a third generation screening.

## *6.3 Discussion*

The study for a better understanding of the parameters governing sol-gel chemistry and the development of a suitable processing method has shown that the structure of the catalyst highly depends on its preparation during the sol-gel process. The type of inorganic or organic precursor influences the specific micro-structure of the catalysts, which affects catalytic activity.

In discovering Mo-based catalyst for propene to acrolein, the primary screening and secondary screening method were implemented. The stage robot reactor as the primary screening tool surveyed the Mo-based catalysts modified with 50 different dopants. At the same time, a new parallel-reactor was developed and used as a secondary screening method. It was used to validate hits of the catalysts discovered in the primary screening and to optimize the activity of the catalysts.

$Mo_{94}Ru_4Te_2$ and $Mo_{88}Sn_8Te_4$ were identified as the best catalysts for selective propene oxidation to acrolein among those investigated. Small amounts of doping with Te increased the catalytic performance. This is in agreement with a previous study that showed that multicomponent oxide systems, based on Mo with Te, are effective catalysts for the selective oxidation of olefins[166].

It was also found that the use of chloride based precursors (RuCl, SnCl) needed aging for more than one month in day light for better activity. It seems that metal-chloride bonds methanolyzed slowly under formation of the more reactive methanolate-species. To develop $Mo_{94}Ru_4Te_2$, Ruthenium(III)chloride was used as starting material, which neighboring stable oxidation states, especially Ru(II)[171], Ru(III)[171], and Ru(IV)[172]. First, it was theorized that aging is necessary to change the oxygen state of Ru(III) to Ru(II) or Ru(IV), which is responsible for the high activity of the catalyst. However, it was found that Ruthenium(III) acetylacetonat is the best precursor for good catalytic activity without a long aging period. Hence, it can be concluded that the alkoxide group of Ruthenium(III) induced the sol-gol process to enhance the catalytic activity.

# Ⅲ. Experiment

The general strategy for high-throughput experimentation in the present study involved not only the validation and development of a new reactor but also the discovery and optimization of new catalyst. To carry out the efficient implementation of high-throughput tests required systematic combinatorial workflow without a bottleneck. Moreover, catalysts are very sensitive depending upon several influences such as composition, exact synthesis protocol, and the precursors used. In this chapter, we will explain how experiments were carried out to discover and to develop new catalysts.

## 7 Work flow overview

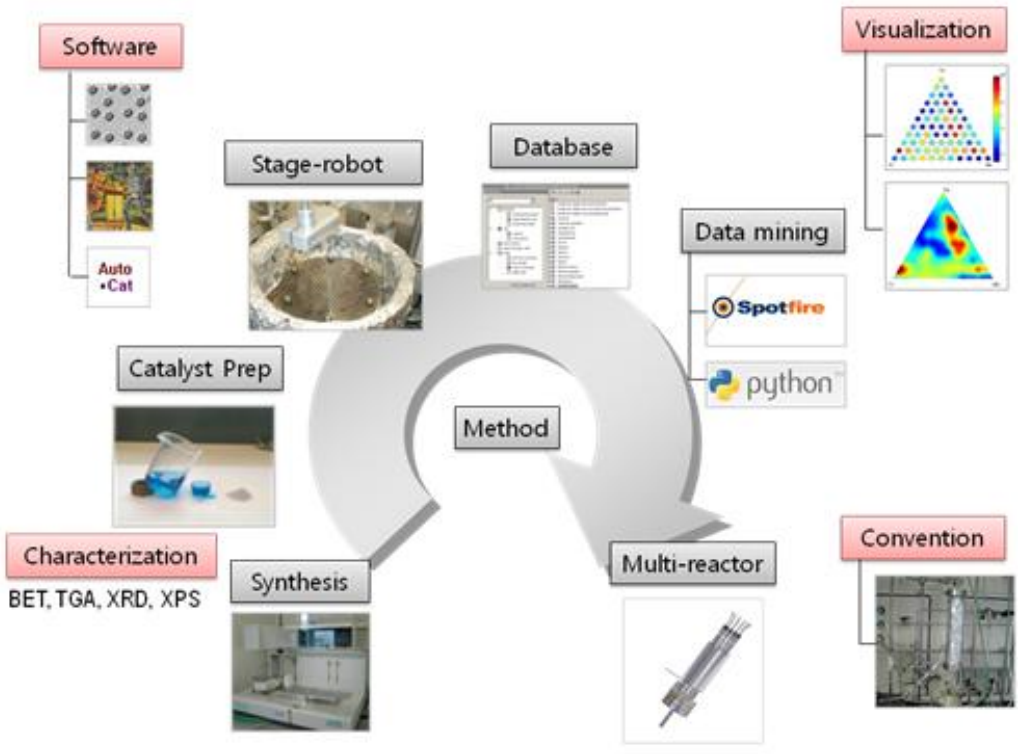


Figure 7.1 Flow chart of experiment procedure under HTE method

As is shown in Figure 7.1, the design of an experiment in this study laid within the combination of automatic synthesis, catalyst preparation by sol-gel method, a stage robot reactor as a primary screening, data mining and a 10-fold parallel reactor as secondary screening including issues of visualization, catalyst characterization and automation program.

## 7.1 Work stream

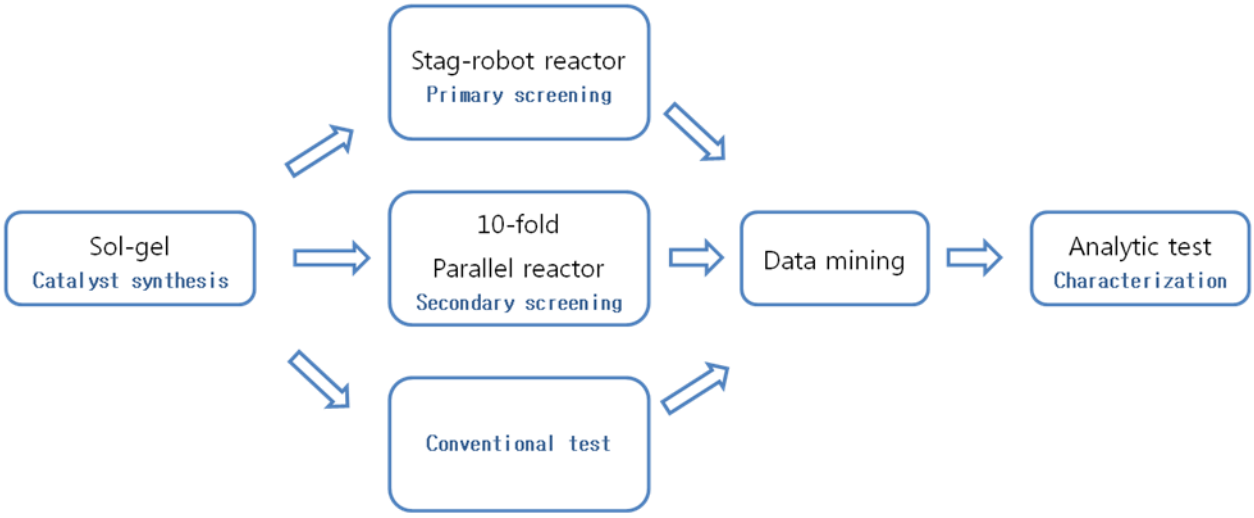


Figure 7.2 Work stream in high-throughput methods

Figure 7.2 illustrates the work stream of catalyst discovery with three screening methods. To carry out the high-throughput experimentation more effectively, this system was planned including six operation units: catalyst preparation; a stage robot reactor; a 10-fold parallel reactor; a conventional test; data mining; and analytical testing. The catalyst preparation step was totally automated by using a pipetting robot (Zinsser Analytic) through the Plattenbau library design software programmed with C++ including the python recipe code[173].

As is well known, it is a complex process to reproduce a catalyst because of several variables, such as composition, morphology, and a pore size contribute to the function of a heterogeneous catalyst. Therefore, it was necessary to classify the process into different screening methods depending on aims. The first phase, known as primary screening using the stage robot, was designed for screening multiple families of metal oxides that logically could perform the desired catalytic performance. The objective of this stage in this work was to discover “hits”, which represent truly new classes of material showing potential for specific applications. Generally, due to achieving sufficient throughput, the sheer volume of experiments often makes it impossible to obtain sufficient reliable data. Thus, "hits" discovered in the primary screening should be validated in the secondary screening process.

Our secondary screening technology using 10-fold parallel fixed bed reactor developed in the in-house workshop provided optimized clues, which assessed the feasibility of hits as development candidates and further optimized the catalyst formulation to improve activity and selectivity. In addition to these uses, it was designed to carry out catalyst kinetic study, as well as mass transfer limitation on operation concepts. Finally, optimized leads entered the third phase of development which showed final validation of the catalyst.

The amount of raw data generated in a short time through the screening method could not be analyzed in a reasonable time without the help of computers and sophisticated software. For this work, Matlab and Spotfire were used to harvest reliable data by visual data mining, which combined data mining techniques with new visualization technologies. Lastly, the obtained catalysts were analyzed by GC-MS and characterized by XRD, BET and XPS.

## *7.2 Stage robot reactor*

The high-throughput reactor system, referred to as the stage robot reactor, was previously developed in our group [78]. The catalyst library was placed between the heating stack and a reaction chamber. The top of the well, an insulating 15 mm thick ceramic mask made of Macor® provided additional reaction volume for the catalytic reaction and insulated the library plate to improve the stability of the reaction temperature on the catalyst surface. A guiding mask helped the sampling needle to thread into each well. Inside the sampling needle, a capillary bundle containing both the educt-gas supply and the product-gas sampling was placed sequentially into each well of the library plate. Since the whole reactor was moved by a xyz-stage, the sampling capillary was moved to reach every single well on the plate. Due to the open boundary conditions on the structure of the reactor, the catalytic reaction was prone to problems. For example, moisture or oxygen from ambient air could enter the reaction chamber. For the oxidation of propene, the total flow (5mL/min) of educt-gas was used with a mixture of 45.6 vol% propene and 54.4 vol % synthetic air ($C_3H_6$:$O_2$=4:1), and a mixture of 64.8 vol% propene and 35.2 vol % synthetic air ($C_3H_6$:$O_2$=9:1).

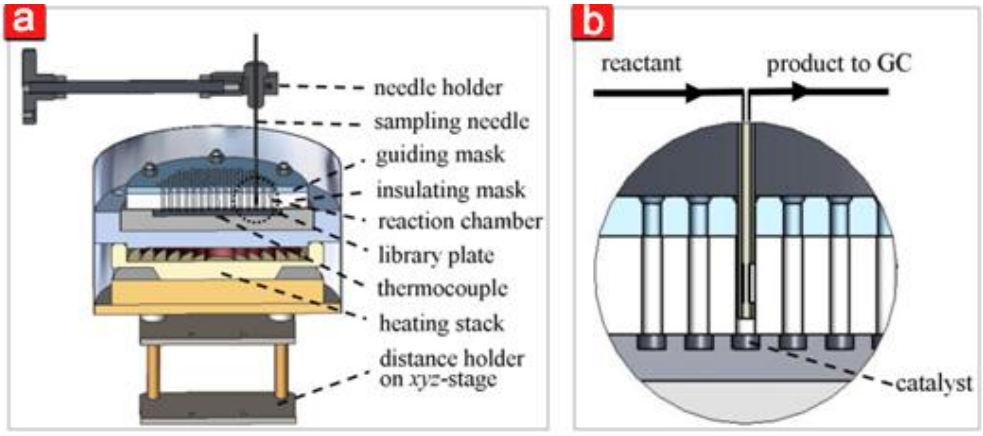


Figure 7.3 (a) Cross-section of the stage robot system (b) Magnification of the reactor chamber [83]

The gas composition of products was analyzed by a micro-gas chromatograph; model CP 4900 Varian, with a thermal conductivity detector. Three packed columns such as Porapak Q and Polar 52CB were used in parallel to separate partial oxidized products and the whole system under this experiment was controlled by TestRig software[174].

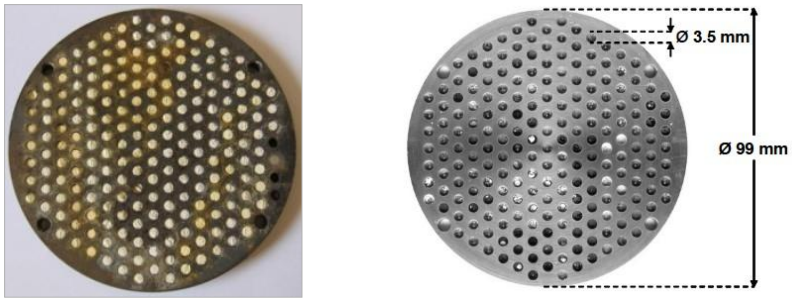


Figure 7.4 Image of a stainless-steel library plate with catalyst samples

As is shown in Figure 7.4, the typical library plates used in our group were made from either stainless-steel (right) or slate (left) plate; they contained 207 separate 2 mm deep drill holes (diameter 3.5 mm), thickness 6 mm, and diameter 99 mm in a hexagonal pattern. For the screening setup with the stage robot reactor as the primary screening process, the steel libraries were used. Some empty wells in the library functioned as background measurement, and at least one well was filled with a reference catalyst. For example, hopcalite, which is an oxide mixture based on copper and manganese oxides[175], was used as a reference catalyst.

## 7.3 10-fold parallel reactor

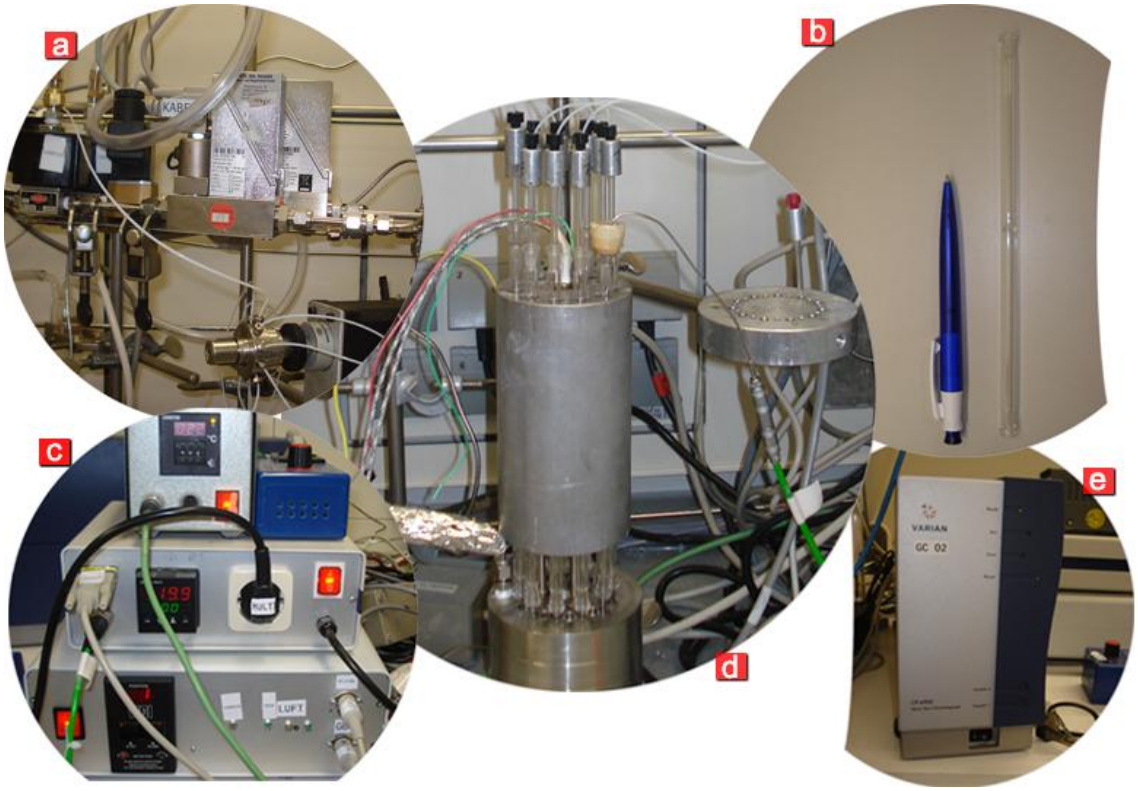


Figure 7.5 Instruments of experimental system: (a) Upstream part, (b) Tube reactor, (c) Controlling part, (d) 10-fold parallel reactor and (e) Micro-GC

As is shown in Figure 7.5, the experimental setup of the 10-fold parallel reactor in the laboratory was divided into 5 parts such as (a) upstream part, (b) tube reactor, (c) controlling part, (d) multi-channel reactor (10-fold parallel reactor) and lastly (e) micro-GC. The upstream part consisting of 3 magnetic valves controlled the feed gas under reaction conditions of 1 bar pressure and a flow rate between 25mL/min and 50 mL/min. The flow rate of feed gas was successfully tested for the same pressure for each channel. Three magnetic valves controlled the composition of the mixed feed-gas, helium and air, respectively. This feed-gas for reaction, as well as the carrier gas for cleaning the channels was flown through each channel in regular sequence controlled by the 10-channel valve. Glass tube reactors (b) were used for the tubular flow reaction. The controlling part (c) functioned to regulate the reactor temperature, control the flow rate, change flow to channels, control the magnetic valves and maintain the temperature in the outlet part at 100 °C. The reaction part (d) was tested to heat up to 400 °C. Lastly, the Micro-GC (e) (CP 4900; Varian) was used to analyze the effluent gas through the signal started by the trigger of controlling part (c).

### *7.3.1 Preparation of tube reactor*

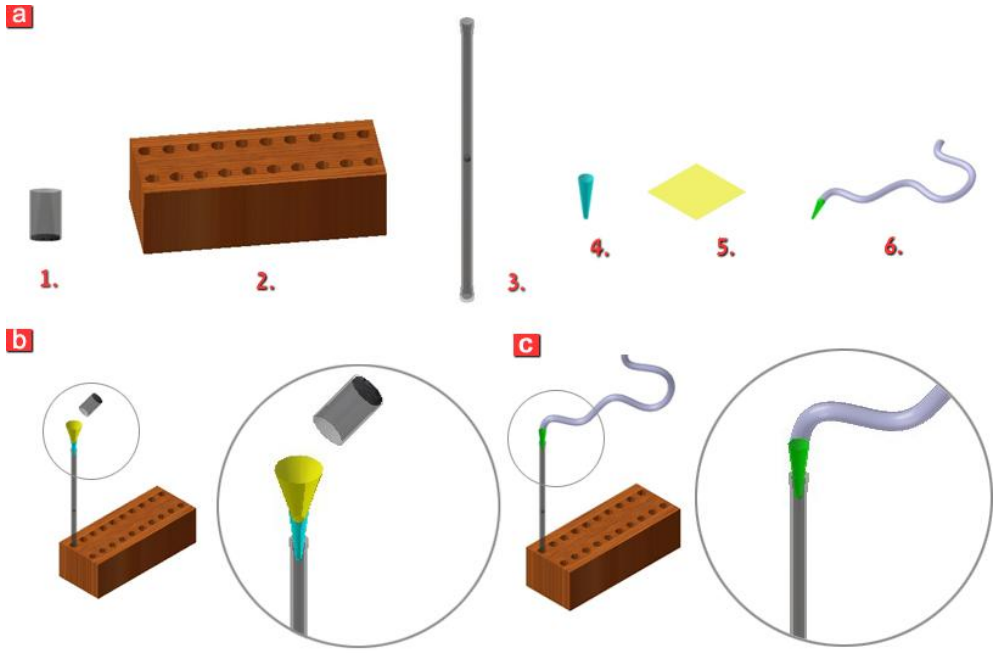


Figure 7.6 Preparation of tube reactors

20 ml flask (1), reactor rack made of wood (2), tube reactor including filter (3), pipetting tip after cutting spire (4), oil blotting paper (5) and air hose (6)

Making quick and accurate measurements of catalyzed reactions from small volumes of catalysts represented considerable problems with regard to handling materials and instruments. To solve these problems, filling a tube reactor with catalysts, as shown in Figure 7.6, followed these steps: (a) prepared (1) a 20 mL flask with catalysts ground by a glass rod after calcinations, (2) a container with 20 wells for tube reactors out of wood, (3) a fixed-bed glass tube reactor (Ø 5 mm i.d., about 220 mm length) with a glass frit, (4) a pipetting tip by cutting a hole in the spire to a diameter large enough for the falling catalysts, (5) oil blotting paper to make a funnel, and (6) a hose to inject the air into the tube reactor. (b) After assembling the tools of part, the tube reactor was filled with a catalyst. Bed (50 mg catalyst diluted with 100 mg sand) resting on a glass frit (Ø 5 mm, porosity = 0.27) in the middle of the reactor fixed in that position throughout the test run. (c) Air gas was injected into the tube reactor to blow off the fine particles of catalysts. In the preparation of small volumes of catalysts, such as 50 mg, particle size could not be controlled. Fine catalysts could contaminate the reactor, increasing the error of experimentations.

### *7.3.2 Cleaning process*

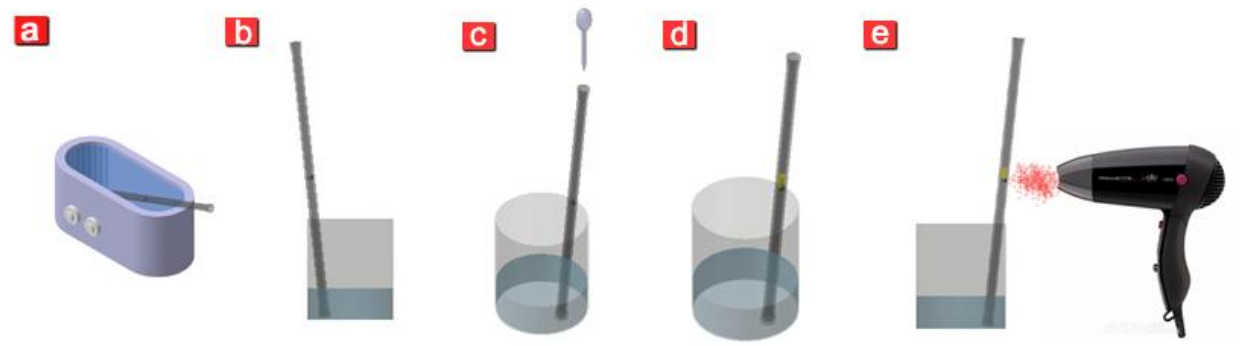


Figure 7.7 Cleaning method of a tube reactor

Increasing the experimental speed with small amounts of catalysts contributes to the problem of contamination by fine catalysts. In order to remove these fine particles in the frit of used reactors, the following 5 cleaning steps were used:

(a) After disposal of the used catalysts, the tube reactor was put in an ultrasonic bath for 30 min at 50 °C to eliminate the rest of catalysts.

(b) The reactor was put in a flask beaker containing water solution.

(c) King's water ($HNO_3$:HCl = 1:3) was dropped into the tube reactor.

(d) The tube reactor remained for a day under this condition.

(e) If the frit was not clean, king's water was again added and heated until the rest of catalysts were removed.

In addition, the splitting module of the 10-fold parallel reactor could be also contaminated by fine catalysts. To monitor this condition, the data of either an empty tube reactor or a bypass were observed. However, serious contamination of fine catalysts in the splitting module was not observed after cleaning. Though contaminated, the low activity of catalysts was apparently due to the low temperature (100 °C) in the splitting module. Generally, the splitting module was dismantled, cleaned with alcohol and dried overnight at 70 °C every half year before new measurements were taken.

## *7.4 Catalyst preparation*

A commercial pipetting robot (Zinsser Analytic) with automation system was used for catalyst synthesis based on the sol-gel method. In the procedure, the prepared metal solutions with precursors were positioned in 10 mL vials. Aliquots of each stock solution were transferred into 2 mL vials in racks of 50 vials to formulate the final reaction mixture. The concept on the combinatorial catalyst library to optimize the speed of the synthesis was applied by using the Plattenbau library design software[173]. This software could calculate the volumes of the different solutions with starting materials according to the formulated recipe written by Python. Finally, it generated a pipetting list, which was transferred to the pipetting robot and provides information with regard to the total volume of each solution needed for synthesis.

After completing the pipetting process into the entire rack, this rack was covered with a lid and placed on an orbital shaker with a maximum of 80 rpm for 15 h to have a homogenous mixture condition. After the lid was removed, the rack was aged for 7 days at room temperature. It was then dried at 40 °C for 7 days in the drying oven to allow gel formation. For calcinations, the oven was maintained at 400 °C for 5 h with a heating rate of 0.2 °C $min^{-1}$. Thereafter, the oven was cooled down to 35 °C with 0.5 °C $min^{-1}$.

After the calcinations, the catalyst powders obtained were ground in HPLC flasks by a glass rod to get better homogeneity in corn sizes, and manually transferred into 207 hexagonally positioned wells (diameter 3.5 mm) in a stainless steel library plate (diameter 99 mm). Some wells were left empty for background screening, and some were filled with a reference catalyst.

Different kinds of modified sol-gel procedures were applied to prepare libraries depending on the matrix metal precursor and different solvents. The detail of information such as catalyst preparation recipe will be introduced as follows, and the information of catalyst composition in specific libraries can be found in the appendix.

### *7.4.1 Sol-gel synthetic recipes*

1) Propene to propene oxide or acrolein

Propionic route

The molar ratio of A (0.25 M solution in methanol): B (0.25 M solution in methanol): complexing agent (4-hydroxy-4-methyl-pentanone): acid (propionic acid) was 50:50:695:2. If B was used as dopant, precious solution was prepared with 0.1 M in methanol. The preparation of $A_{50}B_{50}$ was performed by pipetting the following volumes of single solutions in sequence: 0.25 M, A in methanol (600.0 μL, 0.15 μmol), 0.25 M, B in methanol (600.0 μL, 0.15 μmol), and complexing agent mixed with propionic acid (8.06 M, 259 μL, 2087 μmol).

The list of libraries used in this recipe:

1G1L, 1G2L, 2G1L, 2G3L, 1G3L, 1G4L, 2G4L

M01, M02, M03, M04, M05, M06, M08

T01, T02, T03

Ethylene glycol route

The molar ratio of A (0.25 M solution in the mixture of water and ethylene glycol with 1:1 volume percent): B (0.25 M solution in the mixture of water and ethylene glycol with 1:1 volume percent): acid ($HNO_3$) was 50:50:346. The preparation of $A_{50}B_{50}$ was performed by pipetting the following volumes of single solutions in sequence: 0.25 M, A in water and ethylene glycol (600.0 μL, 0.15 μmol), 0.25 M, B in ethylene glycol (600.0 μL, 0.15 μmol), and nitric acid (8.06 M, 129 μL, 1043 μmol).

The list of libraries used in this recipe:

2G2L

M07

2) Mo based catalyst for propene to acrolein

Catalyst preparation for Hit validation of primary screening

For the validation of hits from primary screening, two generations such as library 1 ($Mo_{96}Sn_4$, $Mo_{96}Ru_4$ $Mo_{96}B_{i4}$, $Mo_{92}Ru_8$, $Mo_{92}Bi_8$, $Mo_{96}Rh_4$, $Mo_{96}Te_4$, $Mo_{92}Er_8$, $Mo_{92}Eu_8$ and $Mo_{92}Y_8$) and library 2 ($Mo_{94}Sn_4Te_2$, $Mo_{94}Ru_4Sb_2$, $Mo_{94}Ru_4Te_2$ and $Mo_{94}Ru_4Bi_2$) were prepared by the modified sol-gel method described in Figure 6.1. $(NH_4)_6Mo_7O_{24}{\cdot}4H_2O$ (0.25 atomic mol/L = 0.035 mol/L) aqueous solution was used containing citric acid in an atomic ratio 3:1 of citric acid (Zitronensäure) and ammonium molybdate. RuCl (Aldrich), SnCl Aldrich, Bi (Strem), Teacid (Fluka), $ErNO_3$ (Aldrich), $YNO_3$ (ABCR), and $EuNO_3$ (STREM) were added into methanol being 0.1 M concentration. The suspensions containing ammonium molybdate were distributed into 20 mL flasks. Doping solutions (0.1 M/methanol) were added into the suspension solution under a vigorous stirring. In addition to these, 1 mL $HNO_3$ was slowly added into each flask, under a stirring. After that, the samples were dried at 373 K for 18 h and calcined at 673K for 4h in air.

Catalyst preparation in secondary screening

- Generation (1-2-3)

$(NH_4)_6Mo_7O_{24}{\cdot}4H_2O$ (0.25 atomic mol/L = 0.035 mol/L) dissolved in distillated water was used containing citric acid in an atomic ratio 3:1 of citric acid (Zitronensäure) and ammonium molybdate. Doping solutions, RuCl (Aldrich) and Teacid (Fluka) with concentration (0.1 M/methanol) were prepared and added into each suspension solution with following volume to get the certain compositions under vigorous stirring with rpm 300. Lastly, $HNO_3$ was slowly added into each flask, under a stirring.

| [ml] | Composition | C/Mo | Mo | Ru | Sn | Te | $HNO_3$ | EG |
|---|---|---|---|---|---|---|---|---|
| Generation 1 | | | | | | | | |
| 1 | $Mo_{94}Ru_4Te_2$ | 3 | 9.4 | 1 | 0 | 0.5 | 1 | |
| 2 | $Mo_{92}Ru_4Te_4$ | 3 | 9.2 | 1 | 0 | 1 | 1 | |
| 3 | $Mo_{90}Ru_4Te_6$ | 3 | 9 | 1 | 0 | 1.5 | 1 | |
| 4 | $Mo_{94}Ru_2Te_4$ | 3 | 9.4 | 0.5 | 0 | 1 | 1 | |
| 5 | $Mo_{96}Ru_2Te_2$ | 3 | 9.6 | 0.5 | 0 | 0.5 | 1 | |
| Generation 2 | | | | | | | | |
| 1 | $Mo_{94}Ru_4Te_2$ | 3 | 9.4 | 1 | 0 | 0.5 | 1 | |
| 2 | $Mo_{94}Ru_4Te_2$ | 3 | 9.4 | 1 | 0 | 0.5 | 1.5 | |
| 3 | $Mo_{94}Ru_4Te_2$ | 3 | 9.4 | 1 | 0 | 0.5 | 1 | 2 |
| 4 | $Mo_{94}Ru_4Te_2$ | 3 | 9.4 | 1 | 0 | 0.5 | 1.5 | 2 |
| 5 | $Mo_{94}Ru_4Te_2$ | 6 | 9.4 | 1 | 0 | 0.5 | 1.5 | 2 |
| Generation 3 | | | | | | | | |
| 1 | $Mo_{88}Ru_8Te_4$ | 3 | 8.8 | 2 | 0 | 1 | 1 | 2 |
| 2 | $Mo_{84}Ru_8Te_8$ | 3 | 8.6 | 2 | 0 | 2 | 1 | 2 |
| 3 | $Mo_{80}Ru_8Te_{12}$ | 3 | 8.2 | 2 | 0 | 3 | 1 | 2 |
| 4 | $Mo_{88}Ru_8Te_4$ | 3 | 8.8 | 2 | 0 | 1 | 2 | 2 |
| 5 | $Mo_{88}Ru_8Te_4$ | 0 | 8.8 | 2 | 0 | 1 | 1 | 2 |

EG: Ethylen glcohol

- Generation 4

Two different Ru precursor solutions were prepared. One (Ru) was just normal RuCl in methanol with 0.1 M. The other (Ru*) was aged for more than one month.

| [ml] | Composition | Mo | Ru | Sn | Te | $HNO_3$ | EG |
|---|---|---|---|---|---|---|---|
| Generation 4 | | | | | | | |
| 1 | $Mo_{94}Ru^*_4Te_2$ | 9.4 | 1 | 0 | 0.5 | 1 | 2 |
| 2 | $Mo_{94}Ru_4Te_2$ | 9.4 | 1 | 0 | 0.5 | 1 | 2 |
| 3 | $Mo_{94}Ru_4Te_2$ | 9.4 | 1 | 0 | 0.5 | 2 | 2 |
| 4 | $Mo_{88}Ru_8Te_{12}$ | 8.2 | 2 | 0 | 1.5 | 1 | 2 |

Ru*: with one month aging

- Generation (5-6-7)

Here, the sol-gel preparation method used was the same as previous used method. During increase of generation, the composition and the amount of citric acid were changed.

| [ml] | Composition | C/Mo | Mo | Ru | Sn | Te | $HNO_3$ | EG |
|---|---|---|---|---|---|---|---|---|
| Generation 5 | | | | | | | | |
| 1 | $Mo_{94}Ru_4Te_2$ | 0 | 9.4 | 1 | 0 | 0.5 | 1 | 2 |
| 2 | $Mo_{94}Ru_4Te_2$ | 1.5 | 9.4 | 1 | 0 | 0.5 | 1 | 2 |
| 3 | $Mo_{92}Ru_4Te_4$ | 1.5 | 9.2 | 1 | 0 | 1 | 1 | 2 |
| 4 | $Mo_{94}Ru_2Te_4$ | 1.5 | 9.2 | 0.5 | 0 | 1 | 1 | 2 |
| 5 | $Mo_{94}Ru_4Te_2$ | 3 | 9.4 | 1 | 0 | 0.5 | 1 | 2 |
| 6 | $Mo_{92}Ru_4Te_4$ | 3 | 9.2 | 1 | 0 | 1 | 1 | 2 |
| 7 | $Mo_{94}Ru_2Te_4$ | 3 | 9.2 | 0.5 | 0 | 1 | 1 | 2 |
| Generation 6 | | | | | | | | |
| 1 | $Mo_{94}Ru_4Te_2$ | 3 | 9.4 | 1 | 0 | 0.5 | 1 | 2 |
| 2 | $Mo_{92}Ru_6e_2$ | 3 | 9.2 | 1.5 | 0 | 0.5 | 1 | 2 |
| 3 | $Mo_{90}Ru_6Te_4$ | 3 | 9.0 | 1.5 | 0 | 1 | 1 | 2 |
| 4 | $Mo_{92}Ru_4Te_4$ | 3 | 9.2 | 1 | 0 | 1 | 1 | 2 |
| 5 | $Mo_{90}Ru_4Te_6$ | 3 | 9.0 | 1 | 0 | 1.5 | 1 | 2 |
| Generation 7 | | | | | | | | |
| 1 | $Mo_{94}Ru_4Te_2$ | 0 | 9.4 | 1 | 0 | 0.5 | 1 | 2 |
| 2 | $Mo_{92}Ru_6Te_2$ | 0 | 9.0 | 1.5 | 0 | 0.5 | 1 | 2 |
| 3 | $Mo_{94}Ru_4Te_2$ | 3 | 9.4 | 1 | 0 | 0.5 | 1 | 2 |
| 4 | $Mo_{92}Ru_6Te_2$ | 3 | 9.0 | 1.5 | 0 | 0.5 | 1 | 2 |
| 5 | $Mo_{96}Ru_4$ | 0 | 9.6 | 1 | 0 | 0 | 1 | 2 |
| 6 | $Mo_{94}Ru_6$ | 0 | 9.4 | 1.5 | 0 | 0 | 1 | 2 |
| 7 | $Mo_{96}Ru_4$ | 3 | 9.6 | 1 | 0 | 0 | 1 | 2 |
| 8 | $Mo_{94}Ru_6$ | 3 | 9.4 | 1.5 | 0 | 0 | 1 | 2 |

EG: Ethylen glcohol

- Generation (8-9-10-11)

Here, in generation 8, several different precursor metals were used to prepare solutions as follows. Mo (Ammonium molybdate tetrahydrate), $Mo^1$ (phosphomolybdic acid), $Mo^2$ (Bi(acetonitrile)molybdenum chloride) were used as Molybdate precursors and Ru*(Ruthenium chloride with more than one month of aging), $Ru^1$(Ammonium hexachlororuthenate) $Ru^2$ (Ruthenium(III) acetylacetonate) were used as Ruthenium precursors. Molybdate (0.25 atomic mol/L = 0.035 mol/L) dissolved in distilled water was used containing citric acid in an atomic ratio

3:1 of citric acid (Zitronensäure) and ammonium molybdate. Doping solutions of three Ruthenium precursors were prepared with concentration (0.1 M/methanol). In generation 10, two rpm (revolution per minute) conditions, rpm 250 and rpm 300, were used to mix solutions.

In generation 11, $Ru^3$ (Ruthenium(IV)oxide anhydrous), $Ru^2$ (Ruthenium(III) acetylacetonate), $Sn^1$(Tintetraisopropoxytin-isoprosal adduct) and $Sn^2$(Tin(IV) acetate) were used for checking the influence of different precursor metals.

| [ml] | Composition | C/Mo | Mo | Ru | Sn | Te | $HNO_3$ | EG |
|---|---|---|---|---|---|---|---|---|
| Generation 8 | | | | | | | | |
| 1 | $Mo_{92}Ru^1{}_6Te_2$ | 3 | 9.2 | 1.5 | 0 | 0.5 | 1 | 2 |
| 2 | $Mo_{92}Ru^2{}_6Te_2$ | 3 | 9.2 | 1.5 | 0 | 0.5 | 1 | 2 |
| 3 | $Mo_{92}Ru^*{}_6Te_2$ | 3 | 9.2 | 1.5 | 0 | 0.5 | 1 | 2 |
| 4 | $Mo^1{}_{92}Ru^1{}_6Te_2$ | 3 | 9.2 | 1.5 | 0 | 0.5 | 1 | 2 |
| 5 | $Mo^1{}_{92}Ru^2{}_6Te_2$ | 3 | 9.2 | 1.5 | 0 | 0.5 | 1 | 2 |
| 6 | $Mo^1{}_{92}Ru^*{}_6Te_2$ | 3 | 9.2 | 1.5 | 0 | 0.5 | 1 | 2 |
| 7 | $Mo^2{}_{92}Ru^1{}_6Te_2$ | 3 | 9.2 | 1.5 | 0 | 0.5 | 1 | 2 |
| 8 | $Mo^2{}_{92}Ru^2{}_6Te_2$ | 3 | 9.2 | 1.5 | 0 | 0.5 | 1 | 2 |
| 9 | $Mo^2{}_{92}Ru^*{}_6Te_2$ | 3 | 9.2 | 1.5 | 0 | 0.5 | 1 | 2 |
| Generation 9 | | | | | | | | |
| 1 | $Mo_{94}Sn_4Te_2$ | 3 | 9.4 | 0 | 1 | 0.5 | 1 | 2 |
| 2 | $Mo_{94}Ru^*{}_4Sb_2$ | 3 | 9.4 | 1 | 0 | 0.5 | 1 | 2 |
| 3 | $Mo_{94}Ru^*{}_4Te_2$ | 3 | 9.4 | 1 | 0 | 0.5 | 1 | 2 |
| 4 | $Mo_{94}Ru^*{}_4Bi_2$ | 3 | 9.4 | 1 | 0 | 0.5 | 1 | 2 |
| 1 | $Mo_{94}Sn_4Te_2$ | 3 | 9.4 | 0 | 1 | 0.5 | 1 | 2 |
| 2 | $Mo_{92}Sn_6Te_2$ | 3 | 9.4 | 0 | 1.5 | 0.5 | 1 | 2 |
| 3 | $Mo_{92}Sn_4Te_4$ | 3 | 9.4 | 0 | 1 | 1 | 1 | 2 |
| 4 | $Mo_{94}Sn_4Te_2$ | 3 | 9.4 | 0 | 1 | 0.5 | 1 | 2 |
| Generation 10 | | | | | | | | |
| 1 | $+Mo_{94}Sn_4Te_2$ | 0 | 9.4 | 0 | 1 | 0.5 | 1 | 2 |
| 2 | $+Mo_{94}Sn_4Te_2$ | 3 | 9.4 | 0 | 1 | 0.5 | 1 | 2 |
| 3 | $+Mo_{92}Ru_8$ | 0 | 9.4 | 2 | 0 | 0 | 1 | 2 |
| 4 | $+Mo_{92}Ru_8$ | 3 | 9.4 | 2 | 0 | 0 | 1 | 2 |
| 5 | $Mo_{94}Sn_4Te_2$ | 0 | 9.4 | 0 | 1 | 0.5 | 1 | 2 |
| 6 | $Mo_{94}Sn_4Te_2$ | 3 | 9.4 | 0 | 1 | 0.5 | 1 | 2 |
| 7 | $Mo_{92}Ru_8$ | 0 | 9.4 | 2 | 0 | 0 | 1 | 2 |
| 8 | $Mo_{92}Ru_8$ | 3 | 9.4 | 2 | 0 | 0 | 1 | 2 |

| Generation 11 | | | | | | | | |
|---|---|---|---|---|---|---|---|---|
| 1 | $Mo_{96}Sn^{1}{}_{1}Te_{2}Ti_{2}$ | 0 | 9.4 | 0 | 0.5 | 0.5 | 1 | 2 |
| 2 | $Mo_{96}Sn^{2}{}_{1}Te_{2}Ti_{2}$ | 0 | 9.4 | 0 | 0.5 | 0.5 | 1 | 2 |
| 3 | $Mo_{94}Ru^{3}{}_{2}Te_{2}Ti_{2}$ | 0 | 9.4 | 1 | 0 | 0.5 | 1 | 2 |
| 4 | $Mo_{94}Ru^{2}{}_{2}Te_{2}Ti_{2}$ | 0 | 9.4 | 1 | 0 | 0.5 | 1 | 2 |
| 5 | $Mo_{94}Sn^{1}{}_{4}Te_{2}$ | 0 | 9.4 | 0 | 2 | 0.5 | 1 | 2 |
| 6 | $Mo_{94}Sn^{2}{}_{4}Te_{2}$ | 0 | 9.4 | 0 | 2 | 0.5 | 1 | 2 |
| 7 | $Mo_{94}Ru^{3}{}_{4}Te_{2}$ | 0 | 9.4 | 2 | 0 | 0.5 | 1 | 2 |
| 8 | $Mo_{94}Ru^{2}{}_{4}Te_{2}$ | 0 | 9.4 | 2 | 0 | 0.5 | 1 | 2 |

Rpm 250: +

Aging more than one month: *

- Generation 12

The last generation, Ammonium molybdate tetrahydrate, $Sn^{3}$ (Tin(II)-2.4-pentanedionate) and $Ru^{2}$ (Ruthenium(III) acetylacetonate) were used as precursor metals without adding citric acid.

| | Generation 12 | | | | | | | |
|---|---|---|---|---|---|---|---|---|
| 1 | $Mo_{94}Sn^{3}{}_{4}Te_{2}$ | 0 | 9.4 | 0 | 2 | 0.5 | 1 | 1 |
| 2 | $Mo_{90}Sn^{3}{}_{8}Te_{2}$ | 0 | 9.4 | 0 | 4 | 0.5 | 1 | 1 |
| 3 | $Mo_{89}Sn^{3}{}_{7}Te_{4}$ | 0 | 9.4 | 0 | 4 | 0.5 | 1 | 1 |
| 4 | $Mo_{94}Sn^{3}{}_{4}Te_{2}$ | 0 | 9.4 | 0 | 1 | 0.5 | 1 | 1 |
| 5 | $Mo_{94}Ru^{2}{}_{4}Te_{2}$ | 0 | 9.4 | 2 | 0 | 0.5 | 1 | 1 |
| 6 | $Mo_{90}Ru^{2}{}_{8}Te_{2}$ | 0 | 9.4 | 2 | 0 | 0.5 | 1 | 1 |
| 7 | $Mo_{89}Ru^{2}{}_{7}Te_{4}$ | 0 | 9.4 | 2 | 0 | 0.5 | 1 | 1 |
| 8 | $Mo_{94}Ru^{2}{}_{4}Te_{2}$ | 0 | 9.4 | 2 | 0 | 0.5 | 1 | 1 |

# Ⅳ. Summary and conclusions

The main objective of this study was to find a high-throughput secondary screening method for two selective oxidation reactions of propene. Due to various products and the complex mechanism for selective reactions, our common high-throughput methods, such as the stage robot reactor (SRR) and the IR-camera, were found unsuitable.

During the new project, a 10-fold parallel reactor for catalytic tests was constructed in the in-house workshop. Ten miniature tube type reactors were installed and automated with regard to adjusting the temperature of the reaction chamber, switching the reactant feed-gases, and controlling the Micro-GC. Control box including an electric circuit was developed on the purpose of transmitting signal to other instruments. For the automation of catalyst experiment, AutoCat was programmed by C++. This software is based on GUI concept and can identify entire process in real-time.

Generally, multi-position valve in parallel reactor was installed downstream since it can avoid the contamination of effluent-gas to be analyzed. However, this concept causes problems either to distribute the flow rate and pressure drop equally through channels or to increase expenses due to feed-gas consumption. In the 10-fold parallel reactor, a multi-position valve was put upstream without these disadvantages. A potential gas contamination problem was solved by the development of the gas splitting module to function minimizing or eliminating the influence of gas contamination between online and offline columns. This secondary screening method replaced the conventional test in the application of hit validation and catalyst optimization.

In order to validate the compatibility of results at each channel, catalyst reaction of carbon-monoxide was applied with Hopcalite. For this, Whisker Diagrams was depicted and showed the deviation of conversion from minimum (2.30; 75 °C) to maximum (5.59; 125°C). To study the distribution of temperature FEA simulation was performed. Apart from this, a new hexagonal aluminum-rack was applied in the entire catalyst processes such as synthesis, aging, heating, cacinations, and testing. In the ternary composition spread of Ag, Cu and Mn, results showed that the new rack is enough to recognize a pattern for decision-making in discovery of catalysts.

Using the stage robot reactor (SRR), the search for catalysts for the conversion of propene to propene oxide was carried out. Five libraries with around 1000 catalysts were synthesized based on the sol-gel method with the binary composition spread of 27 materials. Surprisingly, the results of the conventional tests were incompatible with that of the high-throughput tests. Two reasons, such

as deactivation of catalysts and non-similarity of the structure of the reaction chamber between SRR and PFR were assumed. First, the catalysts developed for the propene epoxidation showed very fast deactivation, and it was found necessary to carry out the reduction with $H_2$ pretreatment. Second, basically, the open structure of SRR makes it difficult to obtain the same result of PFR because of the post-reaction, which may have taken place easily with propene oxide due to its reactivity.

The study of propene to acrolein was performed by using the SRR and the 10-fold parallel reactor. The best catalysts discovered in the primary screening with six libraries were tested to validate the hits in the secondary screening. Subsequently, the optimization process of the catalysts resulted in the catalyst of $Pd_{10}Cu_{30}Ga_{60}$ with the best activity. The result for the composition spread of $Cu_{1-100}Pd_{0-10}Ga_{1-100}$ illustrated that $Pd_{10}Ga_{45}Cu_{45}$ was most active for acrolein production at the mild temperature of 300 °C.

Mo based catalysts were used as starting material for the study of propene to acrolein. Through high-throughput methods, 200 samples in the primary process and 12 generations in the secondary process were tested. Finally, $Mo_{94}Ru_4Te_2$ and $Mo_{88}Sn_8Te_4$ showed very high propene conversion to acrolein with yield of 25% at 375 °C and yield of 28% at 400 °C, respectively. To develop $Mo_{94}Ru_4Te_2$, Ruthenium(III)chloride was used as starting material that needed longer aging. Ruthenium(III) acetylacetonat was found as the best precursor for good catalytic activity without aging. As a result, it seems that the alkoxide group of Ruthenium(III) induced the sol-gol process to enhance the catalytic activity, and metal-chloride bonds was methanolyzed to obtain more reactive methanolate-species.

Consequently, this work indicates that the new developed 10-fold parallel reactor provided a helpful tool for enhancing catalyst discovery in the secondary screening process. Through the experimentation for the search of selective propene oxidation catalysts we reached the goal of our project. This obtained knowledge can be used to extend common high-throughput technology. Especially, it is expected that the combination of the IR-camera method and the 10-fold parallel reactor will provide better benefits in this regard. Nevertheless it is worth mentioning that due to the sensitivity of the catalysts to the preparation, reproduction and scale-up may become difficult.

# Ⅴ. Zusammenfassung und Ausblick

Das Hauptziel dieser Studie bestand darin, die Hochdurchsatz-Methode des sekundären Screenings für zwei selektive Oxidationsreaktionen zu finden. Aufgrund von verschiedenen Produkten und des komplexen Mechanismus für selektive Reaktionen wurden unsere üblichen Hochdurchsatz-Methoden, solche wie der Stage-Robot-Reaktor (SRR) und die IR-Kamera, als ungeeignet befunden. Durch das neue Projekt wurde in der hauseigenen Werkstatt ein 10-fach-Parallel-Reaktor für katalytische Tests konstruiert. Zehn Miniatur-Rohr-Reaktoren wurden installiert und automatisiert in Bezug auf die Einstellung der Temperatur der Reaktionskammer, den Wechseln der Edukt-Gase und die Kontrolle des Mikro-GC. Die Kontrollbox mitsamt der elektrischen Beschaltung wurde mit der Absicht entwickelt, Signale auf andere Instrumente zu übertragen. Für die Atomisierung des Katalysatoren-Experiments wurde AutoCat von C++ programmiert. Diese Software basiert auf dem GUI-Konzept und kann den gesamten Prozess in Echtzeit aufzeigen.

Im Allgemeinen wurde ein Mehrkanal-Ventil im Parallelreaktor ablaufseitig installiert, da sie die Kontaminierungsanalyse von Ausflussgasen verhindern kann. Allerdings verursacht dieses Konzept Probleme, entweder um die Flussrate und Druckverlust gleichmäßig durch die Kanäle zu verteilen, oder in Bezug auf die steigenden Kosten bezüglich der Gaszufuhr-Konsumption. Im 10-fach-Parallelreaktor wurde ein Mehrkanal-Ventil ohne diese Nachteile zulaufseitig angebracht. Ein potenziales Gaskontaminierungsproblem wurde durch die Entwicklung eines Gas-Splitting-Moduls gelöst, welches die Verkleinerung oder Eliminierung des Einflusses der Gaskontamination zwischen online und offline Spalten bewirkt. Diese sekundäre Screening-Methode ersetzte den üblichen Test bei der Anwendung von der Hit-Validierung und Katalysatorenoptimierung.

Um die Kompatibilität der Ergebnisse in jedem Kanal zu validieren, wurde die Katalysatorenreaktion von Kohlenmonoxid mit Hopcalite angewandt. Dafür wurden Whisker Diagramme wiedergegeben, welche die Deviation der Konversion vom Minimum (2.30; 75°C) zum Maximum (5.59; 125°C) zeigten. Um die Distribution von Temperaturen zu studieren, wurde die FEA-Simulation ausgeführt. Davon abgesehen wurde ein neuer hexagonaler Aluminium-Behälter in den gesamten Katalysatorenprozessen wie Synthese, Alterung, Erhitzung, Kalzination und Testung eingesetzt. In der ternären Zusammensetzung von Ag, Cu und Mn zeigten die Ergebnisse, dass der neue Behälter genug ist, um ein Muster für Entscheidungentreffen bei der Entdeckung von Katalysatoren zu erkennen.

Unter Nutzung des Stage-Robot-Reaktors (SRR) wurde die Suche nach Katalysatoren für die Konversion von Propen zu Propenoxid ausgeführt. Fünf Bibliotheken mit etwa eintausend Katalysatoren wurden auf Basis der Sol-Gel-Methode mit der binären Zusammensetzung und Verbreitung von siebenundzwanzig Materialien synthetisiert. Überraschenderweise passten die Ergebnisse der konventionellen Tests nicht mit jenen des Hochdurchsatzverfahrens zusammen. Hierfür wurden zwei Gründe, nämlich die Deaktivierung der Katalysatoren und die Ungleichheit der Struktur der Reaktionskammer zwischen SRR und PFR, vorgelegt. Erstens zeigten die Katalysatoren, welche für die Propenepoxidation entwickelt worden waren, sehr schnelle Deaktivierung, sodass es als nötig befunden wurde, die Reduzierung mit $H_2$-Vorbehandlung auszuführen. Zweitens, und hauptsächlich, macht die offene Struktur von SRR es schwierig, das gleiche Resultat von PFR zu erhalten, aufgrund der Postreaktion, welche mit Propenoxid einfach abläuft aufgrund seiner Reaktionsfähigkeit.

Die Studie von Propen zu Acrolein wurde unter Nutzung der SRR und des 10-fachen-Parallelreaktors durchgeführt. Die besten Katalysatoren der sechs Bibliotheken, entdeckt im primären Screening, wurden getestet, um die Hits im zweiten Screening zu validieren. Anschließend resultierte der Optimierungsprozess der Katalysatoren in dem Katalysator mit den besten Ergebnissen $Pd_{10}Cu_{30}Ga_{60}$. Das Ergebnis für die Komposition aus $Cu_{1–100}Pd_{0-10}Ga_{1-100}$ zeigt auf, dass $Pd_{10}Ga_{45}Cu_{45}$ bei der milden Temperatur von 300°C am aktivsten Acrolein produziert hat.

Mo-basierte Katalysatoren wurden als Startmaterial für die Studie von Propen zu Acrolein genutzt. Durch die Hochdurchsatzverfahren wurden zweihundert Beispiele im primären Prozess und zwölf Generationen im sekundären Prozess getestet. Schließlich zeigten $Mo_{94}Ru_4Te_2$ und $Mo_{88}Sn_8Te_4$ sehr hohe Propenkonversion zu Acrolein mit einer Ausbeute von 25% bei 375 °C beziehungsweise 28% bei 400 °C. Um $Mo_{94}Ru_4Te_2$ zu entwickeln, wurde Ruthenium(III)chloride, welches längeres Altern brauchte, als Startmaterial genutzt. Ruthenium(III) stellte sich als bester Präkursor für gute katalytische Aktivität ohne Altern heraus. Als ein Ergebnis scheint es, dass die Alkoxidgruppe von Ruthenium(III) den Sol-Gel-Prozess einführte zur Förderung der katalytischen Aktivität, und Metall-Chlorid-Anleihen wurden methanolisiert, um mehr reaktionsfähige Methanolat-Spezien zu erhalten.

Infolgedessen zeigt diese Arbeit, dass der neu entwickelte 10-fache-Parallelreaktor ein hilfreiches Werkzeug darstellt zur Förderung der Entdeckung von Katalysatoren im sekundären Screening-Prozess. Durch das Experimentieren für die Suche nach selektiven Propenoxidkatalysatoren

erreichten wir das Ziel unserer Arbeit. Dieses erlangte Wissen kann genutzt werden, um allgemeine Hochdurchsatz-Technologien zu erweitern. Insbesondere wird erwartet, dass die Kombination der IR-Kamera-Methode und des 10-fachen-Parallelreaktors diesbezüglich bessere Leistungen liefern wird. Nichtsdestotrotz sollte erwähnt werden, dass die Reproduktion und der Scale-Up aufgrund der Empfindlichkeit der Katalysatoren in der Vorbereitung schwierig werden könnten.

# Approval


[1] S. Senkan, *Angew. Chem., Int. Ed.* **2001**, *40*, 312.
[2] E. G. Derouane, *CATTECH* **2001**, *5*, 214.
[3] J. H. Clark, *Acc. Chem. Res.* **2002**, *35*, 791.
[4] M. Feher, J. M. Schmidt, *J. Chem. Inf. Comput. Sci.* **2002**, *43*, 218.
[5] F. Roux, R. Lahana, *Drug Discov. Today* **1999**, *4*, 203.
[6] A. Merritt, *Drug Discov. Today* **1999**, *4*, 54.
[7] P. P. Pescarmona, J. C. van der Waal, T. Maschmeyer, *Catal. Today* **2003**, *81*, 347.
[8] J. Jin, M. Prochaska, D. Rochefort, D. K. Kim, L. Zhuang, F. J. DiSalvo, R. B. van Dover, H. t. D. Abru, *Appl. Surf. Sci.* **2007**, *254*, 653.
[9] C. Suh, K. Rajan, *Appl. Surf. Sci.* **2004**, *223*, 148.
[10] W. F. Maier, K. Stowe, S. Sieg, *Angew. Chem. Int. Ed.* **2007**, *46*, 6016.
[11] H. Koinuma, I. Takeuchi, *Nat. Mater.* **2004**, *3*, 429.
[12] X.-D. Xiang, X. Sun, G. Briceno, Y. Lou, K.-A. Wang, H. Chang, W. G. Wallace-Freedman, S.-W. Chen, P. G. Schultz, *Science* **1995**, *268*, 1738.
[13] T. R. Boussie, G. M. Diamond, C. Goh, K. A. Hall, A. M. LaPointe, M. Leclerc, C. Lund, V. Murphy, J. A. W. Shoemaker, U. Tracht, H. Turner, J. Zhang, T. Uno, R. K. Rosen, J. C. Stevens, *J. Am. Chem. Soc.* **2003**, *125*, 4306.
[14] A. Corma, J. M. Serra, *Catal. Today* **2005**, *107-108*, 3.
[15] C. A. Y. Jestin, A. Chiasera, A. Chiappini, M. Ferrari, E. Moser, R. Retoux, and G. C. Righini *Appl. Phys. Lett.* **2007**, *91*.
[16] M. Shimomura, Sawadaishi, Tetsuro, *Curr. Opin. Colloid Interface Sci.* **2001**, *6*, 11.
[17] D. Arcos, M. Vallet-Reg, *Acta Biomater.* **2010**, *In Press, Corrected Proof*, 2874.
[18] B. Y. Ahn, S. I. Seok, I. C. Baek, *Mater. Sci. Eng., C* **2008**, *28*, 1183.
[19] V. G. Gavalas, S. A. Law, J. Christopher Ball, R. Andrews, L. G. Bachas, *Anal. Biochem.* **2004**, *329*, 247.
[20] J.-P. Chen, W.-S. Lin, *Enzyme Microb. Technol.* **2003**, *32*, 801.
[21] M. Lechna, I. Holowacz, A. Ulatowska, H. Podbielska, *Surf. Coat. Technol.* **2002**, *151-152*, 299.
[22] Ebelmen, *Ann. Chim. Phy.* **1845**, *15*, 319.
[23] Ebelmen, *Ann. Chim. Phys.* **1846**, *16*, 129.
[24] Matijevjc, *Conference presented at the Universite de Bordeax I, France June* **1987**, 9.
[25] J. Zarzycki, *J. Sol-Gel Sci. Technol.* **1997**, *8*, 17.
[26] G. W. S. C. Jeffrey Brinker, *The Physics and Chemistry of Sol-Gel Processing*, Elsevier's Science and Technology, **1990**.
[27] G. W. S. C. Jeffrey Brinker, *Sol-Gel Science: The Physics and Chemistry of Sol-Gel Processing* **1990**, *1*, 2.
[28] G. W. S. C. Jeffrey Brinker, *Sol-Gel Science: The Physics and Chemistry of Sol-Gel Processing* **1990**, *1*, 103.
[29] I. C. Tilgner, P. Fischer, F. M. Bohnen, H. Rehage, W. F. Maier, *Microporous Materials* **1995**, *5*, 77.
[30] S. D. Bhagat, A. V. Rao, *Appl. Surf. Sci.* **2006**, *252*, 4289.
[31] L. L. Hench, J. K. West, *Chem. Rev.* **1990**, *90*, 33.

[32] G. W. S. C. Jeffrey Brinker, *Sol-Gel Science: The Physics and Chemistry of Sol-Gel Processing* **1990**, *1*, 130.
[33] W. F. Maier, in *TC5 Kombinatorische Chemie*, **2009**.
[34] J. Klein, T. Zech, J. M. Newsam, S. A. Schunk, *Appl. Catal., A* **2003**, *254*, 121.
[35] L. A. Mitscher, A. Dutta, *Burger's Medicinal Chemistry and Drug Discovery* **2003**, *2*, 1.
[36] B. Yan, *Curr. Opin. Chem. Biol.* **2002**, *6*, 328.
[37] K.Stöwe, in *Dechema Summer School*, Oberthal, **2008**.
[38] A. M. LaPointe, *J. Comb. Chem.* **1998**, *1*, 101.
[39] S. Kalelkar, E. R. Dow, J. Grimes, M. Clapham, H. Hu, *J. Comb. Chem.* **2002**, *4*, 622.
[40] M. Goldberg, K. Mahon, D. Anderson, *Adv. Drug Delivery Rev.* **2008**, *60*, 971.
[41] B. A. Bunin, J. M. Dener, D. A. Livingston, M. D. Annette, in *Annual Reports in Medicinal Chemistry, Vol. 34*, Academic Press, **1999**, pp. 267.
[42] T. Hart, *Drug Discov. Today* **2001**, *6*, 937.
[43] D. Tibiletti, E. A. B. de Graaf, S. Pheng Teh, G. Rothenberg, D. Farrusseng, C. Mirodatos, *J. Catal.* **2004**, *225*, 489.
[44] W. Zhang, Y. Lu, *J. Comb. Chem.* **2006**, *8*, 890.
[45] P. Wentworth, *Trends Biotechnol.* **1999**, *17*, 448.
[46] D. Cao, G. Q. Lu, A. Wieckowski, S. A. Wasileski, M. Neurock, *J. Phys. Chem. B* **2005**, *109*, 11622.
[47] J. Sauer, M. Sierka*, Vol. 21*, John Wiley & Sons, Inc., **2000**, pp. 1470.
[48] H. Kawakami, S. Yoshida, T. Yonezawa, *J. Chem. Soc.* **1984**, *80*, 205.
[49] W.-X. Li, C. Stampfl, M. Scheffler, *Phys. Rev. Lett.* **2003**, *90*, 256102.
[50] J. K. Nørskov, T. Bligaard, A. Logadottir, S. Bahn, L. B. Hansen, M. Bollinger, H. Bengaard, B. Hammer, Z. Sljivancanin, M. Mavrikakis, Y. Xu, S. Dahl, C. J. H. Jacobsen, *J. Catal.* **2002**, *209*, 275.
[51] E. Christoffersen, P. Liu, A. Ruban, H. L. Skriver, J. K. Nørskova, *J. Catal.* **2001**, *199*, 123.
[52] M. Sun, A. E. Nelson, J. Adjaye*, Vol. 222*, **2004**, pp. 243.
[53] K. H. P. Salo, M. Alatalo, K. Laasonen, *Surf. Sci.* **2002**, *516*, 247.
[54] A. E. A.-S. J.W. Andzelm, F.U. Axe, M.W. Doyle, G. Fitzgerald, C.M. Freeman, A.M. Gorman, J.-R. Hill, C.M. Kölmel, S.M. Levine, P.W. Saxe, K. Stark, L. Subramanian, M.A. van Daelen, E. Wimmer, J.M. Newsam, *Catal. Today* **1999**, *50*, 451.
[55] J. Basney, R. Raman, M. Livny, in *Proceedings of the Ninth SIAM Conference on Parallel Processing for Scientific Computing*, San Antonio, Texas, **1999**, pp. 1.
[56] K. Yajima, Y. Ueda, H. Tsuruya, T. Kanougi, Y. Oumi, S. S. C. Ammal, S. Takami, M. Kubo, A. Miyamoto, *Appl. Catal., A* **2000**, *194-195*, 183.
[57] A. Endou, C. Jung, T. Kusagaya, M. Kubo, P. Selvam, A. Miyamoto, *Appl. Surf. Sci.* **2004**, *223*, 159.
[58] S. Sakahara, K. Yajima, R. Belosludov, S. Takami, M. Kubo, A. Miyamoto, *Appl. Surf. Sci.* **2002**, *189*, 253.
[59] M. Kubo, M. Ando, S. Sakahara, C. Jung, K. Seki, T. Kusagaya, A. Endou, S. Takami, A. Imamura, A. Miyamoto, *Appl. Surf. Sci.* **2004**, *223*, 188.
[60] P. B. Wells, S. D. Jackson, R. Whyman, *React. Kinet. Catal. Lett.* **1999**, *68*, 45.
[61] S. Kasztelan, *Catal. Lett.* **1989**, *2*, 165.

[62] R. Chianelli, R., *Oil & Gas Science and Technology - Rev. IFP* **2006**, *61*, 503.
[63] J. Greeley, T. F. Jaramillo, J. Bonde, I. Chorkendorff, J. K. Norskov, *Nat. Mater.* **2006**, *5*, 909.
[64] E. V. Gordeeva, D. E. Lushniknov, N. S. Zefirov, *Tetrahedron* **1992**, *48*, 3789.
[65] S. Rose, *Drug Discov. Today* **2002**, *7*, 133.
[66] O. V. Buyevskaya, D. Wolf, M. Baerns, *Catal. Today* **2000**, *62*, 91.
[67] L. Weber, *Drug Discov. Today* **1998**, *3*, 379.
[68] G. Grubert, S. Kolf, M. Baerns, I. Vauthey, D. Farrusseng, A. C. van Veen, C. Mirodatos, E. R. Stobbe, P. D. Cobden, *Appl. Catal., A* **2006**, *306*, 17.
[69] T. A. B. Beltro-Oviedo, Ildar Domoguez, J. M., *Catal. Today* **2009**, *148*, 28.
[70] U. Rodemerck, M. Baerns, M. Holena, D. Wolf, *Appl. Surf. Sci.* **2004**, *223*, 168.
[71] A. Corma, J. M. Serra, P. Serna, S. Valero, E. Argente, V. Botti, *J. Catal.* **2005**, *229*, 513.
[72] Y. Watanabe, T. Umegaki, M. Hashimoto, K. Omata, M. Yamada, *Catal. Today* **2004**, *89*, 455.
[73] C. Klanner, D. Farrusseng, L. Baumes, M. Lengliz, C. Mirodatos, F. Schüh, *Angew. Chem.* **2004**, *116*, 5461.
[74] S. Sieg, B. Stutz, T. Schmidt, F. Hamprecht, W. Maier, *J. Mol. Model.* **2006**, *12*, 611.
[75] P. Claus, D. Honicke, T. Zech, *Catal. Today* **2001**, *67*, 319.
[76] L. T. Vovoi, Andr Gob, S. dor Margitfalvi, J. sef, *Catal. Today* **2003**, *81*, 517.
[77] J. P. Yi, Z. G. Fan, Z. W. Jiang, W. S. Li, X. P. Zhou, *J. Comb. Chem.* **2007**, *9*, 1053.
[78] J. S. Paul, J. g. Urschey, P. A. Jacobs, W. F. Maier, F. Verpoort, *J. Catal.* **2003**, *220*, 136.
[79] J. Scheidtmann, D. Klär, J. W. Saalfrank, T. Schmidt, W. F. Maier, *QSAR Comb. Sci.* **2005**, *24*, 203.
[80] K. F. Jensen, *Chem. Eng. Sci.* **2001**, *56*, 293.
[81] T. Zech, G. Bohner, J. Klein, *Catal. Today* **2005**, *110*, 58.
[82] A. Allwardt, S. Holzmler-Laue, C. Wendler, N. Stoll, *Catal. Today* **2008**, *137*, 11.
[83] D. K. Kim, W. F. Maier, *J. Catal.* **2006**, *238*, 142.
[84] C. Kiener, M. Kurtz, H. Wilmer, C. Hoffmann, H. W. Schmidt, J. D. Grunwaldt, M. Muhler, F. Schüh, *J. Catal.* **2003**, *216*, 110.
[85] O. C. Gobin, A. Martinez Joaristi, F. Schüh, *J. Catal.* **2007**, *252*, 205.
[86] S. Moehmel, N. Steinfeldt, S. Engelschalt, M. Holena, S. Kolf, M. Baerns, U. Dingerdissen, D. Wolf, R. Weber, M. Bewersdorf, *Appl. Catal., A* **2008**, *334*, 73.
[87] J. B. Poez-Ramoez, Rob J. Mul, Guido Kapteijn, Freek Moulijn, Jacob A., *Catal. Today* **2000**, *60*, 93.
[88] J. S. Paul, P. A. Jacobs, P.-A. W. Weiss, W. F. Maier, *Appl. Catal., A* **2004**, *265*, 185.
[89] H. W. Turner, A. F. Volpe Jr, W. H. Weinberg, *Surf. Sci.* **2009**, *603*, 1763.
[90] S. Thomson, C. Hoffmann, S. Ruthe, H. W. Schmidt, F. Schüh, *Appl. Catal., A* **2001**, *220*, 253.
[91] V. Schurig, *J. Chromatogr. A* **2008**, *1184*, 159.
[92] O. Trapp, *J. Chromatogr. A* **2008**, *1184*, 160.
[93] R. Richmond, E. Gölach, *Anal. Chim. Acta* **1999**, *394*, 33.
[94] K. Eckhard, O. Schluter, V. Hagen, B. Wehner, T. Erichsen, W. Schuhmann, M. Muhler, *Appl. Catal., A* **2005**, *281*, 115.
[95] J. Bner, S. Buchinger, D. Schomburg, *Anal. Biochem.* **2007**, *367*, 143.

[96] K. A. Youdim, K. C. Saunders, *J. Chromatogr. B* **2010**, 11.
[97] M. A. Strege, *J. Chromatogr. B* **1999**, *725*, 67.
[98] W. M. A. Niessen, *J. Chromatogr. A* **2003**, *1000*, 413.
[99] R. P. Singh, S. Sabarinath, S. K. Singh, R. C. Gupta, *J. Chromatogr. B* **2008**, *864*, 52.
[100] J. Scheidtmann, P. A. Weiß, W. F. Maier, *Appl. Catal., A* **2001**, *222*, 79.
[101] P. Rajagopalan, PhD-Thesis, Universität des Saarlandes (Saarbrücken), **2009**.
[102] R. K. Grasselli, *Top. Catal.* **2002**, *21*, 79.
[103] M. M. Bettahar, G. Costentin, L. Savary, J. C. Lavalley, *Appl. Catal., A* **1996**, *145*, 1.
[104] H. K. Harold, *Studies in Surface Science and Catalysis, Vol. 45*, Elsevier, **1989**.
[105] P. D. Emig*, Vol. 1*, Universität Erlangen-Nürnberg Lehrstuhl für Technische Chemie I, Erlangen, **2001**.
[106] G. W. Keulks, M. Y. Lo, *J. Phys. Chem.* **1986**, *90*, 4768.
[107] C. Zhao, I. E. Wachs, *J. Catal.* **2008**, *257*, 181.
[108] M. Imachi, R. L. Kuczkowski, J. T. Groves, N. W. Cant, *J. Catal.* **1983**, *82*, 355.
[109] A. K. Sinha, S. Seelan, S. Tsubota, M. Haruta, *Top. Catal.* **2004**, *29*, 95.
[110] E. Sacaliuc, A. M. Beale, B. M. Weckhuysen, T. A. Nijhuis, *J. Catal.* **2007**, *248*, 235.
[111] O. P. H. Vaughan, G. Kyriakou, N. Macleod, M. Tikhov, R. M. Lambert, *J. Catal.* **2005**, *236*, 401.
[112] J. Lu, M. Luo, H. Lei, X. Bao, C. Li, *J. Catal.* **2002**, *211*, 552.
[113] H. Oryesek, R. P. Schulz, U. Dingerdissen, W. F. Maier, *Chem. Eng. Technol.* **1999**, *22*, 691.
[114] T. A. Nijhuis, M. Makkee, J. A. Moulijn, B. M. Weckhuysen, *Ind. Eng. Chem.* **2006**, *45*, 3447.
[115] E. L. M. a. H. S. Young*, Vol. 3,173,957* (Ed.: U. S. P. Office), United Sates, **1960**.
[116] M. Baerns, O. V. Buyevskaya, M. Kubik, G. Maiti, O. Ovsitser, O. Seel, *Catal. Today* **1997**, *33*, 85.
[117] C.-J. Jia, Y. Liu, W. Schmidt, A.-H. Lu, F. Schüth, *J. Catal.* **2010**, *269*, 71.
[118] L.-Z. Tao, S.-H. Chai, Y. Zuo, W.-T. Zheng, Y. Liang, B.-Q. Xu, *Catal. Today* **2010**, *158*, 310.
[119] S.-H. Chai, H.-P. Wang, Y. Liang, B.-Q. Xu, *J. Catal.* **2007**, *250*, 342.
[120] L. Ning, Y. Ding, W. Chen, L. Gong, R. Lin, L. Yuan, Q. Xin, *Chin. J. Catal.* **2008**, *29*, 212.
[121] A. Corma, G. W. Huber, L. Sauvanaud, P. O'Connor, *J. Catal.* **2008**, *257*, 163.
[122] E. Tsukuda, S. Sato, R. Takahashi, T. Sodesawa, *Catal. Commun.* **2007**, *8*, 1349.
[123] Y.-H. Han, W. Ueda, Y. Moro-Oka, *Appl. Catal., A* **1999**, *176*, 11.
[124] H. Fansuri, G. H. Pham, S. Wibawanta, R. D. Radford, D. K. Zhang, *Developments in Chemical Engineering and Mineral Processing* **2004**, *12*, 333.
[125] B. Zhou, K. T. Chuang, X. Guo, *J. Chem. Soc., Faraday Trans.* **1991**, *87*, 3695.
[126] P. L. N. Botella, J. M. Solsona, B., *J. Mol. Catal. A: Chem.* **2002**, *184*, 335.
[127] W. Ueda, Y. Moro-oka, T. Ikawa, *J. Catal.* **1984**, *88*, 214.
[128] C. Zhao, I. E. Wachs, *Catal. Today* **2006**, *118*, 332.
[129] C. Zhang, C. R. A. Catlow*, Vol. 259*, **2008**, pp. 17.
[130] P. Forzatti, P. L. Villa, N. Ferlazzo, D. Jones, *J. Catal.* **1982**, *76*, 188.
[131] R. Grasselli, C. Lugmair, A. Volpe, *Top. Catal.* **2008**, *50*, 66.
[132] N. Watanabe, W. Ueda, *Ind. Eng. Chem. Res.* **2005**, *45*, 607.

[133] A. Ramli, F. M. Jamil, S. M. Ibrahim, *MJAS* **2007**, *11*, 124.
[134] T. B. Blasco, P. Concepcion, P. Loepez Nieto, J. M. Martinez-Arias, A. Prieto, C., *J. Catal.* **2004**, *228*, 362.
[135] E. K. V. Novakova, Jacques C. Derouane, Eric G., *J. Catal.* **2002**, *211*, 235.
[136] L. Luo, J. A. Labinger, M. E. Davis, *J. Catal.* **2001**, *200*, 222.
[137] J. S. Paul, R. Janssens, J. F. M. Denayer, G. V. Baron, P. A. Jacobs, *J. Comb. Chem.* **2005**, *7*, 407.
[138] J. N. Al-Saeedi, V. V. Guliants, *Appl. Catal., A* **2002**, *237*, 111.
[139] C. Huang, W. Guo, X. Yi, W. Weng, H. Wan, *Catal. Commun.* **2007**, *8*, 162.
[140] O. V. Udalova, D. P. Shashkin, M. D. Shibanova, O. V. Krylov, *Kinet. Catal.* **2008**, *49*, 407.
[141] G. Kirsten, W. F. Maier, *Appl. Surf. Sci.* **2004**, *223*, 87.
[142] J. K. Urschey, Adolf Maier, Wilhelm F., *Appl. Catal., A* **2003**, *252*, 91.
[143] J. Urschey, P.-A. W. Weiss, J. Scheidtmann, R. Richter, W. F. Maier, *Solid State Sci.* **2003**, *5*, 909.
[144] R. J. Hendershot, C. M. Snively, J. Lauterbach, *Chem. Eur. J.* **2005**, *11*, 806.
[145] O. Levenspiel, *Ind. Chem. Eng. Res.* **1999**, *38*, 4140
[146] J. Coronas, J. Santamaría, *Catal. Today* **1999**, *51*, 377.
[147] Y. S. Matros, *Unsteady processes in catalytic reactors*, **1985**.
[148] D. Williamson, in *BoxPlots in Excel 2007, www.duncanwil.co.uk/pdfs/boxplot_07.pdf*, **2010**, p. 12.
[149] S. M. S. Mota, J.-C. Volta, J.-A. Dalmon, *Catal. Today* **2001**, *2398*, 1.
[150] M. A. S. Mota, J. C. Volta, and J. A. Dalmon, *J. Catal.* **2000**, *193*, 308.
[151] M. Kahn, A. Seubsai, I. Onal, S. Senkan, *Comb. Chem. High Throughput Screen.* **2010**, *13*, 67.
[152] S. Lee, L. M. Molina, M. J. López, J. A. Alonso, B. Hammer, B. Lee, S. Seifert, R. E. Winans, J. W. Elam, M. J. Pellin, S. Vajda, *Angew. Chem. Int. Ed.* **2009**, *48*, 1467.
[153] S. g. Jun hak ze, *Introduction to catalyst, Vol. 4*, Hanrimwon, Seoul, **2002**.
[154] J. E. Jaffe, A. Zunger, *Phys. Rev. B: Condens. Matter Mater. Phys.* **1983**, *27*, 5179.
[155] W. Yin, W. Wang, S. Sun, *Catal. Commun.*, *11*, 647.
[156] K. Nagaveni, M. S. Hegde, N. Ravishankar, G. N. Subbanna, G. Madras, *Langmuir* **2004**, *20*, 2900.
[157] C. R. Jung, A. Kundu, S. W. Nam, H.-I. Lee, *Appl. Catal., A* **2007**, *331*, 112.
[158] H. S. Rnkknen, P. Niemel, M. Krause, O., *Fuel Process. Technol.*, *92*, 1881.
[159] G. W. Keulks, M. I. P. R. k, C. Daniel, *Ind. Eng. Chem. Prod. Res. Develop.* **1971**, *10*, 138.
[160] R. MANAILA, N. I. IONESCaUn, M. CALDARARU, *Z. Anorg. Allg. Chem.* **1980**, 221.
[161] A. G. Polkovnikova, A. N. Shatalova, L. L. Zeitina, *Petroleum Chemistry U.S.S.R.* **1964**, *3*, 103.
[162] G. Creten, D. S. Lafyatis, G. F. Froment, *J. Catal.* **1995**, *154*, 151.
[163] H. Fansuri, G. H. Pham, S. Wibawanta, R. D. Radford, D. K. Zhang, *Dev. Chem. Eng. Mineral Process.* **2004**, *12*, 333.
[164] L. M. Thang, V. D. Thang, L. C. Hoa, I. V. Driessche, S. Hoste, Department of Inorganic and Physical Chemistry, Ghent University, Krijgslaan 281-S3, 9000 Gent, Belgium

[165] S. Pudar, J. Oxgaard, K. Chenoweth, A. C. T. van Duin, W. A. Goddard, *J. Phys. Chem. C* **2007**, *111*, 16405.
[166] P. Forzatti, F. Trifitro, *React. Kinet. CataL Lett.* **1979**, *10*, 275.
[167] C. Klanner, D. Farrusseng, L. Baumes, C. Mirodatos, F. Schüh, *QSAR Comb. Sci.* **2003**, *22*, 729.
[168] S. Jouili, S. Tabbone, *Pattern Recogn.* **2012**, *45*, 4054.
[169] W. Liu, E. Ribeiro, *Pattern Recogn.* **2012**, *45*, 3912.
[170] V. H. Nguyen, T. H. B. Nguyen, H. Kim, *Pattern Recogn.* **2012**, *45*, 3853.
[171] G. P. Inzelt, Z., *Electrochem. Commun.* **2004**, *6*, 805.
[172] A. J. Terezo, E. C. Pereira, *Mater. Lett.* **2002**, *53*, 339.
[173] J. Scheidtmann, J. W. Saalfrank, W. F. Maier, M. O. Masakazu Anpo, Y. Hiromi, *Stud. Surf. Sci. Catal.* **2003**, *145*, 13.
[174] J. Scheidtmann, PhD-Thesis, Universität des Saarlandes (Saarbrücken), **2003**.
[175] F. P. F.C. Buciuman, T. Hahn, *Chem. Eng. Process.* **1999**, *38*, 563.

# List of Tables

# List of Figures

# Ⅳ. Appendix

## A List of abbreviations

**Abbreviations**

| Symbol | Meaning |
|---|---|
| ANN | Artificial neural network |
| AA | Acrylic acid |
| AN | Acrylonitrile |
| BC | Boundary condition |
| BET | Brunauer, Emmett and Teller method |
| KB | Complexing agent |
| °C | Degree centigrade |
| °K | Degree Kelvin |
| DOE | Design of Experiment |
| DFT | Density function theory |
| EDX | Energy Dispersive X-ray Analysis |
| EG | Ethylene glycol |
| FEA | Finite Element Analysis |
| GC | Gas chromatography |
| GHSV | Gas hourly space velocity |
| GA | Genetic algorithm |
| GUI | Graphical user interface |
| GNP | Gross national product |
| HPLC | High pressure liquid chromatography |
| HRS | Holographic research strategy |
| HT | High-throughput |
| HTE | High-throughput experimentation |
| h | Hours(s) |
| HPPO | Hydrogen-peroxide-propylen-oxide |

| | |
|---|---|
| IR | Infrared |
| l | Liter |
| LC | Liquid chromatograph |
| MFC | Mass flow controller |
| MC | Monte carlo |
| MS | Mass spectrometry |
| µg | Microgram |
| µl | Microliter |
| µmole | Micromole |
| mg | Milligram |
| mL | Milliliter |
| min | Minutes |
| Mol% | Mole percent |
| MVs | Multi-position valves |
| PFR | Plug flow reactor |
| QCARs | Quantitative composition activity relationships |
| ODOE | Optimal design of experiments |
| PC | Principal components |
| rpm | Revolutions per minute |
| SEM | Scanning electron microscopy |
| SVMs | Support vector machines |
| s, sec | Seconds |
| m sec | Millisecond |
| SRR | Stage robot reactor |
| T | Temperature |
| TCD | Thermal conductivity detector |
| TG | Thermogravimetry |
| Vol% | Volume percent |
| WGSR | Water gas shift reaction |
| XRD | X-ray diffraction |
| XPS | X-ray photoelectron spectroscopy |

# B List of libraries

Occupancy of catalyst library 1G1L

| | | | | | | | |
|---|---|---|---|---|---|---|---|
| 1 | Ag0.5Al0.5 | 51 | Al0.5Bi0.5 | 101 | Cu0.5Ge0.5 | 151 | Ga0.5Sb0.5 |
| 2 | Ag0.5B0.5 | 52 | B0.5Cr0.5 | 102 | Cu0.5Hf0.5 | 152 | Ga0.5Si0.5 |
| 3 | Ag0.5Cr0.5 | 53 | B0.5Cu0.5 | 103 | Cu0.5In0.5 | 153 | Ga0.5Sn0.5 |
| 4 | Ag0.5Cu0.5 | 54 | B0.5Fe0.5 | 104 | Cu0.5La0.5 | 154 | Ga0.5Te0.5 |
| 5 | Ag0.5Fe0.5 | 55 | B0.5Ga0.5 | 105 | Cu0.5Mn0.5 | 155 | Ga0.5W0.5 |
| 6 | Ag0.5Ga0.5 | 56 | B0.5Ge0.5 | 106 | Cu0.5Nb0.5 | 156 | Ga0.5Y0.5 |
| 7 | Ag0.5Ge0.5 | 57 | B0.5Hf0.5 | 107 | Cu0.5Pb0.5 | 157 | Ga0.5Zn0.5 |
| 8 | Ag0.5Hf0.5 | 58 | B0.5In0.5 | 108 | Cu0.5Re0.5 | 158 | Ga0.5Zr0.5 |
| 9 | Ag0.5In0.5 | 59 | B0.5La0.5 | 109 | Cu0.5Ru0.5 | 159 | Ga0.5Ta0.5 |
| 10 | Ag0.5La0.5 | 60 | B0.5Mn0.5 | 110 | Cu0.5Sb0.5 | 160 | Ga0.5Mo0.5 |
| 11 | Ag0.5Mn0.5 | 61 | B0.5Nb0.5 | 111 | Cu0.5Si0.5 | 161 | Ga0.5Bi0.5 |
| 12 | Ag0.5Nb0.5 | 62 | B0.5Pb0.5 | 112 | Cu0.5Sn0.5 | 162 | Ge0.5Hf0.5 |
| 13 | Ag0.5Pb0.5 | 63 | B0.5Re0.5 | 113 | Cu0.5Te0.5 | 163 | Ge0.5In0.5 |
| 14 | Ag0.5Re0.5 | 64 | B0.5Ru0.5 | 114 | Cu0.5W0.5 | 164 | Ge0.5La0.5 |
| 15 | Ag0.5Ru0.5 | 65 | B0.5Sb0.5 | 115 | Cu0.5Y0.5 | 165 | Ge0.5Mn0.5 |
| 16 | Ag0.5Sb0.5 | 66 | B0.5Si0.5 | 116 | Cu0.5Zn0.5 | 166 | Ge0.5Nb0.5 |
| 17 | Ag0.5Si0.5 | 67 | B0.5Sn0.5 | 117 | Cu0.5Zr0.5 | 167 | Ge0.5Pb0.5 |
| 18 | Ag0.5Sn0.5 | 68 | B0.5Te0.5 | 118 | Cu0.5Ta0.5 | 168 | Ge0.5Re0.5 |
| 19 | Ag0.5Te0.5 | 69 | B0.5W0.5 | 119 | Cu0.5Mo0.5 | 169 | Ge0.5Ru0.5 |
| 20 | Ag0.5W0.5 | 70 | B0.5Y0.5 | 120 | Cu0.5Bi0.5 | 170 | Ge0.5Sb0.5 |
| 21 | Ag0.5Y0.5 | 71 | B0.5Zn0.5 | 121 | Fe0.5Ga0.5 | 171 | Ge0.5Si0.5 |
| 22 | Ag0.5Zn0.5 | 72 | B0.5Zr0.5 | 122 | Fe0.5Ge0.5 | 172 | Ge0.5Sn0.5 |
| 23 | Ag0.5Zr0.5 | 73 | B0.5Ta0.5 | 123 | Fe0.5Hf0.5 | 173 | Ge0.5Te0.5 |
| 24 | Ag0.5Ta0.5 | 74 | B0.5Mo0.5 | 124 | Fe0.5In0.5 | 174 | Ge0.5W0.5 |
| 25 | Ag0.5Mo0.5 | 75 | B0.5Bi0.5 | 125 | Fe0.5La0.5 | 175 | Ge0.5Y0.5 |
| 26 | Ag0.5Bi0.5 | 76 | Cr0.5Cu0.5 | 126 | Fe0.5Mn0.5 | 176 | Ge0.5Zn0.5 |
| 27 | Al0.5B0.5 | 77 | Cr0.5Fe0.5 | 127 | Fe0.5Nb0.5 | 177 | Ge0.5Zr0.5 |
| 28 | Al0.5Cr0.5 | 78 | Cr0.5Ga0.5 | 128 | Fe0.5Pb0.5 | 178 | Ge0.5Ta0.5 |
| 29 | Al0.5Cu0.5 | 79 | Cr0.5Ge0.5 | 129 | Fe0.5Re0.5 | 179 | Ge0.5Mo0.5 |
| 30 | Al0.5Fe0.5 | 80 | Cr0.5Hf0.5 | 130 | Fe0.5Ru0.5 | 180 | Ge0.5Bi0.5 |
| 31 | Al0.5Ga0.5 | 81 | Cr0.5In0.5 | 131 | Fe0.5Sb0.5 | 181 | Hf0.5In0.5 |
| 32 | Al0.5Ge0.5 | 82 | Cr0.5La0.5 | 132 | Fe0.5Si0.5 | 182 | Hf0.5La0.5 |
| 33 | Al0.5Hf0.5 | 83 | Cr0.5Mn0.5 | 133 | Fe0.5Sn0.5 | 183 | Hf0.5Mn0.5 |
| 34 | Al0.5In0.5 | 84 | Cr0.5Nb0.5 | 134 | Fe0.5Te0.5 | 184 | Hf0.5Nb0.5 |
| 35 | Al0.5La0.5 | 85 | Cr0.5Pb0.5 | 135 | Fe0.5W0.5 | 185 | Hf0.5Pb0.5 |
| 36 | Al0.5Mn0.5 | 86 | Cr0.5Re0.5 | 136 | Fe0.5Y0.5 | 186 | Hf0.5Re0.5 |
| 37 | Al0.5Nb0.5 | 87 | Cr0.5Ru0.5 | 137 | Fe0.5Zn0.5 | 187 | Hf0.5Ru0.5 |
| 38 | Al0.5Pb0.5 | 88 | Cr0.5Sb0.5 | 138 | Fe0.5Zr0.5 | 188 | Hf0.5Sb0.5 |
| 39 | Al0.5Re0.5 | 89 | Cr0.5Si0.5 | 139 | Fe0.5Ta0.5 | 189 | Hf0.5Si0.5 |
| 40 | Al0.5Ru0.5 | 90 | Cr0.5Sn0.5 | 140 | Fe0.5Mo0.5 | 190 | Hf0.5Sn0.5 |
| 41 | Al0.5Sb0.5 | 91 | Cr0.5Te0.5 | 141 | Fe0.5Bi0.5 | 191 | Hf0.5Te0.5 |
| 42 | Al0.5Si0.5 | 92 | Cr0.5W0.5 | 142 | Ga0.5Ge0.5 | 192 | Hf0.5W0.5 |
| 43 | Al0.5Sn0.5 | 93 | Cr0.5Y0.5 | 143 | Ga0.5Hf0.5 | 193 | Hf0.5Y0.5 |
| 44 | Al0.5Te0.5 | 94 | Cr0.5Zn0.5 | 144 | Ga0.5In0.5 | 194 | Hf0.5Zn0.5 |
| 45 | Al0.5W0.5 | 95 | Cr0.5Zr0.5 | 145 | Ga0.5La0.5 | 195 | Hf0.5Zr0.5 |
| 46 | Al0.5Y0.5 | 96 | Cr0.5Ta0.5 | 146 | Ga0.5Mn0.5 | 196 | Hf0.5Ta0.5 |
| 47 | Al0.5Zn0.5 | 97 | Cr0.5Mo0.5 | 147 | Ga0.5Nb0.5 | 197 | Hf0.5Mo0.5 |
| 48 | Al0.5Zr0.5 | 98 | Cr0.5Bi0.5 | 148 | Ga0.5Pb0.5 | 198 | Hf0.5Bi0.5 |
| 49 | Al0.5Ta0.5 | 99 | Cu0.5Fe0.5 | 149 | Ga0.5Re0.5 | 199 | In0.5La0.5 |
| 50 | Al0.5Mo0.5 | 100 | Cu0.5Ga0.5 | 150 | Ga0.5Ru0.5 | 200 | In0.5Mn0.5 |

## Occupancy of catalyst library 1G2L

| | | | | | | | |
|---|---|---|---|---|---|---|---|
| 1 | In0.5Nb0.5 | 51 | Nb0.5Si0.5 | 101 | Sb0.5Y0.5 | 151 | Mo0.5Bi0.5 |
| 2 | In0.5Pb0.5 | 52 | Nb0.5Sn0.5 | 102 | Sb0.5Zn0.5 | | |
| 3 | In0.5Re0.5 | 53 | Nb0.5Te0.5 | 103 | Sb0.5Zr0.5 | | |
| 4 | In0.5Ru0.5 | 54 | Nb0.5W0.5 | 104 | Sb0.5Ta0.5 | | |
| 5 | In0.5Sb0.5 | 55 | Nb0.5Y0.5 | 105 | Sb0.5Mo0.5 | | |
| 6 | In0.5Si0.5 | 56 | Nb0.5Zn0.5 | 106 | Sb0.5Bi0.5 | | |
| 7 | In0.5Sn0.5 | 57 | Nb0.5Zr0.5 | 107 | Si0.5Sn0.5 | | |
| 8 | In0.5Te0.5 | 58 | Nb0.5Ta0.5 | 108 | Si0.5Te0.5 | | |
| 9 | In0.5W0.5 | 59 | Nb0.5Mo0.5 | 109 | Si0.5W0.5 | | |
| 10 | In0.5Y0.5 | 60 | Nb0.5Bi0.5 | 110 | Si0.5Y0.5 | | |
| 11 | In0.5Zn0.5 | 61 | Pb0.5Re0.5 | 111 | Si0.5Zn0.5 | | |
| 12 | In0.5Zr0.5 | 62 | Pb0.5Ru0.5 | 112 | Si0.5Zr0.5 | | |
| 13 | In0.5Ta0.5 | 63 | Pb0.5Sb0.5 | 113 | Si0.5Ta0.5 | | |
| 14 | In0.5Mo0.5 | 64 | Pb0.5Si0.5 | 114 | Si0.5Mo0.5 | | |
| 15 | In0.5Bi0.5 | 65 | Pb0.5Sn0.5 | 115 | Si0.5Bi0.5 | | |
| 16 | La0.5Mn0.5 | 66 | Pb0.5Te0.5 | 116 | Sn0.5Te0.5 | | |
| 17 | La0.5Nb0.5 | 67 | Pb0.5W0.5 | 117 | Sn0.5W0.5 | | |
| 18 | La0.5Pb0.5 | 68 | Pb0.5Y0.5 | 118 | Sn0.5Y0.5 | | |
| 19 | La0.5Re0.5 | 69 | Pb0.5Zn0.5 | 119 | Sn0.5Zn0.5 | | |
| 20 | La0.5Ru0.5 | 70 | Pb0.5Zr0.5 | 120 | Sn0.5Zr0.5 | | |
| 21 | La0.5Sb0.5 | 71 | Pb0.5Ta0.5 | 121 | Sn0.5Ta0.5 | | |
| 22 | La0.5Si0.5 | 72 | Pb0.5Mo0.5 | 122 | Sn0.5Mo0.5 | | |
| 23 | La0.5Sn0.5 | 73 | Pb0.5Bi0.5 | 123 | Sn0.5Bi0.5 | | |
| 24 | La0.5Te0.5 | 74 | Re0.5Ru0.5 | 124 | Te0.5W0.5 | | |
| 25 | La0.5W0.5 | 75 | Re0.5Sb0.5 | 125 | Te0.5Y0.5 | | |
| 26 | La0.5Y0.5 | 76 | Re0.5Si0.5 | 126 | Te0.5Zn0.5 | | |
| 27 | La0.5Zn0.5 | 77 | Re0.5Sn0.5 | 127 | Te0.5Zr0.5 | | |
| 28 | La0.5Zr0.5 | 78 | Re0.5Te0.5 | 128 | Te0.5Ta0.5 | | |
| 29 | La0.5Ta0.5 | 79 | Re0.5W0.5 | 129 | Te0.5Mo0.5 | | |
| 30 | La0.5Mo0.5 | 80 | Re0.5Y0.5 | 130 | Te0.5Bi0.5 | | |
| 31 | La0.5Bi0.5 | 81 | Re0.5Zn0.5 | 131 | W0.5Y0.5 | | |
| 32 | Mn0.5Nb0.5 | 82 | Re0.5Zr0.5 | 132 | W0.5Zn0.5 | | |
| 33 | Mn0.5Pb0.5 | 83 | Re0.5Ta0.5 | 133 | W0.5Zr0.5 | | |
| 34 | Mn0.5Re0.5 | 84 | Re0.5Mo0.5 | 134 | W0.5Ta0.5 | | |
| 35 | Mn0.5Ru0.5 | 85 | Re0.5Bi0.5 | 135 | W0.5Mo0.5 | | |
| 36 | Mn0.5Sb0.5 | 86 | Ru0.5Sb0.5 | 136 | W0.5Bi0.5 | | |
| 37 | Mn0.5Si0.5 | 87 | Ru0.5Si0.5 | 137 | Y0.5Zn0.5 | | |
| 38 | Mn0.5Sn0.5 | 88 | Ru0.5Sn0.5 | 138 | Y0.5Zr0.5 | | |
| 39 | Mn0.5Te0.5 | 89 | Ru0.5Te0.5 | 139 | Y0.5Ta0.5 | | |
| 40 | Mn0.5W0.5 | 90 | Ru0.5W0.5 | 140 | Y0.5Mo0.5 | | |
| 41 | Mn0.5Y0.5 | 91 | Ru0.5Y0.5 | 141 | Y0.5Bi0.5 | | |
| 42 | Mn0.5Zn0.5 | 92 | Ru0.5Zn0.5 | 142 | Zn0.5Zr0.5 | | |
| 43 | Mn0.5Zr0.5 | 93 | Ru0.5Zr0.5 | 143 | Zn0.5Ta0.5 | | |
| 44 | Mn0.5Ta0.5 | 94 | Ru0.5Ta0.5 | 144 | Zn0.5Mo0.5 | | |
| 45 | Mn0.5Mo0.5 | 95 | Ru0.5Mo0.5 | 145 | Zn0.5Bi0.5 | | |
| 46 | Mn0.5Bi0.5 | 96 | Ru0.5Bi0.5 | 146 | Zr0.5Ta0.5 | | |
| 47 | Nb0.5Pb0.5 | 97 | Sb0.5Si0.5 | 147 | Zr0.5Mo0.5 | | |
| 48 | Nb0.5Re0.5 | 98 | Sb0.5Sn0.5 | 148 | Zr0.5Bi0.5 | | |
| 49 | Nb0.5Ru0.5 | 99 | Sb0.5Te0.5 | 149 | Ta0.5Mo0.5 | | |
| 50 | Nb0.5Sb0.5 | 100 | Sb0.5W0.5 | 150 | Ta0.5Bi0.5 | | |

## Occupancy of catalyst library 1G3L

| | | | | | | | |
|---|---|---|---|---|---|---|---|
| 1 | Co0.3V0.3Ba0.4 | 51 | Ga0.3Cu0.3Hf0.4 | 101 | Ga0.3Fe0.4Sn0.3 | 151 | Cd0.3Nb0.4Ce0.3 |
| 2 | Ni0.3Mn0.4Pb0.3 | 52 | Cu0.3Zr0.3Sn0.4 | 102 | Co0.3Ni0.4Cs0.3 | 152 | Cu0.3Nb0.4Ag0.3 |
| 3 | Cr0.4SrBr0.3Pb0.3 | 53 | Cu0.3Cd0.4Ni0.3 | 103 | Cr0.3Cu0.4Ba0.3 | 153 | Ni0.3Nb0.4SrBr0.3 |
| 4 | Zn0.3Ru0.4Cs0.3 | 54 | Fe0.3Ni0.3Sn0.4 | 104 | Zn0.3Ce0.3Mn0.4 | 154 | Ni0.3Cs0.4Re0.3 |
| 5 | Cu0.4Zn0.3Cs0.3 | 55 | Ga0.3Cr0.4Sn0.3 | 105 | Ga0.3Ni0.4SrBr0.3 | 155 | Co0.3Re0.3Ba0.4 |
| 6 | Co0.3Ca0.4Cs0.3 | 56 | Ni0.3Ca0.3W0.4 | 106 | Cu0.3Zn0.3Hf0.4 | 156 | Cd0.3Co0.3Ru0.4 |
| 7 | Cu0.4Ca0.3W0.3 | 57 | Ni0.4Re0.3Ba0.3 | 107 | Cr0.3Co0.3Sn0.4 | 157 | Ga0.3Co0.3Ce0.4 |
| 8 | Co0.3Zr0.3Zn0.4 | 58 | Mn0.4Ag0.3Cs0.3 | 108 | Co0.4Zn0.3Pd0.3 | 158 | Cu0.3V0.4K0.3 |
| 9 | Cu0.4Ni0.3Hf0.3 | 59 | Co0.4Mn0.3Ba0.3 | 109 | Ni0.3Zr0.3Ba0.4 | 159 | Zn0.3Mn0.4Ba0.3 |
| 10 | Cu0.3W0.3Ba0.4 | 60 | Zr0.4SrBr0.3Ag0.3 | 110 | Co0.3Ni0.3Ca0.4 | 160 | Cr0.4Cd0.3Ca0.3 |
| 11 | Co0.4Ni0.3Bi0.3 | 61 | Fe0.4Ce0.3Pb0.3 | 111 | Ni0.4Zr0.3SrBr0.3 | 161 | Ga0.3Co0.3Zr0.4 |
| 12 | Co0.3Ni0.4Re0.3 | 62 | Co0.3Ni0.3Sn0.4 | 112 | Fe0.3Ni0.3K0.4 | 162 | Fe0.3Ni0.4Pb0.3 |
| 13 | Cu0.4Ni0.3Zr0.3 | 63 | Ni0.4Ce0.3Hf0.3 | 113 | Fe0.4Co0.3Ce0.3 | 163 | Zn0.3Ce0.3Hf0.4 |
| 14 | Ni0.4Ru0.3Ce0.3 | 64 | Cu0.3Ca0.3Ba0.4 | 114 | Cu0.3Co0.3SrBr0.4 | 164 | Ni0.3Zr0.3Pb0.4 |
| 15 | Cr0.4Cu0.3Bi0.3 | 65 | Ni0.3Cs0.3Ba0.4 | 115 | Cd0.4Ni0.3Nb0.3 | 165 | Ga0.3Co0.4Ni0.3 |
| 16 | Cu0.4Ni0.3Pd0.3 | 66 | Co0.3V0.3Ag0.4 | 116 | Cr0.3Co0.3SrBr0.4 | 166 | Cd0.3Zr0.4SrBr0.3 |
| 17 | Cr0.3Cu0.4Ag0.3 | 67 | Ni0.3Ca0.4Ce0.3 | 117 | Ga0.4Cu0.3Pd0.3 | 167 | Co0.3Sn0.3Ru0.4 |
| 18 | Ni0.4Ca0.3Pb0.3 | 68 | Zn0.3Nb0.4Re0.3 | 118 | Cu0.3Hf0.3Re0.4 | 168 | Cd0.3Mn0.4Ba0.3 |
| 19 | Ni0.4Zr0.3Cs0.3 | 69 | Cu0.4Fe0.3Cs0.3 | 119 | Cr0.3Co0.4Ba0.3 | 169 | Ga0.3Sn0.3Nb0.4 |
| 20 | Co0.3Ni0.4Pb0.3 | 70 | Co0.3V0.3Ce0.4 | 120 | Cu0.4Cs0.3W0.3 | 170 | Cr0.3Co0.4Ce0.3 |
| 21 | Ni0.4Cs0.3Re0.3 | 71 | Cr0.4Cd0.3Cs0.3 | 121 | Co0.3Ni0.4Mn0.3 | 171 | Cu0.3Nb0.3Pb0.4 |
| 22 | Ga0.4Ni0.3Cs0.3 | 72 | Cr0.3Co0.3K0.4 | 122 | Co0.4V0.3Bi0.3 | 172 | Co0.3Sn0.3Pd0.4 |
| 23 | Zn0.3W0.4Ba0.3 | 73 | Cu0.3SrBr0.3Hf0.4 | 123 | Ga0.3Cu0.4Pd0.3 | 173 | Ga0.3Cu0.4Ce0.3 |
| 24 | Cu0.3Ni0.4Mn0.3 | 74 | Fe0.3Ni0.3Zn0.4 | 124 | Cu0.3Ni0.3K0.4 | 174 | Cd0.3Ni0.3Nb0.4 |
| 25 | Cu0.3Ce0.4SrBr0.3 | 75 | Ni0.4Nb0.3Pb0.3 | 125 | Fe0.4Zn0.3Ba0.3 | 175 | Co0.4SrBr0.3Pd0.3 |
| 26 | Ni0.4Nb0.3Cs0.3 | 76 | Cu0.3W0.3Re0.4 | 126 | V0.4K0.3Ba0.3 | 176 | Cr0.4Ni0.3Cs0.3 |
| 27 | Co0.3Nb0.3Pb0.4 | 77 | Cu0.3Ni0.3W0.4 | 127 | Cu0.3Fe0.3Pb0.4 | 177 | Cu0.3Ru0.3Bi0.4 |
| 28 | Ga0.4Co0.3Cs0.3 | 78 | Co0.4Ca0.3Mn0.3 | 128 | Cu0.4Sn0.3Ru0.3 | 178 | Ga0.3Cu0.3SrBr0.4 |
| 29 | Co0.3V0.4Pb0.3 | 79 | Co0.4K0.3Pd0.3 | 129 | Zn0.3Hf0.4Ba0.3 | 179 | Co0.4SrBr0.3Ba0.3 |
| 30 | K0.3Nb0.4SrBr0.3 | 80 | Ca0.3Mn0.4Pb0.3 | 130 | Cu0.4Zn0.3Ru0.3 | 180 | Ga0.3Cu0.4Ni0.3 |
| 31 | Nb0.4Ca0.3Pb0.3 | 81 | Ga0.3Zr0.4Zn0.3 | 131 | Co0.3Cs0.4Re0.3 | 181 | Co0.3Ni0.4W0.3 |
| 32 | Cu0.4Sn0.3Pd0.3 | 82 | Co0.3Zr0.4Ce0.3 | 132 | Cu0.4Cd0.3Ba0.3 | 182 | Cu0.4V0.3Re0.3 |
| 33 | Cr0.4Cu0.3Ag0.3 | 83 | Ga0.3Cu0.4Re0.3 | 133 | Ga0.3Cu0.4Fe0.3 | 183 | Ni0.3Ca0.3Ce0.4 |
| 34 | Nb0.4Ag0.3Cs0.3 | 84 | Cu0.4Bi0.3Pd0.3 | 134 | Cd0.3Co0.3Pd0.4 | 184 | Cu0.4V0.3Pb0.3 |
| 35 | Cu0.3Cs0.4W0.3 | 85 | Cu0.3Ca0.4Re0.3 | 135 | Ni0.3Zn0.4Nb0.3 | 185 | Cu0.4Zn0.3Ca0.3 |
| 36 | Ga0.3Ni0.3Re0.4 | 86 | Cu0.3Nb0.3SrBr0.4 | 136 | Ga0.3Cr0.4Ag0.3 | 186 | Cr0.3Cd0.3Co0.4 |
| 37 | Co0.3Hf0.3Pb0.4 | 87 | Cu0.4Sn0.3Ba0.3 | 137 | Cr0.4Cd0.3Ba0.3 | 187 | Ni0.3Nb0.4Ce0.3 |
| 38 | Sn0.3Mn0.4Ba0.3 | 88 | Co0.3Ni0.3Hf0.4 | 138 | Cu0.3Ag0.4W0.3 | 188 | Ni0.3Zr0.3Ce0.4 |
| 39 | Cu0.3Co0.4Ag0.3 | 89 | Cu0.4SrBr0.3Re0.3 | 139 | Fe0.3Co0.4Cs0.3 | 189 | Co0.4Zn0.3Mn0.3 |
| 40 | Cu0.3Zr0.4Ce0.3 | 90 | Zn0.3SrBr0.3Mn0.4 | 140 | Co0.3Zr0.4Cs0.3 | 190 | Co0.3Ni0.3Bi0.4 |
| 41 | Ga0.3Co0.3Cs0.4 | 91 | Cu0.4Mn0.3Ag0.3 | 141 | Cu0.4SrBr0.3Pb0.3 | 191 | Ni0.4Zn0.3Nb0.3 |
| 42 | Fe0.4Cs0.3Bi0.3 | 92 | Ga0.3Co0.3V0.4 | 142 | Cd0.3Ni0.4SrBr0.3 | 192 | Cu0.3K0.4Hf0.3 |
| 43 | Co0.3Hf0.3Bi0.4 | 93 | Ni0.3Nb0.4Cs0.3 | 143 | Co0.3Ni0.4Bi0.3 | 193 | Cu0.3Ni0.4Re0.3 |
| 44 | Ga0.3Ni0.4W0.3 | 94 | Co0.3Ca0.3Ru0.4 | 144 | Ga0.4Ni0.3Zr0.3 | 194 | Cu0.3V0.3Ag0.4 |
| 45 | Ga0.3Co0.4Ce0.3 | 95 | Cu0.3Ni0.4Sn0.3 | 145 | Ga0.3Hf0.4Pb0.3 | 195 | Cr0.4Ca0.3Ag0.3 |
| 46 | Cr0.3Cd0.4Co0.3 | 96 | Cu0.4Cd0.3Nb0.3 | 146 | Co0.3Ni0.4Pd0.3 | 196 | Fe0.3Ni0.4Cs0.3 |
| 47 | Ga0.3V0.4Ag0.3 | 97 | Ga0.3Ni0.3Nb0.4 | 147 | Cd0.3Ce0.3Hf0.4 | 197 | Cd0.3Co0.4Zr0.3 |
| 48 | Sn0.3W0.4Ba0.3 | 98 | Cu0.3Co0.3Ba0.4 | 148 | Cu0.3Fe0.4Ba0.3 | 198 | Cu0.4Ni0.3Ag0.3 |
| 49 | Cd0.3Ce0.3Pd0.4 | 99 | Co0.4Mn0.3Bi0.3 | 149 | Ni0.4Ce0.3W0.3 | 199 | Cu0.3Ce0.4Pd0.3 |
| 50 | Cu0.3Ru0.3Re0.4 | 100 | Nb0.4Cs0.3Bi0.3 | 150 | Cd0.3Cs0.3Pd0.4 | 200 | Cu0.3SrBr0.4W0.3 |

## Occupancy of catalyst library 2G1L

| | | | | | | | |
|---|---|---|---|---|---|---|---|
| 1 | Cu0.3Hf0.2Ti0.5 | 51 | Cu0.5Hf0.2Si0.3 | 101 | Cu0.3Zr0.4Al0.3 | 151 | Cu0.5Zr0.4Sn0.1 |
| 2 | Cu0.3Hf0.2Al0.5 | 52 | Cu0.5Hf0.2Sn0.3 | 102 | Cu0.3Zr0.4Fe0.3 | 152 | Cu0.5Zr0.4Zn0.1 |
| 3 | Cu0.3Hf0.2Fe0.5 | 53 | Cu0.5Hf0.2Zn0.3 | 103 | Cu0.3Zr0.4Mn0.3 | 153 | Cu0.5Zr0.4Ta0.1 |
| 4 | Cu0.3Hf0.2Mn0.5 | 54 | Cu0.5Hf0.2Ta0.3 | 104 | Cu0.3Zr0.4In0.3 | 154 | Cu0.5Zr0.4Ru0.1 |
| 5 | Cu0.3Hf0.2In0.5 | 55 | Cu0.5Hf0.2Ru0.3 | 105 | Cu0.3Zr0.4La0.3 | 155 | Cu0.7Zr0.2Hf0.1 |
| 6 | Cu0.3Hf0.2La0.5 | 56 | Cu0.5Zr0.3Hf0.2 | 106 | Cu0.3Zr0.4Nb0.3 | 156 | Cu0.7Zr0.2Ti0.1 |
| 7 | Cu0.3Hf0.2Nb0.5 | 57 | Cu0.5Hf0.4Ti0.1 | 107 | Cu0.3Zr0.4Sb0.3 | 157 | Cu0.7Zr0.2Al0.1 |
| 8 | Cu0.3Hf0.2Sb0.5 | 58 | Cu0.5Hf0.4Al0.1 | 108 | Cu0.3Zr0.4Si0.3 | 158 | Cu0.7Zr0.2Fe0.1 |
| 9 | Cu0.3Hf0.2Si0.5 | 59 | Cu0.5Hf0.4Fe0.1 | 109 | Cu0.3Zr0.4Sn0.3 | 159 | Cu0.7Zr0.2Mn0.1 |
| 10 | Cu0.3Hf0.2Sn0.5 | 60 | Cu0.5Hf0.4Mn0.1 | 110 | Cu0.3Zr0.4Zn0.3 | 160 | Cu0.7Zr0.2In0.1 |
| 11 | Cu0.3Hf0.2Zn0.5 | 61 | Cu0.5Hf0.4In0.1 | 111 | Cu0.3Zr0.4Ta0.3 | 161 | Cu0.7Zr0.2La0.1 |
| 12 | Cu0.3Hf0.2Ta0.5 | 62 | Cu0.5Hf0.4La0.1 | 112 | Cu0.3Zr0.4Ru0.3 | 162 | Cu0.7Zr0.2Nb0.1 |
| 13 | Cu0.3Hf0.2Ru0.5 | 63 | Cu0.5Hf0.4Nb0.1 | 113 | Cu0.3Zr0.6Hf0.1 | 163 | Cu0.7Zr0.2Sb0.1 |
| 14 | Cu0.3Zr0.5Hf0.2 | 64 | Cu0.5Hf0.4Sb0.1 | 114 | Cu0.3Zr0.6Ti0.1 | 164 | Cu0.7Zr0.2Si0.1 |
| 15 | Cu0.3Hf0.4Ti0.3 | 65 | Cu0.5Hf0.4Si0.1 | 115 | Cu0.3Zr0.6Al0.1 | 165 | Cu0.7Zr0.2Sn0.1 |
| 16 | Cu0.3Hf0.4Al0.3 | 66 | Cu0.5Hf0.4Sn0.1 | 116 | Cu0.3Zr0.6Fe0.1 | 166 | Cu0.7Zr0.2Zn0.1 |
| 17 | Cu0.3Hf0.4Fe0.3 | 67 | Cu0.5Hf0.4Zn0.1 | 117 | Cu0.3Zr0.6Mn0.1 | 167 | Cu0.7Zr0.2Ta0.1 |
| 18 | Cu0.3Hf0.4Mn0.3 | 68 | Cu0.5Hf0.4Ta0.1 | 118 | Cu0.3Zr0.6In0.1 | 168 | Cu0.7Zr0.2Ru0.1 |
| 19 | Cu0.3Hf0.4In0.3 | 69 | Cu0.5Hf0.4Ru0.1 | 119 | Cu0.3Zr0.6La0.1 | 169 | Cu0.1Zr0.9 |
| 20 | Cu0.3Hf0.4La0.3 | 70 | Cu0.5Zr0.1Hf0.4 | 120 | Cu0.3Zr0.6Nb0.1 | 170 | Cu0.2Zr0.8 |
| 21 | Cu0.3Hf0.4Nb0.3 | 71 | Cu0.7Hf0.2Ti0.1 | 121 | Cu0.3Zr0.6Sb0.1 | 171 | Cu0.3Zr0.7 |
| 22 | Cu0.3Hf0.4Sb0.3 | 72 | Cu0.7Hf0.2Al0.1 | 122 | Cu0.3Zr0.6Si0.1 | 172 | Cu0.4Zr0.6 |
| 23 | Cu0.3Hf0.4Si0.3 | 73 | Cu0.7Hf0.2Fe0.1 | 123 | Cu0.3Zr0.6Sn0.1 | 173 | Cu0.5Zr0.5 |
| 24 | Cu0.3Hf0.4Sn0.3 | 74 | Cu0.7Hf0.2Mn0.1 | 124 | Cu0.3Zr0.6Zn0.1 | 174 | Cu0.6Zr0.4 |
| 25 | Cu0.3Hf0.4Zn0.3 | 75 | Cu0.7Hf0.2In0.1 | 125 | Cu0.3Zr0.6Ta0.1 | 175 | Cu0.7Zr0.3 |
| 26 | Cu0.3Hf0.4Ta0.3 | 76 | Cu0.7Hf0.2La0.1 | 126 | Cu0.3Zr0.6Ru0.1 | 176 | Cu0.8Zr0.2 |
| 27 | Cu0.3Hf0.4Ru0.3 | 77 | Cu0.7Hf0.2Nb0.1 | 127 | Cu0.5Zr0.2Hf0.3 | 177 | Cu0.9Zr0.1 |
| 28 | Cu0.3Zr0.3Hf0.4 | 78 | Cu0.7Hf0.2Sb0.1 | 128 | Cu0.5Zr0.2Ti0.3 | 178 | Cu0.1Hf0.9 |
| 29 | Cu0.3Hf0.6Ti0.1 | 79 | Cu0.7Hf0.2Si0.1 | 129 | Cu0.5Zr0.2Al0.3 | 179 | Cu0.2Hf0.8 |
| 30 | Cu0.3Hf0.6Al0.1 | 80 | Cu0.7Hf0.2Sn0.1 | 130 | Cu0.5Zr0.2Fe0.3 | 180 | Cu0.3Hf0.7 |
| 31 | Cu0.3Hf0.6Fe0.1 | 81 | Cu0.7Hf0.2Zn0.1 | 131 | Cu0.5Zr0.2Mn0.3 | 181 | Cu0.4Hf0.6 |
| 32 | Cu0.3Hf0.6Mn0.1 | 82 | Cu0.7Hf0.2Ta0.1 | 132 | Cu0.5Zr0.2In0.3 | 182 | Cu0.5Hf0.5 |
| 33 | Cu0.3Hf0.6In0.1 | 83 | Cu0.7Hf0.2Ru0.1 | 133 | Cu0.5Zr0.2La0.3 | 183 | Cu0.6Hf0.4 |
| 34 | Cu0.3Hf0.6La0.1 | 84 | Cu0.7Zr0.1Hf0.2 | 134 | Cu0.5Zr0.2Nb0.3 | 184 | Cu0.7Hf0.3 |
| 35 | Cu0.3Hf0.6Nb0.1 | 85 | Cu0.3Zr0.2Hf0.5 | 135 | Cu0.5Zr0.2Sb0.3 | 185 | Cu0.8Hf0.2 |
| 36 | Cu0.3Hf0.6Sb0.1 | 86 | Cu0.3Zr0.2Ti0.5 | 136 | Cu0.5Zr0.2Si0.3 | 186 | Cu0.9Hf0.1 |
| 37 | Cu0.3Hf0.6Si0.1 | 87 | Cu0.3Zr0.2Al0.5 | 137 | Cu0.5Zr0.2Sn0.3 | 187 | Cu0.1Ti0.9 |
| 38 | Cu0.3Hf0.6Sn0.1 | 88 | Cu0.3Zr0.2Fe0.5 | 138 | Cu0.5Zr0.2Zn0.3 | 188 | Cu0.2Ti0.8 |
| 39 | Cu0.3Hf0.6Zn0.1 | 89 | Cu0.3Zr0.2Mn0.5 | 139 | Cu0.5Zr0.2Ta0.3 | 189 | Cu0.3Ti0.7 |
| 40 | Cu0.3Hf0.6Ta0.1 | 90 | Cu0.3Zr0.2In0.5 | 140 | Cu0.5Zr0.2Ru0.3 | 190 | Cu0.4Ti0.6 |
| 41 | Cu0.3Hf0.6Ru0.1 | 91 | Cu0.3Zr0.2La0.5 | 141 | Cu0.5Zr0.4Hf0.1 | 191 | Cu0.5Ti0.5 |
| 42 | Cu0.3Zr0.1Hf0.6 | 92 | Cu0.3Zr0.2Nb0.5 | 142 | Cu0.5Zr0.4Ti0.1 | 192 | Cu0.6Ti0.4 |
| 43 | Cu0.5Hf0.2Ti0.3 | 93 | Cu0.3Zr0.2Sb0.5 | 143 | Cu0.5Zr0.4Al0.1 | 193 | Cu0.7Ti0.3 |
| 44 | Cu0.5Hf0.2Al0.3 | 94 | Cu0.3Zr0.2Si0.5 | 144 | Cu0.5Zr0.4Fe0.1 | 194 | Cu0.8Ti0.2 |
| 45 | Cu0.5Hf0.2Fe0.3 | 95 | Cu0.3Zr0.2Sn0.5 | 145 | Cu0.5Zr0.4Mn0.1 | 195 | Cu0.9Ti0.1 |
| 46 | Cu0.5Hf0.2Mn0.3 | 96 | Cu0.3Zr0.2Zn0.5 | 146 | Cu0.5Zr0.4In0.1 | 196 | Cu1.0 |
| 47 | Cu0.5Hf0.2In0.3 | 97 | Cu0.3Zr0.2Ta0.5 | 147 | Cu0.5Zr0.4La0.1 | 197 | Zr1.0 |
| 48 | Cu0.5Hf0.2La0.3 | 98 | Cu0.3Zr0.2Ru0.5 | 148 | Cu0.5Zr0.4Nb0.1 | 198 | Hf1.0 |
| 49 | Cu0.5Hf0.2Nb0.3 | 99 | Cu0.3Zr0.4Hf0.3 | 149 | Cu0.5Zr0.4Sb0.1 | 199 | Ti1.0 |
| 50 | Cu0.5Hf0.2Sb0.3 | 100 | Cu0.3Zr0.4Ti0.3 | 150 | Cu0.5Zr0.4Si0.1 | | |

## Occupancy of catalyst library 2G2L

| | | | | | | | |
|---|---|---|---|---|---|---|---|
| 1 | Cu0.3Hf0.2Ti0.5 | 51 | Cu0.5Hf0.2Si0.3 | 101 | Cu0.3Zr0.4Al0.3 | 151 | Cu0.5Zr0.4 |
| 2 | Cu0.3Hf0.2Al0.5 | 52 | Cu0.5Hf0.2Sn0.3 | 102 | Cu0.3Zr0.4Fe0.3 | 152 | Cu0.5Zr0.4 |
| 3 | Cu0.3Hf0.2Fe0.5 | 53 | Cu0.5Hf0.2Zn0.3 | 103 | Cu0.3Zr0.4Mn0.3 | 153 | Cu0.5Zr0.4 |
| 4 | Cu0.3Hf0.2Mn0.5 | 54 | Cu0.5Hf0.2Ta0.3 | 104 | Cu0.3Zr0.4Ru0.3 | 154 | Cu0.5Zr0.4 |
| 5 | Cu0.3Hf0.2Ru0.5 | 55 | Cu0.5Hf0.2In0.3 | 105 | Cu0.3Zr0.4La0.3 | 155 | Cu0.7Zr0.2 |
| 6 | Cu0.3Hf0.2La0.5 | 56 | Cu0.5Zr0.3Hf0.2 | 106 | Cu0.3Zr0.4Nb0.3 | 156 | Cu0.7Zr0.2 |
| 7 | Cu0.3Hf0.2Nb0.5 | 57 | Cu0.5Hf0.4 | 107 | Cu0.3Zr0.4Sb0.3 | 157 | Cu0.7Zr0.2 |
| 8 | Cu0.3Hf0.2Sb0.5 | 58 | Cu0.5Hf0.4 | 108 | Cu0.3Zr0.4Si0.3 | 158 | Cu0.7Zr0.2 |
| 9 | Cu0.3Hf0.2Si0.5 | 59 | Cu0.5Hf0.4 | 109 | Cu0.3Zr0.4Sn0.3 | 159 | Cu0.7Zr0.2 |
| 10 | Cu0.3Hf0.2Sn0.5 | 60 | Cu0.5Hf0.4 | 110 | Cu0.3Zr0.4Zn0.3 | 160 | Cu0.7Zr0.2 |
| 11 | Cu0.3Hf0.2Zn0.5 | 61 | Cu0.5Hf0.4 | 111 | Cu0.3Zr0.4Ta0.3 | 161 | Cu0.7Zr0.2 |
| 12 | Cu0.3Hf0.2Ta0.5 | 62 | Cu0.5Hf0.4 | 112 | Cu0.3Zr0.4In0.3 | 162 | Cu0.7Zr0.2 |
| 13 | Cu0.3Hf0.2In0.5 | 63 | Cu0.5Hf0.4 | 113 | Cu0.3Zr0.6 | 163 | Cu0.7Zr0.2 |
| 14 | Cu0.3Zr0.5Hf0.2 | 64 | Cu0.5Hf0.4 | 114 | Cu0.3Zr0.6 | 164 | Cu0.7Zr0.2 |
| 15 | Cu0.3Hf0.4Ti0.3 | 65 | Cu0.5Hf0.4 | 115 | Cu0.3Zr0.6 | 165 | Cu0.7Zr0.2 |
| 16 | Cu0.3Hf0.4Al0.3 | 66 | Cu0.5Hf0.4 | 116 | Cu0.3Zr0.6 | 166 | Cu0.7Zr0.2 |
| 17 | Cu0.3Hf0.4Fe0.3 | 67 | Cu0.5Hf0.4 | 117 | Cu0.3Zr0.6 | 167 | Cu0.7Zr0.2 |
| 18 | Cu0.3Hf0.4Mn0.3 | 68 | Cu0.5Hf0.4 | 118 | Cu0.3Zr0.6 | 168 | Cu0.7Zr0.2 |
| 19 | Cu0.3Hf0.4Ru0.3 | 69 | Cu0.5Hf0.4 | 119 | Cu0.3Zr0.6 | 169 | Zr0.9 |
| 20 | Cu0.3Hf0.4La0.3 | 70 | Cu0.5Hf0.4 | 120 | Cu0.3Zr0.6 | 170 | Cu0.2Zr0.8 |
| 21 | Cu0.3Hf0.4Nb0.3 | 71 | Cu0.7Hf0.2 | 121 | Cu0.3Zr0.6 | 171 | Cu0.3Zr0.7 |
| 22 | Cu0.3Hf0.4Sb0.3 | 72 | Cu0.7Hf0.2 | 122 | Cu0.3Zr0.6 | 172 | Cu0.4Zr0.6 |
| 23 | Cu0.3Hf0.4Si0.3 | 73 | Cu0.7Hf0.2 | 123 | Cu0.3Zr0.6 | 173 | Cu0.5Zr0.5 |
| 24 | Cu0.3Hf0.4Sn0.3 | 74 | Cu0.7Hf0.2 | 124 | Cu0.3Zr0.6 | 174 | Cu0.6Zr0.4 |
| 25 | Cu0.3Hf0.4Zn0.3 | 75 | Cu0.7Hf0.2 | 125 | Cu0.3Zr0.6 | 175 | Cu0.7Zr0.3 |
| 26 | Cu0.3Hf0.4Ta0.3 | 76 | Cu0.7Hf0.2 | 126 | Cu0.3Zr0.6 | 176 | Cu0.8Zr0.2 |
| 27 | Cu0.3Hf0.4In0.3 | 77 | Cu0.7Hf0.2 | 127 | Cu0.5Zr0.2Hf0.3 | 177 | Cu0.9 |
| 28 | Cu0.3Zr0.3Hf0.4 | 78 | Cu0.7Hf0.2 | 128 | Cu0.5Zr0.2Ti0.3 | 178 | Hf0.9 |
| 29 | Cu0.3Hf0.6 | 79 | Cu0.7Hf0.2 | 129 | Cu0.5Zr0.2Al0.3 | 179 | Cu0.2Hf0.8 |
| 30 | Cu0.3Hf0.6 | 80 | Cu0.7Hf0.2 | 130 | Cu0.5Zr0.2Fe0.3 | 180 | Cu0.3Hf0.7 |
| 31 | Cu0.3Hf0.6 | 81 | Cu0.7Hf0.2 | 131 | Cu0.5Zr0.2Mn0.3 | 181 | Cu0.4Hf0.6 |
| 32 | Cu0.3Hf0.6 | 82 | Cu0.7Hf0.2 | 132 | Cu0.5Zr0.2Ru0.3 | 182 | Cu0.5Hf0.5 |
| 33 | Cu0.3Hf0.6 | 83 | Cu0.7Hf0.2 | 133 | Cu0.5Zr0.2La0.3 | 183 | Cu0.6Hf0.4 |
| 34 | Cu0.3Hf0.6 | 84 | Cu0.7Hf0.2 | 134 | Cu0.5Zr0.2Nb0.3 | 184 | Cu0.7Hf0.3 |
| 35 | Cu0.3Hf0.6 | 85 | Cu0.3Zr0.2Hf0.5 | 135 | Cu0.5Zr0.2Sb0.3 | 185 | Cu0.8Hf0.2 |
| 36 | Cu0.3Hf0.6 | 86 | Cu0.3Zr0.2Ti0.5 | 136 | Cu0.5Zr0.2Si0.3 | 186 | Cu0.9 |
| 37 | Cu0.3Hf0.6 | 87 | Cu0.3Zr0.2Al0.5 | 137 | Cu0.5Zr0.2Sn0.3 | 187 | Ti0.9 |
| 38 | Cu0.3Hf0.6 | 88 | Cu0.3Zr0.2Fe0.5 | 138 | Cu0.5Zr0.2Zn0.3 | 188 | Cu0.2Ti0.8 |
| 39 | Cu0.3Hf0.6 | 89 | Cu0.3Zr0.2Mn0.5 | 139 | Cu0.5Zr0.2Ta0.3 | 189 | Cu0.3Ti0.7 |
| 40 | Cu0.3Hf0.6 | 90 | Cu0.3Zr0.2Ru0.5 | 140 | Cu0.5Zr0.2In0.3 | 190 | Cu0.4Ti0.6 |
| 41 | Cu0.3Hf0.6 | 91 | Cu0.3Zr0.2La0.5 | 141 | Cu0.5Zr0.4 | 191 | Cu0.5Ti0.5 |
| 42 | Cu0.3Hf0.6 | 92 | Cu0.3Zr0.2Nb0.5 | 142 | Cu0.5Zr0.4 | 192 | Cu0.6Ti0.4 |
| 43 | Cu0.5Hf0.2Ti0.3 | 93 | Cu0.3Zr0.2Sb0.5 | 143 | Cu0.5Zr0.4 | 193 | Cu0.7Ti0.3 |
| 44 | Cu0.5Hf0.2Al0.3 | 94 | Cu0.3Zr0.2Si0.5 | 144 | Cu0.5Zr0.4 | 194 | Cu0.8Ti0.2 |
| 45 | Cu0.5Hf0.2Fe0.3 | 95 | Cu0.3Zr0.2Sn0.5 | 145 | Cu0.5Zr0.4 | 195 | Cu0.9 |
| 46 | Cu0.5Hf0.2Mn0.3 | 96 | Cu0.3Zr0.2Zn0.5 | 146 | Cu0.5Zr0.4 | 196 | Cu1.0 |
| 47 | Cu0.5Hf0.2Ru0.3 | 97 | Cu0.3Zr0.2Ta0.5 | 147 | Cu0.5Zr0.4 | 197 | Zr1.0 |
| 48 | Cu0.5Hf0.2La0.3 | 98 | Cu0.3Zr0.2In0.5 | 148 | Cu0.5Zr0.4 | 198 | Hf1.0 |
| 49 | Cu0.5Hf0.2Nb0.3 | 99 | Cu0.3Zr0.4Hf0.3 | 149 | Cu0.5Zr0.4 | 199 | Ti1.0 |
| 50 | Cu0.5Hf0.2Sb0.3 | 100 | Cu0.3Zr0.4Ti0.3 | 150 | Cu0.5Zr0.4 | | |

## Occupancy of catalyst library 2G3L

| | | | | | | | |
|---|---|---|---|---|---|---|---|
| 1 | Cu0.5Mn0.2Sn0.3 | 51 | Cu0.3Sn0.5In0.2 | 101 | Cu0.7Cr0.2La0.1 | 151 | Cu0.6Mn0.2In0.2 |
| 2 | Cu0.5Mn0.2Sb0.3 | 52 | Cu0.3Sn0.5La0.2 | 102 | Cu0.7Cr0.2Zr0.1 | 152 | Cu0.6Mn0.2La0.2 |
| 3 | Cu0.5Mn0.2Cr0.3 | 53 | Cu0.3Sn0.5Zr0.2 | 103 | Cu0.7In0.2La0.1 | 153 | Cu0.6Mn0.2Zr0.2 |
| 4 | Cu0.5Mn0.2In0.3 | 54 | Cu0.3Sb0.5Cr0.2 | 104 | Cu0.7In0.2Zr0.1 | 154 | Cu0.6Sn0.2Sb0.2 |
| 5 | Cu0.5Mn0.2La0.3 | 55 | Cu0.3Sb0.5In0.2 | 105 | Cu0.7La0.2Zr0.1 | 155 | Cu0.6Sn0.2Cr0.2 |
| 6 | Cu0.5Mn0.2Zr0.3 | 56 | Cu0.3Sb0.5La0.2 | 106 | Cu0.7Mn0.1Sn0.2 | 156 | Cu0.6Sn0.2In0.2 |
| 7 | Cu0.5Sn0.2Sb0.3 | 57 | Cu0.3Sb0.5Zr0.2 | 107 | Cu0.7Mn0.1Sb0.2 | 157 | Cu0.6Sn0.2La0.2 |
| 8 | Cu0.5Sn0.2Cr0.3 | 58 | Cu0.3Cr0.5In0.2 | 108 | Cu0.7Mn0.1Cr0.2 | 158 | Cu0.6Sn0.2Zr0.2 |
| 9 | Cu0.5Sn0.2In0.3 | 59 | Cu0.3Cr0.5La0.2 | 109 | Cu0.7Mn0.1In0.2 | 159 | Cu0.6Sb0.2Cr0.2 |
| 10 | Cu0.5Sn0.2La0.3 | 60 | Cu0.3Cr0.5Zr0.2 | 110 | Cu0.7Mn0.1La0.2 | 160 | Cu0.6Sb0.2In0.2 |
| 11 | Cu0.5Sn0.2Zr0.3 | 61 | Cu0.3In0.5La0.2 | 111 | Cu0.7Mn0.1Zr0.2 | 161 | Cu0.6Sb0.2La0.2 |
| 12 | Cu0.5Sb0.2Cr0.3 | 62 | Cu0.3In0.5Zr0.2 | 112 | Cu0.7Sn0.1Sb0.2 | 162 | Cu0.6Sb0.2Zr0.2 |
| 13 | Cu0.5Sb0.2In0.3 | 63 | Cu0.3La0.5Zr0.2 | 113 | Cu0.7Sn0.1Cr0.2 | 163 | Cu0.6Cr0.2In0.2 |
| 14 | Cu0.5Sb0.2La0.3 | 64 | Cu0.3Mn0.2Sn0.5 | 114 | Cu0.7Sn0.1In0.2 | 164 | Cu0.6Cr0.2La0.2 |
| 15 | Cu0.5Sb0.2Zr0.3 | 65 | Cu0.3Mn0.2Sb0.5 | 115 | Cu0.7Sn0.1La0.2 | 165 | Cu0.6Cr0.2Zr0.2 |
| 16 | Cu0.5Cr0.2In0.3 | 66 | Cu0.3Mn0.2Cr0.5 | 116 | Cu0.7Sn0.1Zr0.2 | 166 | Cu0.6In0.2La0.2 |
| 17 | Cu0.5Cr0.2La0.3 | 67 | Cu0.3Mn0.2In0.5 | 117 | Cu0.7Sb0.1Cr0.2 | 167 | Cu0.6In0.2Zr0.2 |
| 18 | Cu0.5Cr0.2Zr0.3 | 68 | Cu0.3Mn0.2La0.5 | 118 | Cu0.7Sb0.1In0.2 | 168 | Cu0.6La0.2Zr0.2 |
| 19 | Cu0.5In0.2La0.3 | 69 | Cu0.3Mn0.2Zr0.5 | 119 | Cu0.7Sb0.1La0.2 | 169 | Cu0.3Mn0.4Sn0.3 |
| 20 | Cu0.5In0.2Zr0.3 | 70 | Cu0.3Sn0.2Sb0.5 | 120 | Cu0.7Sb0.1Zr0.2 | 170 | Cu0.3Mn0.4Sb0.3 |
| 21 | Cu0.5La0.2Zr0.3 | 71 | Cu0.3Sn0.2Cr0.5 | 121 | Cu0.7Cr0.1In0.2 | 171 | Cu0.3Mn0.4Cr0.3 |
| 22 | Cu0.5Mn0.3Sn0.2 | 72 | Cu0.3Sn0.2In0.5 | 122 | Cu0.7Cr0.1La0.2 | 172 | Cu0.3Mn0.4In0.3 |
| 23 | Cu0.5Mn0.3Sb0.2 | 73 | Cu0.3Sn0.2La0.5 | 123 | Cu0.7Cr0.1Zr0.2 | 173 | Cu0.3Mn0.4La0.3 |
| 24 | Cu0.5Mn0.3Cr0.2 | 74 | Cu0.3Sn0.2Zr0.5 | 124 | Cu0.7In0.1La0.2 | 174 | Cu0.3Mn0.4Zr0.3 |
| 25 | Cu0.5Mn0.3In0.2 | 75 | Cu0.3Sb0.2Cr0.5 | 125 | Cu0.7In0.1Zr0.2 | 175 | Cu0.3Sn0.4Sb0.3 |
| 26 | Cu0.5Mn0.3La0.2 | 76 | Cu0.3Sb0.2In0.5 | 126 | Cu0.7La0.1Zr0.2 | 176 | Cu0.3Sn0.4Cr0.3 |
| 27 | Cu0.5Mn0.3Zr0.2 | 77 | Cu0.3Sb0.2La0.5 | 127 | Cu0.4Mn0.3Sn0.3 | 177 | Cu0.3Sn0.4In0.3 |
| 28 | Cu0.5Sn0.3Sb0.2 | 78 | Cu0.3Sb0.2Zr0.5 | 128 | Cu0.4Mn0.3Sb0.3 | 178 | Cu0.3Sn0.4La0.3 |
| 29 | Cu0.5Sn0.3Cr0.2 | 79 | Cu0.3Cr0.2In0.5 | 129 | Cu0.4Mn0.3Cr0.3 | 179 | Cu0.3Sn0.4Zr0.3 |
| 30 | Cu0.5Sn0.3In0.2 | 80 | Cu0.3Cr0.2La0.5 | 130 | Cu0.4Mn0.3In0.3 | 180 | Cu0.3Sb0.4Cr0.3 |
| 31 | Cu0.5Sn0.3La0.2 | 81 | Cu0.3Cr0.2Zr0.5 | 131 | Cu0.4Mn0.3La0.3 | 181 | Cu0.3Sb0.4In0.3 |
| 32 | Cu0.5Sn0.3Zr0.2 | 82 | Cu0.3In0.2La0.5 | 132 | Cu0.4Mn0.3Zr0.3 | 182 | Cu0.3Sb0.4La0.3 |
| 33 | Cu0.5Sb0.3Cr0.2 | 83 | Cu0.3In0.2Zr0.5 | 133 | Cu0.4Sn0.3Sb0.3 | 183 | Cu0.3Sb0.4Zr0.3 |
| 34 | Cu0.5Sb0.3In0.2 | 84 | Cu0.3La0.2Zr0.5 | 134 | Cu0.4Sn0.3Cr0.3 | 184 | Cu0.3Cr0.4In0.3 |
| 35 | Cu0.5Sb0.3La0.2 | 85 | Cu0.7Mn0.2Sn0.1 | 135 | Cu0.4Sn0.3In0.3 | 185 | Cu0.3Cr0.4La0.3 |
| 36 | Cu0.5Sb0.3Zr0.2 | 86 | Cu0.7Mn0.2Sb0.1 | 136 | Cu0.4Sn0.3La0.3 | 186 | Cu0.3Cr0.4Zr0.3 |
| 37 | Cu0.5Cr0.3In0.2 | 87 | Cu0.7Mn0.2Cr0.1 | 137 | Cu0.4Sn0.3Zr0.3 | 187 | Cu0.3In0.4La0.3 |
| 38 | Cu0.5Cr0.3La0.2 | 88 | Cu0.7Mn0.2In0.1 | 138 | Cu0.4Sb0.3Cr0.3 | 188 | Cu0.3In0.4Zr0.3 |
| 39 | Cu0.5Cr0.3Zr0.2 | 89 | Cu0.7Mn0.2La0.1 | 139 | Cu0.4Sb0.3In0.3 | 189 | Cu0.3La0.4Zr0.3 |
| 40 | Cu0.5In0.3La0.2 | 90 | Cu0.7Mn0.2Zr0.1 | 140 | Cu0.4Sb0.3La0.3 | 190 | Cu0.3Mn0.3Sn0.4 |
| 41 | Cu0.5In0.3Zr0.2 | 91 | Cu0.7Sn0.2Sb0.1 | 141 | Cu0.4Sb0.3Zr0.3 | 191 | Cu0.3Mn0.3Sb0.4 |
| 42 | Cu0.5La0.3Zr0.2 | 92 | Cu0.7Sn0.2Cr0.1 | 142 | Cu0.4Cr0.3In0.3 | 192 | Cu0.3Mn0.3Cr0.4 |
| 43 | Cu0.3Mn0.5Sn0.2 | 93 | Cu0.7Sn0.2In0.1 | 143 | Cu0.4Cr0.3La0.3 | 193 | Cu0.3Mn0.3In0.4 |
| 44 | Cu0.3Mn0.5Sb0.2 | 94 | Cu0.7Sn0.2La0.1 | 144 | Cu0.4Cr0.3Zr0.3 | 194 | Cu0.3Mn0.3La0.4 |
| 45 | Cu0.3Mn0.5Cr0.2 | 95 | Cu0.7Sn0.2Zr0.1 | 145 | Cu0.4In0.3La0.3 | 195 | Cu0.3Mn0.3Zr0.4 |
| 46 | Cu0.3Mn0.5In0.2 | 96 | Cu0.7Sb0.2Cr0.1 | 146 | Cu0.4In0.3Zr0.3 | 196 | Cu0.3Sn0.3Sb0.4 |
| 47 | Cu0.3Mn0.5La0.2 | 97 | Cu0.7Sb0.2In0.1 | 147 | Cu0.4La0.3Zr0.3 | 197 | Cu0.3Sn0.3Cr0.4 |
| 48 | Cu0.3Mn0.5Zr0.2 | 98 | Cu0.7Sb0.2La0.1 | 148 | Cu0.6Mn0.2Sn0.2 | 198 | Cu0.3Sn0.3In0.4 |
| 49 | Cu0.3Sn0.5Sb0.2 | 99 | Cu0.7Sb0.2Zr0.1 | 149 | Cu0.6Mn0.2Sb0.2 | 199 | Cu0.3Sn0.3La0.4 |
| 50 | Cu0.3Sn0.5Cr0.2 | 100 | Cu0.7Cr0.2In0.1 | 150 | Cu0.6Mn0.2Cr0.2 | 200 | Cu0.3Sn0.3Zr0.4 |

## Occupancy of catalyst library 1G4L

| | | | | | | | |
|---|---|---|---|---|---|---|---|
| 1 | Ga0.4Cr0.4Cu0.2 | 51 | Ga0.5Cr0.4Fe0.1 | 101 | Ga0.4Cr0.4Ni0.2 | 151 | Ga0.5Cr0.4V0.1 |
| 2 | Ga0.4Cr0.4Cd0.2 | 52 | Ga0.5Cr0.4Co0.1 | 102 | Ga0.4Cr0.4Zr0.2 | 152 | Ga0.5Cr0.4Zn0.1 |
| 3 | Ga0.4Cr0.4Fe0.2 | 53 | Ga0.5Cr0.4Ni0.1 | 103 | Ga0.4Cr0.4V0.2 | 153 | Ga0.5Cr0.4Sn0.1 |
| 4 | Ga0.4Cr0.4Co0.2 | 54 | Ga0.5Cr0.4Zr0.1 | 104 | Ga0.4Cr0.4Zn0.2 | 154 | Ga0.5Cr0.4K0.1 |
| 5 | Ga0.4Cr0.4Ni0.2 | 55 | Ga0.5Cr0.4V0.1 | 105 | Ga0.4Cr0.4Sn0.2 | 155 | Ga0.5Cr0.4Nb0.1 |
| 6 | Ga0.4Cr0.4Zr0.2 | 56 | Ga0.5Cr0.4Zn0.1 | 106 | Ga0.4Cr0.4K0.2 | 156 | Ga0.5Cr0.4Ca0.1 |
| 7 | Ga0.4Cr0.4V0.2 | 57 | Ga0.5Cr0.4Sn0.1 | 107 | Ga0.4Cr0.4Nb0.2 | 157 | Ga0.5Cr0.4Ru0.1 |
| 8 | Ga0.4Cr0.4Zn0.2 | 58 | Ga0.5Cr0.4K0.1 | 108 | Ga0.4Cr0.4Ca0.2 | 158 | Ga0.5Cr0.4Ce0.1 |
| 9 | Ga0.4Cr0.4Sn0.2 | 59 | Ga0.5Cr0.4Nb0.1 | 109 | Ga0.4Cr0.4Ru0.2 | 159 | Ga0.5Cr0.4SrBr0.1 |
| 10 | Ga0.4Cr0.4K0.2 | 60 | Ga0.5Cr0.4Ca0.1 | 110 | Ga0.4Cr0.4Ce0.2 | 160 | Ga0.5Cr0.4Ag0.1 |
| 11 | Ga0.4Cr0.4Nb0.2 | 61 | Ga0.5Cr0.4Ru0.1 | 111 | Ga0.4Cr0.4SrBr0.2 | 161 | Ga0.5Cr0.4Hf0.1 |
| 12 | Ga0.4Cr0.4Ca0.2 | 62 | Ga0.5Cr0.4Ce0.1 | 112 | Ga0.4Cr0.4Ag0.2 | 162 | Ga0.5Cr0.4Cs0.1 |
| 13 | Ga0.4Cr0.4Ru0.2 | 63 | Ga0.5Cr0.4SrBr0.1 | 113 | Ga0.4Cr0.4Hf0.2 | 163 | Ga0.5Cr0.4W0.1 |
| 14 | Ga0.4Cr0.4Ce0.2 | 64 | Ga0.5Cr0.4Ag0.1 | 114 | Ga0.4Cr0.4Cs0.2 | 164 | Ga0.5Cr0.4Re0.1 |
| 15 | Ga0.4Cr0.4SrBr0.2 | 65 | Ga0.5Cr0.4Hf0.1 | 115 | Ga0.4Cr0.4W0.2 | 165 | Ga0.5Cr0.4Ba0.1 |
| 16 | Ga0.4Cr0.4Ag0.2 | 66 | Ga0.5Cr0.4Cs0.1 | 116 | Ga0.4Cr0.4Re0.2 | 166 | Ga0.5Cr0.4Bi0.1 |
| 17 | Ga0.4Cr0.4Hf0.2 | 67 | Ga0.5Cr0.4W0.1 | 117 | Ga0.4Cr0.4Ba0.2 | 167 | Ga0.5Cr0.4Pb0.1 |
| 18 | Ga0.4Cr0.4Cs0.2 | 68 | Ga0.5Cr0.4Re0.1 | 118 | Ga0.4Cr0.4Bi0.2 | 168 | Ga0.5Cr0.4Hf20.1 |
| 19 | Ga0.4Cr0.4W0.2 | 69 | Ga0.5Cr0.4Ba0.1 | 119 | Ga0.4Cr0.4Pb0.2 | 169 | Ga0.4Cr0.5Cu0.1 |
| 20 | Ga0.4Cr0.4Re0.2 | 70 | Ga0.5Cr0.4Bi0.1 | 120 | Ga0.4Cr0.4Hf20.2 | 170 | Ga0.4Cr0.5Cd0.1 |
| 21 | Ga0.4Cr0.4Ba0.2 | 71 | Ga0.5Cr0.4Pb0.1 | 121 | Ga0.45Cr0.45Cu0.1 | 171 | Ga0.4Cr0.5Fe0.1 |
| 22 | Ga0.4Cr0.4Bi0.2 | 72 | Ga0.5Cr0.4Hf20.1 | 122 | Ga0.45Cr0.45Cd0.1 | 172 | Ga0.4Cr0.5Co0.1 |
| 23 | Ga0.4Cr0.4Pb0.2 | 73 | Ga0.4Cr0.5Cu0.1 | 123 | Ga0.45Cr0.45Fe0.1 | 173 | Ga0.4Cr0.5Ni0.1 |
| 24 | Ga0.4Cr0.4Hf20.2 | 74 | Ga0.4Cr0.5Cd0.1 | 124 | Ga0.45Cr0.45Co0.1 | 174 | Ga0.4Cr0.5Zr0.1 |
| 25 | Ga0.45Cr0.45Cu0.1 | 75 | Ga0.4Cr0.5Fe0.1 | 125 | Ga0.45Cr0.45Ni0.1 | 175 | Ga0.4Cr0.5V0.1 |
| 26 | Ga0.45Cr0.45Cd0.1 | 76 | Ga0.4Cr0.5Co0.1 | 126 | Ga0.45Cr0.45Zr0.1 | 176 | Ga0.4Cr0.5Zn0.1 |
| 27 | Ga0.45Cr0.45Fe0.1 | 77 | Ga0.4Cr0.5Ni0.1 | 127 | Ga0.45Cr0.45V0.1 | 177 | Ga0.4Cr0.5Sn0.1 |
| 28 | Ga0.45Cr0.45Co0.1 | 78 | Ga0.4Cr0.5Zr0.1 | 128 | Ga0.45Cr0.45Zn0.1 | 178 | Ga0.4Cr0.5K0.1 |
| 29 | Ga0.45Cr0.45Ni0.1 | 79 | Ga0.4Cr0.5V0.1 | 129 | Ga0.45Cr0.45Sn0.1 | 179 | Ga0.4Cr0.5Nb0.1 |
| 30 | Ga0.45Cr0.45Zr0.1 | 80 | Ga0.4Cr0.5Zn0.1 | 130 | Ga0.45Cr0.45K0.1 | 180 | Ga0.4Cr0.5Ca0.1 |
| 31 | Ga0.45Cr0.45V0.1 | 81 | Ga0.4Cr0.5Sn0.1 | 131 | Ga0.45Cr0.45Nb0.1 | 181 | Ga0.4Cr0.5Ru0.1 |
| 32 | Ga0.45Cr0.45Zn0.1 | 82 | Ga0.4Cr0.5K0.1 | 132 | Ga0.45Cr0.45Ca0.1 | 182 | Ga0.4Cr0.5Ce0.1 |
| 33 | Ga0.45Cr0.45Sn0.1 | 83 | Ga0.4Cr0.5Nb0.1 | 133 | Ga0.45Cr0.45Ru0.1 | 183 | Ga0.4Cr0.5SrBr0.1 |
| 34 | Ga0.45Cr0.45K0.1 | 84 | Ga0.4Cr0.5Ca0.1 | 134 | Ga0.45Cr0.45Ce0.1 | 184 | Ga0.4Cr0.5Ag0.1 |
| 35 | Ga0.45Cr0.45Nb0.1 | 85 | Ga0.4Cr0.5Ru0.1 | 135 | Ga0.45Cr0.45SrBr0.1 | 185 | Ga0.4Cr0.5Hf0.1 |
| 36 | Ga0.45Cr0.45Ca0.1 | 86 | Ga0.4Cr0.5Ce0.1 | 136 | Ga0.45Cr0.45Ag0.1 | 186 | Ga0.4Cr0.5Cs0.1 |
| 37 | Ga0.45Cr0.45Ru0.1 | 87 | Ga0.4Cr0.5SrBr0.1 | 137 | Ga0.45Cr0.45Hf0.1 | 187 | Ga0.4Cr0.5W0.1 |
| 38 | Ga0.45Cr0.45Ce0.1 | 88 | Ga0.4Cr0.5Ag0.1 | 138 | Ga0.45Cr0.45Cs0.1 | 188 | Ga0.4Cr0.5Re0.1 |
| 39 | Ga0.45Cr0.45SrBr0.1 | 89 | Ga0.4Cr0.5Hf0.1 | 139 | Ga0.45Cr0.45W0.1 | 189 | Ga0.4Cr0.5Ba0.1 |
| 40 | Ga0.45Cr0.45Ag0.1 | 90 | Ga0.4Cr0.5Cs0.1 | 140 | Ga0.45Cr0.45Re0.1 | 190 | Ga0.4Cr0.5Bi0.1 |
| 41 | Ga0.45Cr0.45Hf0.1 | 91 | Ga0.4Cr0.5W0.1 | 141 | Ga0.45Cr0.45Ba0.1 | 191 | Ga0.4Cr0.5Pb0.1 |
| 42 | Ga0.45Cr0.45Cs0.1 | 92 | Ga0.4Cr0.5Re0.1 | 142 | Ga0.45Cr0.45Bi0.1 | 192 | Ga0.4Cr0.5Hf20.1 |
| 43 | Ga0.45Cr0.45W0.1 | 93 | Ga0.4Cr0.5Ba0.1 | 143 | Ga0.45Cr0.45Pb0.1 | 193 | Ga0.5Cr0.5 |
| 44 | Ga0.45Cr0.45Re0.1 | 94 | Ga0.4Cr0.5Bi0.1 | 144 | Ga0.45Cr0.45Hf20.1 | 194 | Ga0.5Cr0.5 |
| 45 | Ga0.45Cr0.45Ba0.1 | 95 | Ga0.4Cr0.5Pb0.1 | 145 | Ga0.5Cr0.4Cu0.1 | 195 | Ga0.4Cr0.6 |
| 46 | Ga0.45Cr0.45Bi0.1 | 96 | Ga0.4Cr0.5Hf20.1 | 146 | Ga0.5Cr0.4Cd0.1 | 196 | Ga0.4Cr0.6 |
| 47 | Ga0.45Cr0.45Pb0.1 | 97 | Ga0.4Cr0.4Cu0.2 | 147 | Ga0.5Cr0.4Fe0.1 | 197 | Ga0.6Cr0.4 |
| 48 | Ga0.45Cr0.45Hf20.1 | 98 | Ga0.4Cr0.4Cd0.2 | 148 | Ga0.5Cr0.4Co0.1 | 198 | Ga0.6Cr0.4 |
| 49 | Ga0.5Cr0.4Cu0.1 | 99 | Ga0.4Cr0.4Fe0.2 | 149 | Ga0.5Cr0.4Ni0.1 | 199 | Ga0.7Cr0.3 |
| 50 | Ga0.5Cr0.4Cd0.1 | 100 | Ga0.4Cr0.4Co0.2 | 150 | Ga0.5Cr0.4Zr0.1 | 200 | Ga0.7Cr0.3 |

## Occupancy of catalyst library 3G1L

| | | | | | | | |
|---|---|---|---|---|---|---|---|
| 1 | Cu(a)1.0 | 51 | Cu(a)0.1Zr0.4Sn0.5 | 101 | Cu(a)0.2Hf0.2Sn0.6 | 151 | Hf0.7Sn0.2Cu(b)0.1 |
| 2 | Cu(a)0.9Zr0.1 | 52 | Cu(a)0.1Zr0.3Sn0.6 | 102 | Cu(a)0.2Hf0.1Sn0.7 | 152 | Hf0.6Sn0.3Cu(b)0.1 |
| 3 | Cu(a)0.9Sn0.1 | 53 | Cu(a)0.1Zr0.2Sn0.7 | 103 | Cu(a)0.1Hf0.9 | 153 | Hf0.5Sn0.4Cu(b)0.1 |
| 4 | Cu(a)0.8Zr0.2 | 54 | Cu(a)0.1Zr0.1Sn0.8 | 104 | Cu(a)0.1Hf0.8Sn0.1 | 154 | Hf0.4Sn0.5Cu(b)0.1 |
| 5 | Cu(a)0.8Zr0.1Sn0.1 | 55 | Cu(a)0.1Sn0.9 | 105 | Cu(a)0.1Hf0.7Sn0.2 | 155 | Hf0.3Sn0.6Cu(b)0.1 |
| 6 | Cu(a)0.8Sn0.2 | 56 | Zr1.0 | 106 | Cu(a)0.1Hf0.6Sn0.3 | 156 | Hf0.2Sn0.7Cu(b)0.1 |
| 7 | Cu(a)0.7Zr0.3 | 57 | Zr0.9Sn0.1 | 107 | Cu(a)0.1Hf0.5Sn0.4 | 157 | Hf0.1Sn0.8Cu(b)0.1 |
| 8 | Cu(a)0.7Zr0.2Sn0.1 | 58 | Zr0.8Sn0.2 | 108 | Cu(a)0.1Hf0.4Sn0.5 | 158 | Hf0.7Cu(b)0.3 |
| 9 | Cu(a)0.7Zr0.1Sn0.2 | 59 | Zr0.7Sn0.3 | 109 | Cu(a)0.1Hf0.3Sn0.6 | 159 | Hf0.5Cu(b)0.5 |
| 10 | Cu(a)0.7Sn0.3 | 60 | Zr0.6Sn0.4 | 110 | Cu(a)0.1Hf0.2Sn0.7 | 160 | Hf0.3Cu(b)0.7 |
| 11 | Cu(a)0.6Zr0.4 | 61 | Zr0.5Sn0.5 | 111 | Cu(a)0.1Hf0.1Sn0.8 | 161 | Zr0.1Sn0.1Cu(b)0.8 |
| 12 | Cu(a)0.6Zr0.3Sn0.1 | 62 | Zr0.4Sn0.6 | 112 | Hf1.0 | 162 | Zr0.2Sn0.1Cu(b)0.7 |
| 13 | Cu(a)0.6Zr0.2Sn0.2 | 63 | Zr0.3Sn0.7 | 113 | Hf0.9Sn0.1 | 163 | Zr0.1Sn0.2Cu(b)0.7 |
| 14 | Cu(a)0.6Zr0.1Sn0.3 | 64 | Zr0.2Sn0.8 | 114 | Hf0.8Sn0.2 | 164 | Zr0.3Sn0.1Cu(b)0.6 |
| 15 | Cu(a)0.6Sn0.4 | 65 | Zr0.1Sn0.9 | 115 | Hf0.7Sn0.3 | 165 | Zr0.2Sn0.2Cu(b)0.6 |
| 16 | Cu(a)0.5Zr0.5 | 66 | Sn1.0 | 116 | Hf0.6Sn0.4 | 166 | Zr0.1Sn0.3Cu(b)0.6 |
| 17 | Cu(a)0.5Zr0.4Sn0.1 | 67 | Cu(a)0.9Hf0.1 | 117 | Hf0.5Sn0.5 | 167 | Zr0.4Sn0.1Cu(b)0.5 |
| 18 | Cu(a)0.5Zr0.3Sn0.2 | 68 | Cu(a)0.8Hf0.2 | 118 | Hf0.4Sn0.6 | 168 | Zr0.3Sn0.2Cu(b)0.5 |
| 19 | Cu(a)0.5Zr0.2Sn0.3 | 69 | Cu(a)0.8Hf0.1Sn0.1 | 119 | Hf0.3Sn0.7 | 169 | Zr0.2Sn0.3Cu(b)0.5 |
| 20 | Cu(a)0.5Zr0.1Sn0.4 | 70 | Cu(a)0.7Hf0.3 | 120 | Hf0.2Sn0.8 | 170 | Zr0.1Sn0.4Cu(b)0.5 |
| 21 | Cu(a)0.5Sn0.5 | 71 | Cu(a)0.7Hf0.2Sn0.1 | 121 | Hf0.1Sn0.9 | 171 | Zr0.5Sn0.1Cu(b)0.4 |
| 22 | Cu(a)0.4Zr0.6 | 72 | Cu(a)0.7Hf0.1Sn0.2 | 122 | Hf0.1Sn0.1Cu(b)0.8 | 172 | Zr0.4Sn0.2Cu(b)0.4 |
| 23 | Cu(a)0.4Zr0.5Sn0.1 | 73 | Cu(a)0.6Hf0.4 | 123 | Hf0.2Sn0.1Cu(b)0.7 | 173 | Zr0.3Sn0.3Cu(b)0.4 |
| 24 | Cu(a)0.4Zr0.4Sn0.2 | 74 | Cu(a)0.6Hf0.3Sn0.1 | 124 | Hf0.1Sn0.2Cu(b)0.7 | 174 | Zr0.2Sn0.4Cu(b)0.4 |
| 25 | Cu(a)0.4Zr0.3Sn0.3 | 75 | Cu(a)0.6Hf0.2Sn0.2 | 125 | Hf0.3Sn0.1Cu(b)0.6 | 175 | Zr0.1Sn0.5Cu(b)0.4 |
| 26 | Cu(a)0.4Zr0.2Sn0.4 | 76 | Cu(a)0.6Hf0.1Sn0.3 | 126 | Hf0.2Sn0.2Cu(b)0.6 | 176 | Zr0.6Sn0.1Cu(b)0.3 |
| 27 | Cu(a)0.4Zr0.1Sn0.5 | 77 | Cu(a)0.5Hf0.5 | 127 | Hf0.1Sn0.3Cu(b)0.6 | 177 | Zr0.5Sn0.2Cu(b)0.3 |
| 28 | Cu(a)0.4Sn0.6 | 78 | Cu(a)0.5Hf0.4Sn0.1 | 128 | Hf0.4Sn0.1Cu(b)0.5 | 178 | Zr0.4Sn0.3Cu(b)0.3 |
| 29 | Cu(a)0.3Zr0.7 | 79 | Cu(a)0.5Hf0.3Sn0.2 | 129 | Hf0.3Sn0.2Cu(b)0.5 | 179 | Zr0.3Sn0.4Cu(b)0.3 |
| 30 | Cu(a)0.3Zr0.6Sn0.1 | 80 | Cu(a)0.5Hf0.2Sn0.3 | 130 | Hf0.2Sn0.3Cu(b)0.5 | 180 | Zr0.2Sn0.5Cu(b)0.3 |
| 31 | Cu(a)0.3Zr0.5Sn0.2 | 81 | Cu(a)0.5Hf0.1Sn0.4 | 131 | Hf0.1Sn0.4Cu(b)0.5 | 181 | Zr0.1Sn0.6Cu(b)0.3 |
| 32 | Cu(a)0.3Zr0.4Sn0.3 | 82 | Cu(a)0.4Hf0.6 | 132 | Hf0.5Sn0.1Cu(b)0.4 | 182 | Zr0.7Sn0.1Cu(b)0.2 |
| 33 | Cu(a)0.3Zr0.3Sn0.4 | 83 | Cu(a)0.4Hf0.5Sn0.1 | 133 | Hf0.4Sn0.2Cu(b)0.4 | 183 | Zr0.6Sn0.2Cu(b)0.2 |
| 34 | Cu(a)0.3Zr0.2Sn0.5 | 84 | Cu(a)0.4Hf0.4Sn0.2 | 134 | Hf0.3Sn0.3Cu(b)0.4 | 184 | Zr0.5Sn0.3Cu(b)0.2 |
| 35 | Cu(a)0.3Zr0.1Sn0.6 | 85 | Cu(a)0.4Hf0.3Sn0.3 | 135 | Hf0.2Sn0.4Cu(b)0.4 | 185 | Zr0.4Sn0.4Cu(b)0.2 |
| 36 | Cu(a)0.3Sn0.7 | 86 | Cu(a)0.4Hf0.2Sn0.4 | 136 | Hf0.1Sn0.5Cu(b)0.4 | 186 | Zr0.3Sn0.5Cu(b)0.2 |
| 37 | Cu(a)0.2Zr0.8 | 87 | Cu(a)0.4Hf0.1Sn0.5 | 137 | Hf0.6Sn0.1Cu(b)0.3 | 187 | Zr0.2Sn0.6Cu(b)0.2 |
| 38 | Cu(a)0.2Zr0.7Sn0.1 | 88 | Cu(a)0.3Hf0.7 | 138 | Hf0.5Sn0.2Cu(b)0.3 | 188 | Zr0.1Sn0.7Cu(b)0.2 |
| 39 | Cu(a)0.2Zr0.6Sn0.2 | 89 | Cu(a)0.3Hf0.6Sn0.1 | 139 | Hf0.4Sn0.3Cu(b)0.3 | 189 | Zr0.8Sn0.1Cu(b)0.1 |
| 40 | Cu(a)0.2Zr0.5Sn0.3 | 90 | Cu(a)0.3Hf0.5Sn0.2 | 140 | Hf0.3Sn0.4Cu(b)0.3 | 190 | Zr0.7Sn0.2Cu(b)0.1 |
| 41 | Cu(a)0.2Zr0.4Sn0.4 | 91 | Cu(a)0.3Hf0.4Sn0.3 | 141 | Hf0.2Sn0.5Cu(b)0.3 | 191 | Zr0.6Sn0.3Cu(b)0.1 |
| 42 | Cu(a)0.2Zr0.3Sn0.5 | 92 | Cu(a)0.3Hf0.3Sn0.4 | 142 | Hf0.1Sn0.6Cu(b)0.3 | 192 | Zr0.5Sn0.4Cu(b)0.1 |
| 43 | Cu(a)0.2Zr0.2Sn0.6 | 93 | Cu(a)0.3Hf0.2Sn0.5 | 143 | Hf0.7Sn0.1Cu(b)0.2 | 193 | Zr0.4Sn0.5Cu(b)0.1 |
| 44 | Cu(a)0.2Zr0.1Sn0.7 | 94 | Cu(a)0.3Hf0.1Sn0.6 | 144 | Hf0.6Sn0.2Cu(b)0.2 | 194 | Zr0.3Sn0.6Cu(b)0.1 |
| 45 | Cu(a)0.2Sn0.8 | 95 | Cu(a)0.2Hf0.8 | 145 | Hf0.5Sn0.3Cu(b)0.2 | 195 | Zr0.2Sn0.7Cu(b)0.1 |
| 46 | Cu(a)0.1Zr0.9 | 96 | Cu(a)0.2Hf0.7Sn0.1 | 146 | Hf0.4Sn0.4Cu(b)0.2 | 196 | Zr0.1Sn0.8Cu(b)0.1 |
| 47 | Cu(a)0.1Zr0.8Sn0.1 | 97 | Cu(a)0.2Hf0.6Sn0.2 | 147 | Hf0.3Sn0.5Cu(b)0.2 | 197 | Zr0.7Cu(b)0.3 |
| 48 | Cu(a)0.1Zr0.7Sn0.2 | 98 | Cu(a)0.2Hf0.5Sn0.3 | 148 | Hf0.2Sn0.6Cu(b)0.2 | 198 | Zr0.5Cu(b)0.5 |
| 49 | Cu(a)0.1Zr0.6Sn0.3 | 99 | Cu(a)0.2Hf0.4Sn0.4 | 149 | Hf0.1Sn0.7Cu(b)0.2 | 199 | Zr0.3Cu(b)0.7 |
| 50 | Cu(a)0.1Zr0.5Sn0.4 | 100 | Cu(a)0.2Hf0.3Sn0.5 | 150 | Hf0.8Sn0.1Cu(b)0.1 | 200 | Cu(b)1.0 |

Occupancy of catalyst library 1G5L

| | | | | | | | |
|---|---|---|---|---|---|---|---|
| 1 | Mo0.96Sb0.04 | 26 | Mo0.96Co0.04 | 51 | Mo0.92Sb0.08 | 76 | Mo0.92Co0.08 |
| 2 | Mo0.96Sc0.04 | 27 | Mo0.96B0.04 | 52 | Mo0.92Sc0.08 | 77 | Mo0.92B0.08 |
| 3 | Mo0.96Li0.04 | 28 | Mo0.96Al0.04 | 53 | Mo0.92Li0.08 | 78 | Mo0.92Al0.08 |
| 4 | Mo0.96Lu0.04 | 29 | Mo0.96Ag0.04 | 54 | Mo0.92Lu0.08 | 79 | Mo0.92Ag0.08 |
| 5 | Mo0.96Mg0.04 | 30 | Mo0.96Ca0.04 | 55 | Mo0.92Mg0.08 | 80 | Mo0.92Ca0.08 |
| 6 | Mo0.96Mn0.04 | 31 | Mo0.96In0.04 | 56 | Mo0.92Mn0.08 | 81 | Mo0.92In0.08 |
| 7 | Mo0.96Ni0.04 | 32 | Mo0.96Zr0.04 | 57 | Mo0.92Ni0.08 | 82 | Mo0.92Zr0.08 |
| 8 | Mo0.96Pd0.04 | 33 | Mo0.96Y0.04 | 58 | Mo0.92Pd0.08 | 83 | Mo0.92Y0.08 |
| 9 | Mo0.96Na0.04 | 34 | Mo0.96Si0.04 | 59 | Mo0.92Na0.08 | 84 | Mo0.92Si0.08 |
| 10 | Mo0.96Sn0.04 | 35 | Mo0.96Sr0.04 | 60 | Mo0.92Sn0.08 | 85 | Mo0.92Sr0.08 |
| 11 | Mo0.96Cs0.04 | 36 | Mo0.96Te0.04 | 61 | Mo0.92Cs0.08 | 86 | Mo0.92Te0.08 |
| 12 | Mo0.96Rb0.04 | 37 | Mo0.96Sn0.04 | 62 | Mo0.92Rb0.08 | 87 | Mo0.92Sn0.08 |
| 13 | Mo0.96Re0.04 | 38 | Mo0.96Ho0.04 | 63 | Mo0.92Re0.08 | 88 | Mo0.92Ho0.08 |
| 14 | Mo0.96Rh0.04 | 39 | Mo0.96Ce0.04 | 64 | Mo0.92Rh0.08 | 89 | Mo0.92Ce0.08 |
| 15 | Mo0.96Cu0.04 | 40 | Mo0.96Cr0.04 | 65 | Mo0.92Cu0.08 | 90 | Mo0.92Cr0.08 |
| 16 | Mo0.96Dy0.04 | 41 | Mo0.96Zn0.04 | 66 | Mo0.92Dy0.08 | 91 | Mo0.92Zn0.08 |
| 17 | Mo0.96Er0.04 | 42 | Mo0.96Bi0.04 | 67 | Mo0.92Er0.08 | 92 | Mo0.92Bi0.08 |
| 18 | Mo0.96Eu0.04 | 43 | Mo0.96Mo0.04 | 68 | Mo0.92Eu0.08 | 93 | Mo0.92Mo0.08 |
| 19 | Mo0.96Ga0.04 | 44 | Mo0.96V0.04 | 69 | Mo0.92Ga0.08 | 94 | Mo0.92V0.08 |
| 20 | Mo0.96Hf0.04 | 45 | Mo0.96Ti0.04 | 70 | Mo0.92Hf0.08 | 95 | Mo0.92Ti0.08 |
| 21 | Mo0.96Au0.04 | 46 | Mo0.96Pd0.04 | 71 | Mo0.92Au0.08 | 96 | Mo0.92Pd0.08 |
| 22 | Mo0.96Ir0.04 | 47 | Mo0.96Nb0.04 | 72 | Mo0.92Ir0.08 | 97 | Mo0.92Nb0.08 |
| 23 | Mo0.96La0.04 | 48 | Mo0.96K0.04 | 73 | Mo0.92La0.08 | 98 | Mo0.92K0.08 |
| 24 | Mo0.96Ru0.04 | 49 | Mo0.96NaW0.04 | 74 | Mo0.92Ru0.08 | 99 | Mo0.92NaW0.08 |
| 25 | Mo0.96Fe0.04 | 50 | Mo0.96Ba0.04 | 75 | Mo0.92Fe0.08 | 100 | Mo0.92Ba0.08 |

Occupancy of catalyst library 2G6L

| | | | | | | | |
|---|---|---|---|---|---|---|---|
| 1 | Mo0.94Sn0.4Sb0.2 | 26 | Mo0.94Sn0.4Co0.2 | 51 | Mo0.94Ru0.4Sb0.2 | 76 | Mo0.94Ru0.4Co0.2 |
| 2 | Mo0.94Sn0.4Sc0.2 | 27 | Mo0.94Sn0.4B0.2 | 52 | Mo0.94Ru0.4Sc0.2 | 77 | Mo0.94Ru0.4B0.2 |
| 3 | Mo0.94Sn0.4Li0.2 | 28 | Mo0.94Sn0.4Al0.2 | 53 | Mo0.94Ru0.4Li0.2 | 78 | Mo0.94Ru0.4Al0.2 |
| 4 | Mo0.94Sn0.4Lu0.2 | 29 | Mo0.94Sn0.4Ag0.2 | 54 | Mo0.94Ru0.4Lu0.2 | 79 | Mo0.94Ru0.4Ag0.2 |
| 5 | Mo0.94Sn0.4Mg0.2 | 30 | Mo0.94Sn0.4Ca0.2 | 55 | Mo0.94Ru0.4Mg0.2 | 80 | Mo0.94Ru0.4Ca0.2 |
| 6 | Mo0.94Sn0.4Mn0.2 | 31 | Mo0.94Sn0.4In0.2 | 56 | Mo0.94Ru0.4Mn0.2 | 81 | Mo0.94Ru0.4In0.2 |
| 7 | Mo0.94Sn0.4Ni0.2 | 32 | Mo0.94Sn0.4Zr0.2 | 57 | Mo0.94Ru0.4Ni0.2 | 82 | Mo0.94Ru0.4Zr0.2 |
| 8 | Mo0.94Sn0.4Pd0.2 | 33 | Mo0.94Sn0.4Y0.2 | 58 | Mo0.94Ru0.4Pd0.2 | 83 | Mo0.94Ru0.4Y0.2 |
| 9 | Mo0.94Sn0.4Na0.2 | 34 | Mo0.94Sn0.4Si0.2 | 59 | Mo0.94Ru0.4Na0.2 | 84 | Mo0.94Ru0.4Si0.2 |
| 10 | Mo0.94Sn0.4Sn0.2 | 35 | Mo0.94Sn0.4Sr0.2 | 60 | Mo0.94Ru0.4Sn0.2 | 85 | Mo0.94Ru0.4Sr0.2 |
| 11 | Mo0.94Sn0.4Cs0.2 | 36 | Mo0.94Sn0.4Te0.2 | 61 | Mo0.94Ru0.4Cs0.2 | 86 | Mo0.94Ru0.4Te0.2 |
| 12 | Mo0.94Sn0.4Rb0.2 | 37 | Mo0.94Sn0.4Sn0.2 | 62 | Mo0.94Ru0.4Rb0.2 | 87 | Mo0.94Ru0.4Sn0.2 |
| 13 | Mo0.94Sn0.4Re0.2 | 38 | Mo0.94Sn0.4Ho0.2 | 63 | Mo0.94Ru0.4Re0.2 | 88 | Mo0.94Ru0.4Ho0.2 |
| 14 | Mo0.94Sn0.4Rh0.2 | 39 | Mo0.94Sn0.4Ce0.2 | 64 | Mo0.94Ru0.4Rh0.2 | 89 | Mo0.94Ru0.4Ce0.2 |
| 15 | Mo0.94Sn0.4Cu0.2 | 40 | Mo0.94Sn0.4Cr0.2 | 65 | Mo0.94Ru0.4Cu0.2 | 90 | Mo0.94Ru0.4Cr0.2 |
| 16 | Mo0.94Sn0.4Dy0.2 | 41 | Mo0.94Sn0.4Zn0.2 | 66 | Mo0.94Ru0.4Dy0.2 | 91 | Mo0.94Ru0.4Zn0.2 |
| 17 | Mo0.94Sn0.4Er0.2 | 42 | Mo0.94Sn0.4Bi0.2 | 67 | Mo0.94Ru0.4Er0.2 | 92 | Mo0.94Ru0.4Bi0.2 |
| 18 | Mo0.94Sn0.4Eu0.2 | 43 | Mo0.94Sn0.4Mo0.2 | 68 | Mo0.94Ru0.4Eu0.2 | 93 | Mo0.94Ru0.4Mo0.2 |
| 19 | Mo0.94Sn0.4Ga0.2 | 44 | Mo0.94Sn0.4V0.2 | 69 | Mo0.94Ru0.4Ga0.2 | 94 | Mo0.94Ru0.4V0.2 |
| 20 | Mo0.94Sn0.4Hf0.2 | 45 | Mo0.94Sn0.4Ti0.2 | 70 | Mo0.94Ru0.4Hf0.2 | 95 | Mo0.94Ru0.4Ti0.2 |
| 21 | Mo0.94Sn0.4Au0.2 | 46 | Mo0.94Sn0.4Pd0.2 | 71 | Mo0.94Ru0.4Au0.2 | 96 | Mo0.94Ru0.4Pd0.2 |
| 22 | Mo0.94Sn0.4Ir0.2 | 47 | Mo0.94Sn0.4Nb0.2 | 72 | Mo0.94Ru0.4Ir0.2 | 97 | Mo0.94Ru0.4Nb0.2 |
| 23 | Mo0.94Sn0.4La0.2 | 48 | Mo0.94Sn0.4K0.2 | 73 | Mo0.94Ru0.4La0.2 | 98 | Mo0.94Ru0.4K0.2 |
| 24 | Mo0.94Sn0.4Ru0.2 | 49 | Mo0.94Sn0.4NaW0.2 | 74 | Mo0.94Ru0.4Ru0.2 | 99 | Mo0.94Ru0.4NaW0.2 |
| 25 | Mo0.94Sn0.4Fe0.2 | 50 | Mo0.94Sn0.4Ba0.2 | 75 | Mo0.94Ru0.4Fe0.2 | 100 | Mo0.94Ru0.4Ba0.2 |

Occupancy of catalyst T01

| | | | |
|---|---|---|---|
| 1 | Cu0.8Mn0.1Ag0.1 | 26 | Cu0.2Mn0.3Ag0.5 |
| 2 | Cu0.7Mn0.2Ag0.1 | 27 | Cu0.2Mn0.2Ag0.6 |
| 3 | Cu0.7Mn0.1Ag0.2 | 28 | Cu0.2Mn0.1Ag0.7 |
| 4 | Cu0.6Mn0.3Ag0.1 | 29 | Cu0.1Mn0.8Ag0.1 |
| 5 | Cu0.6Mn0.2Ag0.2 | 30 | Cu0.1Mn0.7Ag0.2 |
| 6 | Cu0.6Mn0.1Ag0.3 | 31 | Cu0.1Mn0.6Ag0.3 |
| 7 | Cu0.5Mn0.4Ag0.1 | 32 | Cu0.1Mn0.5Ag0.4 |
| 8 | Cu0.5Mn0.3Ag0.2 | 33 | Cu0.1Mn0.4Ag0.5 |
| 9 | Cu0.5Mn0.2Ag0.3 | 34 | Cu0.1Mn0.3Ag0.6 |
| 10 | Cu0.5Mn0.1Ag0.4 | 35 | Cu0.1Mn0.2Ag0.7 |
| 11 | Cu0.4Mn0.5Ag0.1 | 36 | Cu0.1Mn0.1Ag0.8 |
| 12 | Cu0.4Mn0.4Ag0.2 | 37 | Cu0.2Mn0.8 |
| 13 | Cu0.4Mn0.3Ag0.3 | 38 | Cu0.4Mn0.6 |
| 14 | Cu0.4Mn0.2Ag0.4 | 39 | Cu0.6Mn0.4 |
| 15 | Cu0.4Mn0.1Ag0.5 | 40 | Cu0.8Mn0.2 |
| 16 | Cu0.3Mn0.6Ag0.1 | 41 | Mn0.2Ag0.8 |
| 17 | Cu0.3Mn0.5Ag0.2 | 42 | Mn0.4Ag0.6 |
| 18 | Cu0.3Mn0.4Ag0.3 | 43 | Mn0.6Ag0.4 |
| 19 | Cu0.3Mn0.3Ag0.4 | 44 | Mn0.8Ag0.2 |
| 20 | Cu0.3Mn0.2Ag0.5 | 45 | Cu0.2Ag0.8 |
| 21 | Cu0.3Mn0.1Ag0.6 | 46 | Cu0.4Ag0.6 |
| 22 | Cu0.2Mn0.7Ag0.1 | 47 | Cu0.6Ag0.4 |
| 23 | Cu0.2Mn0.6Ag0.2 | 48 | Cu0.8Ag0.2 |
| 24 | Cu0.2Mn0.5Ag0.3 | 49 | Cu1.0 |
| 25 | Cu0.2Mn0.4Ag0.4 | 50 | Mn1.0 |

Occupancy of catalyst T02

| | | | |
|---|---|---|---|
| 1 | Cu0.8Mn0.1Ag0.1 | 26 | Cu0.2Mn0.3Ag0.5 |
| 2 | Cu0.7Mn0.2Ag0.1 | 27 | Cu0.2Mn0.2Ag0.6 |
| 3 | Cu0.7Mn0.1Ag0.2 | 28 | Cu0.2Mn0.1Ag0.7 |
| 4 | Cu0.6Mn0.3Ag0.1 | 29 | Cu0.1Mn0.8Ag0.1 |
| 5 | Cu0.6Mn0.2Ag0.2 | 30 | Cu0.1Mn0.7Ag0.2 |
| 6 | Cu0.6Mn0.1Ag0.3 | 31 | Cu0.1Mn0.6Ag0.3 |
| 7 | Cu0.5Mn0.4Ag0.1 | 32 | Cu0.1Mn0.5Ag0.4 |
| 8 | Cu0.5Mn0.3Ag0.2 | 33 | Cu0.1Mn0.4Ag0.5 |
| 9 | Cu0.5Mn0.2Ag0.3 | 34 | Cu0.1Mn0.3Ag0.6 |
| 10 | Cu0.5Mn0.1Ag0.4 | 35 | Cu0.1Mn0.2Ag0.7 |
| 11 | Cu0.4Mn0.5Ag0.1 | 36 | Cu0.1Mn0.1Ag0.8 |
| 12 | Cu0.4Mn0.4Ag0.2 | 37 | Cu0.2Mn0.8 |
| 13 | Cu0.4Mn0.3Ag0.3 | 38 | Cu0.4Mn0.6 |
| 14 | Cu0.4Mn0.2Ag0.4 | 39 | Cu0.6Mn0.4 |
| 15 | Cu0.4Mn0.1Ag0.5 | 40 | Cu0.8Mn0.2 |
| 16 | Cu0.3Mn0.6Ag0.1 | 41 | Mn0.2Ag0.8 |
| 17 | Cu0.3Mn0.5Ag0.2 | 42 | Mn0.4Ag0.6 |
| 18 | Cu0.3Mn0.4Ag0.3 | 43 | Mn0.6Ag0.4 |
| 19 | Cu0.3Mn0.3Ag0.4 | 44 | Mn0.8Ag0.2 |
| 20 | Cu0.3Mn0.2Ag0.5 | 45 | Cu0.2Ag0.8 |
| 21 | Cu0.3Mn0.1Ag0.6 | 46 | Cu0.4Ag0.6 |
| 22 | Cu0.2Mn0.7Ag0.1 | 47 | Cu0.6Ag0.4 |
| 23 | Cu0.2Mn0.6Ag0.2 | 48 | Cu0.8Ag0.2 |
| 24 | Cu0.2Mn0.5Ag0.3 | 49 | Cu1.0 |
| 25 | Cu0.2Mn0.4Ag0.4 | 50 | Mn1.0 |
| | | 51 | Ag1.0 |

Occupancy of catalyst T03

| | | | |
|---|---|---|---|
| 1 | Ga0.275Cu0.7Pd0.025 | 26 | Ga0.45Cu0.5Pd0.05 |
| 2 | Ga0.25Cu0.7Pd0.05 | 27 | Ga0.425Cu0.5Pd0.075 |
| 3 | Ga0.225Cu0.7Pd0.075 | 28 | Ga0.4Cu0.5Pd0.1 |
| 4 | Ga0.2Cu0.7Pd0.1 | 29 | Ga0.375Cu0.5Pd0.125 |
| 5 | Ga0.175Cu0.7Pd0.125 | 30 | Ga0.35Cu0.5Pd0.15 |
| 6 | Ga0.15Cu0.7Pd0.15 | 31 | Ga0.325Cu0.5Pd0.175 |
| 7 | Ga0.125Cu0.7Pd0.175 | 32 | Ga0.3Cu0.5Pd0.2 |
| 8 | Ga0.1Cu0.7Pd0.2 | 33 | Ga0.275Cu0.5Pd0.225 |
| 9 | Ga0.075Cu0.7Pd0.225 | 34 | Ga0.25Cu0.5Pd0.25 |
| 10 | Ga0.05Cu0.7Pd0.25 | 35 | Ga0.225Cu0.5Pd0.275 |
| 11 | Ga0.025Cu0.7Pd0.275 | 36 | Ga0.2Cu0.5Pd0.3 |
| 12 | Cu0.7Pd0.3 | 37 | Ga0.575Cu0.4Pd0.025 |
| 13 | Ga0.375Cu0.6Pd0.025 | 38 | Ga0.55Cu0.4Pd0.05 |
| 14 | Ga0.35Cu0.6Pd0.05 | 39 | Ga0.525Cu0.4Pd0.075 |
| 15 | Ga0.325Cu0.6Pd0.075 | 40 | Ga0.5Cu0.4Pd0.1 |
| 16 | Ga0.3Cu0.6Pd0.1 | 41 | Ga0.475Cu0.4Pd0.125 |
| 17 | Ga0.275Cu0.6Pd0.125 | 42 | Ga0.45Cu0.4Pd0.15 |
| 18 | Ga0.25Cu0.6Pd0.15 | 43 | Ga0.425Cu0.4Pd0.175 |
| 19 | Ga0.225Cu0.6Pd0.175 | 44 | Ga0.4Cu0.4Pd0.2 |
| 20 | Ga0.2Cu0.6Pd0.2 | 45 | Ga0.375Cu0.4Pd0.225 |
| 21 | Ga0.175Cu0.6Pd0.225 | 46 | Ga0.35Cu0.4Pd0.25 |
| 22 | Ga0.15Cu0.6Pd0.25 | 47 | Ga0.325Cu0.4Pd0.275 |
| 23 | Ga0.125Cu0.6Pd0.275 | 48 | Ga0.3Cu0.4Pd0.3 |
| 24 | Ga0.1Cu0.6Pd0.3 | 49 | Ga0.4Cu0.3Pd0.3 |
| 25 | Ga0.475Cu0.5Pd0.025 | 50 | Ga0.3Cu0.3Pd0.4 |

# C Used chemicals for libraries

| Num | Label | El. | Connection | Company | ID-Nr. |
|---|---|---|---|---|---|
| 1 | $AgNO_3M$ | Ag | $NO_3$ | ABCR | 1571 |
| 2 | $AlNO_3M$ | Al | $NO_3$ | Alfa | 100 |
| 3 | AuBrM | Au | Br | | 1997 |
| 4 | BAcidM | B | Acid | Fluka | 191 |
| 5 | BaClM | Ba | Cl | | 144 |
| 6 | Bi2EthylhexanoatM | Bi | 2Ethylhexanoat | Strem | 1409 |
| 7 | $CaNO_3M$ | Ca | $NO_3$ | Merck | 212 |
| 8 | $CeNO_3M$ | Ce | $NO_3$ | Fluka | 1953 |
| 9 | $CoNO_3M$ | Co | $NO_3$ | Fluka | 898 |
| 10 | $CrNO_3M$ | Cr | $NO_3$ | Aldrich | 900 |
| 11 | CsClM | Cs | Cl | unb. | 219 |
| 12 | $CuNO_3M$ | Cu | $NO_3$ | Fluka | 869 |
| 13 | $DyNO_3M$ | Dy | $NO_3$ | Aldrich | 286 |
| 14 | $ErNO_3M$ | Er | $NO_3$ | Aldrich | 1537 |
| 15 | $EuNO_3M$ | Eu | $NO_3$ | STREM | 1536 |
| 16 | $FeNO_3M$ | Fe | $NO_3$ | k.A. | 1221 |
| 17 | $GaNO_3M$ | Ga | $NO_3$ | Aldrich | 1031 |
| 18 | GeO*i*PrM | Ge | O*i*Pr | Aldrich | 915 |
| 19 | HfClM | Hf | Cl | Aldrich | 1634 |
| 20 | $HoNO_3M$ | Ho | $NO_3$ | STREM | 1395 |
| 21 | $InNO_3M$ | In | $NO_3$ | Aldrich | 1621 |
| 22 | IrClM | Ir | Cl | Aldrich | 374 |
| 23 | $KNO_3M$ | K | $NO_3$ | | 394 |
| 24 | $LaNO_3M$ | La | $NO_3$ | Fluka | 424 |
| 25 | $LiNO_3M$ | Li | $NO_3$ | Fluka | 440 |
| 26 | $LuNO_3M$ | Lu | $NO_3$ | Aldrich | 1538 |
| 27 | $MgNO_3M$ | Mg | $NO_3$ | Merck | 1034 |
| 28 | $MnNO_3M$ | Mn | $NO_3$ | Merck | 464 |
| 29 | MoO*i*PrI | Mo | O*i*Pr | AlfaAesar | 498 |
| 30 | $NaNO_3M$ | Na | $NO_3$ | Merck | 531 |
| 31 | NbOEtM | Nb | OEt | | 1038 |
| 32 | $NiNO_3M$ | Ni | $NO_3$ | Aldrich | 559 |
| 33 | $PbClO_4M$ | Pb | ClO4 | | 182 |
| 34 | PdOAcM | Pd | OAc | | 579 |
| 35 | $PrNO_3M$ | Pr | $NO_3$ | k.A. | 639 |
| 36 | PtBrM | Pt | Br | | 1234 |
| 37 | RbacacM | Rb | acac | Aldrich | 1033 |
| 38 | ReClM | Re | Cl | Aldrich | 1161 |
| 39 | RhClM | Rh | Cl | Aldrich | 1223 |
| 40 | RuClM | Ru | Cl | Aldrich | 681 |
| 41 | SbClM | Sb | Cl | J.T.Baker | 128 |
| 42 | $ScNO_3M$ | Sc | $NO_3$ | ABCR | 1664 |
| 43 | $SiNO_3M$ | Si | $NO_3$ | | 1876 |
| 44 | $SmNO_3M$ | Sm | $NO_3$ | Riedel | 1747 |
| 45 | SnClM | Sn | Cl | Aldrich | 841 |
| 46 | SrClM | Sr | Cl | Merck | 1880 |
| 47 | TaOEtM | Ta | OEt | ABCR | 1617 |
| 48 | TeacidM | Te | Acid | Fluka | 1601 |
| 49 | TiO*i*PrM | Ti | O*i*Pr | Lancaster | 1898 |
| 50 | VOO*i*Pr3M | V | $OO*i*Pr_3$ | ABCR | 1492 |
| 51 | WClM | W | Cl | Fluka | 1688 |
| 52 | $YNO_3M$ | Y | $NO_3$ | ABCR | 905 |
| 53 | ZnOAcM | Zn | OAc | Fluka | 836 |
| 54 | $ZrONO_3M$ | Zr | $ONO_3$ | Johnson | 860 |

# D Sketch of splitting module in the 10-fold parallel reactor

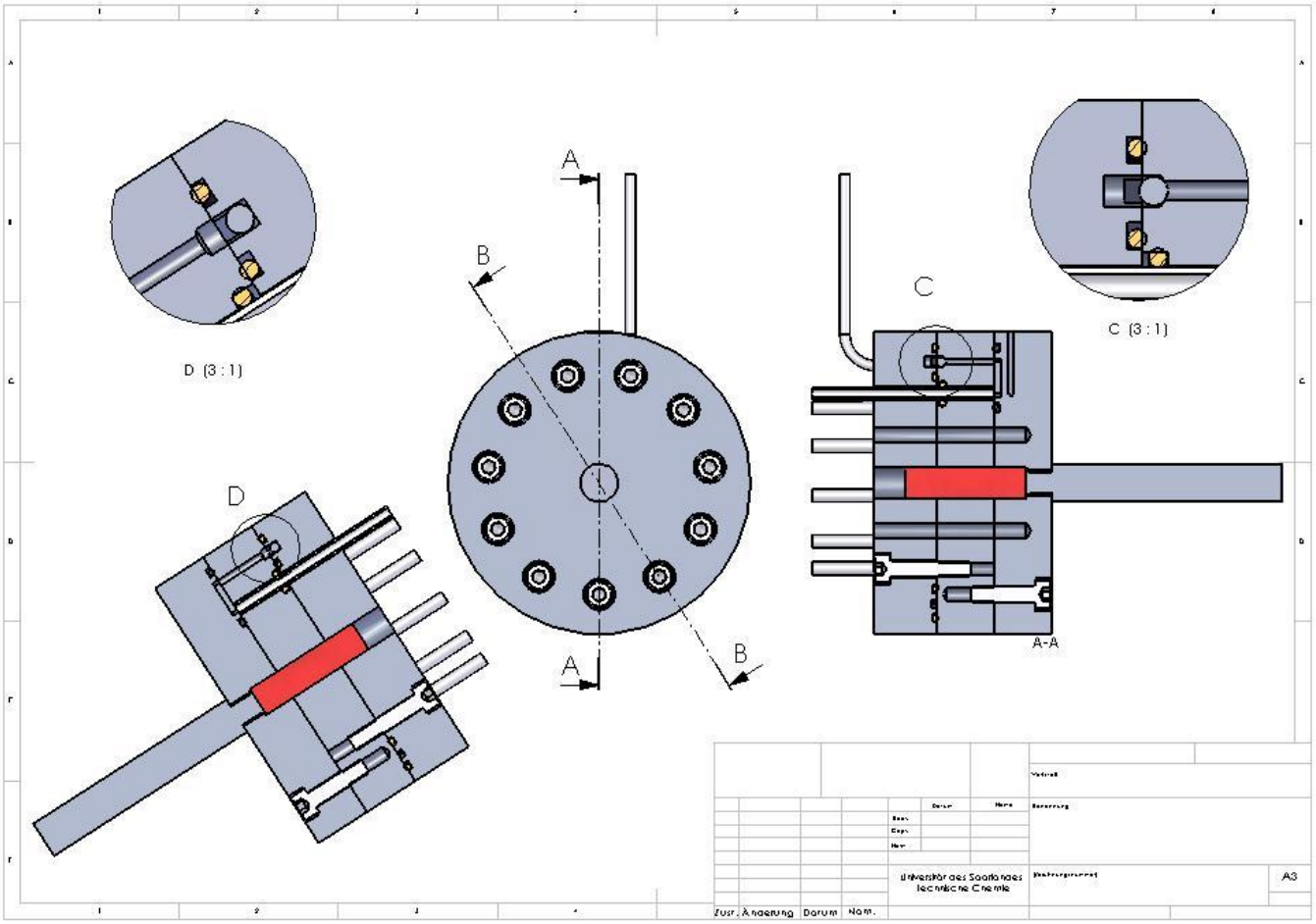

# E Ignition

## 1) Ignition temperature and ratio of propene

Ignition temperature: 458 °C

Lower explosive limit: 2% at 20 °C

Upper explosive limit: 11.1% at 20 °C

Reference: www.engineeringtoolbox.com

## 2) Temperature dependence of ignition limits

$Z_u(t) = Z_{u,20°C} \cdot (1 - c \cdot (t - 20°C))$ $Z_u$ : Lower explosive limit

$Z_o(t) = Z_{o,20°C} \cdot (1 + c \cdot (t - 20°C))$ $Z_o$ : Upper explosive limit

c = 0.000721 for many hydrocarbons for $H_2$ (and other fuels), c can differ

Note: Range of ignitable mixture increases for higher temperature

Reference: combustion lecture slide

by Dr. F. Dinkelacker and Prof. A.Leipertz in Erlangnen-Nuernberg

| Temperature (°C) | Lower Explosive | Upper Explosive |
|---|---|---|
| 20 | 2 | 11.1 |
| 50 | 1.95674 | 11.34009 |
| 100 | 1.88464 | 11.74025 |
| 150 | 1.81254 | 12.1404 |
| 200 | 1.74044 | 12.54056 |
| 250 | 1.66834 | 12.94071 |
| 300 | 1.59624 | 13.34087 |
| 350 | 1.52414 | 13.74102 |
| 400 | 1.45204 | 14.14118 |
| 450 | 1.37994 | 14.54133 |
| 500 | 1.30784 | 14.94149 |
| 550 | 1.23574 | 15.34164 |
| 600 | 1.16364 | 15.7418 |

## 3) Ignition temperature and flammable limit of Chemicals

| Fuel or Chemical | Temperature | | Fuel or Chemical | "Lower Explosive or Flammable Limit" | "Upper Explosive or Flammable Limit" |
|---|---|---|---|---|---|
| | (°C) | (°F) | | (LEL/LFL)% | (UEL/UFL)% |
| Acetaldehyde | 175 | 347 | Acetaldehyde | 4 | 60 |
| Acetone | 465 | 869 | Acetone | 2.6 | 12.8 |
| Acetylene | 305 | 581 | Acetylene | 2.2 | 85 |
| Benzene | 560 | 1040 | Benzene | 1.3 | 7.1 |
| Butane | 420 | 788 | Butane | 1.8 | 8.4 |
| Carbon monoxide | 609 | 1128 | Carbon Monoxide | 12 | 75 |
| Cyclohexane | 245 | 473 | Cyclohexane | 1.3 | 8 |
| Diethyl ether | 160 | 320 | Diethyl Ether | 1.9 | 36 |
| Ethane | 515 | 859 | Ethane | 3 | 12.4 |
| Ethylene | 490 | 914 | Ethylene | 2.7 | 36 |
| Ehtyl Alcohol | 365 | 689 | Ethyl Alcohol | 3.3 | 19 |
| Fuel Oil No.1 | 210 | 410 | Fuel Oil No.1 | 0.7 | 5 |
| Hydrogen | 500 | 932 | Hydrogen | 4 | 75 |
| Isobutane | 462 | 864 | Isobutane | 1.8 | 9.6 |
| Isobutene | 465 | 869 | Isobutene | 1.8 | 9 |
| Isooctane | 447 | 837 | Isooctane | 0.79 | 5.94 |
| Isopentane | 420 | 788 | Isopentane | 1.32 | 9.16 |
| Isopropyl Alcohol | 399 | 750 | Isopropyl Alcohol | 2 | 12 |
| Methane (Natural Gas) | 580 | 1076 | Methane | 5 | 15 |
| Methyl Alcohol | 385 | 725 | Methyl Alcohol | 6.7 | 36 |
| Naphtha | 550 | 1022 | Naphthalene | 0.9 | 5.9 |
| n-Heptane | 215 | 419 | n-Heptane | 1.05 | 6.7 |
| n-Hexane | 225 | 437 | n-Hexane | 1.1 | 7.5 |
| n-Pentane | 260 | 500 | Pentane | 1.5 | 7.8 |
| Propane | 480 | 842 | Propane | 2.1 | 10.1 |
| Propylene | 458 | 856 | Propylene | 2 | 11.1 |
| Toluene | 530 | 849 | Toluene | 1.2 | 7.1 |
| Xylene | 463 | 867 | p-Xylene | 1.1 | 7 |

# F List of products

| Name | Another name | Structure | Formula | Mw[g/mol] |
|---|---|---|---|---|
| Propylene | Propene |  | $C_3H_6$ | 42.08064 |
| 1,5-Hexadien | 1,5-Hexadiene<br>Biallyl<br>Diallyl | 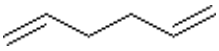 | $C_6H_{10}$ | 82.1454 |
| Propylenoxid | 1,2-Epoxipropan<br>Methyloxiran<br>Propylenether | 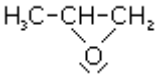 | $C_3H_6O$ | 58.08004 |
| Propionaldehyd | Propanal<br>Propionaldehyde<br>Methylacetaldehyde<br>Propionic aldehyde | 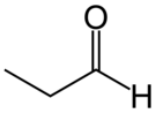 | $C_3H_6O$ | 58.08004 |
| Aceton | Propanone<br>β-ketopropane<br>Dimethyl ketone | 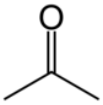 | $CH_3COCH_3$ | 58.08004 |
| Acrolein | 2-Propenal<br>Acraldehyde<br>Acrylic Aldehyde<br>Allyl Aldehyde | 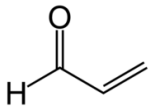 | $C_3H_4O$ | 56.06416 |
| Benzol | Benzene | 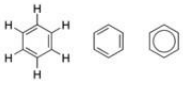 | $C_6H_6$ | 78.11364 |
| Allylalkohol | 2-Propen-1-ol<br>2-Propenol | 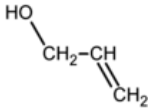 | $C_3H_6O$ | 58.08004 |
| 1,3-butadiene | Buta-1,3-diene<br>Biethylene<br>Erythrene<br>Divinyl | 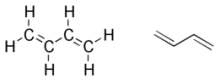 | C4H6 | 54.09164 |
| THF | Tetrahydrofuran THF<br>Hydrofuran<br>oxolane |  | $C_4H_8O$ | 72.10692 |
| Water | | | $H_2O$ | 18.01528 |
| carbon dioxide | | | $CO_2$ | 44.0098 |
| Hydrogen | | | $H_2$ | 2.01588 |

# G Source codes

Matlab source code for the visualization with conversion vs selectivity

```
%%%%%%%%%%%%%%%%%%%%%%%%%%%%%%%%%%%%%%%%%%%%%%%%%%%%%%%%%%%%%%%%%%%%%%%%%%%%%%%%
% Main file for Conversion vs Selectivity
% File=visualstart.m
% Chemical Engineer, Woongsik Su in 2009
% Saarbrücken Univeristy
%%%%%%%%%%%%%%%%%%%%%%%%%%%%%%%%%%%%%%%%%%%%%%%%%%%%%%%%%%%%%%%%%%%%%%%%%%%%%%%%

close all;clear all
warning off MATLAB:griddata:DuplicateDataPoints

[get,path]=uigetfile('.txt');
A=load(get);
v=A(:,5);


figure
hold on
labnum=A(:,1)
x=A(:,2)/max(A(:,2));
y=A(:,3);
scatter(x,y,8,colorchange(A(:,5)),'filled')
grid off
axis on
text(0.8,-0.08,'Conversion','Fontsize',10);
text(-0.08,0.6,'Selectivity','Fontsize',10,'Rotation',90);
text(x+0.0008,y+0.0008,int2str(labnum),'FontSize',8);
set(1,'color','white');

rectangle('Position',[0.89,0.79,0.1,0.208])
scatter(0.91,0.99,15,[0 1 0],'filled');
text(0.92,0.99,'150° C','FontSize',8);
scatter(0.91,0.95,15,[0 0 0],'filled');
text(0.92,0.95,'200° C','FontSize',8);
scatter(0.91,0.91,15,[0 0 1],'filled');
text(0.92,0.91,'250° C','FontSize',8);
```

## Matlab source code for visualization in ternary composition

```
%%%%%%%%%%%%%%%%%%%%%%%%%%%%%%%%%%%%%%%%%%%%%%%%%%%%%%%%%%%%%%%%%%%%%%%%%%%%%%%%
% Main file for visualization in ternary composition
% File=terstart.m
% original source from Uli Theune, Geophysics, University of Alberta
% Source has been modified by Su Woongsik in 2008
% To visualize the ternary composition
% Chemical Engineer, Woongsik Su in 2009
% Saarbrücken Univeristy
%%%%%%%%%%%%%%%%%%%%%%%%%%%%%%%%%%%%%%%%%%%%%%%%%%%%%%%%%%%%%%%%%%%%%%%%%%%%%%%%

close all;clear all
warning off MATLAB:griddata:DuplicateDataPoints
%load data
[get,path]=uigetfile('.txt');
A=load(get);
el1='Cr'
el2='Mo'
el3='Ni'


l=length(A);
v=A(:,4);

figure;
colormap(jet)
[hg,htick,hcb]=tersurf(A(:,1),A(:,2),A(:,3),v);
hlabels=terlabel(el1,el2,el3);

set(hg(:,3),'color','m')
set(hg(:,2),'color','c')
set(hg(:,1),'color','y')

set(hlabels,'fontsize',12)
set(hlabels(3),'color','m')
set(hlabels(2),'color','c')
set(hlabels(1),'color','y')
set(htick(:,1),'color','y','linewidth',3)
set(htick(:,2),'color','c','linewidth',3)
set(htick(:,3),'color','m','linewidth',3)

set(hcb,'xcolor','w','ycolor','w')
set(gcf,'color',[0 0 0.3])
set(gcf,'paperpositionmode','auto','inverthardcopy','off')
```

```
function [hg,htick,hcb]=tersurf(c1,c2,c3,d)
%%%%%%%%%%%%%%%%%%%%%%%%%%%%%%%%%%%%%%%%%%%%%%%%%%%%%%%%%%%%%%%%%%%%%%%%%%%%%%%
%FUNCTION [HG,HTICK,HCB]=TERSURF(C1,C2,C3,D) plots the values in the vector d
% The three vectors c1,c2,c3 define the position of a data value within the
% Uli Theune, Geophysics, University of Alberta
% 2002 - ...
%%%%%%%%%%%%%%%%%%%%%%%%%%%%%%%%%%%%%%%%%%%%%%%%%%%%%%%%%%%%%%%%%%%%%%%%%%%%%%%

if nargin < 4
    error('Error: Not enough input arguments.');
    return
end
if (length(c1)+length(c2)+length(c3))/length(c1) ~=3
    error('Error: all arrays must be of equal length.');
    return
end

% Check if the data need to be normalized
if max(c1+c2+c3)>1
    for i=1:length(c1)
        c1(i)=c1(i)/(c1(i)+c2(i)+c3(i));
        c2(i)=c2(i)/(c1(i)+c2(i)+c3(i));
        c3(i)=c3(i)/(c1(i)+c2(i)+c3(i));
    end
end

hold on
% Calculate the position of the data points in the ternary diagram
x=0.5-c1*cos(pi/3)+c2/2;
y=0.866-c1*sin(pi/3)-c2*cot(pi/6)/2;

% Create short vectors for the griding
tri=delaunay(x,y);
trisurf(tri,x,y,d);
shading interp

% Add the axis system now
d1=cos(pi/3);
d2=sin(pi/3);
l=linspace(0,1,6);
zmax=max(d);
for i=2:length(l)-1
   hg(i-1,3)=plot3([l(i)*d1 1-l(i)*d1],[l(i)*d2 l(i)*d2],[zmax zmax]*1.1,':k','linewidth',0.25);
   hg(i-1,1)=plot3([l(i) l(i)+(1-l(i))*d1],[0 (1-l(i))*d2],[zmax zmax]*1.1,':k','linewidth',0.25);
   hg(i-1,2)=plot3([(1-l(i))*d1 1-l(i)],[(1-l(i))*d2 0],[zmax zmax]*1.1,':k','linewidth',0.25);
end
plot([0 1 0.5 0],[0 0 sqrt(3)/2 0],'k','linewidth',1)
% Make x-tick labels
for i=1:length(l)
    htick(i,1)=text(l(i),-0.025,num2str(l(i)));
    htick(i,3)=text(1-l(i)*cos(pi/3)+0.025,l(i)*sin(pi/3)+0.025,num2str(l(i)));
    htick(i,2)=text(0.5-l(i)*cos(pi/3)-0.06,sin(pi/3)*(1-l(i)),num2str(l(i)));
end
hold off
axis image
axis off
caxis([min(d) max(d)])
view(2)
hcb=colorbar;
```

## Matlab source code for visualization of library in the results of SRR

```
%%%%%%%%%%%%%%%%%%%%%%%%%%%%%%%%%%%%%%%%%%%%%%%%%%%%%%%%%%%%%%%%%%%%%%%%%%%%
% file name = circle_test.m
% for visulalization of library in the results of SRR
% Chemical Engineer, Woongsik Su in 2009
% Saarbrücken Univeristy
%%%%%%%%%%%%%%%%%%%%%%%%%%%%%%%%%%%%%%%%%%%%%%%%%%%%%%%%%%%%%%%%%%%%%%%%%%%%

%%%%%%%%%%%%%%%
% import data %
%%%%%%%%%%%%%%%
center=[17 16]; %%%%%%%% Center of the circle
r=19; %%%%%%%% Radius of the circle
N=300; %%%%%%%% Number of dividing
theta=linspace(0,2*pi,N); %%%%%%%% Angle of the circle(Radian)
x=r*cos(theta)+center(1); %%%%%%%% x coordinate
y=r*sin(theta)+center(2); %%%%%%%% y coordinate
hold on;
plot(x,y,'black'); %%%%%%%% Plot the circle

%load data
[get,path]=uigetfile('.txt');
Datenmatrix=load(get);

B=[22  20  18  16  14  12  10  23  21  19  17  15  13  11
   9   26  24  22  20  18  16  14  12  10  8   6   27
   25  23  21  19  17  15  13  11  9   7   5   28  26
   24  22  20  18  16  14  12  10  8   6   4   29  27
   25  23  21  19  17  15  13  11  9   7   5   3   30
   28  26  24  22  20  18  16  14  12  10  8   6   4
   2   31  29  27  25  23  21  19  17  15  13  11  9
   7   5   3   1   30  28  26  24  22  20  18  16  14
   12  10  8   6   4   2   31  29  27  25  23  21  19
   17  15  13  11  9   7   5   3   1   30  28  26  24
   22  20  18  16  14  12  10  8   6   4   2   29  27
   25  23  21  19  17  15  13  11  9   7   5   3   28
   26  24  22  20  18  16  14  12  10  8   6   4   27
   25  23  21  19  17  15  13  11  9   7   5   26  24
   22  20  18  16  14  12  10  8   6   23  21  19  17
   15  13  11  9   22  20  18  16  14  12  10]
A=[1   1   1   1   1   1   1   3   3   3   3   3   3   3
   3   5   5   5   5   5   5   5   5   5   5   5   7
   7   7   7   7   7   7   7   7   7   7   7   9   9
   9   9   9   9   9   9   9   9   9   9   9   11  11
   11  11  11  11  11  11  11  11  11  11  11  11  13
   13  13  13  13  13  13  13  13  13  13  13  13  13
   13  15  15  15  15  15  15  15  15  15  15  15  15
   15  15  15  15  17  17  17  17  17  17  17  17  17
   17  17  17  17  17  17  19  19  19  19  19  19  19
   19  19  19  19  19  19  19  19  19  21  21  21  21
   21  21  21  21  21  21  21  21  21  21  21  23  23
   23  23  23  23  23  23  23  23  23  23  23  23  25
   25  25  25  25  25  25  25  25  25  25  25  25  27
   27  27  27  27  27  27  27  27  27  27  27  29  29
   29  29  29  29  29  29  29  29  29  31  31  31  31
   31  31  31  31  33  33  33  33  33  33  33]
```

```
scatter(A(:),B(:),200,Datenmatrix(:),'filled')

axis equal, axis([-3 36 -3 36]), zoom on

   grid off
   colorbar
   axis off
 %  hold on
   text(38,38,'Activity','Fontsize',12)
 grid on;
set(gcf,'color',[1 1 1]);
```

## C++ source code in AutoCat

```
// testform.cpp : implementation file
// written by Woongsik Su in Saarbruecken at Technical University in 2009
// c++ for the automation of 10-fold parallel reactor
//

#include "stdafx.h"
#include "irtestrig.h"
#include "testform.h"
#include "LevelTrace.h"
#include "Multioptions.h"
#include "Tvichw32.h"
#include "lpt.h"
#include "MainFrm.h"
#ifdef _DEBUG
#define new DEBUG_NEW
#undef THIS_FILE
static char THIS_FILE[] = __FILE__;
#endif

/////////////////////////////////////////////////////////////////////////////
// testform dialog

IMPLEMENT_DYNCREATE(testform, CPanelInstrument)

/////////////////////////////////////////////////////////////////////////////
// CRobbiCtrlView diagnostics

#ifdef _DEBUG
void testform::AssertValid() const
{
	CPanelInstrument::AssertValid();
}

void testform::Dump(CDumpContext& dc) const
{
	CPanelInstrument::Dump(dc);
}
#endif //_DEBUG

/////////////////////////////////////////////////////////////////////////////

testform::testform()
	: CPanelInstrument(testform::IDD)
{
	//{{AFX_DATA_INIT(testform)
	m_bRunning = FALSE;
	//}}AFX_DATA_INIT
	m_bWaiting = FALSE;
	m_WaitTime = 100;
	m_WaitCarrier = 10;
	m_WaitFeed = 20;
	m_WaitInHoleAfter = 0;
	m_WaitInHole = 100;
	m_WaitOver = 0;
	m_WaitStatus = "";
```

```
        m_WaitStr = "";
        m_SuctionTime = 50;
        //      HW32 = NULL;
//      m_bEnableGC = FALSE;
//      m_RunDirectory = _T("");
        m_bGCForceReady = FALSE;
        m_Cleaning=FALSE;
        m_Pretreat=FALSE;
        m_Singlerun=FALSE;
        m_RunPointsAct=1;
        m_initialchanel=1;
        m_numberGC=2;
        m_TotalTime=0;
// Multi
        //m_FeedVentileUse=TRUE;
        //m_CarrierVentileUse=TRUE;
        //m_FeedWaitingTime=100;
        //m_CarrierWaitingTime=200;
        //m_MicroGcUse=TRUE;
        static BOOL bFirst = TRUE;
        if (bFirst) {
                bFirst = FALSE;

// Read Values from Setup
                ASSERT(theSetup != NULL);
                if (!theSetup->fOpenSection("Multi")) {
                        SetupDefault();
                        VERIFY(theSetup->fOpenSection("Multi"));
                }
                theSetup->Get("FeedVentileUse", m_FeedVentileUse);
                theSetup->Get("CarrierVentileUsebefore", m_CarrierVentileUsebefore);
                theSetup->Get("CarrierVentileUseafter", m_CarrierVentileUseafter);
                theSetup->Get("FeedWaitingTime", m_FeedWaitingTime);
                theSetup->Get("CarrierWaitingTimebefore", m_CarrierWaitingTimebefore);
                theSetup->Get("CarrierWaitingTimeafter", m_CarrierWaitingTimeafter);
                theSetup->Get("MicroGcUse", m_MicroGcUse);
                theSetup->Get("SuctionTime", m_SuctionTime);
                theSetup->Get("DoubleMeasurements", m_DoubleMeasurements);
                theSetup->Get("GCRunTime", m_GCRunTime);
                theSetup->Get("CleaningTime", m_CleaningTime);
                theSetup->Get("PretreatingTime", m_PretreatingTime);
                theSetup->Get("SinglerunningTime", m_SinglerunningTime);
                theSetup->Get("SinglewaitingTime", m_SinglewaitingTime);
                theSetup->Get("SinglerunningChannel", m_SinglerunningChannel);
                theSetup->Get("CleanGCUse", m_CleanGCUse);
                //c_StartGC.EnableWindow(m_MicroGcUse);
                //c_StartGC.EnableWindow(false);

                //c_StartGC.EnableWindow(m_bEnableGC);

                theSetup->CloseSection();



                // SetupReadRuns();

//              c_DoRun.EnableWindow(FALSE);

// Open Lpt Port
                if (m_MicroGcUse) {
```

```
                        CLpt::Init();

                        USHORT IRQNumber=7;
                        UCHAR ucPortNum;
                        ucPortNum = GetLPTNumber(CLpt::GetHandle());
                        SetPin(CLpt::GetHandle(),2,true);

                        TRACE("IRQNum:%d PortNum:%d IRQCounter:%d₩n",
                                IRQNumber,ucPortNum,GetIRQCounter(CLpt::GetHandle(),IRQNumber));
                }

                SetPin(CLpt::GetHandle(), (unsigned char) m_FeedPinNo, false);
                SetPin(CLpt::GetHandle(), (unsigned char) m_CarrierPinNo, false);
                SetPin(CLpt::GetHandle(), (unsigned char) m_PretreatPinNo, false);



                }
        //end Multiinitial

                if (!theSetup->fOpenSection("Feed")) {
                        VERIFY(theSetup->fOpenSection("Feed"));
                }
                theSetup->Get("PinNo", m_FeedPinNo);
                theSetup->CloseSection();

                if (!theSetup->fOpenSection("Carrier")) {
                        VERIFY(theSetup->fOpenSection("Carrier"));
                }
                theSetup->Get("PinNo", m_CarrierPinNo);
                theSetup->CloseSection();

                if (!theSetup->fOpenSection("Pretreat")) {
                        VERIFY(theSetup->fOpenSection("Pretreat"));
                }
                theSetup->Get("PinNo", m_PretreatPinNo);
                theSetup->CloseSection();
}

testform::~testform()
{
        // Also see OnDestroy !

}


void testform::DoDataExchange(CDataExchange* pDX)
{
        CPanelInstrument::DoDataExchange(pDX);
        //{{AFX_DATA_MAP(testform)
        DDX_Control(pDX, IDC_STARTGC, c_StartGC);
        DDX_Check(pDX, IDC_STARTGC, m_bRunning);
        //}}AFX_DATA_MAP
}



BEGIN_MESSAGE_MAP(testform, CPanelInstrument)
        //{{AFX_MSG_MAP(testform)
        ON_BN_CLICKED(IDC_STARTGC, OnStartGC)
        ON_BN_CLICKED(IDC_BUTTON1, OnButton1)
```

```
        ON_BN_CLICKED(IDC_BUTTON2, OnButton2)
        ON_BN_CLICKED(IDC_BUTTON3, OnButton3)
        ON_BN_CLICKED(IDC_BUTTON4, OnButton4)
        ON_BN_CLICKED(IDC_BUTTON5, OnButton5)
        ON_BN_CLICKED(IDC_BUTTON6, OnButton6)
        ON_BN_CLICKED(IDC_BUTTON7, OnButton7)
        ON_BN_CLICKED(IDC_BUTTON8, OnButton8)
        ON_BN_CLICKED(IDC_BUTTON9, OnButton9)
        ON_BN_CLICKED(IDC_BUTTON10, OnButton10)
        ON_BN_CLICKED(IDC_DORUN, OnDoRun)
        ON_BN_CLICKED(IDC_MULTOPTIONS, OnMultoptions)
        ON_BN_CLICKED(IDC_START_GC, OnButton12)
        ON_BN_CLICKED(IDC_CleanRun, OnCleanRun)
        ON_BN_CLICKED(IDC_Pretreat, OnPretreat)
        ON_BN_CLICKED(IDC_SingleRun, OnSingleRun)
        //}}AFX_MSG_MAP
END_MESSAGE_MAP()

/////////////////////////////////////////////////////////////////////////////
// testform message handlers

void testform::OnStartGC()
{
        // TODO: Add your control notification handler code here
                if (m_MicroGcUse) {
                c_StartGC.SetCheck(1);
                SetPin(CLpt::GetHandle(),2,false);
                Sleep(200);
                SetPin(CLpt::GetHandle(),2,true);
                c_StartGC.SetCheck(0);
                c_StartGC.EnableWindow(FALSE);
        }
}

BOOL testform::IsGCReady(void) {
        if (CLpt::GetHandle() != NULL && m_MicroGcUse)
                return GetPin(CLpt::GetHandle(),13);
        else
                return FALSE;

}

void testform::OnButton1()
{
        // TODO: Add your control notification handler code here
        m_Serial.Open(_T("COM2"));
        m_Serial.Setup(CSerial::EBaud9600,CSerial::EData8,CSerial::EParNone,CSerial::EStop1);
        m_Serial.SetupHandshaking(CSerial::EHandshakeOff);

        m_Serial.Write("1go1₩n");
        m_Serial.Close();

}

void testform::OnButton2()
{
        // TODO: Add your control notification handler code here
        m_Serial.Open(_T("COM2"));
        m_Serial.Setup(CSerial::EBaud9600,CSerial::EData8,CSerial::EParNone,CSerial::EStop1);
        m_Serial.SetupHandshaking(CSerial::EHandshakeOff);
```

```
        m_Serial.Write("1go2₩n");
        m_Serial.Close();
}

void testform::OnButton3()
{
        // TODO: Add your control notification handler code here
        m_Serial.Close();
        m_Serial.Open(_T("COM2"));
        m_Serial.Setup(CSerial::EBaud9600,CSerial::EData8,CSerial::EParNone,CSerial::EStop1);
        m_Serial.SetupHandshaking(CSerial::EHandshakeOff);

        m_Serial.Write("1go3₩n");
        m_Serial.Close();
}

void testform::OnButton4()
{
        // TODO: Add your control notification handler code here
        m_Serial.Open(_T("COM2"));
        m_Serial.Setup(CSerial::EBaud9600,CSerial::EData8,CSerial::EParNone,CSerial::EStop1);
        m_Serial.SetupHandshaking(CSerial::EHandshakeOff);

        m_Serial.Write("1go4₩n");
        m_Serial.Close();
}

void testform::OnButton5()
{
        // TODO: Add your control notification handler code here
        m_Serial.Open(_T("COM2"));
        m_Serial.Setup(CSerial::EBaud9600,CSerial::EData8,CSerial::EParNone,CSerial::EStop1);
        m_Serial.SetupHandshaking(CSerial::EHandshakeOff);

        m_Serial.Write("1go5₩n");
        m_Serial.Close();
}

void testform::OnButton6()
{
        // TODO: Add your control notification handler code here
        m_Serial.Open(_T("COM2"));
        m_Serial.Setup(CSerial::EBaud9600,CSerial::EData8,CSerial::EParNone,CSerial::EStop1);
        m_Serial.SetupHandshaking(CSerial::EHandshakeOff);

        m_Serial.Write("1go6₩n");
        m_Serial.Close();
}

void testform::OnButton7()
{
        // TODO: Add your control notification handler code here
        m_Serial.Open(_T("COM2"));
        m_Serial.Setup(CSerial::EBaud9600,CSerial::EData8,CSerial::EParNone,CSerial::EStop1);
        m_Serial.SetupHandshaking(CSerial::EHandshakeOff);

        m_Serial.Write("1go7₩n");
        m_Serial.Close();
}

void testform::OnButton8()
```

```
{
	// TODO: Add your control notification handler code here
	m_Serial.Open(_T("COM2"));
	m_Serial.Setup(CSerial::EBaud9600,CSerial::EData8,CSerial::EParNone,CSerial::EStop1);
	m_Serial.SetupHandshaking(CSerial::EHandshakeOff);

	m_Serial.Write("1go8Wn");
	m_Serial.Close();
}

void testform::OnButton9()
{
	// TODO: Add your control notification handler code here
	m_Serial.Open(_T("COM2"));
	m_Serial.Setup(CSerial::EBaud9600,CSerial::EData8,CSerial::EParNone,CSerial::EStop1);
	m_Serial.SetupHandshaking(CSerial::EHandshakeOff);

	m_Serial.Write("1go9Wn");
	m_Serial.Close();
}

void testform::OnButton10()
{
	// TODO: Add your control notification handler code here
	m_Serial.Open(_T("COM2"));
	m_Serial.Setup(CSerial::EBaud9600,CSerial::EData8,CSerial::EParNone,CSerial::EStop1);
	m_Serial.SetupHandshaking(CSerial::EHandshakeOff);

	m_Serial.Write("1go10Wn");
	m_Serial.Close();
}

void testform::CmdTgtDoRegisterCommands(void) {
	CExpCommand *cmd = CmdTgtGetCommando();
	ASSERT(cmd != NULL);
	cmd->ExpCmdRegisterCmd(CmdTgtGetID(), CMD_RUN, "Run", "Starte Run.");
	cmd->ExpCmdRegisterCmd(CmdTgtGetID(), CMD_CLEAN, "Clean", "Starte Clean.");
	cmd->ExpCmdRegisterCmd(CmdTgtGetID(), CMD_PRETREAT, "Pretreat", "Starte Pretreat.");
	cmd->ExpCmdRegisterCmd(CmdTgtGetID(), CMD_SINGLERUN, "Singlerun", "Starte Singlerun.");

}

BOOL testform::CmdTgtValidateOptions(int /* CmdID */, const CString & /* Options */, CString & /* ErrMsg */ )
{
	// Nothing to do
	return TRUE;
}

void testform::CmdTgtDoCommand(int CmdID, const CString & /* Options */) {
	switch (CmdID) {
	case CMD_START:
	case CMD_STOP:
	case CMD_PAUSE:
	case CMD_RESUME:
		break;
	case CMD_RUN:
		CmdTgtSetState(INDI_NOT_READY);
		UpdateData();
		m_bRunning = TRUE;
		UpdateData(FALSE);
		OnDoRun();
```

```
		break;
		case CMD_CLEAN:
			CmdTgtSetState(INDI_NOT_READY);
			UpdateData();
			m_bRunning = TRUE;
			UpdateData(FALSE);
			OnCleanRun();
		break;
		case CMD_PRETREAT:
			CmdTgtSetState(INDI_NOT_READY);
			UpdateData();
			m_bRunning = TRUE;
			UpdateData(FALSE);
			OnPretreat();
		break;
			case CMD_SINGLERUN:
			CmdTgtSetState(INDI_NOT_READY);
			UpdateData();
			m_bRunning = TRUE;
			UpdateData(FALSE);
			OnSingleRun();
		break;
		default:
			TRACE("Unknown CommandWn");
			ASSERT(FALSE);
			break;
		}
}

void testform::OnDoRun()
		// TODO: Add your control notification handler code here
{
		 //CString str_1,str_2;
		 //str_1.Format("%d",m_RunPoints.GetSize());
		 //str_2.Format("%d",m_RunPointsAct);
		 // MessageBox(str_2,str_1,MB_OK);
		// Kommt noch weg
		{
		UpdateData();

		m_RunState = MULTI_CHANNEL;

		// Call this in every case, will deactivate the DoRun Button.
		m_Cleaning=FALSE;
		DoRun();
		}
}



void testform::OnCleanRun()
{
		// TODO: Add your control notification handler code here
			{
		UpdateData();

		m_RunState = MULTI_CHANNEL;

		// Call this in every case, will deactivate the DoRun Button.
		m_Pretreat=FALSE;
		m_Cleaning=TRUE;
```

```
        DoRun();
        }
}


void testform::DoRun(void) {

//      ASSERT(m_bRunning);
//      m_RackDisplay.ResumeRun();
        //CPoint p;
        CString str;
        m_bRunning=TRUE;

        //m_FeedVentileUse;
        //m_CarrierVentileUse;
        //m_MicroGcUse;
        //SetPin(CLpt::GetHandle(), (unsigned char) m_CarrierPinNo, false);
        //SetPin(CLpt::GetHandle(), (unsigned char) m_FeedPinNo, false);
        //SetPin(CLpt::GetHandle(), (unsigned char) m_PretreatPinNo, false);

        switch (m_RunState) {
        case MULTI_CHANNEL: // First Movement is sent in OnDoRun
                m_numberGC=2;
                if (m_Singlerun)
                {
                str.Format("Moving to Channel(%d)", m_SinglerunningChannel);
                DisplayStatusStr(str);
                OnStartMULTI(m_SinglerunningChannel);
                m_RunPointsAct=10;
                }
                else
                {
                str.Format("Moving to Channel(%d)", m_RunPointsAct);
                DisplayStatusStr(str);
                OnStartMULTI(m_RunPointsAct);
                }

                if (m_Cleaning)
                {m_RunState=MULTI_CLEAN;
                }
                else if (m_Pretreat)
                {m_RunState=MULTI_PRETREAT;
                }
                else if (m_Singlerun)
                {m_RunState=MULTI_SINGLERUN;
                }
                else
                {m_RunState=MULTI_CARRIER;
                }
                DoRun();
                break;
        case MULTI_CARRIER:
                m_RunState=MULTI_FEED;
                if (!m_CarrierVentileUsebefore)
                {Wait(0);}
                else
                {
                        SetPin(CLpt::GetHandle(), (unsigned char) m_CarrierPinNo, true);
                        Wait(m_CarrierWaitingTimebefore);
                }
                //
```

```
            if (m_CleanGCUse)
            {m_RunState=MULTI_CLEANGC;
            }
            else
            {
            }
            //
            break;
    case MULTI_CLEANGC:
            m_RunState=MULTI_CLEANGCWAIT;
            OnStartGC();
            DoRun();
            break;
    case MULTI_CLEANGCWAIT:
            m_RunState=MULTI_FEED;
            SetPin(CLpt::GetHandle(), (unsigned char) m_CarrierPinNo, true);
            Wait(m_SuctionTime);
            break;
    case MULTI_FEED:
            m_RunState = MULTI_STARTGC;
            if (!m_FeedVentileUse)
            {Wait(0);}
            else
            //FEED
            {SetPin(CLpt::GetHandle(), (unsigned char) m_CarrierPinNo, false);
            SetPin(CLpt::GetHandle(), (unsigned char) m_FeedPinNo, true);
            Wait(m_FeedWaitingTime);
            }
            break;
    case MULTI_STARTGC:
            if (!m_MicroGcUse)
            {
            m_RunState = MULTI_CARRIER2;
            DoRun();
            }
            else
            {
            m_RunState = MULTI_WAITING;
            OnStartGC();
            m_numberGC=m_numberGC-1;
            DoRun();
            }
            break;
    case MULTI_WAITING:
            if ((!m_DoubleMeasurements)|(m_numberGC==0))
            {
            m_TotalTime=m_SuctionTime;
            }
            else
            {
            m_TotalTime=m_SuctionTime+m_GCRunTime;
            }
            if (m_FeedVentileUse)
            {
            SetPin(CLpt::GetHandle(), (unsigned char) m_CarrierPinNo, false);
            SetPin(CLpt::GetHandle(), (unsigned char) m_FeedPinNo, true);
            Wait(m_TotalTime);
            }
            else
            {
            SetPin(CLpt::GetHandle(), (unsigned char) m_CarrierPinNo, true);
```

```
        SetPin(CLpt::GetHandle(), (unsigned char) m_FeedPinNo, false);
        Wait(m_TotalTime);
        }
        if ((!m_DoubleMeasurements)|(m_numberGC==0))
        {
        m_RunState = MULTI_CARRIER2;
        }
        else
        {
        m_RunState = MULTI_STARTGC;
        }
        break;
case MULTI_CARRIER2:
        m_RunState = MULTI_WAITEND;
        if (!m_CarrierVentileUseafter)
        {Wait(0);}
        else
        {
        SetPin(CLpt::GetHandle(), (unsigned char) m_CarrierPinNo, true);
        SetPin(CLpt::GetHandle(), (unsigned char) m_FeedPinNo, false);
        Wait(m_CarrierWaitingTimeafter);
        }
        break;
case MULTI_CLEAN:
        m_RunState=MULTI_WAITEND;
        if (m_RunPointsAct)
        {SetPin(CLpt::GetHandle(), (unsigned char) m_CarrierPinNo, true);}
        Wait(m_CleaningTime);
        break;
case MULTI_PRETREAT:
        m_RunState=MULTI_WAITEND;
        if (m_RunPointsAct)
        {SetPin(CLpt::GetHandle(), (unsigned char) m_PretreatPinNo, true);}
        Wait(m_PretreatingTime);
        break;
case MULTI_SINGLERUN:
        m_RunState=MULTI_SINGLEGCRUN;
        if (m_RunPointsAct)
        {SetPin(CLpt::GetHandle(), (unsigned char) m_FeedPinNo, true);}
        Wait(m_SinglerunningTime);
        break;
case MULTI_SINGLEGCRUN:
        m_RunState=MULTI_SINGLEGCWAIT;
        OnStartGC();
        DoRun();
        break;
case MULTI_SINGLEGCWAIT:
        m_RunState=MULTI_WAITEND;
        Wait(m_SinglewaitingTime);
        break;
case MULTI_WAITEND:
        m_RunPointsAct++;
        if (m_RunPointsAct < 11) {
                m_RunState = MULTI_CHANNEL;
                DoRun();
        } else {
                m_RunState = MULTI_STOP;
                DoRun();
        }
        break;
case MULTI_STOP:
```

```
                if (m_Singlerun)
                {
                }
                else
                {
                        OnStartMULTI(m_initialchanel);
                        SetPin(CLpt::GetHandle(), (unsigned char) m_CarrierPinNo, false);
                        SetPin(CLpt::GetHandle(), (unsigned char) m_FeedPinNo, false);
                        SetPin(CLpt::GetHandle(), (unsigned char) m_PretreatPinNo, false);
                        m_bRunning = FALSE;
                        m_Cleaning= FALSE;
                        m_RunPointsAct=1;
                }
                UpdateData();
                DisplayStatusStr("Stopped");

                UpdateData(FALSE);
                CmdTgtSetState(INDI_READY);
                break;
        default:
                ASSERT(FALSE);
                break;
        }

}



void testform::OnThreadCheck(void) {
        if (m_bWaiting) {
                m_WaitTime--;
                TRACE("Waiting: %dWn", m_WaitTime);

                        // Display progress in Status Bar.
                CString str;
                if (m_WaitTime % 10 == 0) {
                        str.Format("%d", m_WaitTime);
                } else
                        str = ".";
                m_WaitStr += str;
                CIRTestRigApp *pApp = static_cast<CIRTestRigApp *>(AfxGetApp());
                ASSERT_VALID(pApp);
                CMainFrame *pWnd = static_cast<CMainFrame *>(pApp->GetMainWnd());
                ASSERT_VALID(pWnd);
                pWnd->m_wndStatusBar.SetWindowText(m_WaitStr);

                        // then call DoRun if necessary.
                if (m_WaitTime <= 0) {
                        m_bWaiting = FALSE;
                        if (m_bRunning)
                                DoRun();
                }
        }

        c_StartGC.EnableWindow(IsGCReady());
}

void testform::Wait(int Seconds) {
        m_WaitStr.Format("%sWaiting: %d", m_WaitStatus, Seconds);
        m_WaitTime = Seconds;
                // Display in StatusBar.
```

```
	DisplayStatusStr(m_WaitStr);

	if (m_WaitTime == 0)
		// Do immediately.
		DoRun();
	else
		m_bWaiting = TRUE;
}

void testform::DisplayStatusStr(const CString &str) {
	CIRTestRigApp *pApp = static_cast<CIRTestRigApp *>(AfxGetApp());
	ASSERT_VALID(pApp);
	CMainFrame *pWnd = static_cast<CMainFrame *>(pApp->GetMainWnd());
	ASSERT_VALID(pWnd);
	pWnd->m_wndStatusBar.SetWindowText(str);
}


void testform::OnStartMULTI(int Channel_num)
{
	// TODO: Add your control notification handler code here
	m_Serial.Open(_T("COM2"));
	m_Serial.Setup(CSerial::EBaud9600,CSerial::EData8,CSerial::EParNone,CSerial::EStop1);
	m_Serial.SetupHandshaking(CSerial::EHandshakeOff);
	m_ChannelStr.Format("1go%dWn", Channel_num);
	m_Serial.Write(m_ChannelStr);
	m_Serial.Close();
}

void testform::OnMultoptions()
{
	// TODO: Add your control notification handler code here
	CMultioptions dlg;
	dlg.m_FeedVentileUse = m_FeedVentileUse;
	dlg.m_CarrierVentileUsebefore = m_CarrierVentileUsebefore;
	dlg.m_CarrierVentileUseafter = m_CarrierVentileUseafter;
	dlg.m_FeedWaitingTime = m_FeedWaitingTime;
	dlg.m_CarrierWaitingTimebefore = m_CarrierWaitingTimebefore;
	dlg.m_CarrierWaitingTimeafter = m_CarrierWaitingTimeafter;
	dlg.m_MicroGcUse = m_MicroGcUse;
	dlg.m_SuctionTime = m_SuctionTime;
	dlg.m_DoubleMeasurements = m_DoubleMeasurements;
	dlg.m_GCRunTime = m_GCRunTime;
	dlg.m_CleaningTime = m_CleaningTime;
	dlg.m_PretreatingTime = m_PretreatingTime;
	dlg.m_SinglerunningTime = m_SinglerunningTime;
	dlg.m_SinglewaitingTime = m_SinglewaitingTime;
	dlg.m_SinglerunningChannel = m_SinglerunningChannel;

	dlg.m_CleanGCUse= m_CleanGCUse;
	//dlg.SetParent(this);
	if (dlg.DoModal() == IDOK) {

	m_FeedVentileUse = dlg.m_FeedVentileUse;
	m_CarrierVentileUsebefore = dlg.m_CarrierVentileUsebefore;
	m_CarrierVentileUseafter = dlg.m_CarrierVentileUseafter;
	m_FeedWaitingTime = dlg.m_FeedWaitingTime;
	m_CarrierWaitingTimebefore = dlg.m_CarrierWaitingTimebefore;
	m_CarrierWaitingTimeafter = dlg.m_CarrierWaitingTimeafter;
	m_MicroGcUse = dlg.m_MicroGcUse;
	m_SuctionTime = dlg.m_SuctionTime;
```

```
		m_DoubleMeasurements = dlg.m_DoubleMeasurements;
		m_GCRunTime = dlg.m_GCRunTime;
		m_CleaningTime = dlg.m_CleaningTime;
		m_PretreatingTime = dlg.m_PretreatingTime;
		m_SinglerunningTime = dlg.m_SinglerunningTime;
		m_SinglewaitingTime = dlg.m_SinglewaitingTime;

		m_SinglerunningChannel = dlg.m_SinglerunningChannel;

		m_CleanGCUse = dlg.m_CleanGCUse;

		SetupSave();
		}

}

void testform::SetupDefault(void)
{
		ASSERT(theSetup != NULL);
		theSetup->InsertSection("Multi");
		VERIFY(theSetup->fOpenSection("Multi"));

		theSetup->RegisterKey("FeedVentileUse", CSetup::KEY_INT);
		theSetup->RegisterDefault("FeedVentileUse", 0);

		theSetup->RegisterKey("CarrierVentileUsebefore", CSetup::KEY_INT);
		theSetup->RegisterDefault("CarrierVentileUsebefore", 0);

		theSetup->RegisterKey("CarrierVentileUseafter", CSetup::KEY_INT);
		theSetup->RegisterDefault("CarrierVentileUseafter", 0);

		theSetup->RegisterKey("FeedWaitingTime", CSetup::KEY_INT);
		theSetup->RegisterDefault("FeedWaitingTime", 100);

		theSetup->RegisterKey("CarrierWaitingTimebefore", CSetup::KEY_INT);
		theSetup->RegisterDefault("CarrierWaitingTimebefore", 50);

		theSetup->RegisterKey("CarrierWaitingTimeafter", CSetup::KEY_INT);
		theSetup->RegisterDefault("CarrierWaitingTimeafter", 50);

		theSetup->RegisterKey("MicroGcUse", CSetup::KEY_INT);
		theSetup->RegisterDefault("MicroGcUse", 0);

		theSetup->RegisterKey("SuctionTime", CSetup::KEY_INT);
		theSetup->RegisterDefault("SuctionTime", 50);

		theSetup->RegisterKey("DoubleMeasurements", CSetup::KEY_INT);
		theSetup->RegisterDefault("DoubleMeasurements", 0);

		theSetup->RegisterKey("GCRunTime", CSetup::KEY_INT);
		theSetup->RegisterDefault("GCRunTime", 0);

		theSetup->RegisterKey("CleaningTime", CSetup::KEY_INT);
		theSetup->RegisterDefault("CleaningTime", 0);

		theSetup->RegisterKey("CleanGCUse", CSetup::KEY_INT);
		theSetup->RegisterDefault("CleanGCUse", 0);

		theSetup->RegisterKey("PretreatingTime", CSetup::KEY_INT);
		theSetup->RegisterDefault("PretreatingTime", 0);
```

```
	theSetup->RegisterKey("SinglerunningTime", CSetup::KEY_INT);
	theSetup->RegisterDefault("SinglerunningTime", 0);

	theSetup->RegisterKey("SinglerunningChannel", CSetup::KEY_INT);
	theSetup->RegisterDefault("SinglerunningChannel", 0);

	theSetup->RegisterKey("SinglewaitingTime", CSetup::KEY_INT);
	theSetup->RegisterDefault("SinglewaitingTime", 0);


	theSetup->CloseSection();
}

void testform::SetupSave(void)
{
	ASSERT(theSetup != NULL);
	VERIFY(theSetup->fOpenSection("Multi"));

	theSetup->Set("FeedVentileUse", m_FeedVentileUse);
	theSetup->Set("CarrierVentileUsebefore", m_CarrierVentileUsebefore);
	theSetup->Set("CarrierVentileUseafter", m_CarrierVentileUseafter);
	theSetup->Set("FeedWaitingTime", m_FeedWaitingTime);
	theSetup->Set("CarrierWaitingTimebefore", m_CarrierWaitingTimebefore);
	theSetup->Set("CarrierWaitingTimeafter", m_CarrierWaitingTimeafter);
	theSetup->Set("MicroGcUse", m_MicroGcUse);
	theSetup->Set("SuctionTime", m_SuctionTime);
	theSetup->Set("DoubleMeasurements", m_DoubleMeasurements);
	theSetup->Set("GCRunTime", m_GCRunTime);
	theSetup->Set("CleaningTime", m_CleaningTime);
	theSetup->Set("PretreatingTime", m_PretreatingTime);
	theSetup->Set("SinglerunningTime", m_SinglerunningTime);
	theSetup->Set("SinglewaitingTime", m_SinglewaitingTime);
	theSetup->Set("SinglerunningChannel", m_SinglerunningChannel);

	theSetup->Set("CleanGCUse", m_CleanGCUse);
	theSetup->CloseSection();
}

void testform::OnButton12()
{
	// TODO: Add your control notification handler code here
	//	if (m_bEnableGC) {
	//	c_StartGC.SetCheck(1);
	//	SetPin(CLpt::GetHandle(),2,false);
	//	Sleep(200);
	//	SetPin(CLpt::GetHandle(),2,true);
	//	c_StartGC.SetCheck(0);
//		c_StartGC.EnableWindow(FALSE);
	//}
}

void testform::OnPretreat()
{
	// TODO: Add your control notification handler code here
		{
	UpdateData();

	m_RunState = MULTI_CHANNEL;

	// Call this in every case, will deactivate the DoRun Button.
	//m_Cleaning=TRUE;
```

```
        m_Cleaning=FALSE;
        m_Pretreat=TRUE;
        DoRun();
        }

}

void testform::OnSingleRun()
{
        // TODO: Add your control notification handler code here
        {
        UpdateData();

        m_RunState = MULTI_CHANNEL;

        // Call this in every case, will deactivate the DoRun Button.
        m_Cleaning=FALSE;
        m_Pretreat=FALSE;
        m_Singlerun=TRUE;
        DoRun();
        }
}
```